AN INDUSTRIAL ECOLOGY APPROACH TO SULPHIDE-CONTAINING MINERAL WASTES TO MINIMISE ARD FORMATION

Susan T.L. Harrison, Jennifer L. Broadhurst, Precious Hlongwane, Didi X. Makaula, Alexander K.B. Opitz, Mhlangabezi T. Golela and Mariette Smart

Part 1:
Characterising Potential for ARD

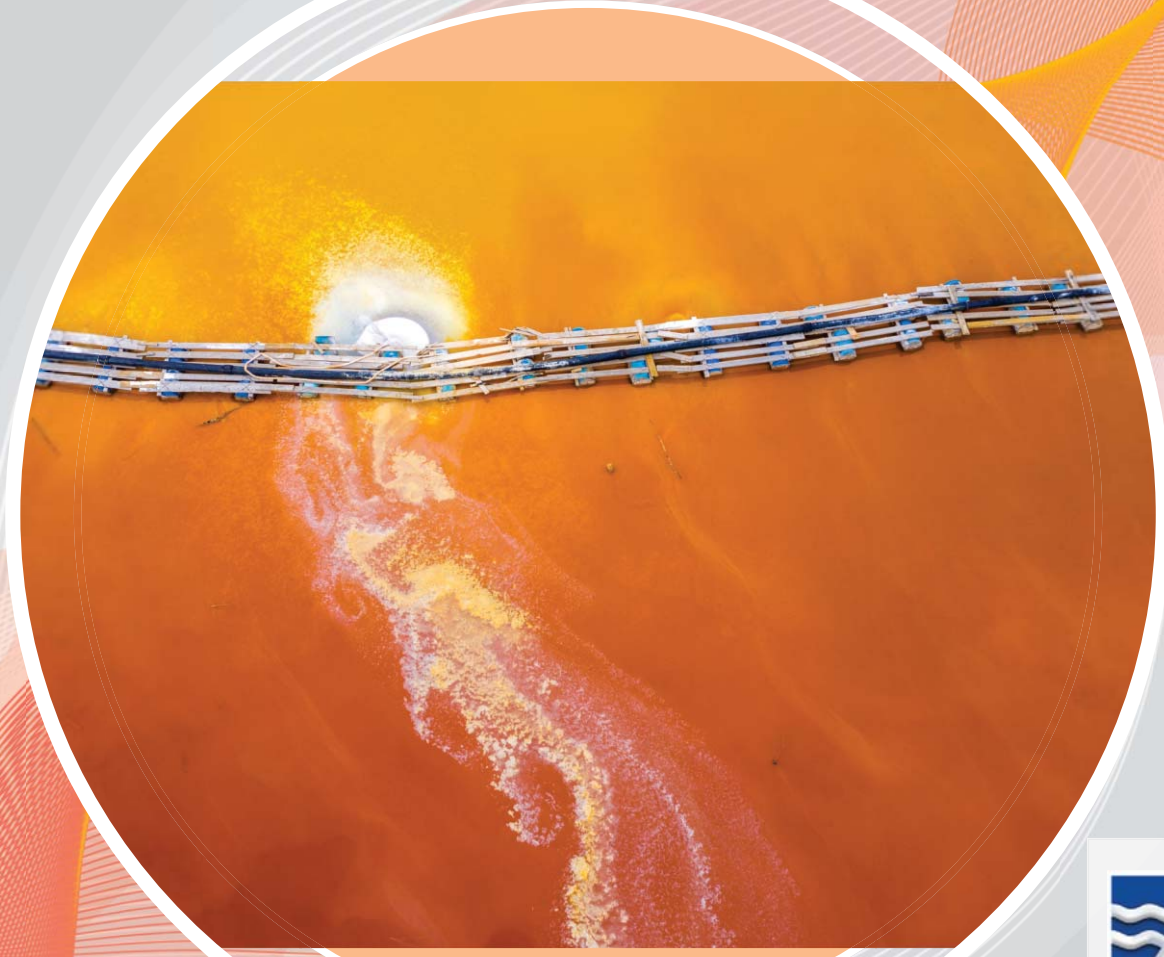

WATER RESEARCH COMMISSION

TT 822/1/20

An Industrial Ecology Approach to Sulphide-containing Mineral Wastes to Minimise ARD Formation

Part 1:
Characterising Potential for ARD

Report to the
Water Research Commission

by

Susan T.L. Harrison, Jennifer L. Broadhurst,
Precious Hlongwane, Didi X. Makaula,
Alexander K.B. Opitz, Mhlangabezi T. Golela and Mariette Smart

Centre for Bioprocess Engineering Research
Department of Chemical Engineering, University of Cape Town

WRC Report No. TT 822/1/20
ISBN 978-0-6392-0155-9

June 2020

Obtainable from
Water Research Commission
Private Bag X03
GEZINA, 0031

orders@wrc.org.za or download from www.wrc.org.za

EXECUTIVE SUMMARY

Acid rock drainage (ARD) represents a major potential environmental impact of mining of sulphidic minerals and pyritic coal. To prevent its formation, appropriate handling of waste rock or interburden, coal discards, fine coal waste and hard rock tailings is required. In this study, presented as WRC K5/2231, we have addressed both the categorisation of the ARD-generating potential of the waste material and routes towards the prevention of ARD formation from the waste. Our work is informed by the over-arching premise that the re-purposing of benign mineral wastes to other uses, using an industrial ecology focus, is preferable to its long-term disposal, hence we explore this approach. The findings of this project "An Industrial Ecology Approach to Sulphide-containing Mineral Wastes to Minimise ARD Formation" are reported in two parts, presented as two separate reports:

Part 1: Characterising potential for ARD formation

Part 2: Design for Disposal and Extraction of Products of Value

In this report, Part 1, the focus is on achieving the characterisation of waste rock and tailings fractions within an acceptable time period and in such a manner that the data gathered can inform modelling of the prediction of ARD formation. In review of the typically used static and long-term kinetic tests, these data were not previously available within an acceptable time frame for use in planning studies; hence, we developed and introduced the flask based 'biokinetic' test operated over a 30 to 90 day period. Together with this, we have compiled a set of ARD and metal mobilisation tests that allow for data collection to be completed within a 3- to 4-month period and for these data to include relative kinetic data in terms of acidification and neutralisation.

On review of the standard static tests typically used to provide an indication of whether a material is potentially acid forming or not, we observe that, owing to the extreme oxidant, these are largely 'worst-case scenario' tests; however, they are also batch endpoint tests, allowing neutralisation of the acid generated by the acid neutralising capacity (ANC), regardless of relative rates. As a result, this does not necessarily represent the acid forming potential across time. The humidity cell test requires at least 20 weeks, with complete data often requiring substantial extension of this time-line.

To address the time-line issue, we have acknowledged two important time-frames for ARD generation: 1) the time for onset of active ARD generation through acidification, and 2) the level or degree of acidification achieved. The time frame of the testwork can be shortened significantly by separating out these components.

We have developed the biokinetic test, first reported by our team in 2010, and refined it to provide an improved data set on ARD formation by taking into account the microbial activity catalysing, and thereby speeding up, ARD formation. To further refine the biokinetic test to address its consistent operation and enhance its sensitivity and accuracy, a number of operating variables are considered; most importantly particle size (and hence degree of liberation) and solids loading. The role of microbial inoculum in the biokinetic test was explored.

Further, the biokinetic test provides kinetic data on the neutralisation and acidification components of the material. By manipulating its operation to work from neutral pH or to start under acidified conditions, the data generated can be used to characterise the onset of acidification or the degree of acidification or both. In this report, we have concentrated our study largely on the latter owing to this being required to characterise the materials as acid forming (AF), potentially acid forming (PAF) or non-acid forming (NAF).

Following a review of static tests, humidity tests and the set-up of the biokinetic test, the data extractable from static and biokinetic tests is compared across a range of samples, showing that the essence of the static test data can be extracted from the biokinetic test. Thereafter we extend the analysis of both these tests to study the release or deportment of metals during the acidification process to further assess the environmental burden. This is extended to implement the sequential chemical extraction protocol to shed light on metal deportment under conditions ranging from neutral and non-oxidative through varying levels of acidity to highly acid and oxidising conditions. These data are critical for confirming whether a "benign" categorisation is relevant for de-sulphurised tailings material or NAF materials.

This report presents an improvement on the approaches to characterising ARD potential of mine waste rock and tailings or fines. It highlights use of the semi-continuous or flow-through biokinetic test, using a representative sample size and a particle size distribution ensuring sufficient liberation. Through these approaches or the combined use of the batch test with and without pH-control for rapidly neutralising samples, an appropriate environment can be created to simulate the biotic environment conducive to ARD generation for assessing the potential for a mine waste to generate ARD. It thus better informs the disposal of such materials. This suite of tests is also critical for consideration of re-purposing of mine wastes, an area of increasing importance as we work towards the circular economy. Our ongoing research further extends our studies on ARD characterisation through the reports being generation for WRC projects WRC K5/2580 and WRC K5/2946 and on the re-purposing of mine waste through our studies reported through WRC projects WRC K5/2761 and WRC K5/2844.

ACKNOWLEDGEMENTS

The project team gratefully acknowledge the funding and technical contribution received from the Water Research Commission. Further, thanks is expressed to the Reference Group for their technical input and assistance with logistic matters such as securing appropriate samples. Particular thanks goes to the following members of the Reference Group:

Reference Group	Affiliation
Dr Chris Broukaert	Pollution Research Group, UKZN
Dr Phil Hobbs	Hydrogeologist, CSIR
Ms Ritva Muhlbauer	Anglo Thermal Coal
Mr Rod Schwab	Department of Water and Sanitation

This page was intentionally left blank

Contents

LIST OF FIGURES

LIST OF TABLES

PUBLICATIONS DERIVING FROM WRC K5/2231

In peer-reviewed journals:

1. Becker M., Dyanti N., Broadhurst J., Harrison S.T.L. and Franzidis J-P. (2015). A mineralogical approach to evaluating laboratory scale acid rock drainage characterisation tests. *Minerals Engineering* 80, 33-36. Doi.org/10.1016/j.mineng.2015.06.015
2. Kotsiopoulos A. and Harrison S.T.L. (2017). Application of fine desulfurised coal tailings as a neutralising barrier in the prevention of acid rock drainage. *Hydrometallurgy* 168, 159-166. Doi: 10.1016/j.hydromet.2016.10.004
3. Kotsiopoulos A. and Harrison S.T.L. (2018). Co-disposal of benign desulfurised tailings with sulfidic waste rock to mitigate ARD generation: influence of flow and contact surface. Minerals Engineering, 116, 62-71. DOI: 10.1016/j.mineng.2017.03.003
4. Amaral Filho J.R., Firpo B., Broadhurst J.L. and Harrison S.T.L. On the feasibility of South African coal waste for production of "FabSoil', a technosol. Minerals Engineering (in press).
5. Amaral Filho J.R., Stander H.-M., Firpo B., Broadhurst J.L. and Harrison S.T.L. Opportunities for soil-related applications of fine coal processing wastes in South Africa. Minerals Engineering (under review).
6. Golela M.T., Opitz A.K.B., Smart M., Ntwampe S.K.O., Broadhurst J.L. and Harrison S.T.L. The semi-continuous UCT biokinetic test provides improved characterization of acid rock drainage potential of sulfidic waste rock by inoculated and naturally occurring microorganisms. Minerals Engineering (under review).
7. Stander H.-M., Harrison S.T.L. and Broadhurst J.L. Assessment of opportunities, barriers and drivers for the transfer of technologies for mine waste valorization: a case study of coal processing wastes in South Africa (in preparation).

In peer-reviewed conference proceedings:

1. Broadhurst J.L., Bryan C.G., Becker M., Franzidis J.-P. and Harrison S.T.L. (2013). Characterising the acid generating potential of mine water by means of laboratory-scale static and biokinetic tests. Proceedings of IMWA 2013 (Wolkersdorfer, Brown and Figueroa (Eds)), Golden, Colorado, USA. pp 33-38
2. Dyanti N., Becker M., Broadhurst J.L., Harrison S.T.L. and Franzidis J.-P. (2013). Use of mineralogy to interpret laboratory-scale acid rock drainage prediction tests – a gold case study. World Gold Conference 2013: Challenges in Gold Mining: 26-29 Sept 2013. pp. 519-525
3. Simunika N., Broadhurst J., Petersen J., Harrison S.T.L., Franzidis J-P. (2013). Predicting the time-related generation of acid rock drainage from mine waste: a copper case study. 3rd International Seminar on Environmental Issues in Mining. ISBN 978 956 9393 04 4
4. Broadhurst J.L. and Harrison, S.T.L. (2015). A desulfurization flotation approach for the integrated management of sulfide wastes and acid rock drainage risks. In: A Brown, C Bucknam, M Carballo et al. (eds), 10th International Conference on Acid Rock Drainage & IMWA Annual Conference, Chapter 2: Applied Mineralogy and Geoenvironmental Units, Santiago, Chile, 20-25 April 2015, Gecamin
5. Kotsiopoulos A. and Harrison S.T.L. (2015). Enhancing ARD mitigation by application of benign tailings to reduce the permeability of waste rock dumps. International Biohydrometallurgy Symposium, October 2015, Bali
6. Opitz A.K.B., Broadhurst J.L. and Harrison S.T.L. (2015). Assessing environmental risks associated with ultrafine coal wastes using laboratory-scale tests. International Biohydrometallurgy Symposium, October 2015, Bali
7. Opitz A.K.B, Becker M., Broadhurst J.L., Bradshaw D. and Harrison S.T.L. (2016). The biokinetic test as a geometallurgical indicator for acid rock drainage potentials. In Proceedings of 3rd AUSIMM International Geometallurgy conference, Perth, WA, June 2016. pp. 183-191

8. Opitz A.K.B., Becker M., Harrison S.T.L. and Broadhurst J.L. (2016). Characterising environmental risks associated with sulphide-bearing gold wastes. In Mining Meets Water – Conflicts and Solutions: Proceedings IMWA 2016, pp. 957-964. Freiberg Germany

9. Becker M., Charikinya E., Ntlhabane S., Voigt M., Broadhurst J.L., Harrison S.T.L. and Bradshaw D. (2018). An integrated mineralogy-based modelling framework for the simultaneous assessment of plant operational parameters with acid rock drainage potential of tailings. Proceedings 11th ICARD | IMWA, Wolkersdorfer, Ch.; Sartz, L.; Weber, A.; Burgess, J.; Tremblay, G. (eds.) | MWD Conference – "Risk to Opportunity"

10. Makaula D.X., Huddy R.J., Fagan-Endres M.A. and Harrison S.T.L. (2018). A flow-through biokinetic test for characterizing ARD potential: investigating the microbial metabolic activity on pyrite-bearing waste rock surfaces in an unsaturated ore bed. Proceedings 11th ICARD | IMWA, Wolkersdorfer, Ch.; Sartz, L.; Weber, A.; Burgess, J.; Tremblay, G. (eds.) | MWD Conference – "Risk to Opportunity"

11. Stander H.-M., Harrison S.T.L. and Broadhurst J.L. (2018). Re-purposing of acid generating fine coal waste: an assessment and analysis of opportunities. Proceedings 11th ICARD | IMWA, Wolkersdorfer, Ch.; Sartz, L.; Weber, A.; Burgess, J.; Tremblay, G. (eds.) | MWD Conference – "Risk to Opportunity"

Theses and Dissertations completed:

1. Hlongwane, Precious. MSc(Eng), University of Cape Town
2. Golela, Mhlangabezi Tolbert. M.Tech, Cape Peninsula University of Technology
3. Makaula, Didi Xhanti. PhD, University of Cape Town

Theses and Dissertations to be completed

4. Stander, Helene-Marie. PhD, University of Cape Town
5. Opitz, Alexander. PhD, University of Cape Town

ACRONYMS & ABBREVIATIONS

AAS	Atomic Absorption Spectroscopy
ABA	Acid Base Accounting
ABS	Autotrophic Basal Salt
AF	Acid Forming
ANC	Acid Neutralising Capacity
APHA	American Public Health Association
ARD	Acid Rock Drainage
CBS	Copper Bearing Sample
GARD	Global Acid Rock Drainage
GBS	Gold Bearing Sample
INAP	International Network for Acid Prevention
NAF	Non-Acid Forming
NAG	Net Acid Generation
NAPP	Net Acid Producing Potential
PAF	Potentially Acid Forming
PSD	Particle Size Distribution
QEMSCAN	Quantitative Evaluation of minerals
QXRD	Quantitative X-Ray Diffraction
RISC	Reduced Inorganic Sulphur Compounds
SCE	Sequential Chemical Extraction
SSA	Specific Surface Area
XRD	X-Ray Diffraction
XRF	X-Ray Fluorescence Spectroscopy

GLOSSARY OF TERMS

Acid Base Accounting	classifies the waste sample according to its potential for acid generation and neutralisation
Acid Generating Potential	potential in a waste sample for the formation of acid under the correct conditions
Acid Neutralising Capacity (ANC)	inherent potential in a waste sample for neutralising acid determined experimentally
Acid Rock Drainage (ARD)	Oxidation of sulphidic minerals results in acidic sulphate products which cause increased salinity and acidity of water run-off, leachate and water bodies, mobilisation of heavy metals, and contamination of the environment
acidophilic microorganisms	microbial organisms which thrive in an acidic environment
biokinetic tests	tests which include the role of microorganisms in the formation of acid in the waste sample
containment	acid rock drainage mitigation by preventing the leachate from entering the environment
kinetic tests	tests which quantify the rate of generation and quality of the acid generation, informing on the duration of the potential ARD formation, the relative contributions of the acid forming and acid neutralising components and the effectiveness of control measures used to limit sulphide oxidation
leachate	the solution after water has percolated through the rock
Maximum Potential Acidity (MPA)	the theoretical maximum acid which a waste sample could generate determined from its composition
mobilisation (of metals)	The movement or deportment of metals from the rock into the environment, typically carried by a water stream
Net Acid Generation (NAG)	a rapid ‘static’ field test for ARD determined experimentally, allowing simultaneous acid generation and neutralisation
Net Acid Producing Potential (NAPP)	the difference between MPA and ANC
static tests	tests which quantify only an end point of acid generation

This page was intentionally left blank

CHAPTER 1: BACKGROUND

1.1 Introduction

Wastes from the extraction and beneficiation of sulphide-bearing hard rock ores and coal deposits may contain significant quantities of sulphide minerals, particularly pyrite susceptible to oxidative dissolution in the presence of water and oxygen and giving rise to the formation of acid rock drainage (ARD). ARD is recognized as a significant problem in South Africa. Oxidation of sulphidic minerals results in acidic sulphate products which cause increased salinity and acidity of water run-off, leachate and water bodies, mobilisation of metals, and environmental contamination. Following mining of sulphide-bearing ores, generation of ARD is a long-lived problem, extending for 10s to 100s of years after mine closure. It is critical to handle waste materials and their disposal to prevent or minimise the generation of ARD.

Formation of ARD requires the reaction of a combination of sulphide, water and oxygen and is often catalysed by microorganisms. Hence, the long-term prevention of its formation requires the removal of these components from the reaction surface. Most typically, exclusion of oxygen and water is sought; however, this is required on an ongoing basis. Conversely removal of sulphide presents a permanent solution in which the risk of ARD formation is completely removed. This is the preferred approach.

On testing this concept of risk removal initially, the separation was motivated to produce a bulk fraction of benign tailings and a small fraction of sulphide rich materials for containment. This was initially tested as an end-of-pipe treatment approach; however, the value of integrating such separation into the upstream process stages was highlighted. The technological feasibility of this approach of complete removal of the risk of ARD formation from tailings and fine waste fractions by sulphide separation at the end-of-pipe has been demonstrated (Harrison et al., 2013). It is apparent that the prevention of ARD from the fines fraction by sulphide removal has good potential; further, this enables appropriate disposal of or re-purposing of the resultant waste streams produced. Addressing this holistically can provide significant additional benefit. This approach, underpinned by industrial ecology, forms a central thrust of this project. The implementation of this approach to minimising ARD formation from the tailings and fine wastes is further informed by techno-economic and environmental analysis, initiated in Harrison et al. (2013) and extended in these further studies.

In addressing these aspects, the ability to assess potential for the formation of ARD, both in terms of the extent of formation and the time frame of this, are essential. Currently accepted standard methods have significant shortcomings with respect to providing rigorous data for prediction of ARD and typically not considered on the basis of the relative time frame of acid formation and acid neutralisation. This first report from this study (provided here as Part 1) focuses on assessing appropriate methods for determining the potential ARD problem resulting from the waste material disposed and further developing the suite of methods as required. It is accompanied by a second report (Part 2) in which the techno-economic feasibility and environmental benefit of the two stage separation for risk removal and appropriate disposal are considered. Importantly Part B is extended based on an industrial ecology approach to consider potential for the re-purposing of the ensuing tailings streams, i.e. sulphide-rich and sulphide-lean streams to products of value.

The aim of the study presented as Part 1 of the report, as expressed in the proposal, is:

“Develop a method for characterizing the long term ARD generation potential that takes into account the likely impact of microbial colonisation and the relative time frame of acidification and neutralisation, building on the proposed concept of the biokinetic test, described by Hesketh et al. (2010a).”

The value of moving beyond considering acidity to include the fate of salts and metals mobilised from the waste rock should be recognised.

1.2 Project Background Leading to Scope

Characterisation of ARD generation potential plays an important role in planning for mine waste disposal. Typically, the data used to characterise the potential of a deposit or waste to form ARD are obtained from chemically-based static tests or humidity cell tests (International Network for Acid Prevention, 2013). However, in most real-world situations active microbial populations contribute substantially to ARD formation, even under extreme conditions (Bryan, 2006). Hence, the reaction kinetics and role of microbial activity are integral to understanding the potential for ARD generation and need to be addressed in addition to the standard characterisation tests for ARD.

ARD is formed through the oxidation of exposed or liberated sulphide minerals (typically pyrite FeS_2 but also other metal sulphides) and is accelerated by microbially catalysed exothermic reactions (Parker & Robertson, 1999). These oxidation reactions require oxygen and water as well as free Fe^{3+} ions in solution. At neutral to alkaline pH, pyrite is oxidised by dissolved oxygen (Schumann, et al., 2012), but this reaction is slow under ambient temperatures. In the presence of acid, acidophilic micro-organisms catalyse the oxidation of Fe^{2+} ions, producing Fe^{3+} which in turn leach pyrite and other mineral sulphides exposed at the surface of the material. Further acid is generated through microbially catalysed oxidation of reduced sulphur.

Current laboratory scale tests for ARD characterisation are typically fast chemical tests, referred to as static tests, or long-term kinetic tests such as the humidity cell. Static tests include acid base accounting (ABA) and net acid generation (NAG) tests. Neither the static or kinetic tests typically account for microbial factors. In addition, the static tests do not take into account the relative kinetics of acid generating and acid consuming reactions across the range of materials present. They also do not provide information on the lag associated with ARD generation, due to the establishment of communities of ferrous iron and sulphur oxidising micro-organisms. Details and discussions on these tests can be found in Smart et al. (2002) and Stewart et al. (2006).

Microbial oxidation tests for the prediction of ARD generation potential have been proposed previously. In the British Columbia Research Confirmation Test, *Acidithiobacillus ferrooxidans*, an iron and sulphur oxidising bacterium, was added to an acid stabilised (pH 2.5) suspension of mineral particulates, crushed to an average particle size of 200 µm. The flasks were incubated at 35˚C and the pH was maintained below pH 2.8 for the first three days, to allow for microbial adaptation, after which additional sample material was added. The solution pH was tested regularly. If it increased above pH 3.5, the test was terminated and the sample classified as most likely non-acid forming. A decrease in solution pH indicated microbial activity and provided a strong indication that the sample was acid forming. Limitations of this test include the acidification of samples to the ideal conditions for microbial activity as well as the use of a single microbial species (Bruynesteyn & Hackl, 1984), giving an over-estimation of final acidity, inability to study initial ARD generation at natural pH ranges and the synergistic microbial activity of mixed cultures. We introduced the biokinetic shake flask test (Hesketh, et al., 2010a). Through the use of finely milled whole ore or tailings, the characterisation of the potential for microbially-mediated ARD formation is sought, while minimising the time of assay required. The environments used both mimic the biologically active environment that typically develops with time as well as investigating the potential to generate such an environment. The defined microbial consortium is representative of those typically associated with the generation of ARD (Bryan, 2006). While this test has provided new insight into the tendency to establish a microbially catalysed environment (Hesketh, et al., 2010a; Kazadi Mbamba, et al., 2012), the relative kinetic rates of acid generation and acid neutralisation and the probability of the sulphur species present to contribute to ARD, refinement of the test is required to maximise information provided while ensuring its reproducibility and standard performance. This forms the focus of the study. Further to this, we also consider the potential for the aqueous environment, whether or not acidic or oxidising or both, to cause deportment of metals from the waste rock.

CHAPTER 2: APPROACHES TO CHARACTERISING ARD POTENTIAL

2.1 Review of Approaches to Characterising ARD Potential

In order to be effectively managed, it is necessary to characterise the long-term acid generating potential of mine wastes accurately and reliably using simple, robust and precise testing procedures. Whilst the chemical oxidation of pyrite occurs at a relatively slow rate, the formation of ARD is greatly accelerated in the presence of naturally-occurring acidophilic microorganisms (Bryan, 2006; Johnson & Hallberg, 2005).

As illustrated in Figure 2-1, ARD characterisation and prediction tools can be categorised into three groups: analytical characterisation methods which include chemical, physical and mineralogical characterisation; geochemical tests at the laboratory or field test scale; and mathematical models, including engineering, empirical and geochemical models for ARD prediction.

In practice, the reliable prediction of ARD is likely to require combined application of several different tools with selection of specific tests, the combination of tests being dictated by the required outcomes and decision-making context (i.e. fit for purpose).

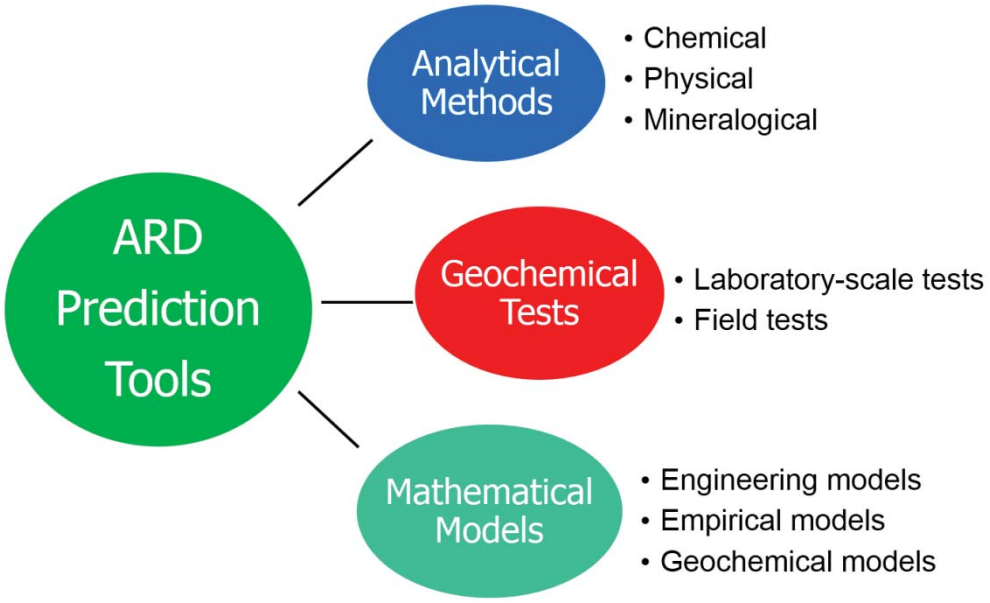

Figure 2-1 Categorisation of ARD characterisation and prediction tools

Laboratory-scale geochemical tests are a typical starting place for the characterising of ARD potential. These can be subdivided further into three main categories. The first two are the well-known static tests and conventional kinetic tests (International Network for Acid Prevention, 2013; Smart, et al., 2002; Price, 2009) while the third is the more recently added biokinetic shake flask test. Key strengths, weaknesses and applications of these tests are described below. Their key focus is on determining the acid generation as illustrated in Figure 2-2, traditionally the endpoint acid generation.

Static chemical tests, such as acid base accounting (ABA) and net acid generation (NAG), provide an indication of the absolute potential of a material to generate acid over time. They are simple and inexpensive tests with short turn-around times. However, they utilise aggressive conditions in

comparison with those found in natural environment and provide no information on reaction rates, especially the relative rates of acid neutralisation and acidification. These tests are thus mainly used as initial screening tests, whereby materials are classified in accordance with universally accepted criteria. These tests lead to an indicative categorisation but are not absolute.

Kinetic tests are designed to provide information on the time-related acid generating potential of a material. The most common conventional kinetic tests include humidity cells and column leach tests. These provide an estimate of weathering kinetics and lag time under conditions which more closely simulate those expected in a disposal scenario. They are thus useful in predicting the time-related drainage quality. A major drawback of these standard kinetic tests is the time required to generate meaningful data. They are thus resource extensive and time consuming, and typically require operation for several months or even years to provide meaningful information. This makes them expensive and their application tends to be limited to specific (and usually site-specific) studies. Other disadvantages relate to poor reproducibility aggravated by the heterogeneity of the large samples of coarse particle size distribution, and their uncertainties around scale-up. The standard procedures also tend to ignore the role of microbial activity in ARD generation, despite the fact that microbial colonisation of sulphide-bearing waste rock or tailings is inevitable (Bryan, 2006). Most importantly, their required time frame for reliable and meaningful results often precludes their robust use to inform the design of the waste disposal strategies.

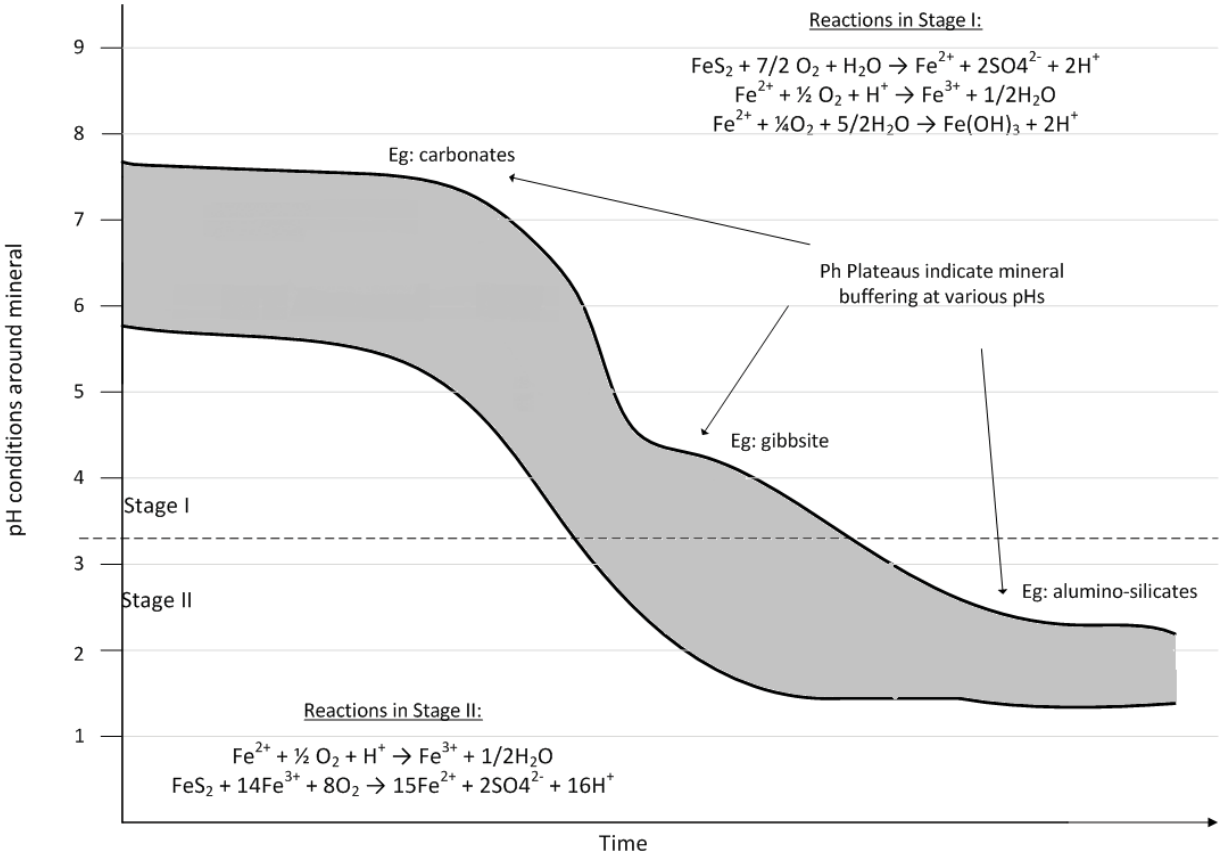

Figure 2-2 The time scale associated with the onset of acidification and generation of ARD from mineral deposits expands over years. To provide effective characterisation and prediction tools, the 'onset' and 'acidification' stages can be analysed separately.

In an attempt to address the short-comings of standard humidity and leach column tests, a microbial shake flask test was proposed by Duncan and Bruynesteyn (1979) but found little traction. Subsequently, Hesketh et al. (2010a) developed a more rigorous biokinetic test through application of the knowledge base from mineral bioleaching to the measurement of ARD generation potential. As the name implies, this test is specifically designed to provide information on the kinetics of ARD drainage under conditions of microbial activity. It is relatively rapid in comparison with other kinetic tests.

The predictive capabilities of this type of test, and indeed the static tests, are limited by both the use of finely milled materials and aggressive leach conditions. The latter effectively eliminates the lag period leading up to the onset of conditions conducive to microbial activity (see Figure 2-2), and can thus be considered to provide a realistic simulation of the aggressive microbially-assisted phase. In other words, the biokinetic test is a characterisation test, providing input to prediction methods but does not provide direct prediction which depends on both the conditions leading to onset of ARD and the degree of liberation of the sulphide mineral. Although it still requires refinement and standardisation, this test is a very useful tool in the ARD potential characterisation and prediction toolbox, particularly in terms of providing information that both enhances and validates the results of static tests in a time and cost effective way, providing information on the relative timescale of acidification and neutralisation and providing information within a biotic and acidic environment likely to develop in long-term humidity cell and other kinetic tests.

Hesketh et al. (2010a) originally developed the biokinetic test for copper-bearing hard rock. The teams from Minerals to Metals and the Centre for Bioprocess Engineering at UCT have extended the data sets collected across additional hardrock samples and coal. In this project, we consider the application of the biokinetic shake flask tests to a range of sulphide-bearing mine wastes from different sources and origins. Through analysis of the data sets collected to date, in this section we demonstrate its role in both validating and enhancing the results and nature of the data obtained from standard static chemical tests. Further we identify areas for refinement.

Figure 2-3 provides a summary of these laboratory scale geochemical tests for use in ARD characterisation and prediction in combination with modelling and simulation. Current characterisation follows a sequential process to minimise the required time and costs associated with the assessment. ARD characterisation commences with static ARD chemical tests that have been designed to quantify the acid-neutralizing and acid-generating components present in the waste samples. Such tests provide information concerning the maximum generation and neutralisation of acidity. Following the classification of the waste sample, standard laboratory-based kinetic tests (ASTM, 2012) are performed to inform on the rates of the reactions involved and the composition of the pollution generated. The combined results of the laboratory-scale tests, often coupled to data from field tests, are subsequently used for prediction of ARD generation under field conditions (Verburg, et al., 2009; Price, 1997).

The detailed overview of the laboratory and conventional methods is provided by Harrison et al. (2010) and in the Global Acid Rock Drainage (GARD) guide (International Network for Acid Prevention, 2013), prepared by the International Network for Acid Prevention (INAP). A brief overview is given in Section 2.2.

The quality of the characterisation and prediction data resulting from these analyses is strongly affected by the sampling protocol used and the selection of an appropriate suite of tests. The choice of tests for analysis of a particular waste rock is informed by the geology of the sample, cost and time available (Harrison, et al., 2010). Ideally, characterisation of the material designated for both value recovery and waste disposal should be carried out during the exploratory phase of a new operation. Outcrop exposures, exploration drill cores, geological sections and core assays may be used, with the same sampling techniques as those used to evaluate material in terms of recoverable resources, thus providing rigorous data to inform processing decisions and design for disposal. In practice, in most cases testing is confined to waste rock dumps and tailings impoundments at operational or legacy sites.

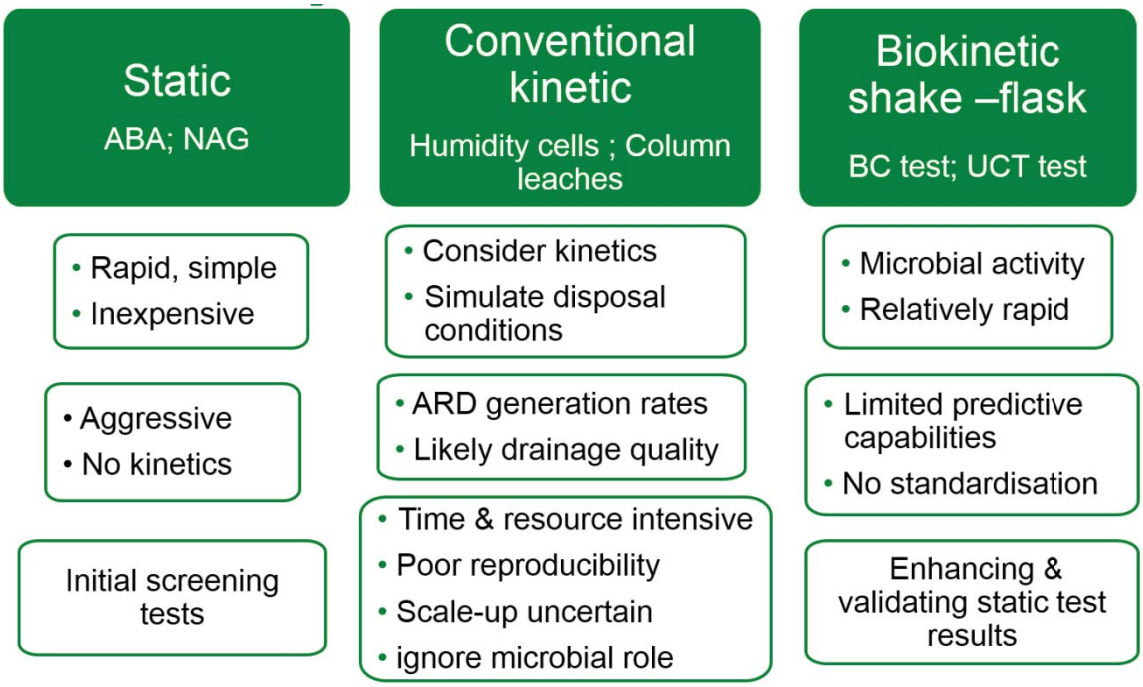

Figure 2-3 Summary and comparison of laboratory scale geochemical tests for ARD characterisation and prediction

2.2 Summary and Overview of Static and Conventional Methods

2.2.1 Static characterisation tests

The most commonly used static ARD test is Acid-Base Accounting (Ferguson & Erickson, 1988) which classifies the waste sample according to its potential for acid generation. For this quantification, both the inherent neutralising potential, i.e. the acid neutralising capacity (ANC), and the acid generating potential, i.e. the maximum potential acidity (MPA), are determined from experimental and theoretical calculations respectively. An overall value, the net acid producing potential (NAPP), with units of equivalent kilograms H_2SO_4 per ton or kilograms $CaCO_3$ per ton, is determined (Smart, et al., 2002; Miller & Jeffery, 1995). Samples with NAPP values greater than 20 and less than -20 kg H_2SO_4 per ton are classified as potentially acid forming and acid neutralising respectively.

The standard ANC test was developed by Sobek et al. (1978) using a back-titration after acid digestion with hydrochloric acid, with the quantity and molarity based on a preliminary reactive carbonate test to determine the fizz rating. The fizz rating is a qualitative test which is subjective and open to personal bias (Evans & Skousen, 1995; Skousen, et al., 1997) and remains a main source of error in the ANC test (Paktunc, et al., 2001). Variations in ANC test methods stem mainly from the observed incomplete oxidation of ferrous iron to ferric iron and the temperature at which the acid digestion reactions occur. Analysis of samples containing significant quantities of siderite (an Fe-carbonate) have been found to overestimate ANC values due to incomplete ferric iron precipitation during back-titration; an acid generation process (Skousen et al., 1997). The authors suggested the addition of H_2O_2 to oxidise Fe^{2+} to Fe^{3+} before back titration, thus accounting for the acid generated during ferric iron precipitation. White et al. (White III, et al., 1999) in experiments comparing the Sobek (1978) and Standard Skousen (1997) methods in the presence of siderite, found that there was insufficient reaction time in the Sobek method for the complete hydrolysis of the ferric iron; resulting in a significant difference between the values from these methods. During modification of the Sobek method with the addition of H_2O_2, Weber et al. (2004a) found that the H_2O_2 addition resulted in the oxidation of sulphide minerals within the ore sample leading to an under-estimation of the ANC. The authors suggested a drop-wise addition might limit this oxidation. Stewart et al. (2006) outlined a methodology which included the filtering of the ore sample,

as per the Skousen method, and the drop-wise addition of the H_2O_2 after each titration step to ensure complete ferrous iron oxidation.

The level of detection of the tests is not sufficient to provide an accurate, quantitative analysis but is useful for waste classification (Lawrence & Scheske, 1997). The ANC test does not account for the relative reactivity of the acid consuming minerals, particularly the reactive silicate minerals (Paktunc, 1999). The high temperatures experienced during the tests, improbable in a waste heap situation, also enhanced the rate of acid consumption for many minerals; especially true for the silicates in the ore sample (Lawrence & Scheske, 1997; Jambor, et al., 2000). ANC test methods which include acid digestion at room temperatures have been developed (Lawrence & Wang, 1997); however, this method remains outside standard classification protocols.

The maximum potential acidity (MPA) of a waste sample is estimated from the total sulphur content. It is assumed that all the sulphur present is available for acid production according to the stoichiometry of pyrite oxidation, allowing easy calculation of the MPA value (Weber, et al., 2004a; Weber, et al., 2004b). The accuracy of the MPA value is thus dependent on the measurement of the total sulphur content. Problems associated with the use of total sulphur and associated assumptions have been discussed extensively (Paktunc, 1999; White III, et al., 1999; Jennings & Dollhopf, 1995). Hedin and Erickson (1988) found that leachate results were more strongly related to the total sulphur content of a sample than the pyritic sulphur. In a study which compared techniques for the determination of total sulphur, Czerewko et al. (2003) suggested thermal decomposition combustion infrared spectrophotometry as a method of choice when dealing with many samples due its reliable results, ease and rapidity. Where sulphur is present as sulphates and organic sulphur, the assumptions that all sulphur is available for acid production and that this production follows pyrite stoichiometry may cause an overestimation of the MPA and thus NAPP value (Kania, 1998). This overestimation of the NAPP value (NAPP = MPA – ANC) led Lapakko (2002) to suggest that classification results using the ABA tests represent a worst case scenario for the formation of acid rock drainage and should be interpreted with caution. Further, we acknowledge that these tests do not consider the relative rates of acidification and neutralisation. In an open system, differing rates affect the neutralisation of acid generation achieved.

In conjunction with the ABA tests, net acid generation (NAG) experiments are used to classify the ARD potentials of ore samples. The NAG test was developed in response to a demand for a rapid field test for ARD characterisation (Coastech Research Inc, 1989). Stewart et al. (2006) suggested that the use both NAPP and NAG methods for sample classification may highlight potential issues in the ANC and MPA estimations and reduce the likelihood of mis-classification of ore samples. Both tests, therefore, are included in ARD characterisation protocols (Verburg, et al., 2009). During the NAG tests, the reaction of ore samples with a 30% H_2O_2 solution allows for simultaneous acid-generation and acid-neutralisation (Adam, et al., 1997). Acid-generation is facilitated through reaction of the sulphide species with the H_2O_2, with the level of neutralisation dependent on the ore composition. Following this reaction, the measurement of the solution pH and its subsequent back titration, firstly to a pH of 4.5 and secondly to pH 7.0, allows for quantification of the equivalent net acid production potential of a sample. Titration to pH 4.5 accounts for the acidity produced from sulphide oxidation while titration to pH 7.0 accounts for the acid generation from the hydrolysis and precipitation of divalent metal ions (Stewart, et al., 2006).

Although the NAPP and NAG tests both aim to quantify the overall acid producing potential of waste samples, Miller et al. (1991a) found that NAG results often yielded much lower values than the corresponding NAPP tests. The authors reported NAG values at approximately two-thirds of the corresponding NAPP values and suggested incomplete oxidation of sulphide minerals as an explanation of the reported inconsistencies (Lapakko & Lawrence, 1993). In fact, Mirza et al. (1992) tested the use of hydrogen peroxide to oxidise sulphide minerals in coal, coal-pyrite and ore-pyrite samples and confirmed incomplete oxidation of the sulphide minerals. Modification of the NAG tests for

use on coal wastes (O'Shay, et al., 1990) demonstrated good sulphide oxidation (97-102%). Results from a similarly modified method, used on mine waste samples, however, showed some discrepancies between the NAPP and NAG results (Lapakko & Lawrence, 1993). The authors suggested that the accuracy was linked to the elevated neutralising potential values due to the incomplete oxidation of ferrous iron released from certain minerals during hydrogen peroxide oxidation. This discrepancy was found to be elevated in samples with a high ANC: MPA ratio (Lapakko & Lawrence, 1993). Irrespective of these limitations, however, the qualitative assessment of waste samples provided by the NAG tests is still useful in waste characterisation, especially in field conditions where quantitative, analytical assessment of the total sulphur content of the samples is difficult (Lapakko & Lawrence, 1993). Miller et al. (1991a) suggested that measurement of the pH of the solution after hydrogen peroxide decomposition was sufficient to provide sample classification as potentially acid forming or not. This idea was used in the formation of the waste characterisation using the ARD Classification Plot (Miller, et al., 1997), where samples are classified by the NAPP value and the solution pH from the NAG test.

2.2.2 Kinetic characterisation tests

Following the initial screening of the potential of waste samples for acid generation, kinetic ARD test are conducted to quantify the rate of generation and quality of the ARD generated. These test results inform the duration of the potential ARD formation, the relative contributions of the acid forming and acid neutralising components and the effectiveness of control measures used to limit sulphide oxidation (Lapakko, 2002). Kinetic ARD techniques range in size from laboratory scale tests to large scale physical dump sites (Blowes, et al., 2003). Laboratory scale chemical tests, such as flask experiments, leach columns and humidity cell experiments, aim to provide kinetic data on ARD generation (Sapsford, et al., 2009; Environment Australia, 1997) by simulating the mineral weathering and ARD formation under exposure to moisture and oxygen.

As a direct extension of a static ARD test, kinetic NAG experiments involve the continuous measurements of the pH and temperature during reaction of the sample with H_2O_2 (Lapakko, 2002). This test aims to provide information on the rate of sulphide mineral oxidation by H_2O_2 as well as the rate of neutralisation of the acid produced. Aside from information regarding the rate of reaction of the sample with H_2O_2, the results from these experiments may, at best, provide worst case scenario data. In addition, this test work is time consuming, with the same limitations as the static NAG experiments (Stewart, et al., 2006). Furthermore, shake flask experiments often necessitate the milling of ore samples and thus do not represent particle sizes of the wastes accurately (Lapakko, 2002). This reduction in particle size, and associated increase in mineral liberation, also leads to an over-estimation of the rate of ARD formation (Mitchell, 2000) and potentially the extent of ARD generation. These rates should thus only be considered on a relative basis for characterisation or to inform modelling for predicting ARD generation (Malmström, et al., 2000).

While shake flask tests require size reduction and the submergence of the waste sample, column experiments allow for the study of ARD generation from larger particle sizes as well as under flow regimes more representative of waste dump conditions (Opitz, et al., 2015). Additionally, kinetic leach column experiments may be conducted to assess independently several factors (Mitchell, 2000) and may be used as a relatively simple method for the assessment of potential remediation options (Environment Australia, 1997; US Environmental Protection Agency, 1994). However, the lack of standard operation procedures (Smart, et al., 2002), in conjunction with the time necessary for the simulation of ARD generation (Lapakko, 2002), is a major disadvantage when compared to the quicker flask characterisation tests.

The most commonly used laboratory-scale, kinetic ARD test for the characterisation of ARD generation is the humidity cell experiment (Caruccio (1968) as cited in Lapakko (2002)). These tests are used to assess relative ARD formation potential between ore samples (Mitchell, 2000) and determine rates of mineral dissolution under moist disposal conditions. The conditions under which humidity cell

experiments are performed include aeration with dry air (3 days), aeration with humid air (3 days), and a water flush to collect the acidity formed and dissolved metal and salt species (ASTM, 2012). The standard method allows for comparison of the ARD characterisation between waste samples analysed in different laboratories; however, this method focuses exclusively on ARD generation under abiotic, water-flushed conditions, and fails to account for ARD generation under the acidic conditions formed once microbial populations are well established with waste rock dumps. Furthermore, the experimental conditions may not be representative of waste rock dumps; the assumption that the waste rock is exposed to moist conditions at all times provides a major source of error for this technique and may lead to an over-estimation in the ARD potential and rate of ARD formation (Ardau, et al., 2009; Lapakko, 2002).

Overall, the major limitation in the use of kinetic experiments for the characterisation of the ARD potentials lie in the time required for accurate assessment (Räisänen, et al., 2010; Villeneuve, et al., 2009; Hesketh, et al., 2010a), often leading to added expense in comparison to static tests as well as their not being available during the decision-making period of developing waste disposal or re-purposing approaches. Reduction in the experimental time, however, precludes accurate representation of field conditions (Lapakko, 2002).

CHAPTER 3: ASSESSMENT OF THE BIOKINETIC ASSAY AS DEVELOPED PREVIOUSLY PAND REFINEMENT OF DATA EVALUATION

3.1 Current Methodology for the Biokinetic Test

Although chemical characterisation tests can be used to inform on ARD generation under abiotic conditions, they fail to provide insight into the role of microorganisms on the rate of ARD generation (Hesketh, et al., 2010a). Further, extended so-called chemical tests often become biotic with time owing to the natural microbial community on the ore surface, thereby influencing results unintentionally and reducing reproducibility. Inclusion of a microbial component to ARD characterisation has previously been suggested by Bruynesteyn and Hackl (1984). This idea was extended to develop the 'version 1' biokinetic test utilising shake flasks experiments on finely ground samples inoculated with micro-organisms implicated in the bioleaching of mineral sulphides (Hesketh, et al., 2010a). These tests aim to focus on the characterisation of the waste rock or tailings sample to provide appropriate kinetic data for ARD prediction.

Current ARD characterisation methods focus on the overall potential for ARD generation or, during kinetic tests, the initial time-frame where oxygen is the primary oxidant. Although kinetic ARD characterisation tests provide information regarding initial pollution generation, this biokinetic test is the first standard laboratory-scale test to account for ARD generation once acidification and microbial colonisation of the mine wastes has occurred. The test has substantial potential. The study of initial ARD generation within natural pH ranges on operation of the biokinetic test at circum-neutral pH is focussed on the Stage I onset of acidification shown in Figure 2-2. The acidified tests focus on the characterisation of stage II ARD generation. These data, in combination with data on mineral liberation and particle size pre-comminution can be used for ARD prediction.

3.1.1 Developing the current method for the UCT biokinetic test

Hesketh et al. (2010a) proposed the use of a refined biokinetic shake flask test using a mixed microbial culture for the characterisation of ARD from tailings samples. The authors found good comparison between the data obtained using static tests and biokinetic shake flask results.

Biokinetic tests were carried out on all waste samples in accordance with the standard batch method described in Hesketh et al. (2010a). In this test, 7.5 g of sample, with a particle size of <150 µm was added to a basal salts medium (ABS) at pH 2.0, prior to inoculation with an active, mixed microbial bioleaching culture. The prepared flasks are subsequently maintained at 37^{o}C on an orbital shaker at 150 rpm for a period of approximately 90 days.

3.1.2 Microorganisms used in biokinetic tests

For best applicability of this test, the indigenous microorganisms on the waste rock form the best inoculum; however, it is not practicable to generate a tailored inoculum for each rock sample in the preliminary testing. To ensure the establishment of an effective microbial environment, the inoculum used contains both a strong iron-oxidiser and a strong sulphur oxidiser. While these are used as the dominant microbes to ensure that consistent microbial loads can be used, these are intentionally not selected from pure cultures to ensure a range of other microbial species, in addition to the indigenous microbial community, that can contribute to the microbial colonisation, as is appropriate for the specific waste rock. An inoculum, made up of a 1:1 ratio of a *Leptospirillum ferriphilum* dominated culture and an *Acidithiobacillus caldus* dominated culture, both grown on pyrite at 37°C, was used. The presence of other iron- and sulphur oxidising micro-organisms is noted and contributes to inoculum robustness (Smart, et al., 2018). Direct microscopic cell counts of the inoculum were used to calculate the inoculum volume required.

3.1.3 Biokinetic test procedure

Batch biokinetic tests without pH control were carried out using a refined protocol developed from our preceding studies. For each biokinetic test, 150 mL ABS solution at pH 2.0 was added to 7.5 g of waste rock material, milled to less than 150 µm, in a 500 ml flask. To achieve the size fraction <150 µm, the sample was milled, screened using a 150 µm mesh and that fraction not passing through the mesh re-milled and re-screened. Tests were inoculated with 10^9 cells from the prepared inoculum to achieve a final microbial concentration of 6.67 x 10^6 cells/mL. Un-inoculated controls were included for each test. Flasks were incubated at 37°C and 150 rpm for the duration of the test, typically 90 days. The biokinetic test flasks were compensated for evaporation daily by the addition of acidified water to correct for volume loss by weight, prior to sampling. In the pH controlled tests, pH was corrected to pH 2.0 daily. For the batch tests, analytical measurements of pH and redox potential were performed within flasks and a small sample volume withdrawn for iron and sulphate assay. All physicochemical tests were conducted in triplicate, using triplicate flasks for each test condition.

3.1.4 Analytical methods

The pH was recorded using a 713 Metrohm pH meter while the redox potential was measured using a 703 Metrohm Eh meter and an Ag/AgCl reference electrode. The modified 1-10 phenanthroline method was used to measure ferrous iron (Komadel and Stucki, 1988) and total iron, the latter following conversion of ferric to ferrous iron by addition of hydroxylammonium chloride. The sulfate concentration was determined using the $BaCl_2$ turbidity method (APHA, 1998).

3.2 Characterising the Acid-generating Potential of Mine Wastes using the Laboratory Scale Biokinetic Test

3.2.1 Introduction to application of the biokinetic test

This section explores the application of a novel biokinetic test (Hesketh, et al., 2010a), in combination with conventional static chemical tests, for the rapid and effective characterisation of the acid generating potential of a number of mine wastes from the processing of both hardrock ores and coal.

Chemical static and biokinetic shake flask tests were carried out on the following mine waste samples:

- *Untreated copper sulphide tailings:* Sample represented typical tailings from the flotation of porphyry-type copper sulphide ores, with the sulphide minerals comprising mainly pyrite (~7% by mass) and minor quantities of chalcopyrite (~0.5% by mass) (Hesketh, et al., 2010b).
- *Desulphurised copper sulphide tailings*: Sample prepared from the untreated copper sulphide tailings in a two-stage batch desulphurisation flotation process, as described in Hesketh et al. (2010b).
- *Copper sulphide waste rock: S*ample of waste rock prepared from a blend of low-grade porphyry copper sulphide and complex base-metal sulphide ores. The sulphide minerals comprised mainly pyrite (~2.6%) and no carbonate minerals were detected by XRD (Opitz, 2013).
- *Nickel-pyrrhotite flotation tailings: S*ample prepared from a low-grade nickel sulphide (pentlandite) ore in a laboratory-scale batch flotation cell (Chimbganda, et al., 2013). Pyrrhotite was identified as the major sulphide mineral and calcite as the major carbonate. The ore also contained relatively reactive silicate minerals, such as olivine (~4%).
- *Gold tailings*: Sample prepared through the crushing and screening of a Witwatersrand gold ore. Mineralogical analysis indicated that pyrite is the major sulphide mineral (~1%) and calcite the major carbonate mineral (Dyantyi, et al., 2013).
- *Coal waste slurry:* Two samples of fresh ultra-fine thickener underflow procured from two different coal processing plants in the Middelburg area, South Africa. Sample One was screened into various size fractions, prior to further test work (Kotelo, 2013). The coal slurry samples contained

25-40% ash-forming minerals, comprising mainly quartz and kaolinite with minor quantities (<5%) of pyrite, calcite, dolomite and sulphate minerals (Kotelo, 2013; Amaral Filho, 2012).

- *Untreated coal discard:* Sample generated at a South African power station, through the destoning of a low-grade coal by means of an experimental X-ray sorter. The discard had an ash content of 56.4% (Amaral Filho, 2012).
- *Desulphurised coal discard:* Sample prepared from the untreated coal discard sample in a two-stage flotation process as described by Kazadi Mbamba et al. (2012), using oleic acid to recover coal in the first-stage float and xanthate to remove sulphide minerals in the second flotation stage. The desulphurised tailings comprised 36% of the feed discards and had an ash content of 82.4% (Amaral Filho, 2012).

Static tests were conducted on all samples using both the ABA and NAG test methodologies. The ABA test was used to report the net acid producing potential (NAPP), measured as the balance between the maximum potential acidity (MPA) and the acid neutralising capacity (ANC). The MPA was based on the total LECO sulphur concentration in the case of the wastes from the processing of hard-rock ores, and the sulphide sulphur content (as determined by the standard ISO 157: 1996 method) in the case of coal wastes. ANC was determined empirically in accordance with the method proposed by Skousen et al. (Skousen, et al., 1977). NAG tests were conducted according to the method described by Smart et al. (2002). This method measures the acid forming potential, by allowing both the acid-forming and neutralising reactions to occur simultaneously using H_2O_2 as an oxidant. The waste samples were subsequently classified using a slightly modified version of the combined ABA/NAG classification system, proposed by Smart et al. (2002). In the modified classification plot, samples with a NAG pH of <4.5 and NAPP values of more than 20 are classified as acid forming, those with NAG pH values < 4.5 and NAPP values of between -20 and 20 are potentially acid forming, and those with NAG pH values > 4.5 and NAPP values of <0 are non-acid forming. Where results of the ABA and NAG tests contradict each other, the classification of samples is considered to be uncertain.

Biokinetic tests were carried out on all waste samples using the standard batch method described in Hesketh et al. (2010a) and detailed in Section 3.1. In order to better present an open flow-through system, a un-optimised dynamic (semi-continuous) version of the standard batch biokinetic test was also carried out on selected samples (coal waste slurry, with reference to coal (Kotelo, 2013)) under circum-neutral pH conditions. In these tests, the initial pH of the basal salts medium was adjusted to a value of 6 prior to the introduction of the waste sample. This was followed by intermittent removal and replacement of 90% of the supernatant during the course of the shake flask test. The draw-and-fill semi-continuous method was developed rigorously in a later part of this study and is reported in Chapter 6.

3.2.2 Comparative characterisation test results

Static test results for the wastes from the processing of hardrock ores (Table 3-1 and Figure 3-1) indicate that the untreated sulphide tailings and waste rock samples investigated are all classified as acid generating. The low-sulphur copper tailings sample, generated through the desulphurisation flotation of the copper sulphide tailings, is classified as non-acid forming.

Table 3-1 Static ARD results, summarised for wastes from hard-rock processing

Waste description	Total S (%)	ANC (kg/t H_2SO_4)	NAPP (kg/t H_2SO_4)	NAG pH
Untreated copper sulphide tailings	3.84	23.2	94.8	2.57
Desulphurised copper sulphide tailings	0.21	28.7	-22.3	5.71
Copper sulphide waste rock	3.39	3.39	92.8	2.63
Nickel-pyrrhotite flotation tailings	3.59	89.4	20.3	3.19
Gold tailings	1.41	16.5	24.9	2.51

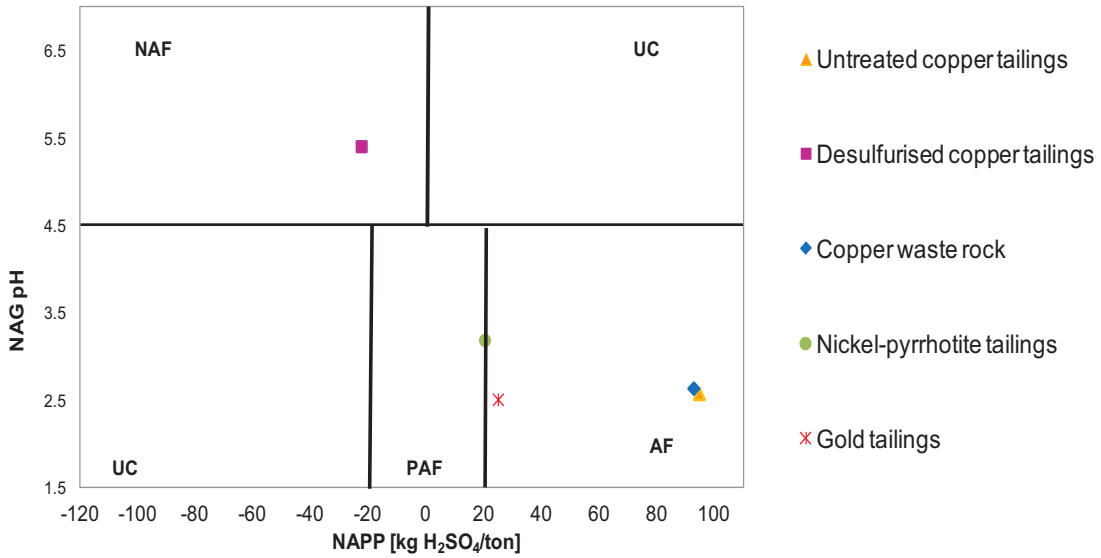

Figure 3-1 Static ARD classification plot for wastes from hard-rock processing
(NAF: non-acid forming, UC: uncertain, PAF: potentially acid forming and AF: acid forming)

The results of standard batch biokinetic tests, given in Figure 3-2, yielded results consistent with the static tests in terms of classification, i.e. all untreated mine waste samples tested were net acid generating, under conditions of microbial activity, whilst removal of the sulphide by means of flotation effectively removed the long-term ARD risk.

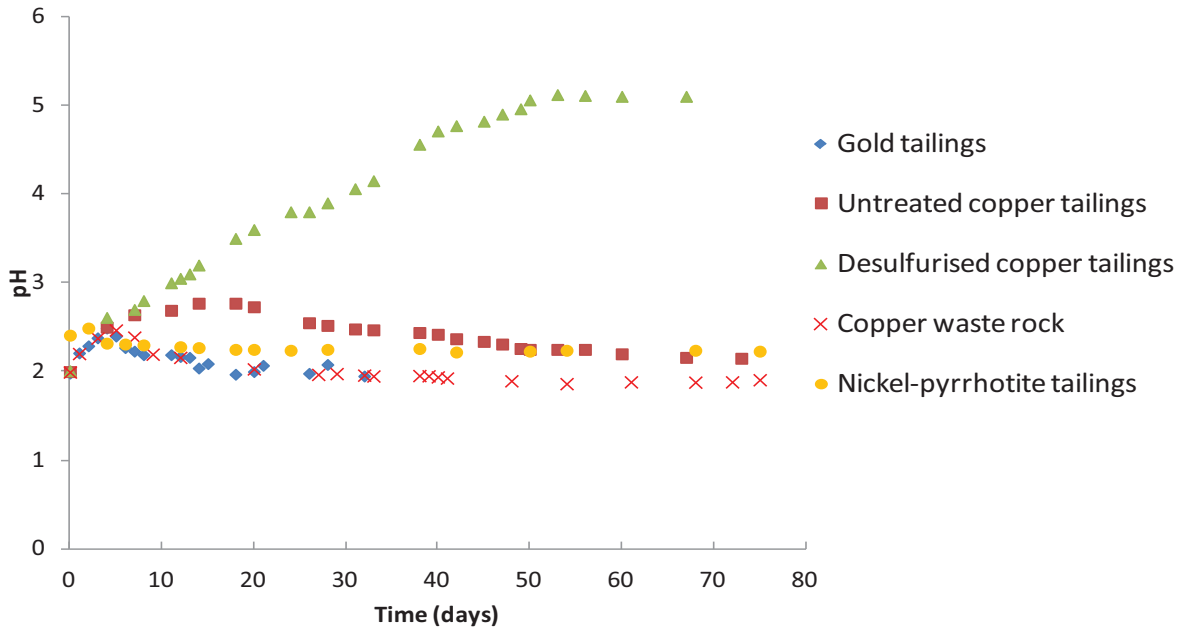

Figure 3-2 Batch biokinetic test results for wastes from the processing of hard-rock ores

The biokinetic test results also show that, in the hard rock waste samples studied, the acid neutralising reactions occur more rapidly than pyrite oxidation, with the pyrite-bearing wastes becoming net acid consuming as the acidification rate exceeds the neutralisation rate. The difference in the time-frame of acid generation and neutralisation and its impact on the quality of the effluent from waste rock dumps

has been demonstrated in the column studies of Opitz (2013) and reported in Harrison et al. (2010), highlighting the importance of the kinetic information provided through the laboratory-scale biokinetic test but not through the static tests. For the waste ores studied, this neutralising capacity was, however, generally short-lived in the acidic environment (<15 days) for those wastes that had not been desulphurised, and the acidification observed in the biokinetic tests thus ultimately exceeded that predicted by the static tests (final biokinetic pH values are lower than the NAG pH values). This is particularly the case for the pyrrhotite-bearing nickel sulphide tailings which, despite the relatively high ANC, exhibited acid generating behaviour after the first day. This can be attributed to the relatively rapid kinetics of pyrrhotite oxidation in comparison to that of pyrite (Janzen, et al., 2000).

Static test results for the coal waste samples (Table 3-2 and Figure 3-3) indicate that the untreated coal discards are acid forming, the coal waste slurry 1 potentially acid forming, and the coal waste slurry 2 and the desulphurised coal discards both non-acid forming.

Table 3-2 Summary of static ARD test results for coal processing wastes

Waste description	Total S (%)	S^{2-} (%)	ANC (kg/t H_2SO_4)	NAPP (kg/t H_2SO_4)	NAG pH
Coal waste slurry 1: -75 µm	2.08	1.00	27.7	2.9	2.50
Coal waste slurry 1: +212-315 µm	1.03	0.64	28.2	-8.6	2.97
Coal waste slurry 2	0.82	0.50	131.9	-116.6	5.20
Untreated coal discards	5.11	3.30	55.6	101.0	2.20
Desulphurised coal discards	0.21	n/d	76.7	-70.6	5.90

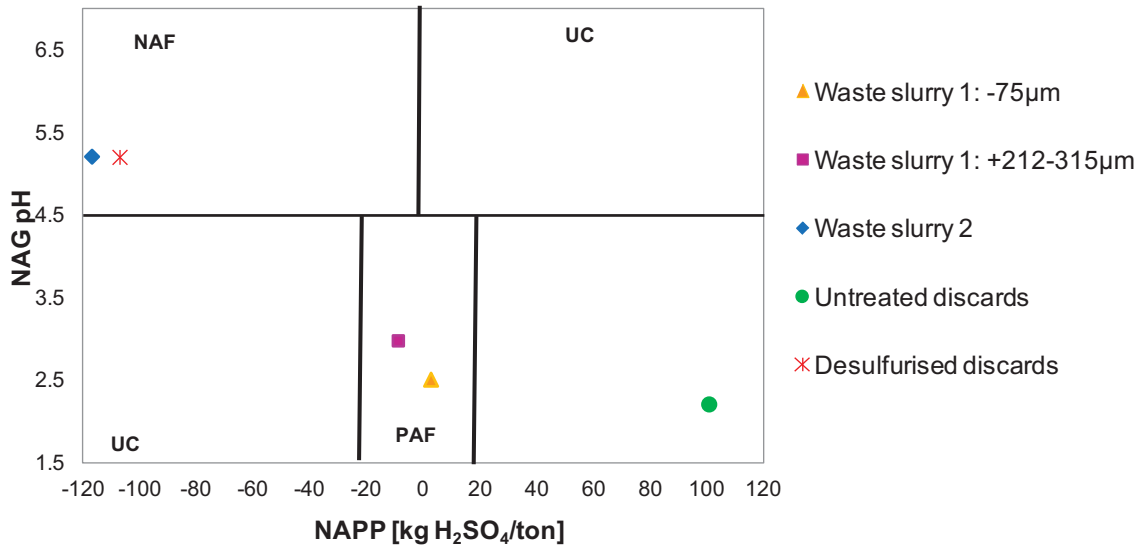

Figure 3-3 Static ARD classification plot for the coal processing wastes

In accordance with Miller (2008), the standard NAG test may overestimate the acid generating potential of samples with relatively low acid generating potential (i.e. those falling in the PAF region of the graph), due to organic acid effects. However, biokinetic tests (Figure 3-4) confirmed that samples classified as either acid forming or *potentially* acid forming on the basis of static chemical tests are also acid forming under conditions of microbial colonisation. In agreement with the static chemical tests, biokinetic tests indicate that coal waste slurry 2 and the desulphurised coal discards are both non-acid generating over the duration of the test. A comparison of the leach behaviour of the -75 µm fraction of coal slurry waste 1 under biotic and abiotic conditions confirms, furthermore, that microbial activity plays a significant role

in acid generating behaviour. As in the case of the wastes from hard-rock ore processing, the biokinetic test results indicate that, although the samples classified as PAF and AF are initially acid consuming, this acid neutralising capacity is consumed relatively rapidly. This is of relevance when considering a tailings deposit where soluble neutralising capacity is transported away from the waste material, hence not available to neutralise acid generated through the oxidation of pyrite over the longer term.

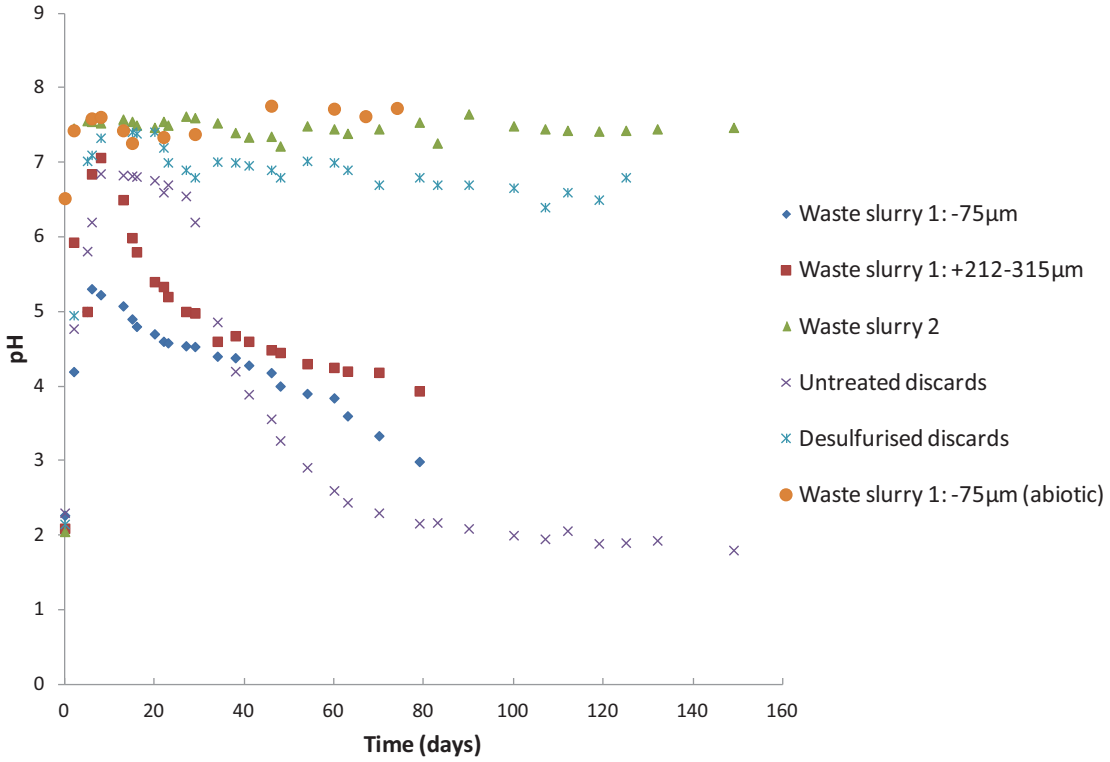

Figure 3-4 Batch biokinetic test results for wastes from coal processing

Dynamic biokinetic leach tests on the two size fractions of coal waste slurry 1 (Figure 3-5) confirm that these samples eventually become net acid generating under conditions of microbial colonisation in a semi-continuous flow scenario, even when using a leach solution with a relatively mild circum-neutral pH, i.e. pH 6. Mineralogical analysis of the leach residues indicated incomplete oxidation of pyrite over the 87 day biokinetic test period, particularly in the case of the coarser size fraction.

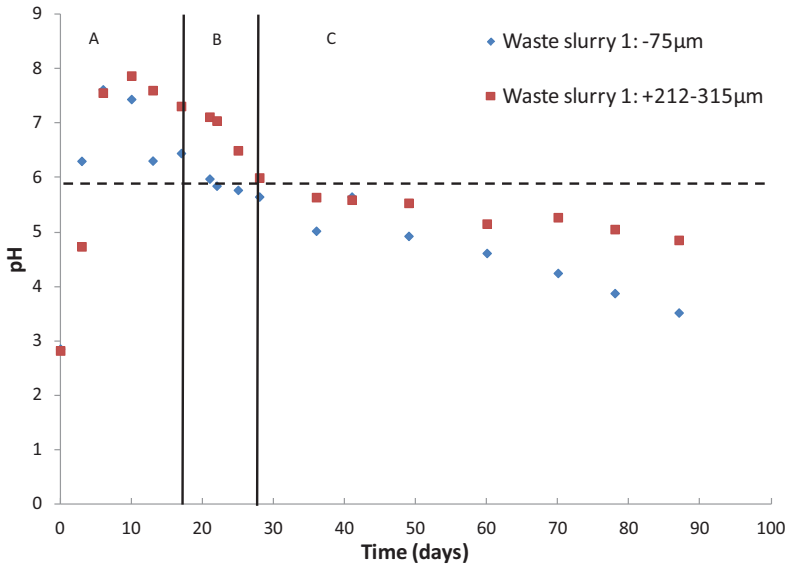

Figure 3-5 Dynamic biokinetic test results for wastes from coal processing at circum-neutral pH conditions (where A, B and C correspond to supernatant replacement intervals of 3, 8 and 14 days respectively)

3.3 Detailed Discussion of Selected Case Studies Using the Laboratory-scale Biokinetic Assay

3.3.1 A copper sulphide tailings desulphurisation case study

The first case study entails the pre-disposal treatment of conventional tailings by means of a two-stage desulphurisation flotation process for removal of sulphide minerals (Hesketh, et al., 2010b). This process resulted in three output streams: a value-rich concentrate which could be fed back to the main metal recovery plant, a small volume pyrite rich waste and a large volume fraction, containing the majority of the gangue minerals (Figure 3-6).

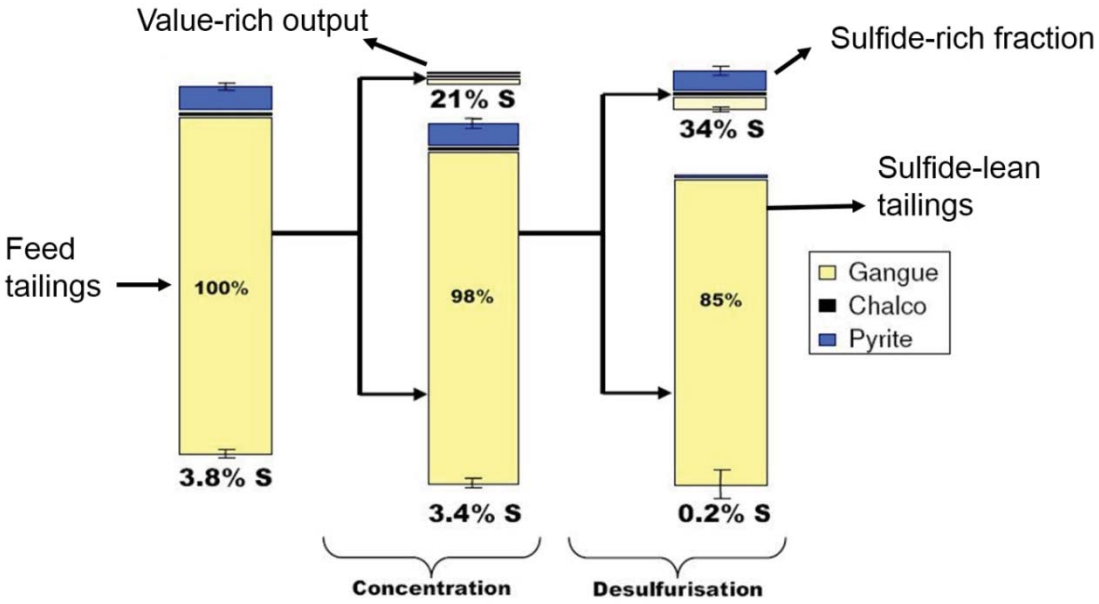

Figure 3-6 Two-stage desulphurisation flotation of a copper sulphide tailings sample (Hesketh, et al., 2010b)

ARD characterisation tests, as described in Section 3.1 and Section 3.2, were carried out on the feed (untreated) and sulphide-lean (desulphurised) tailings, to establish the effectiveness of the desulphurisation process in terms of reducing ARD risks. Results of the conventional Acid Base Accounting (ABA) tests for the untreated and desulphurised tailings are superimposed on the plot of acid neutralising capacity (ANC) as a function of total sulphur classification in Figure 3-7. These results indicate that, although the untreated and desulphurised tailings samples have similar acid neutralising capacities, the relatively high sulphide content of the tailings before desulphurisation resulted in it being classified as acid forming, whilst the sample after desulphurisation by flotation can be classified as non-acid forming.

As shown in Figure 3-8, NAG test results confirmed those of the ABA tests with the untreated tailings sample (before desulphurisation) falling into the acid forming region, and the desulphurised sample into the non-acid forming region, of the combined NAG/ABA classification plot.

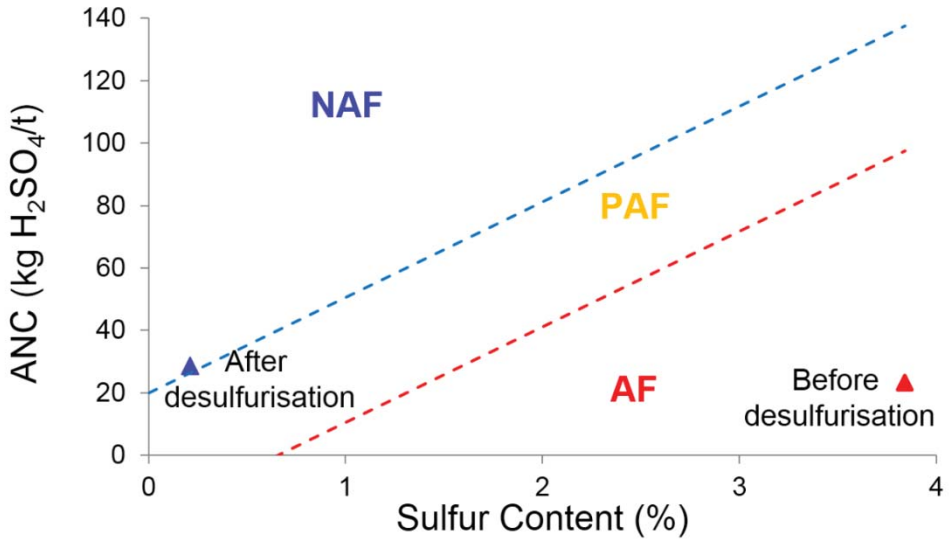

Figure 3-7 ABA test results for the untreated and desulphurised copper sulphide tailings. Where AF is acid forming, PAF is potentially acid forming and NAF is non-acid forming.

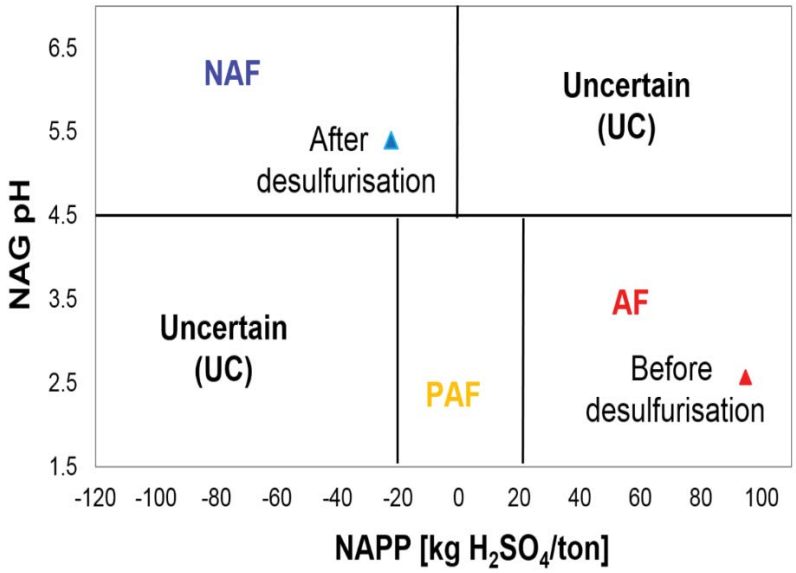

Figure 3-8 Combined NAG/ABA classification plot for the copper sulphide tailings sample, before and after desulphurisation. (AF is acid forming, PAF is potentially acid forming and NAF is non-acid forming).

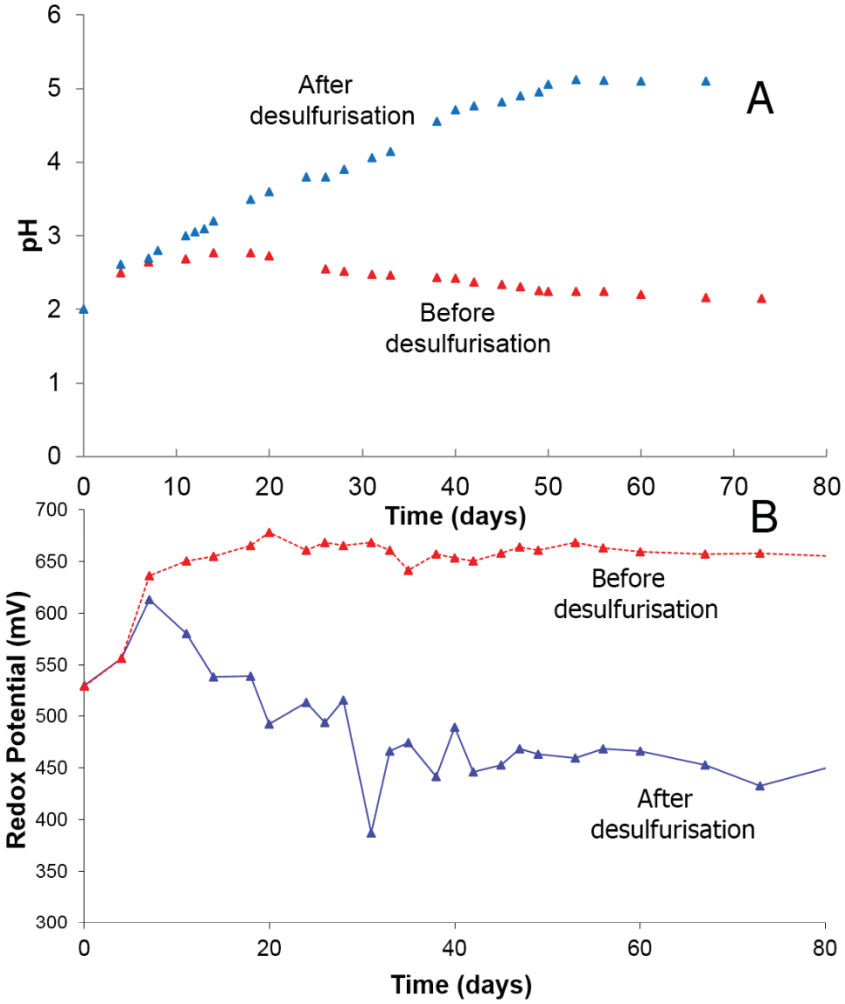

Figure 3-9 Biokinetic test results for the untreated (red markers) and desulphurised (blue markers) copper sulphide tailings.

The time-related changes in pH and redox potential under biokinetic test results are presented in Figure 3-9A and B respectively. Initially both the untreated and desulphurised tailings gave rise to an increase in pH, which is consistent with acid leaching of gangue material. For the desulphurised tailings sample (represented by the blue markers), this trend continued for approximately 2 months, indicating that the sample remains net acid neutralising during this phase. Thereafter the pH stabilised at a value of just over pH 5. In contrast, pH values for the untreated tailings with the higher sulphide content peaked at 12 days and then declined steadily until day 70, indicating that the sample remained net acid generating over this period. The high redox potentials obtained for the untreated tailings sample were, furthermore, consistent with microbially mediated oxidation of pyrite through the microbial oxidation of ferrous iron in solution to ferric iron which subsequently acts as a leach agent of pyrite and other base metal sulphides present. Conversely, the low redox potentials for the desulphurised samples were indicative of the absence of any significant microbial activity.

3.3.2 A comparative case study on copper sulphide tailings and waste rock

A comparison of the results of static tests, described in Section 3.2 for the untreated copper sulphide tailings and copper waste rock samples (Opitz, 2013), indicate that these two samples had similar NAPP and NAG pH values, and hence occur at a similar location in the acid forming region of the combined ABA/NAG classification plot (Figure 3-10).

The classification graph of ANC as a function of total sulphur, shown in Figure 3-11, based on ABA test results, indicates, however, that the copper waste rock sample has a slightly lower total sulphur and significantly lower ANC content than the tailings sample.

These differences were reflected by the results of the biokinetic tests, conducted according to the method outlined in Section 3.1 and are shown in terms of pH as a function of time in Figure 3-12. While both samples exhibit acid neutralising behaviour in the initial leach stages, the lag period before onset of acid generation is much shorter, and the rate of subsequent acid generation is faster in the case of the waste rock sample with the lower acid neutralising capacity.

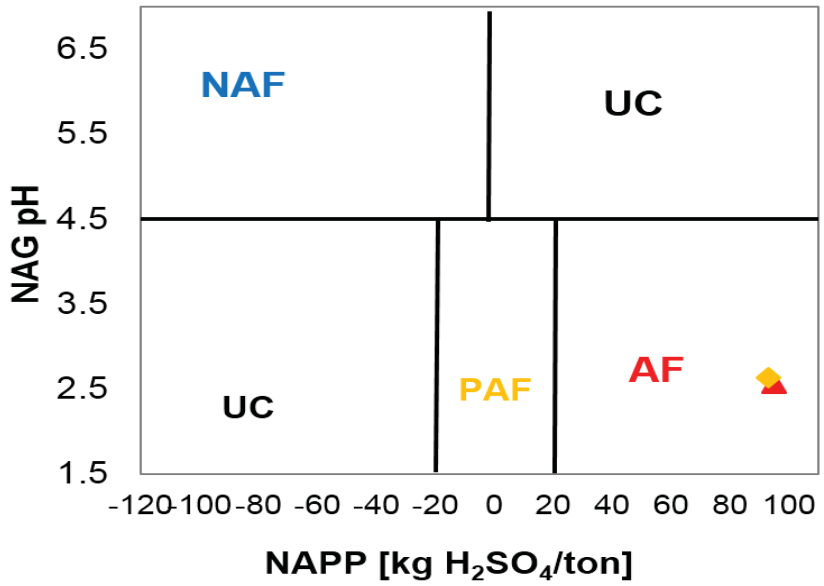

Figure 3-10 Combined NAG/ABA classification plot for the untreated copper sulphide tailings and waste rock samples. (AF is acid forming, PAF is potentially acid forming and NAF is non-acid forming).

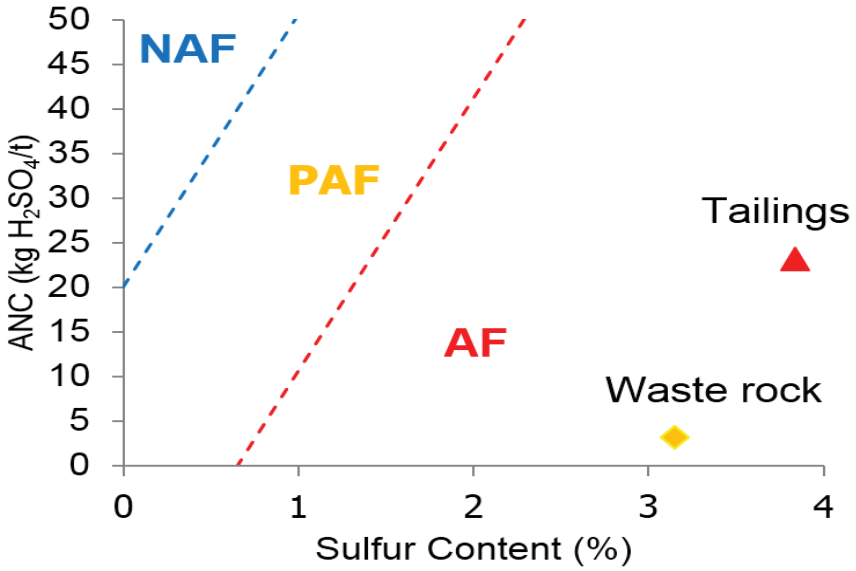

Figure 3-11 ABA test results for the untreated copper sulphide tailings and waste rock samples. (AF is acid forming, PAF is potentially acid forming and NAF is non-acid forming).

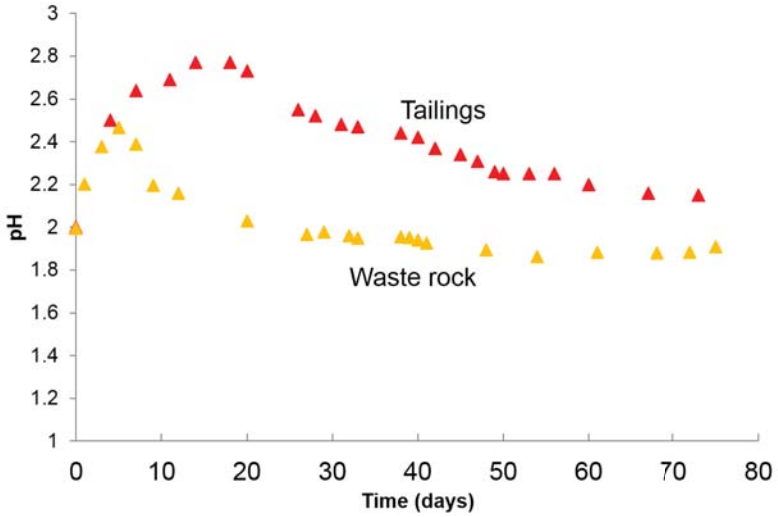

Figure 3-12 Biokinetic test results for the untreated copper sulphide tailings and waste rock samples

3.3.3 A coarse coal waste desulphurisation case study

The concept of the removal of sulphide from base metal wastes pre-disposal was extended to the coal sector, with the investigation of a two-stage flotation process for the simultaneous recovery of coal (in stage 1) and removal of sulphide (in stage 2) from pulverised coal discard, as presented diagrammatically in Figure 3-13 (Amaral Filho, 2012).

Comparative ARD characterisation tests were carried out on the feed and desulphurised discards, in order to assess the effectiveness of the desulphurisation process in terms of removing ARD risks. As in the case of the copper sulphide tailings, the static ARD tests inidcate desulphurisation flotation of coal discards results in a drastic reduction in sulphide concentration, effectively changing the characteristics of the sample from acid forming to non-acid forming (Figure 3-14).

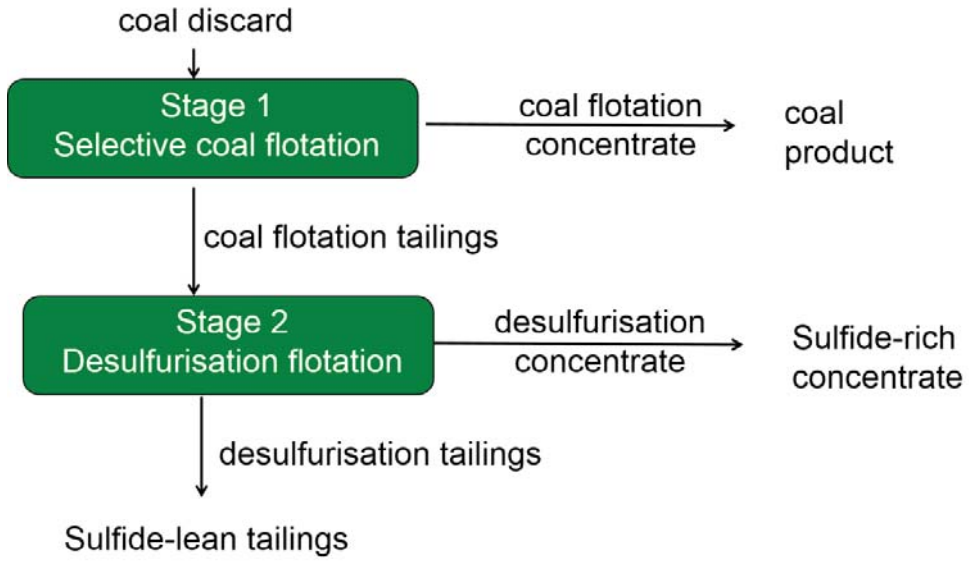

Figure 3-13 Two-stage flotation process for the recovery of coal and removal of sulphide sulphur from coal wastes.

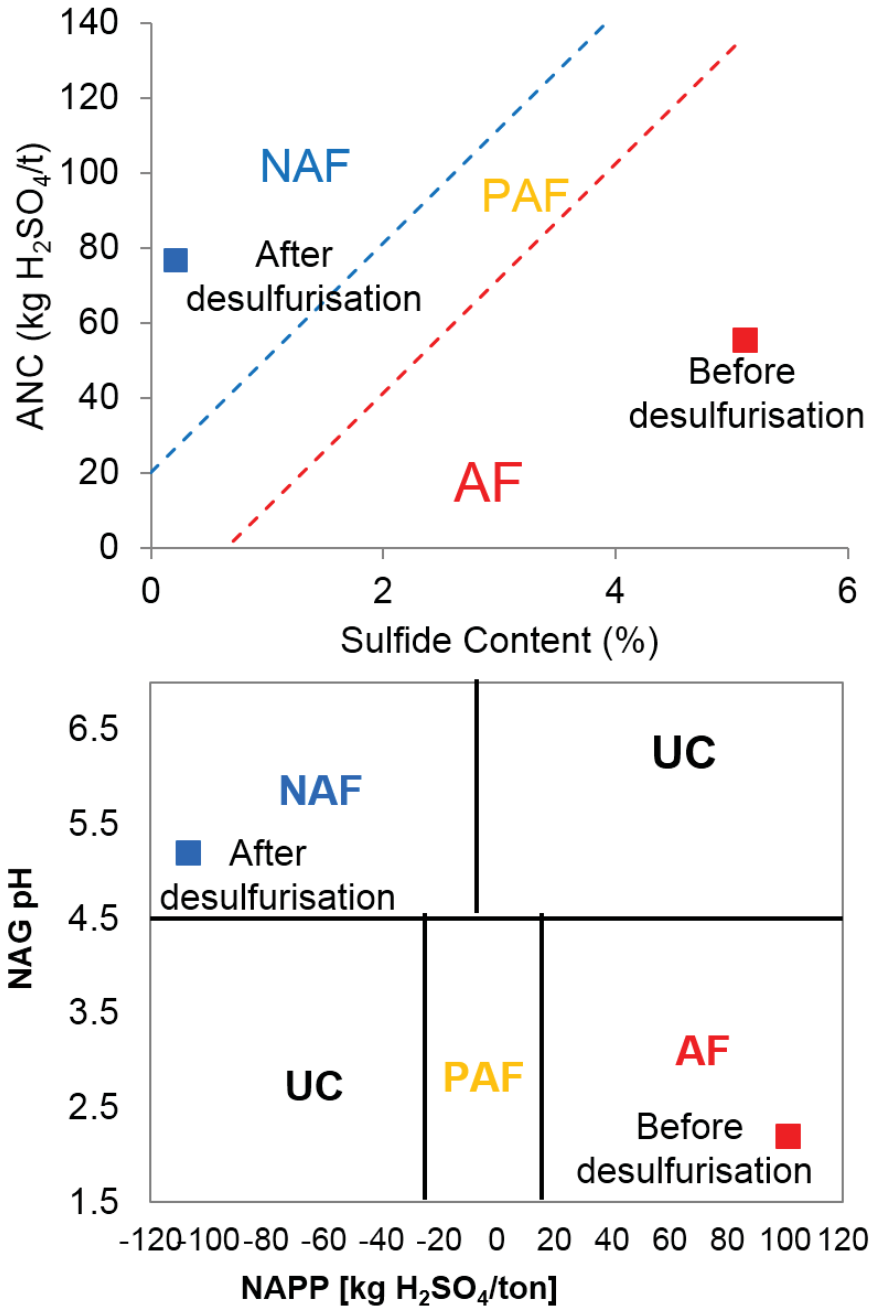

Figure 3-14 Static tests results for the coal discard sample before and after desulphurisation flotation. (AF is acid forming, PAF is potentially acid forming and NAF is non-acid forming).

Having conducted the shake flask biokinetic assay according to Section 3.1, the biokinetic pH values are given as a function of leach time in Figure 3-15B. This shows an increase in initial pH for both the untreated and desulphurised discard sample which can be attributed to dissolution of acid-neutralising reactive gangue minerals such as carbonates. The relatively high initial pH values in comparison to the copper sulphide waste samples (see previous sub-sections) are consistent with the higher concentration of acid neutralising minerals and corresponding ANC values. Despite the high acid neutralising capacity of the untreated discard sample, the initial net acid neutralising phase is followed by a relatively sharp decline in pH as the reactive acid neutralising minerals become depleted and the acid forming sulphide oxidation reactions become dominant. The onset of microbially catalysed oxidation of pyrite oxidation is demonstrated by the sudden increase in redox potential for the untreated sample after day 30, shown in Figure 3-15A and attributable to microbially catalysed Fe^{2+} oxidation. In the case of the desulphurised discards, however, the pH values remained elevated and the redox

potentials low throughout the leach period, consistent with the non-acid generating classification of this sample.

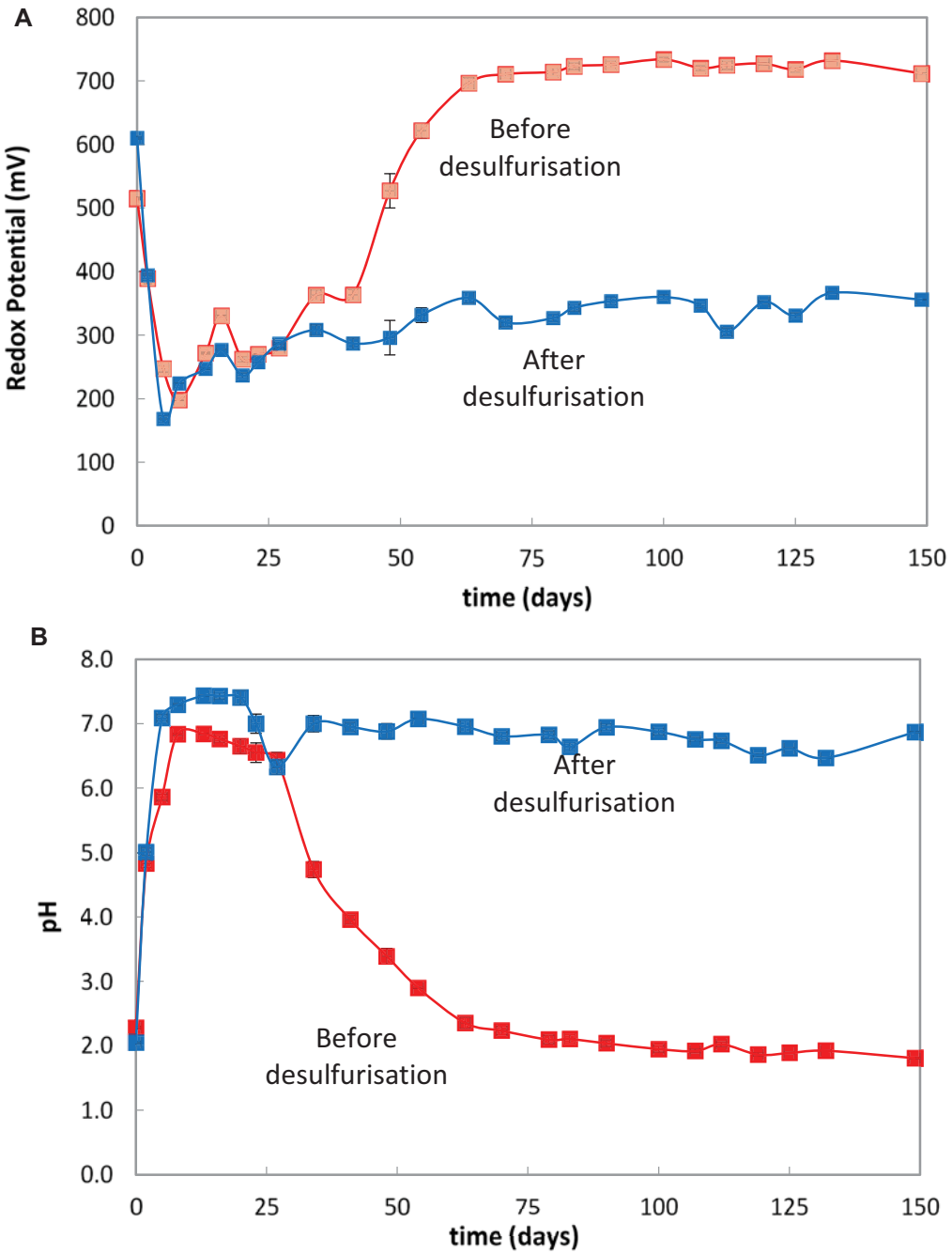

Figure 3-15 Biokinetic test results for the coal discard samples before (red symbols) and after (blue symbols) desulphurisation by flotation

3.3.4 An ultra-fine coal waste study

As indicated in Figure 3-16, static tests on a sample of ultra-fine coal waste (-75 µm) investigated by Kotelo (2013) were somewhat inconclusive, with both the ABA and NAG tests indicating this sample to be potentially acid forming.

Three different biokinetic tests were carried out on this sample, namely a standard batch test, an abiotic test without inoculation and a dynamic biokinetic test. In the dynamic test, conducted under semi-

continuous leach conditions, 90% of the supernatant was replaced with fresh basal salt solution, the pH of which was first adjusted to pH 6. Initially this solution was replaced every three days, then later every 8 days and finally every 14 days (Figure 3-17).

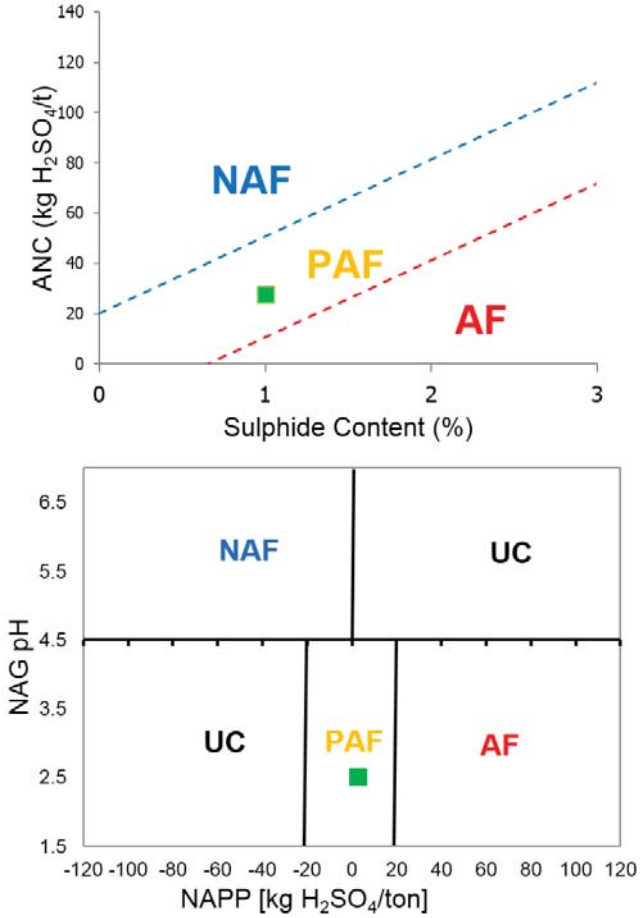

Figure 3-16 Static test results on a sample of ultra-fine coal waste. (AF is acid forming, PAF is potentially acid forming and NAF is non-acid forming).

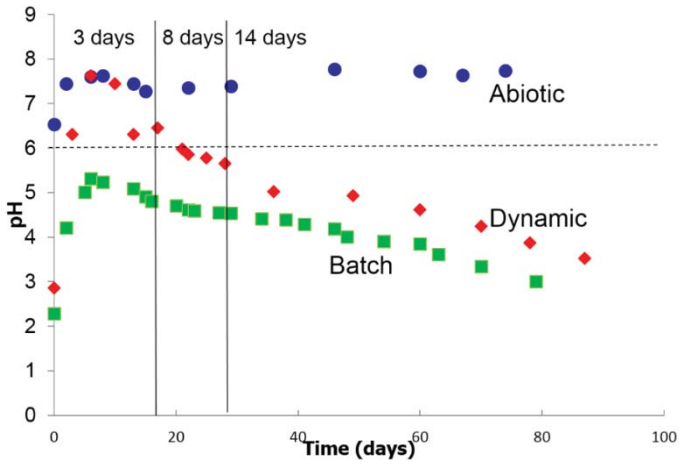

Figure 3-17 The pH data collected as a function of time for the laboratory-scale biokinetic test on an ultrafine coal waste under abiotic (blue), batch microbial (green) and dynamic microbial (red) conditions. The time period for replacement of 90% supernatant with solution at pH 6.0 in the dynamic test is indicated above the graph.

As shown in the earlier biokinetic tests, an initial increase in pH was observed for all biokinetic tests due to rapid acid dissolution of carbonates. In the inoculated tests, this is followed by a gradual decrease in pH as reactive acid neutralising minerals became depleted and the acid generating sulphide oxidation reactions became dominant. The dynamic tests indicated that replacement of the supernatant with circumneutral solution resulted in a higher initial pH owing to the regular removal of acidity. However, after the 3rd replacement, the pH started to decrease fairly rapidly, with the sample becoming net acid generating (acidifying the circumneutral leach solution) within 20 days. The net acid generating behaviour under circum-neutral pH conditions is unexpected, given these conditions are generally not considered to be optimal for ferrous iron and sulphur oxidising micro-organisms implicated in generating the ferric and acid leach agents for oxidation of pyrite and other base metal sulphides. These data provide some support for the postulation of strong surface attachment and the robust nature of the micro-organisms as well as the presence of a range of microbial species tolerating differing pH conditions but contributing to acidification. The pH-time trends for the inoculated tests indicate, furthermore, that the pH had not yet stabilised at the termination of the biokinetic tests (76-80 days), indicating that pyrite oxidation and, consequently, ongoing associated acid generation was incomplete. This was supported by mineralogical analysis of the biokinetic leach residue from the dynamic leach tests, which showed the presence of residual sulphide (Kotelo, 2013). Mineralogical analysis also indicated that the reactive neutralising minerals (i.e. calcite and dolomite) had been depleted, whilst weathering of the silicate minerals (i.e. kaolinite and quartz) appeared to be negligible.

Comparison of biotic and abiotic test results clearly indicated the crucial role that microbial activity plays in the generation of ARD from coal wastes, with the abiotic sample remaining essentially non-acid generating in the absence of microbial colonisation.

3.3.5 Summary of initial findings of the biokinetic test

While the biokinetic test results are consistent with the static tests in general, the biokinetic tests provide additional information. Firstly, the relative onset of neutralisation and acidification is observed, giving preliminary kinetic data on these. The role of endemically-occurring micro-organisms in speeding up ARD formation is shown. Data of the nature summarised has previously been gleaned from humidity cell or column tests with more rapid observation here. These tests, however, also require finely milled sample, thus limiting direct prediction results and rather providing characterisation of ARD potential.

The batch nature of the first version of the biokinetic test is similar to the static test in giving the final net acid formation. By expanding the test to an open system, the washout of neutralisation capacity can better mimic the real world system.

3.4 Conclusions with respect to the Biokinetic Assay

This study has demonstrated that the biokinetic test can be used to both validate and enhance the results of simple static tests. It can be used to provide additional insight where inconclusive results are obtained from the combined analysis of NAPP and NAG results, as proposed by Smart et al. (2002). Further it can provide valuable additional information on the effect of microbial activity on the potential for ARD formation. This laboratory-scale test can provide relative kinetics of the acid forming and neutralising reactions under stagnant and dynamic flow conditions. Such information provides a measure of the potential for conditions that promote bioleaching to be established. Further, it provides data that can potentially be used for the prediction of ARD formation through simulation modelling as described by Simunika et al. (2013). Ultimately, it has potential to assist in the implementation of waste management strategies that are effective in both the short and long-term. The advantages of the biokinetic test over other conventional kinetic tests include its relatively simple and inexpensive methodology. The biokinetic test also delivers meaningful results pertaining to the long-term ARD generating potential of both fine and coarse wastes in a relatively short period of time (< 3 months for wastes from hard-rock ore processing, and 4-5 months for coal processing wastes).

To date, such systems have not been used routinely for the characterisation of ARD potential from waste rock due to the perceived limitations placed on the reaction conditions necessary for active microbial growth. As with the static tests, questions exist around the representative nature of the particle sizes used. Furthermore, concerns have been expressed around the relevance of the laboratory microbial communities compared to those found in natural ARD environments (Mitchell, 2000); these were alluded to in Section 3.1.2 and are investigated in CHAPTER 6:. No standard method has previously been put forward for the characterisation of microbially-mediated ARD generation from waste rock. From the studies summarised in this chapter, it is clear that, while baseline standard conditions will be sought, variation will be required in response to the waste mineral type and this should be recognised, with guidelines provided, to inform the tailoring of the test to the waste mineral studied.

CHAPTER 4: CHARACTERISING WATER-RELATED ENVIRONMENTAL IMPACTS ASSOCIATED WITH COAL AND GOLD MINE WASTES: DE-SULPHURISATION, ACIDIFICATION AND METAL DEPORTMENT

The extraction of metals from ores generates large amounts of waste material through both mining and mineral processing practice. The environmental effects arising from the disposal of such wastes are far reaching and long-term (Koehnken, et al., 2003), with formation of water pollution originating from the runoff of mine waste disposal sites being a major polluting factor. For sulphide-bearing wastes, the generation of acid rock drainage (ARD) is of particular concern. Characterised by low pH values, the highly acidic nature of the solution results in the mobilisation of deleterious elements contained within the mine waste (Nordstrom, 2011).

ARD poses a major environmental concern for the mining of both hard-rock and coal. ARD is formed from the oxidation of sulphide minerals within mining wastes in the presence of oxygen and water. Mineral sulphide oxidation is further accelerated in the presence of naturally-occurring iron- and sulphur-oxidising micro-organisms. The acidic drainage resulting from these reactions, in addition to affecting the surrounding environments adversely due to the low pH and high salinity, promotes the deportment of metal species from the mineral wastes. These are transported into local aquifers, where the elevated metal concentrations may cause significant environmental damage.

In this chapter, we consider the acidification through ARD generation from coal wastes and the potential to mitigate this through desulphurisation in Section 4.1. We extend this to consider the impact of conditions to which the coal waste material is exposed on potential for metal deportment in Section 4.2. In Section 4.3, we explore the equivalent studies on sulphidic waste materials from the gold-mining sector.

4.1 Processing Waste from the Coal Mining Sector: Desulphurisation as a Route to Minimise Acidification

In South Africa, ARD generation is of particular concern to the coal mining industry, where the majority of the mineral sulphides exist as pyrite mineral. Other associated sulphide mineral species, however, include galena (PbS), sphalerite (ZnS) and chalcocite (Cu_2S), amongst others. In addition to the potential for these associated cations to be released as a result of sulphide mineral oxidation, other mineral phases within coal wastes may pose significant environmental risks as a result of mobilisation of metal cations. Major metals such as Al, K, Mg and Fe have been found to occur in coal wastes, which, whilst having a low toxicity limit, may accumulate within local environments to concentrations above the accepted toxicity limits. Additionally, the presence of metals with high toxicity often exist in the waste dumps and slimes dams. Metals such as V, Cu, Cr, As, Pb, U, Co, Th and, particularly, Cd, Sb, Se, Mo and Hg are found in coal wastes in concentrations which pose significant risks to the environment. Commonly determined trace metal concentrations are presented in Table 4-1.

Table 4-1 Concentrations of trace metals typically found in South African ROM coals as compared to the global average (after Bergh et al. (2013))

Coal Deposit	Metal Concentration [ppm]								Reference
	As	Cd	Hg	Pb	Se	V	U	Th	
Witbank 4 Seam	5.5	0.3	0.29	15	0.8	39	2.6	8.9	Bergh (2009)

Coal Deposit	Metal Concentration [ppm]								Reference
	As	Cd	Hg	Pb	Se	V	U	Th	
Witbank 2 Seam	4.6	0.6	0.12	10	0.9	27	4	15	Cairncross (1990)
Waterberg Upper Ecc	11.4	0.2	0.37	76	1.3	96	4.7	9.3	Bergh (2009)
Waterberg Deposit	9.3	0.13	0.9	23.4	1.19	55	3.07	7.5	Wagner & Tloteng (2012)
Highveld 4 Seam	3.1	0.4	0.2	7	1	33	-	-	Wagner & Tloteng (2012)
Global Average	5	0.6	0.12	25	3	25	1.2	3.1	Zhang et al. (2004)

On applying our concept of desulphurisation of fine coal waste (or other hard rock tailings), we separate the non-economic sulphide minerals into a low-volume waste stream, leaving the bulk waste volume with a low sulphide mineral content, which is thus non-acid generating. Kazadi Mbamba et al. (2012) suggested the use of froth flotation for the desulphurisation of coal ultrafine wastes, with the addition of a coal flotation stage prior to desulphurisation for the recovery of a clean coal product. Iroala (2014) discusses the use of reflux classification as an alternative to flotation to achieve these separations. Following this process, the high-sulphide, low-volume waste stream may be deposited selectively with containment to prevent ARD generation while the low-sulphide, high-volume waste may be safely deposited within slimes dams, or re-purposed (see Part 2 of WRC K5/2231). The coal product stream may be sold due to its acceptable calorific, ash and sulphur composition.

In the Kazadi Mbamba (2012) and Iroala (2014) studies, standard static ARD classification methods were used, in conjunction with total sulphur deportment across the flotation process, to measure success in reduction of ARD potential of coal waste. No analysis of the major and trace metal content of the coal waste streams produced as a result of the desulphurisation process was conducted. The focus of the present study extends the studies of Kazadi Mbamba (2012) and Iroala (2014) to investigate the two-stage desulphurisation process on two ultrafine coal wastes, giving particular consideration to the analysis of the metal content of the waste streams and its potential for mobilisation, together with the standard ARD classification and biokinetic accelerated weathering tests, to assess the environmental risk associated with the product streams following desulphurisation via froth flotation.

4.1.1 Materials and methods

4.1.1.1 Sample description

In this study, two coal waste samples were obtained, representing two major coalfields in South Africa, Witbank & Waterberg. A 71 kg cyclone waste sample (-500 µm) was received from the selected colliery from the Witbank coalfield and a 64 kg thickener feed sample (-180 µm) from a colliery in the Waterberg coalfield. Representative sampling of the received wastes was conducted using a Dickie & Stockler rotary splitter, with resulting samples of approximately 210 g used in the 2-stage desulphurisation, froth flotation experiments. The particle size distributions of the Witbank and Waterberg coal waste samples (Figure 4-1) were performed using a dry test sieving method as outlined in ISO 153:1993 in the Centre for Minerals Research (CMR) laboratories at the University of Cape Town.

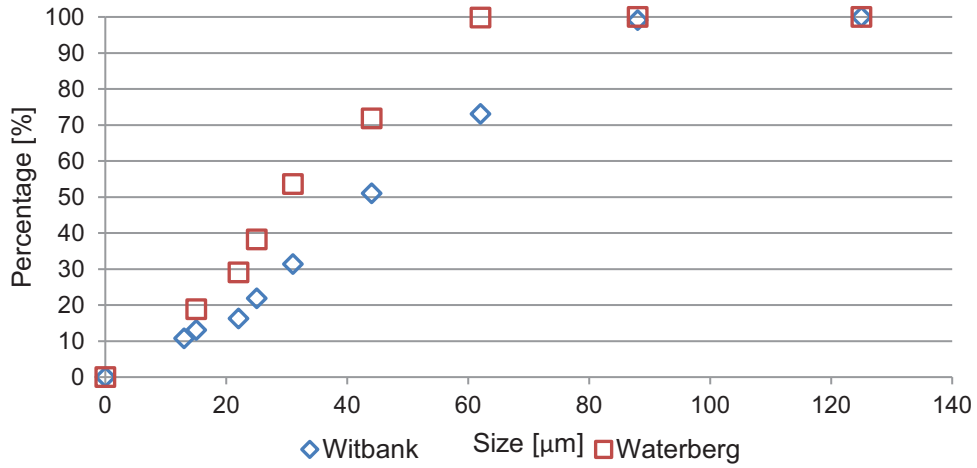

Figure 4-1 Particle size distributions of the Witbank and Waterberg coal waste samples analysed using a Malvern Particle Analyser

4.1.1.2 Two-stage desulphurisation via froth flotation

Physical desulphurisation of the coal waste samples was conducted using laboratory-scale froth flotation by means of a 3L Leeds-type flotation cell (Figure 4-2). The operating variables used in the 2-stage froth flotation experiments are presented in Table 4-2.

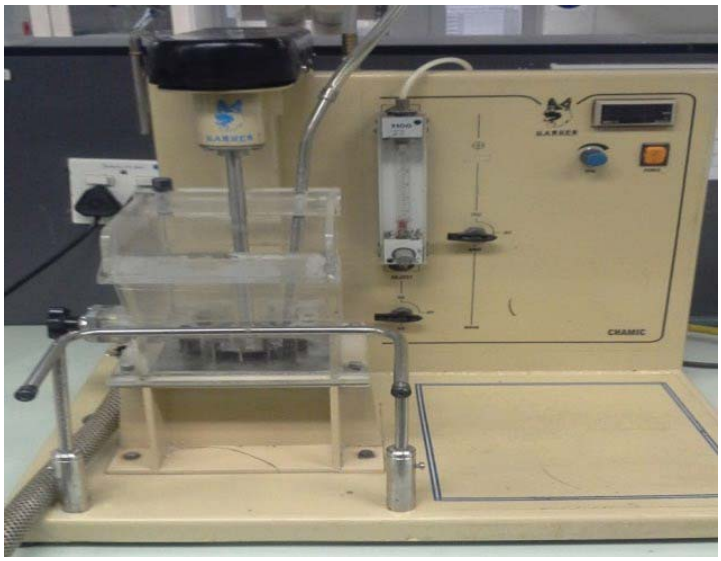

Figure 4-2 Laboratory-scale, 3ℓ batch flotation cell

Table 4-2 Operating variables for the 2-stage froth flotation experiments

Variable	Operating Condition
Impeller Speed	1200 rpm
Froth height	30 cm
Pulp density	10%
Aeration	5-6 L/min

4.1.2 Characterisation of environmental risk

Characterisation of the environmental risk associated with the coal waste samples produced from the froth flotation experiments was performed through investigation of the ARD potentials of the feed,

concentrate and tails streams from the coal and sulphide flotation stages. Additionally, the mobility of the major metals associated with the coal wastes was investigated under the ARD test conditions. The overall environmental risk associated with the metals mobilised under the test conditions was assessed using the protocol as outlined by Broadhurst & Petrie (2010). To better understand the partitioning of the metal species within the mineral phases, and the associated metal mobility under disposal conditions, sequential chemical extractions, as outlined by Broadhurst et al. (2009), were performed on the coal waste streams.

4.1.2.1 ARD classification tests

ARD classification tests were conducted on the feed, concentrates and tailings samples following both coal flotation and subsequent desulphurisation via froth flotation. Standard acid-base accounting (ABA), in conjunction with the net acid generation (NAG) tests (Stewart, et al., 2006), were used in the assessment of the ARD potentials of each of the product streams. To assess potential ARD generation under microbially-mediated conditions, batch biokinetic tests (Hesketh, et al., 2010a) were performed in duplicate on selected streams according to sample availability.

4.1.2.2 Leachate analysis for metal mobility

The mobility of the major metal species was investigated through analysis of the leachate solutions following ABA and NAG test work. The metal concentrations within the leach solutions were analysed using inductively coupled plasma-optical emission spectroscopy (ICP-OES) at the Analytical Laboratory of the Department of Chemical Engineering at the University of Cape Town.

4.1.2.3 Sequential Chemical Extraction Tests

Sequential chemical extraction (SCE) tests were performed on the coal waste samples according to the protocol outlined by Broadhurst et al. (2009). The SCE tests entail the seven stage, sequential reaction of the waste sample using leaching agents of increasing strengths. Following each leaching stage, the waste samples were centrifuged at 10 000 rpm using the Beckman JA-20 rotor, equivalent to 12 000 g, for 10 minutes at ambient conditions. The recovered leachate solution was analysed for the metals of interest. The sequential leaching stages are described in Table 4-3.

Table 4-3 Sequential chemical extraction test conditions

Leaching Stage	Leaching Agent	Leaching Conditions	Targeted Mineral Phases
1	40 mL H_2O	Ambient conditions	Water-soluble constituents
2	20 mL 1 M NH_3-acetate	Ambient conditions	Exchangeable constituents
3	20 mL 1 M Na-acetate	Ambient conditions	Soluble carbonate constituents
4	20 mL $NH_2OH.HCL$	Agitate for 2 hrs at 50°C	Amorphous Mn- & Fe-oxyhydroxides
5	30 mL 2M $NH_2OH.HCl$	Agitate for 3 hrs at 90°C	Crystalline Mn- & Fe-oxyhydroxides
6	750 mg $KClO_3$; 5 mL 12 M HCl; 10 mL 4 M HNO_3	Agitate for 1 hr at 90°C	Primary & Secondary sulphides and organics
7	Aqua Regia	15 min at 90°C	Residual silicates

4.1.2.4 Environmental risk assessment using ranking & scoring

The environmental risks associated with the soluble metal concentrations were assessed according to the ranking scoring method developed by Broadhurst & Petrie (2010). The soluble metal concentrations are used, together with the water quality limits and the natural background concentrations specific to each metal species, in the calculation of hazard potential factors and risk potential factors. These factors are then ranked using a unique ranking system to determine which metal species has the potential to

be of risk in the environment. The total available metal concentrations were determined by total digestion using extraction in aqua regia (step 7) and metal analysis using ICP-OES.

4.1.3 Results of the two-stage desulphurisation using froth flotation

Two-stage flotation was conducted according to the methodology outlined by Kazadi Mbamba et al. (2012) and described in Section 4.1.1.2. The first flotation stage was conducted to recover a coal concentrate, with its tails (1st Tails) progressing to the second flotation stage where a sulphide-rich concentrate (sulphur concentrate) and sulphide-lean tails (2nd Tails) were recovered. A block flow diagram of the two-stage flotation process is presented in Figure 4-3.

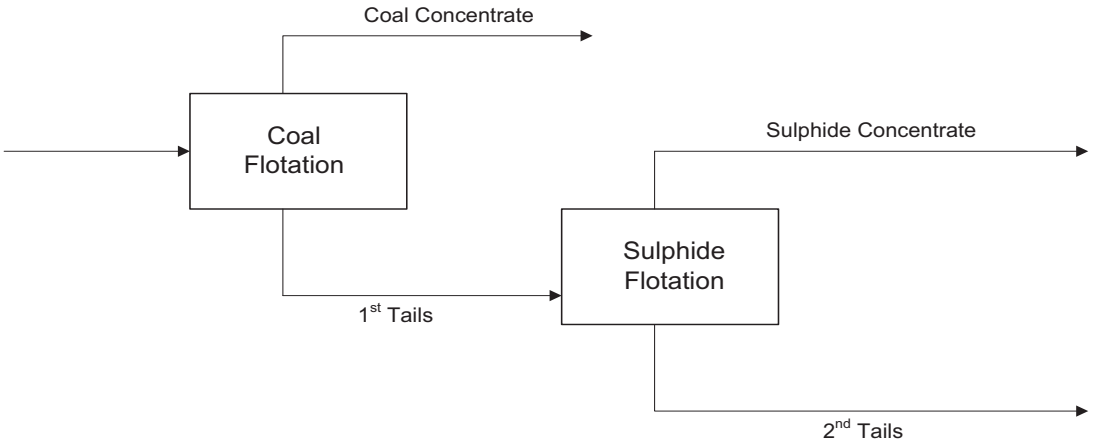

Figure 4-3 Schematic of the 2-stage desulphurisation process using froth flotation

The mass, total sulphur and ash recoveries for each of the process streams for the Witbank coal waste is presented in Figure 4-4 and that for the Waterberg coal waste Figure 4-5. The associated ash and sulphur grades of the Witbank coal waste process streams are presented in Table 4-4 and those of the Waterberg coal waste streams in Table 4-5.

On processing the Witbank colliery coal waste stream, approximately 26% of the feed material was recovered in the coal concentrate stream during coal flotation stage. The ash and sulphur grade for the coal product stream were approximately 22% and 2.3% respectively. The relatively high sulphur grade obtained in this case may be problematic with respect to this saleable product and the necessary specifications required for the coal feed streams for the purpose of energy generation in South Africa; it suggests that further sulphide liberation may be necessary to achieve 'in-spec' coal. However, the majority of the ash and sulphur deported to the tails stream of the coal flotation process (1st Tails).

The 1st tails stream proceeded to sulphide flotation where approximately 10% of the total initial mass reported to the sulphide concentrate (15% of Tails 1) and the majority of the ash content of Tails 1 (approx.. 90%) reported to the tails (2nd Tails) which made up some two-thirds of the initial coal waste stream entering the overall process. The ash grade of the concentrate stream, however, remained high at approximately 36%. Separation of the total sulphur components within this flotation stage was poor, with approximately equal amounts of total sulphur reporting to the sulphide concentrate and tails streams, again suggesting limited sulphide liberation. The differences in mass recovery, however, did result in a substantial increase in the sulphur grade of the sulphide concentrate stream relative to the feed stream to the sulphide flotation process. However, the total sulphur grade in the tails stream remained above 2% total sulphur.

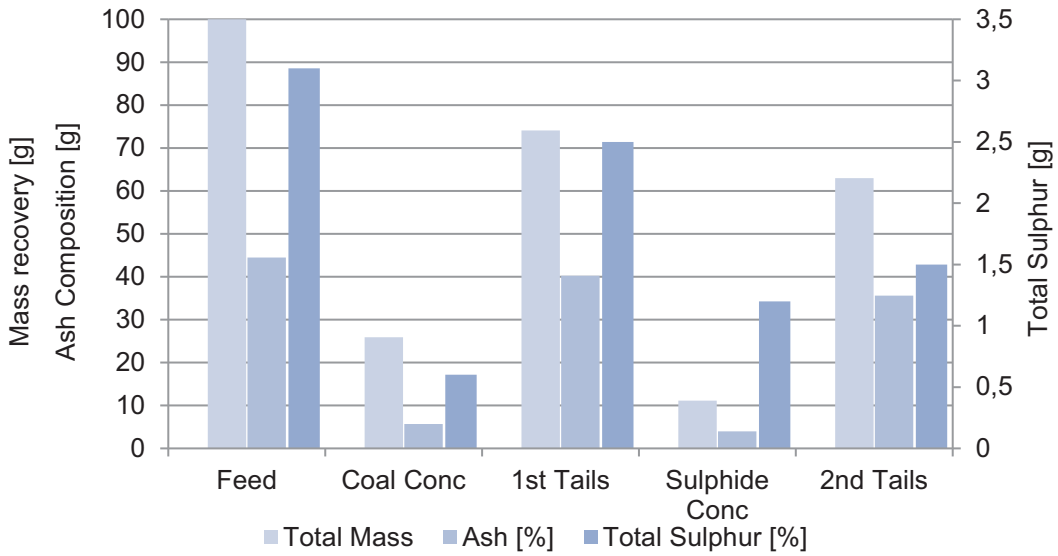

Figure 4-4 Deportment of the total mass, ash (primary y-axis) and total sulphur (secondary y-axis) for the two-stage flotation of the Witbank coal waste sample

Table 4-4 Ash and sulphur grades of the 2-stage flotation streams for the Witbank coal waste sample

Component	Feed	Coal Conc	1st Tails	Sulphide Conc	2nd Tails
Total Mass [g]	100	25.9	74.1	11.1	63
Ash [%] in stream	44.5	22.0	54.3	36.0	56.5
Total Sulphur [%] in stream	3.1	2.3	3.4	10.8	2.4
Recovery of ash present in feed stream [%] (mass balance closures of 102% and 99%)	100	12	90	9	80
Recovery of sulphur present in feed stream [%] (mass balance closures of 100% and 106%)	100	19	81	38	48

A similar total mass recovery was achieved for the flotation of the Waterberg sample, with approximately 30% of the total mass reporting to the coal concentrate product stream (Table 4-5). Here, the sulphur grade of the coal concentrate was below 1.5%; the specification for coal combustion for electricity generation in South Africa. The majority of the ash and sulphur reported to the tails stream (Tails 1).

Table 4-5 Ash and sulphur grades of the 2-stage flotation streams for the Waterberg coal waste sample

Component	Feed	Coal Conc	1st Tails	Sulphide Conc	2nd Tails
Total Mass [g]	100	30	70	2	68
Ash (g)	49.4	7.4	42.0	1.2	42.6
Total Sulphur (g)	1.1	0.39	0.63	0.36	0.41
Ash [%] in stream	49.4	24.5	60.2	59.5	62.7
Total Sulphur [%] in stream	1.1	1.3	0.9	18.0	0.6
Recovery of ash present in feed stream [%] (mass balance closures of 100% and 104%)	100	15	85	2.4	86
Recovery of sulphur present in feed stream [%] (mass balance closures of 92% and 122%)	100	35	57	33	37

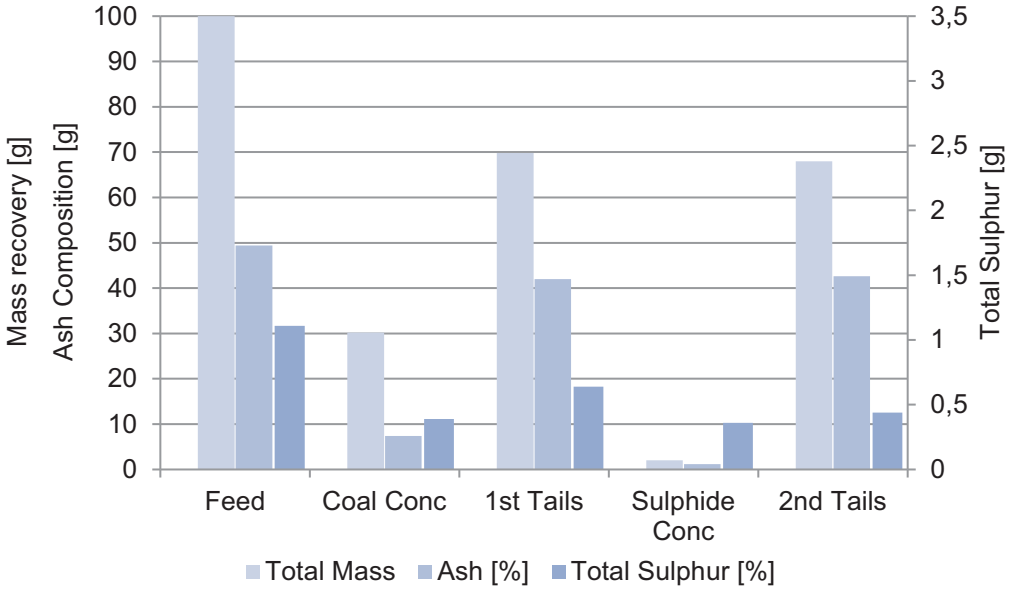

Figure 4-5 Mass, Ash and Sulphur deportment of the Waterberg coal waste sample following 2-stage flotation

Approximately equal proportions of total sulphur reported to the concentrate and tails streams of the sulphide flotation process while some 97% of the ash in Tails 1 reported to Tails 2. Given the differences in mass between these two streams, this resulted in an increase in sulphur grade of the concentrate from 0.9% to 18%. The bulk of the mass of the feed stream reports to Tails 2, i.e. some 68% (Table 4-5, Figure 4-5). The poor closure of the mass balances across this case study are noted.

4.1.4 The environmental risks associated with coal desulphurisation

4.1.4.1 ARD characterisation tests

Acid-base accounting classification tests estimate the potential for ARD generation through a balance of the maximum potential acidity (MPA) and the acid neutralising capacity (ANC). The MPA value is estimated from quantification of total sulphur, together with the assumption that all the sulphur is present as pyrite mineral and available for oxidation. Thus, in the estimation of this value, no provision is made for the presence of non-pyritic sulphur species. The ANC value is quantified experimentally through titration of the leachate recovered following acid digestion of the waste sample. The results of the ARD characterisation tests using acid-base accounting are presented in Table 4-6 and Table 4-7 for the Witbank and Waterberg coal wastes respectively.

Table 4-6 ARD classification results for the Witbank ultrafine coal waste following acid-base accounting test work

Sample	Sulphur Grade [%]	MPA [kg H_2SO_4 /ton]	ANC [kg H_2SO_4 /ton]	NAPP [kg H_2SO_4 /ton]	ABA Classification
Feed	3.1	95	3.8	91	AF
Coal Concentrate	2.16	66	4.1	62	AF
Coal Tails 1	3.43	105	4.2	101	AF
Sulphur Concentrate	10.7	327	4.1	323	AF
Benign Tails 2	2.37	72	4.2	68	AF

Both Witbank and Waterberg feed samples were classified as potentially acid forming, with low acid neutralising capacities observed for both feed samples. This was unexpected given the high ash content. Coal flotation of the Witbank sample resulted in deportment of the sulphur to the tailings. Both the coal concentrate and coal tails (Tails 1) were estimated to neutralise approximately 4 kg-H_2SO_4/ton of waste. The sulphide flotation stage resulted in an accumulation of the total sulphur in the sulphur concentrate stream, however, separation was not achieved to remove the potential for ARD generation from the 2nd stage tails entirely, with NAPP values for the sulphide concentrate and final tailings of 323 and 68 kg-H_2SO_4/ton per ton respectively.

Table 4-7 ARD classification results for the Waterberg ultrafine coal waste following acid-base accounting test work

Sample	**Sulphur Grade** [%]	**MPA** [kg H_2SO_4 /ton]	**ANC** [kg H_2SO_4 /ton]	**NAPP** [kg H_2SO_4 /ton]	**ABA** Classification
Feed	1.11	34	10	24	AF
Coal Concentrate	1.28	39	7	32	AF
Coal Tails	0.92	32	121	-89	NAF
Sulphur Concentrate	17.6	539	7	532	AF
Benign Tails	0.65	20	121	-101	NAF

Flotation of the Waterberg sample resulted in poor separation of the total sulphur during the coal flotation stage (Table 4-7). A discrepancy in the ANC results, however, resulted in a non-acid forming classification of the tailings from this flotation stage, while the coal concentrate stream retained the potential for acid generation. The total sulphur fraction, however, was concentrated to the second concentrate stream during the sulphide flotation stage, with a non-acid forming classification achieved for the 2nd stage tails, due to both its lower MPA and its higher ANC. As noted previously, the sulphur imbalance may have resulted in a mis-classification of the sulphur concentrate sample.

Further ARD classification was conducted on both samples using a combination of the ABA and NAG_{pH}, with the results shown graphically in characterisation plots Figure 4-6 and Figure 4-7. The NAPP value on the x-axis was calculated from the ABA results while the NAG_{pH} was measured after complete reaction of the sample with a known quantity of 15% H_2O_2 solution. The resulting pH values from the NAG tests following two-stage flotation of the Witbank coal waste support the acid forming (AF) classification as provided by the acid-base accounting test protocol (Figure 4-6). Although the 2-stage desulphurisation decreased the NAPP value, the pH of the solution following reaction with 15% H_2O_2 remained approximately pH 2.0 for all concentrate and tails streams. Hence, while acid generating capacity was concentrated into the sulphide concentrate, the 2nd tailings stream remained acid generating, albeit less so.

In contrast, the combined NAPP-NAG test results for the Waterberg coal waste, presented in Figure 4-7, indicated some contradictory results when compared to those obtained following acid-base accounting. Here, the pH after reaction of the feed and waste coal concentrate material was above pH 4.5, suggesting a non-acid-forming classification for these samples. Classification of the remaining samples, however, support acid-base accounting, with the tails from both flotation experiments being classified as non-acid-forming, while the sulphur concentrate product indicated the potential for acid generation.

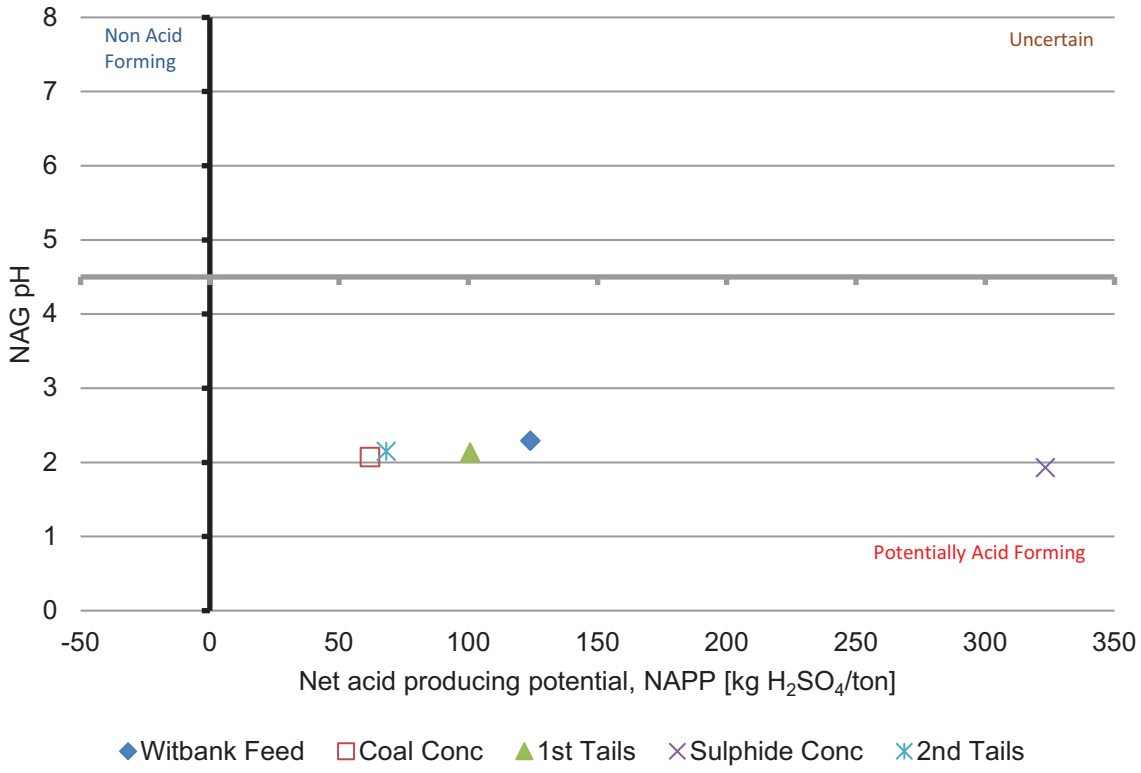

Figure 4-6 Characterisation plot showing the classification of the Witbank sample using the NAG_{pH} and NAPP values showing acid generating classification for all flotation streams

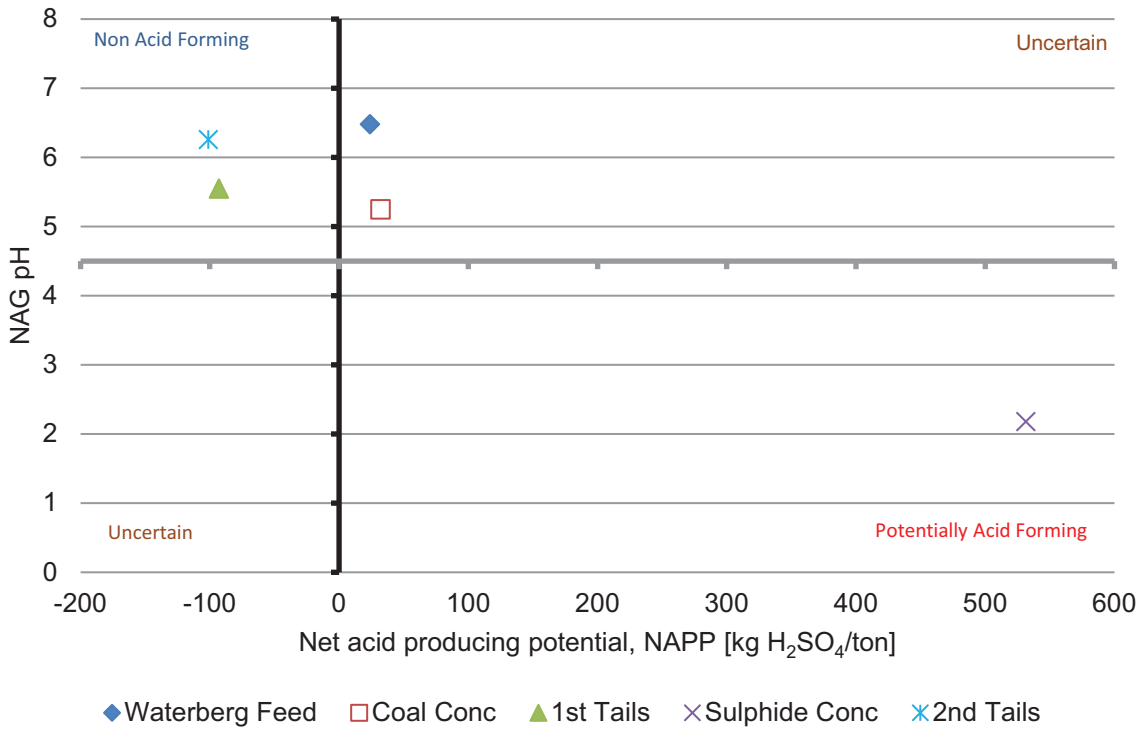

Figure 4-7 Characterisation plot showing the classification of the Waterberg coal wastes using the NAG_{pH} and NAPP values.

Although the standard ABA (acid-base accounting) method is routinely used for the classification of the ARD potentials of solid wastes, the method does not account for the presence of organic sulphur in relation to its pyritic counterpart adequately. The estimation of the MPA, used in the calculation above, uses the total sulphur content of the waste as determined by LECO analysis, and thus, any organic sulphur present in the sample is assumed to behave as pyrite mineral.

Thus, the discrepancies observed between the ABA and the NAG test results, in particular those of the feed and coal concentrate streams, may be as a result of the over-estimation of the maximum potential acidity as estimated using the total sulphur content. For the Witbank sample, however, the low ANC value, and possibly poor pyritic-sulphur separation in the flotation stages, results in a "potentially acid forming" classification during both ABA and NAG tests, regardless of any over-estimation due to the presence of organic sulphur.

4.1.4.2 ARD characterisation using biokinetic test

To assess ARD generation under biotically-mediated conditions and gather data on the relative rates of acidification and neutralisation, the UCT biokinetic test, also referred to as the biokinetic accelerated weathering test, was performed as described in Section 3.1. The finely-milled coal waste sample was suspended in media and inoculated with a mixed mesophilic culture consisting of both iron- and sulphur-oxidising microorganisms. Monitoring of the flask experiments was performed through measurement of the solution pH, redox potential, ferrous iron and total iron concentrations. These variables give an indication of acid generation under submerged conditions in the presence of ARD-generating microbes.

The pH profile for the Witbank coal waste streams is presented in Figure 4-8. From an initial pH of approximately pH 2.0, the pH of the coal waste slurries remained constant over the initial 4 days of the experiment. This supported the low ANC values reported in the ABA static tests, with a lack of significant change in pH indicating the low acid neutralisation capacity of the wastes. Thereafter, the pH of the Feed and 2nd Tails stream decreased over the 20 days of the flask experiment to pH 1.7 and pH 1.8 respectively. This decrease in pH indicated the acid generation characteristics of these wastes, confirming the NAPP-NAG characterisation. Over this time period of 25 days, no significant change in the pH of the coal concentrate and 1st Tails waste streams was observed.

As an indication of the activity of the iron-oxidising microorganisms in the experiments, the redox potential, a function of the ratio of the concentrations of ferrous iron to ferric iron, of the flasks was monitored over the course of the experiment. These results are presented in Figure 4-9. Initially, the potentials of approximately 450 mV indicated the relative dominance of ferrous iron over ferric iron with the flask experiments. After approximately 3 days, the rise in the redox potentials of the feed waste as well as the tails following sulphide flotation (2nd Tails) indicated the oxidation of the soluble ferrous iron to ferric iron. For the feed sample, the rise in potential to reach 700 mV of day 5 correlated with a decrease in the pH of the test, suggesting sulphide mineral oxidation via ferric iron. A pH of 1.6 was recorded on day 60 and remained little changed to day 90. For the 2nd Tails, however, no immediate correlation between the initial rise in redox potential and a decrease in test pH was observed, with this difference possibly due to the lower sulphide mineral content and the removal of well-liberated sulphide following the sulphide flotation process. In this test, the redox potential reached 700 mV on day 10 at which point pH decrease was observed. A pH of 1.75 was recorded on day 60 and remained little changed to day 90.

In the test on the coal tailings (Tails 1), the increase in redox potential was seen on day 12, reaching 620 mV on day 14 and 680 mV on day 25 at which point acidification started. A pH of 1.75 was recorded on day 60 and remained little changed to day 90, as shown for Tails 2.

In the coal concentrate test, the redox potential started to decrease on day 22, reaching 680 mV on day 28 at which point a decrease in pH was observed. A pH of 1.7 was observed by day 60 and decrease to a minimum of pH 1.6 by day 90. These data suggest effect of both sulphur liberation and propensity for microbial activity on the rate of acidification.

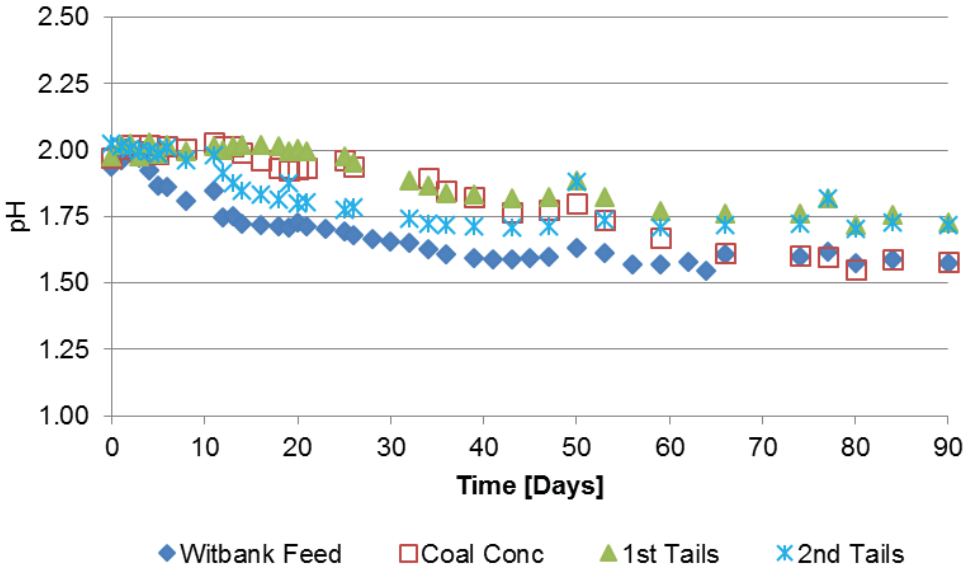

Figure 4-8 pH profiles of the Witbank coal wastes under biokinetic accelerated weathering conditions

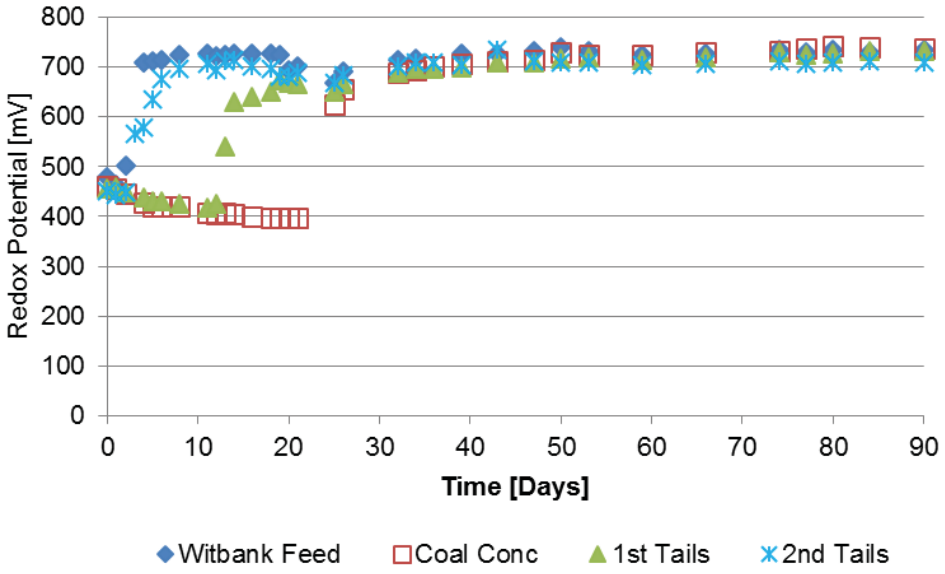

Figure 4-9 Redox potential measurements of the biokinetic tests using Witbank coal waste samples indicating the rate of microbial ferrous iron oxidation relative to that of mineral leaching with ferric iron

The redox potential data is supported by the ferrous iron (Figure 4-10) and total iron (Figure 4-11) concentration curves, the difference indicating the concentrations of ferric iron available for mineral oxidation. The ferrous iron concentration for the Witbank feed sample increased over the initial 2 days due to the solubilisation of iron-bearing components in the coal. The lack of a similar increase in the concentrate and tails streams following coal flotation suggests the dissolution and removal of the easily-soluble iron-bearing minerals during the 1st flotation process. After the initial 3 days, the ferrous concentration for all Witbank samples remained below 200 mg/ℓ due to the action of the iron-oxidising microorganisms for the feed sample. A small increase in ferrous iron was observed in each test up until the point at which the redox potential increased and the pH started to decrease, typically reflecting the onset of microbial action, i.e. day 22, 12 and 3 for the coal concentrate, Tails 1 and Tails 2 streams. In these three cases, the ferrous iron concentration did not exceed 200 mg/L.

Following the decrease in ferrous iron concentration (Figure 4-10), and associated increased in ferric iron, an increase in total iron concentration was observed in all samples (Figure 4-11). This suggests the presence of an iron-bearing mineral, e.g. pyrite which is not solubilised under acidic conditions alone but requires the presence of an oxidising agent, such as ferric iron, for its dissolution. By the end of test at 90 days, the total iron concentration in solution had increased to >1600 mg/L in the feed test, >1200 mg/L in the coal concentrate test and approximately 600 mg/L in the tests on Tails 1 and Tails 2. This further supports the desulphurisation of the feed waste material by the flotation process, but suggests incomplete separation during the sulphide flotation stage. The latter may be the result of incomplete sulphide liberation as suggested above.

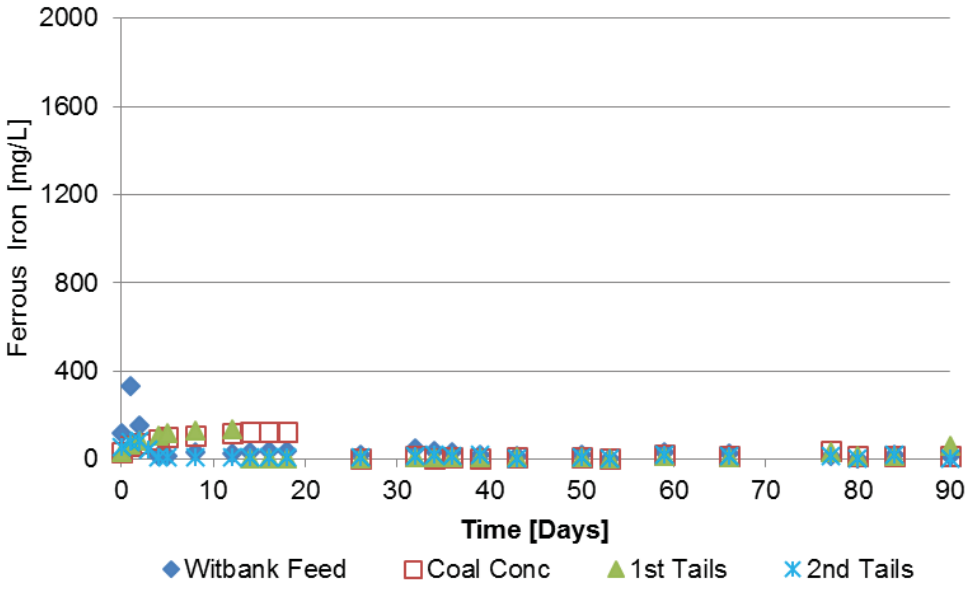

Figure 4-10 Ferrous iron concentration curves for the biokinetic flask experiments using Witbank coal waste samples

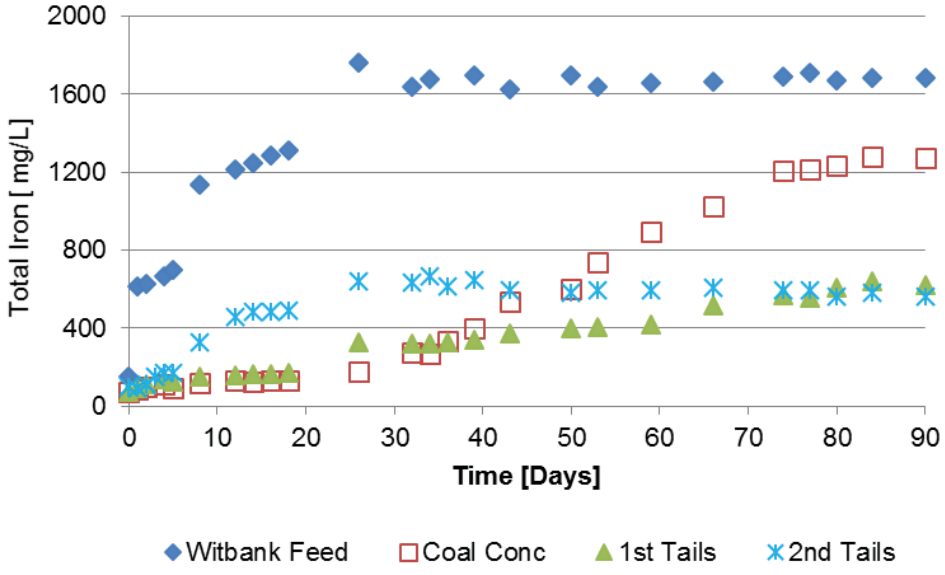

Figure 4-11 Total iron concentration curves from the biokinetic flasks using the Witbank coal waste streams following 2-stage froth flotation.

The pH profiles for the Waterberg samples (Figure 4-12) reflected the inherent acid neutralising capacity of the coal waste samples which led to an increase in pH to approximately pH 7.0 over the initial 4 days. The profiles were similar for the concentrate and tails streams following coal flotation and the tails following sulphide flotation, presenting a non-acid-forming characterisation consistent with the ABA and NAG test results. The near-neutral pH values resulted in precipitation of the ferric iron within the biokinetic flasks, resulting in low redox potential values of approximately 200 mV (Figure 4-13).

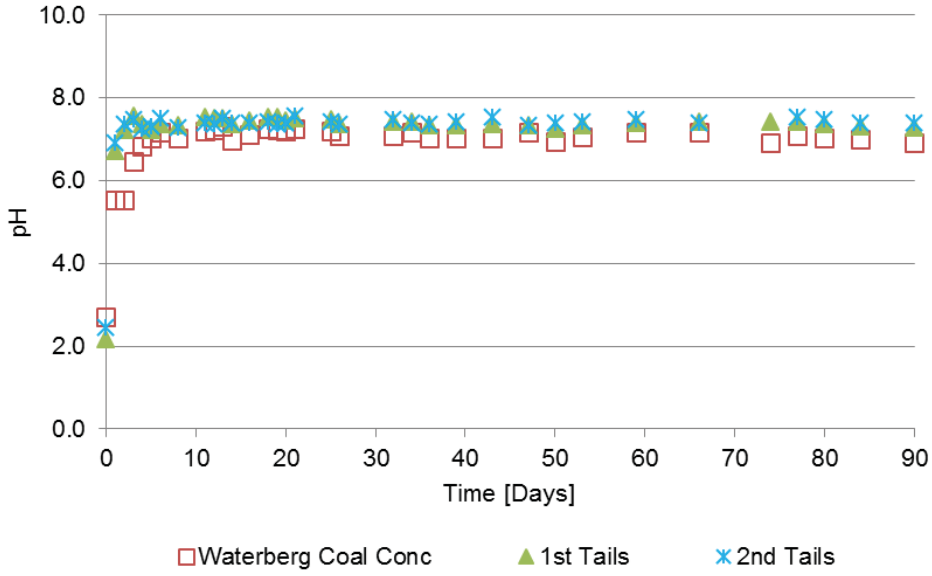

Figure 4-12 pH curves for selected Waterberg samples following ARD characterisation using biokinetic testing

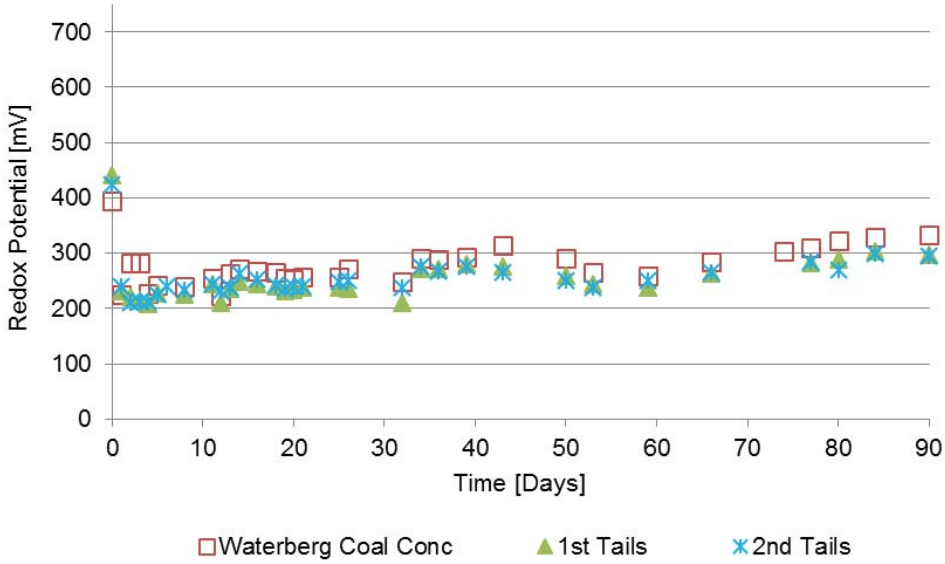

Figure 4-13 Redox potential curves for the Waterberg samples as measured from biokinetic test flasks.

4.2 Metal Deportment from Coal Waste Streams Pre- and Post Desulphurisation under ARD Characterisation Test Conditions

4.2.1 Metal risks associated with the coal samples pre and post separation, based on metal content

The standard ARD characterisation and biokinetic tests focus exclusively on the generation of acidity as an indicator for environmental risk. In these tests, however, little provision is made for the risks associated with the deportment of toxic metal anions under conditions experienced in typical waste deposits. To identify elements of potential environmental risk, trace metal analysis of the leachate solutions following total digestions of both the Witbank and Waterberg coal samples, reported in Section 0, were performed. These microwave digestions were carried out in a mixed HCl (3 parts), HNO_3 (1 part) and HF (1 part) environment. The potential environmental risks associated with the total metal deportment, estimated through a risk assessment analysis (Broadhurst & Petrie, 2010), were conducted and used to identify the particular elements of interest within each coal waste sample. The risks associated with the desulphurisation flotation streams are presented in Table 4-8 and Table 4-9 for the Witbank and Waterberg ultrafine wastes respectively.

Significant differences were observed in the potential environmental risks associated with these two ultrafine coal wastes. Prior to the desulphurisation flotation process being conducted, significant risks were observed with the potential mobility of Fe, As, Al and Pb for the Witbank coal waste (Table 4-8). Of these elements, the As and Fe exhibited a “high” environmental risk, while the Al and Pb exhibited ‘moderate’ risk potentials. Following the coal flotation step within the two-stage desulphurisation process, risks remained with the deportment of the Fe, As and Al, suggesting a significant quantity of the Pb-bearing phases reported to the coal concentrate stream. Following the 2nd stage of the desulphurisation process, however, significant environmental risks associated with the deportment of As and Fe remained, albeit in lower quantities relative to the initial coal waste sample. The remaining presence of these elements, predominantly associated with sulphide minerals, within the sulphide tailings stream further indicated the poor separation experienced within this flotation stage.

The potential mobility of Al, As, Cr, Fe, Mn, Pb and Zn posed an environmental hazard for the Waterberg ultrafine coal waste. Following the 2-stage desulphurisation process, however, the potential risk associated with the deportment of the Cr and Zn elements were decreased in the final tailings stream, suggesting a significant portion of the associated mineral phases deported to the sulphide concentrate stream. This deportment has potential to impact the further uses of this sulphide-rich process stream. For the non-acid forming Tails 2 stream, a “high” environmental risk remained for potential deportment of As and Fe elements.

Table 4-8 The overall environmental risk associated with metal mobility from process streams following 2-stage desulphurisation of the Witbank ultrafine coal tailings

Environmental Significance		RPF / 1000	Coal Waste Feed	Coal Flotation Concentrate	Coal Flotation Tails	Sulphide Flotation Tails
High	A	1000-10000				
	B	100-1000	As < Fe		As	
	C	10-100		As < Fe	Al < Fe	Fe < As
Moderate		1-10	Al < Pb	Al		Al
Low		0.1-1	U<Cr<Ti<Ni<Zn	U<Cr<Zn<Ti<Pb	Zn<Pb<Ti<Cr	Ni<Zn<Pb<Ti
Negligible		<0.1	Ca<K<Co<Mn <Cu<Ba<V	Ca<K<Ba<Co <Mn<Cu<V<Ni	Ca<K<Co<Ba <Mn<Cu<V<U <Ni	Ca<K<Ba<C <Mn<Cr<Cu<U <V

Table 4-9 The environmental risk associated with the total available metal deportment for the tails process streams from the 2-stage flotation process performed on the Waterberg coal sample

Environmental Significance		RPF / 1000	Coal Flotation Tails	Sulphide Flotation Tails
High	A	1000-10000		
	B	100-1000	Fe	Fe<As
	C	10-100	Cr < As	
Moderate		1-10	Zn < Pb	Al<Mn<Pb
Low		0.1-1	Ca<Ti<Ni<U<Al	Ca<V<Ti<Ni<Cr<Zn<U
Negligible		<0.1	K<Co<Mn<Ba<Cu<V	K<Ba<Co<Cu

4.2.2 Metal deportment under ANC and NAG test conditions

Following the identification of the elements with the potential environmental risk, their deportment under ANC and NAG test conditions was investigated. Elemental mobilisation under ANC conditions occurred because of leaching of the acid-soluble mineral phases at elevated temperatures. The element with the highest mobility for the Witbank sample under ANC conditions (Figure 4-14: Mobilisation of the environmentally significant elements for the Witbank ultrafine coal waste following acid digestion under ANC conditions) was Fe, with approximately 33% of the total available content deporting under the acidic conditions. The similar percentage deportment obtained for the tailings stream following coal flotation (1st Tails) suggested that most of the acid-soluble Fe-bearing phases reported to the 1st Tails. Analysis of the tailings following sulphide flotation (2nd Tails) exhibited residual Fe mobilisation which further supported the poor separation during the sulphide flotation stage, as observed from the significant quantity of ash in the sulphide concentrate stream (Table 4-4).

The other elements of interest exhibited much lower mobilisation percentages. While the Al solubilisation remained low for all streams in the two-stage flotation process, significant mobilisation of the Pb-bearing minerals in the concentrate and tailings streams following coal flotation suggested poor separation of this element. The lack of significant mobilisation in the Witbank 2nd Tails suggests the majority of the minerals containing the metals of concern deported to the sulphide concentration stream. Similar behaviour was displayed by As-bearing components. Such potential deportment requires clear understanding prior to proposed downstream uses of fractions of Witbank ultrafine coal waste.

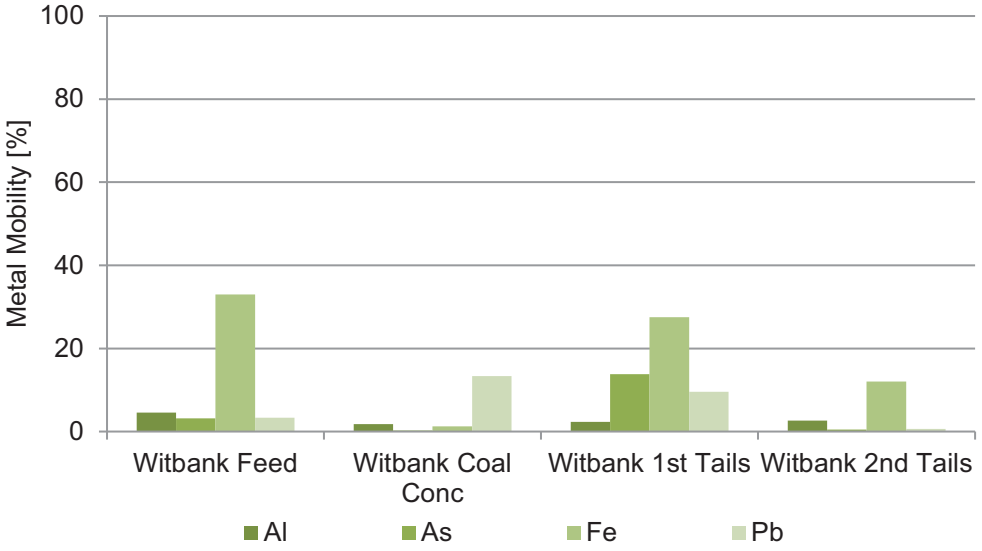

Figure 4-14 Mobilisation of the environmentally significant elements for the Witbank ultrafine coal waste following acid digestion under ANC conditions

Significant mobilisation of the Mn element was observed under the acidic leaching conditions for the Waterberg 1st Tails, with the difference in mobilisation of this element with that observed from the 2nd Tails process stream suggesting the deportment of the Mn-bearing components to the sulphide concentrate stream. With the exception of the mobilisation of the Al element in the 1st Tails stream (16%), solubilisation of the other elements of concern was below 10%.

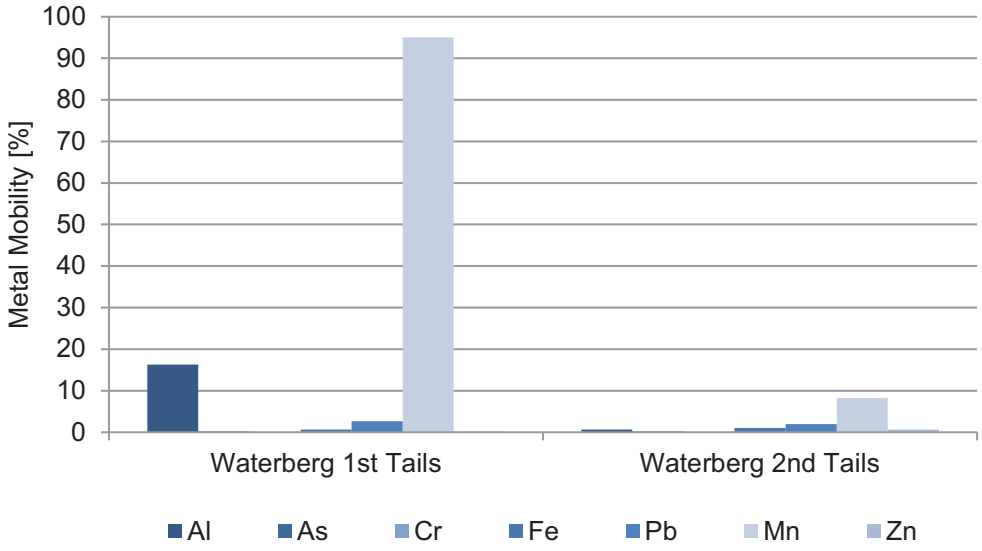

Figure 4-15 Mobilisation of the environmentally significant elements for the Waterberg ultrafine coal waste following acid digestion under ANC conditions

Solubilisation of the elemental species under NAG test conditions resulted from mineral oxidation by H_2O_2 in conjunction with acid reaction as a result of the acidity generation by this oxidation. Mobilisation of those elements with the potential for environmental degradation from the Witbank and Waterberg ultrafine coal wastes are presented in Figure 4-16 and Figure 4-17 respectively.

The differences in solubilisation of the Fe element between the ANC and NAG tests for the Witbank sample was a result of the presence of Fe-bearing mineral phases which do not undergo acid

solubilisation, such as pyrite mineral, within the ultrafine coal waste. Thus, the significant mobilisation of this element, together with the potential risks observed previously, suggests the necessity of oxidation of the Fe-bearing minerals as a precursor to potential for environmental degradation. Lower mobilities of As and Pb were observed under NAG conditions as compared to the ANC conditions. This may be because of the lower elemental solubilities at the elevated pH, although both tests displayed acidic conditions.

For the Waterberg coal wastes, the mobility of the elements was affected by the elevated pH conditions (pH > 5.0) for all process streams. Thus, although Fe solubilisation was expected under the oxidative conditions, the elevated pH conditions led to the precipitation of this element. Similarly, the potential for adsorption of the elements of interest, particularly onto Fe precipitates formed at elevated pH, led to the removal of these elements from the leachate solutions. Thus, lower concentrations of the elements were observed under NAG test conditions.

With the exception of the Fe concentrations for the Witbank sample, only small concentrations, and thus mobilities, for the other elements were observed. The high toxicities of the elements of interest means that only low concentrations within the leachate solutions are necessary for potential negative environmental consequence. Investigation of the elemental concentrations and mobilities informs the potential for environmental risk which is proportional to their toxic limits. Furthermore, concentrations mobilised under representative conditions are important to discern.

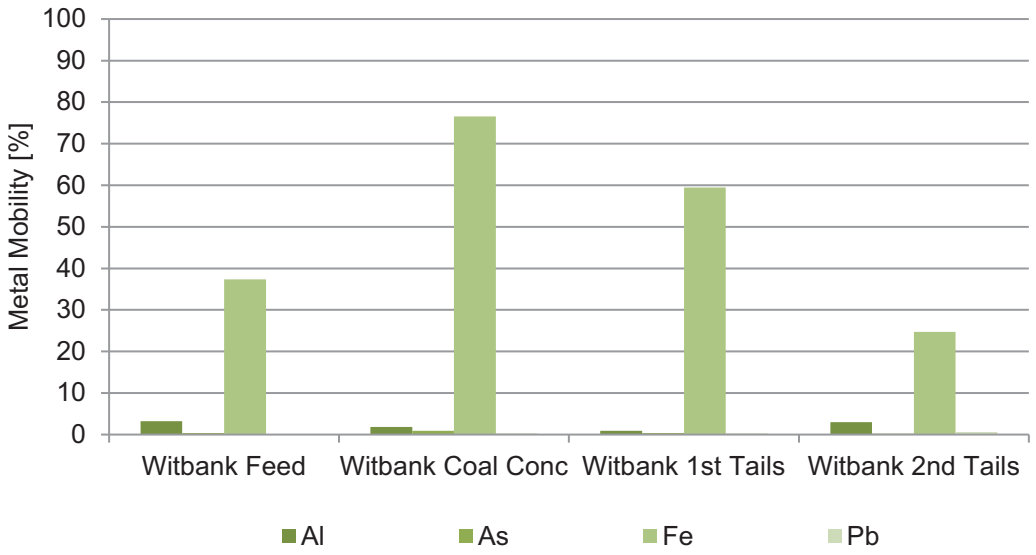

Figure 4-16 Mobilisation of the major metals for Witbank ultrafine coal waste under oxidative conditions during NAG conditions

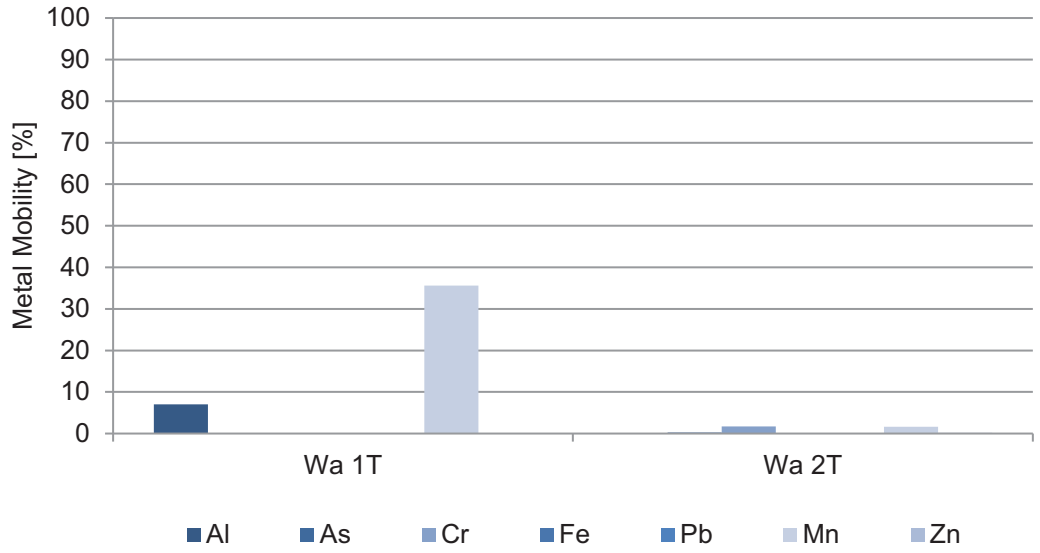

Figure 4-17 Mobilisation of the major metals for Waterberg coal wastes after reaction with 15% H_2O_2 solution during NAG conditions

4.2.3 Risk Assessment under ANC and NAG test conditions

Using the concentrations measured within the ANC (Table 4-10) and NAG (Table 4-11) test flasks for the Witbank and Waterberg ultrafine coal wastes, the risk assessment factors were calculated. Under ANC conditions, there exists a potential for negative environmental effects associated with the mobility of Fe and As elements. This was in contrast to the direct mobility results, where Pb solubilisation was higher than the As element. Similarly, for the Waterberg coal waste, although a high mobility of the Mn was observed, the concentration of this element was sufficiently low to result in a negligible environmental risk. Furthermore, a similar negligible environmental risk profile was observed for the elements of interest for the Waterberg sample.

Table 4-10 Risk assessment of the metal mobility under ANC conditions for the Witbank ultrafine coal sample

Environmental Significance		RPF / 1000	Coal Tailings Feed	Coal Flotation Concentrate	Coal Flotation Tails	Sulphide Flotation Tails
High	A	1000-10000				
	B	100-1000				
	C	10-100	Fe			
Moderate		1-10				As < Fe
Low		0.1-1	As	As		
Negligible		<0.1	Al<Pb	Al<Pb	As<Al<Fe<Pb	Pb<Al

Table 4-11 The environmental risks associated with the deportment of the elements of interest from the Waterberg coal waste following acid digestion during the ANC test

Environmental Significance		RPF / 1000	Coal Flotation Tails	Sulphide Flotation Tails
High	A	1000-10000		
	B	100-1000		
	C	10-100		
Moderate		1-10		
Low		0.1-1		
Negligible		<0.1	Al<As<Cr<Fe<Mn<Pb<Zn	Al<As<Cr<Fe<Mn<Pb<Zn

The risks associated with the elemental mobility under NAG testing are presented in Table 4-12 and Table 4-13 for the Witbank and Waterberg ultrafine coal wastes respectively. The increases in Fe mobility from the Witbank coal waste observed under the NAG conditions as compared to the ANC test conditions resulted in a “high” environmental risk potential of this element. A lower environmental risk was associated with the other elements of interest, possibly due to the lower H^+ concentrations in the NAG test flasks as indicated by the higher pH value. The elevated pH conditions observed in the leachate solution following NAG testing on the Waterberg coal waste led to a decrease in the leachate concentration of the elements of interest, particularly Fe, leading to a decrease in the associated risk for environmental degradation.

Table 4-12 Risk assessment of the elements mobilised under NAG test conditions highlighting the effects of the different test conditions on elemental deportment and subsequent environmental risk

Environmental Significance		RPF / 1000	Coal Tailings Feed	Coal Flotation Concentrate	Coal Flotation Tails	Sulphide Flotation Tails
High	A	1000-10000				
	B	100-1000				
	C	10-100	Fe	Fe	Fe	
Moderate		1-10				Fe
Low		0.1-1	As			
Negligible		<0.1	Al<Pb	As<Al<Pb	Pb<Al<As	Pb<As<Al

Table 4-13 Environmental significance of the elements mobilised under oxidative condtions during the NAG tests for the Waterberg ultrafine coal waste sample

Environmental Significance		RPF / 1000	Coal Flotation Tails	Sulphide Flotation Tails
High	A	1000-10000		
	B	100-1000		
	C	10-100		
Moderate		1-10		
Low		0.1-1		
Negligible		<0.1	Al<As<Cr<Fe<Mn<Pb<Zn	Al<As<Cr<Fe<Mn<Pb<Zn

4.2.4 Sequential Chemical Extraction tests and risk assessment

Analysis of the elemental concentrations and the associated risk factors following static ARD testing provided information regarding the mobility of the elements within these tests; however, the static ARD tests are conducted under severe chemical conditions. To gain a better understanding of the elemental deportment under conditions likely to occur within waste disposal scenarios, sequential chemical extractions were performed on both the Witbank and Waterberg process streams, with the measured elemental concentrations at each stage used to quantify the environmental risk associated with these concentrations.

The sequential chemical extraction tests consisted of sequential leaching of the coal wastes under increasing chemical reactivity. Following each leaching stage, the leachate solutions were collected, and the concentrations of the elements of interest quantified. These concentrations were used to partition the elements into the mineral phases targeted by each leaching stage. The results of the apportioning for the Witbank and Waterberg process streams are presented in Figure 4-18 and Figure 4-19 respectively.

Analysis of the elemental partitioning for the Witbank feed and de-sulphurised streams supported the separation results observed from the leachate chemistry. The Al-bearing phases associated with the Fe-oxyhydroxide and sulphide mineral phases reported in greater quantity to the coal concentrate stream than the 1st Tails stream. Similarly, a larger proportion of the Fe-bearing minerals which reported to 1st Tails was associated with the sulphide leaching conditions as compared to the coal concentrate stream. Furthermore, most of the Pb-bearing minerals associated with Fe-oxyhydroxides reported to the 1st Tails, with little reporting to the coal concentrate. With respect to the 2nd stage of the de-sulphurisation process, the Fe-bearing minerals associated with the sulphide minerals in the 2nd Tails were similar to those in the 1st Tails stream, suggesting a poor separation of the sulphide minerals under the conditions of the 2nd flotation stage in this instance. Similarly, the Pb-bearing, sulphide-like mineral phases were concentrated to the 2nd Tails stream, rather than the sulphide concentrate. The partitioning of the As-bearing minerals appeared similar throughout the de-sulphurisation process streams, suggesting equal deportment of the As-bearing mineral phases into all the process streams. The higher proportion of Fe-bearing mineral sulphides as compared to Fe-oxyhydroxides confirmed the Fe mobility results observed under the ANC and NAG tests, further suggesting the presence of an acid-insoluble sulphide mineral phase, most likely pyrite.

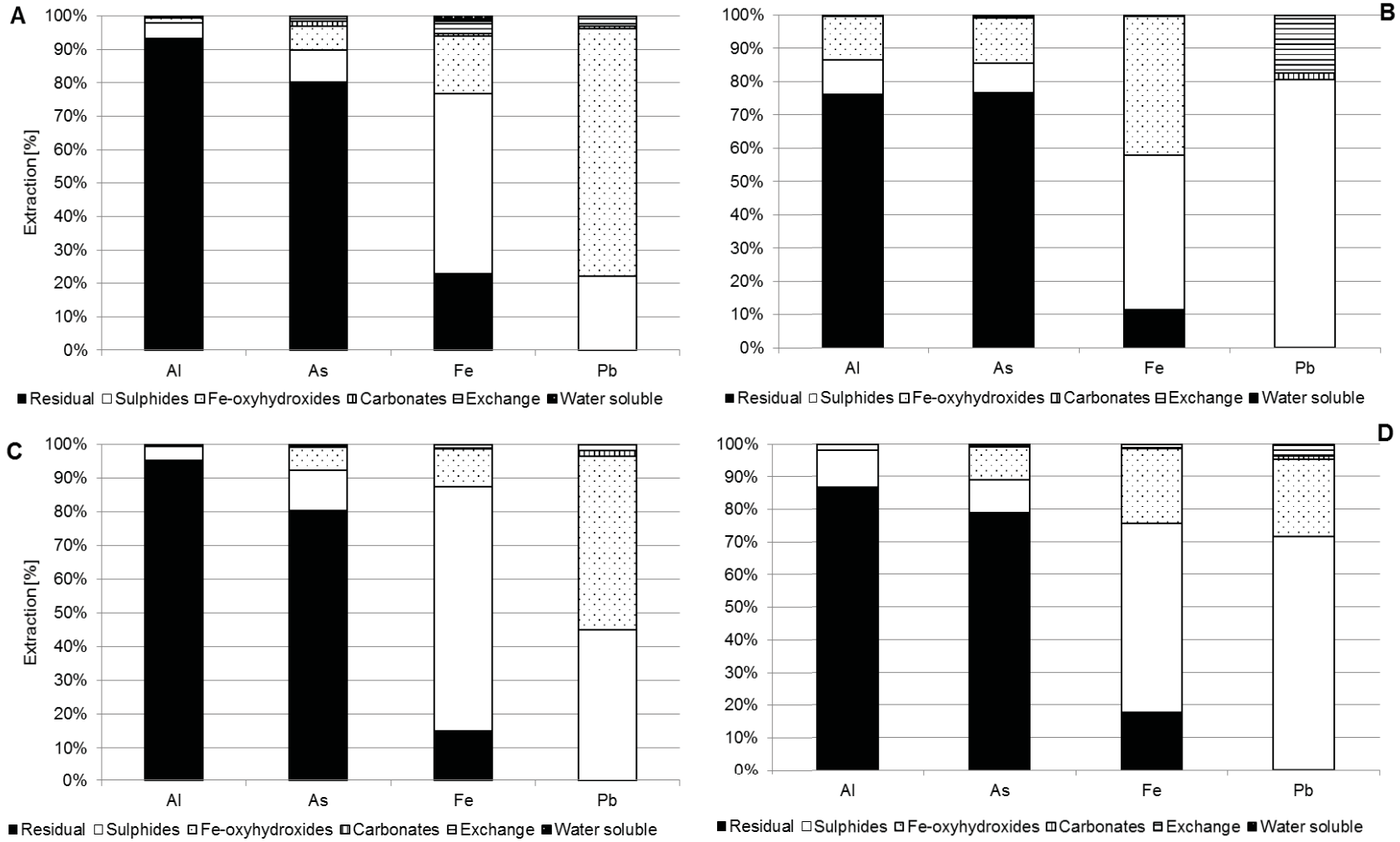

Figure 4-18 Partitioning of elements following sequential chemical extraction tests for the Witbank tailings feed stream (A), the Witbank coal concentrate stream (B), the coal flotation tails stream (C) and the sulphide flotation tails stream (D).

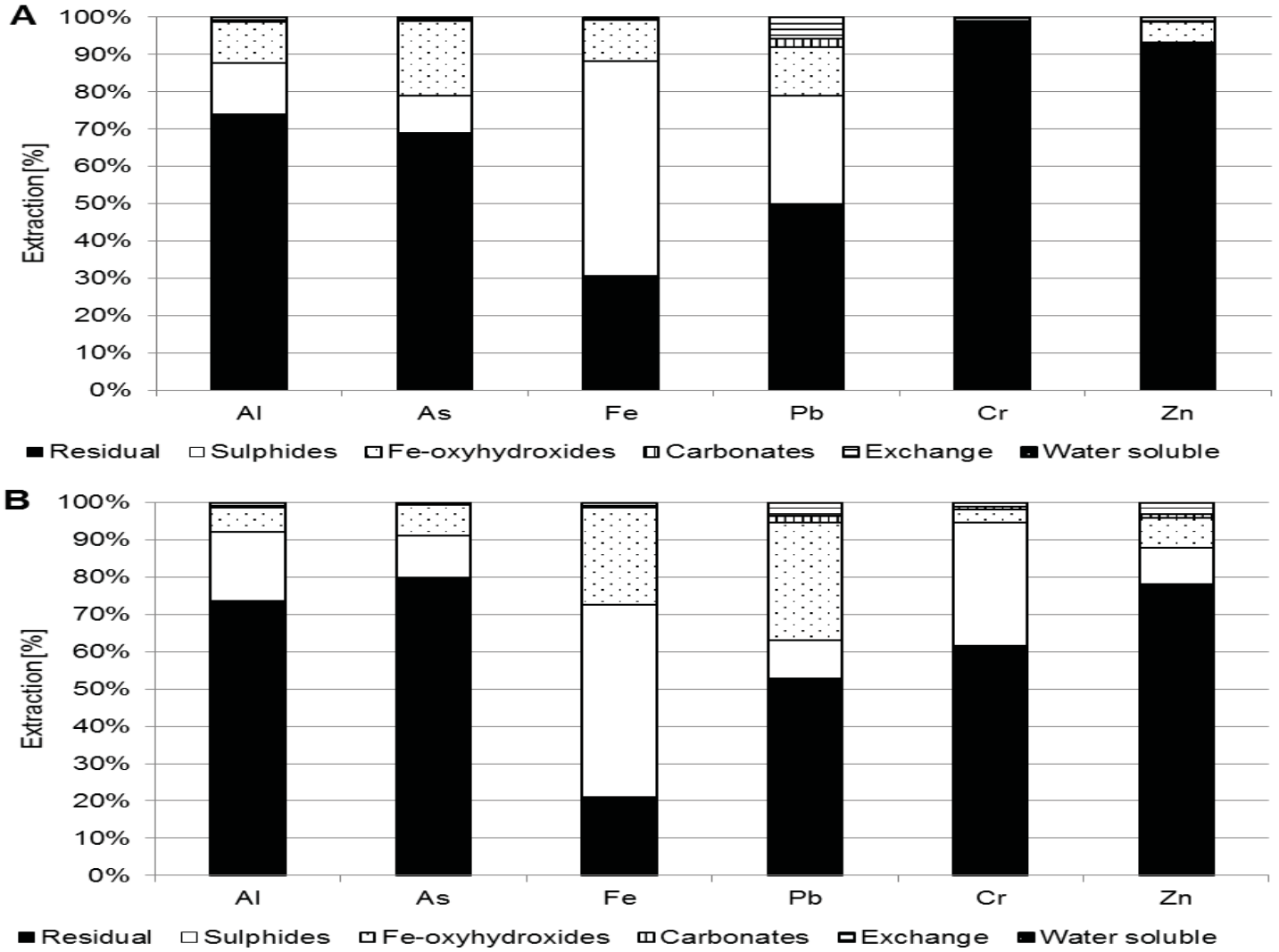

Figure 4-19 Sequential chemical extraction results for the Waterberg ultrafine coal floatation tails stream (A) and the sulphide flotation tails stream (B) showing the partitioning of the potential hazardous elements according to their reactivity phases

Similarly, analysis of the elemental partitioning for the Waterberg 1st and 2nd Tails process streams allowed for observations into the efficacy of the sulphide flotation stage for this coal waste sample. The similar partitioning profiles for the Al, As and Fe elements indicated a poor separation of the mineral phases bearing these elements within the sulphide flotation stage for this coal waste. In contrast, the differences observed in the partitioning of the Pb, Cr and Zn bearing minerals suggested the deportment of the Pb-bearing sulphides to the coal concentrate stream, while a concentration of the non-silicate associated Cr and Zn mineral phases to the 2nd Tails. The predominance of the sulphide mineral phases within the coal waste suggested a potential for significant elemental mobility under oxidative conditions, a result masked by precipitation reactions which would have occurred at the elevated pH conditions with the NAG tests.

Following an understanding of the elemental deportment with respect to the chemical leaching conditions gained from the sequential chemical extraction tests, environmental risk assessments were performed using the extents of mineral dissolution at each stage for both the Witbank and Waterberg coal samples. Throughout all stages of the SCE tests, the dissolution of Al metal anions did not pose an environmental risk. The Al element is largely concentrated within the silicate gangue minerals present within the coal wastes, which exhibit limited reactivity under ARD generating conditions. Therefore, although a total digestion of the coal waste indicated the potential for environmental degradation, no significant risks are associated with this element under disposal conditions.

Low and negligible environmental risks were obtained from the dissolution results for the first three stages of the sequential chemical extraction test, encompassing element deportment for the water soluble, exchangeable and carbonate fractions for the Witbank ultrafine processing streams. Significant environmental risks, however, were observed for dissolution of minerals within the Fe-oxyhydroxide and sulphide fractions (Table 4-14 and Table 4-15). Environmentally significant concentrations of the Pb and Fe elements were present in this phase for the 2nd Tails process stream, presenting a concern for the deportment of this element under acidic conditions within a waste deposit scenario. For these elements, the environmental risk associated with the potential elemental mobility remains the same between the feed and the 2nd Tails sample. However, the recovery of the sulphide concentrate streams as potential products from this coal waste, may hold potential for the desulphurisation process as the separation process did not add to the environmental risks associated with the disposal of the coal ultrafine wastes.

Table 4-14 Elements of environmental concern mobilised during the SCE test phase aimed at the dissolution of the Fe-oxyhydroxide minerals within the Witbank ultrafine coal waste

Environmental Significance		RPF / 1000	Coal Tailings Feed	Coal Flotation Concentrate	Coal Flotation Tails	Sulphide Flotation Tails
High	A	1000-10000				
	B	100-1000				
	C	10-100				
Moderate		1-10	Fe < Pb	As < Pb		Fe < Pb
Low		0.1-1	As	Fe	Fe < As < Pb	As
Negligible		<0.1	Al	Al	Al	Al

Table 4-15 Elements posing an environmental risk associated with the sulphide mineral phases and mobilised during stage 6 of the SCE test conducted on the Witbank ultrafine coal waste samples

Environmental Significance		RPF / 1000	Coal Tailings Feed	Coal Flotation Concentrate	Coal Flotation Tails	Sulphide Flotation Tails
High	A	1000-10000				
	B	100-1000				
	C	10-100	Fe	Fe	Fe	Fe
Moderate		1-10	As		As	
Low		0.1-1	Pb	As < Pb	Pb	Pb < As
Negligible		<0.1	Al	Al	Al	Al

Similarly, elemental concentrations posing a potential environmental risk were observed within stages 5 and 6 of the sequential chemical extraction method, targeting the Fe-oxyhydroxides and the sulphide minerals respectively for the Waterberg coal waste sample (Table 4-16). Significant risks exist with the dissolution of Fe and, to a lesser extent, As and Pb under the conditions experienced at these stages of leaching. Importantly, the conditions under which dissolution of the Fe-oxyhydroxides and sulphide minerals occur may easily be obtainable within waste disposal situations over time, even for samples with an overall “non-acid forming” classification as is the case for the Waterberg sample. Thus, the potential risk associated with the deportment of these elements is a true reflection of the environmental concerns associated with the disposal of the Waterberg ultrafine coal waste sample.

Table 4-16 The environmental risks associated with metal deportment for stage 5 and stage 6 of the sequential chemical extraction test performed on the Waterberg ultrafine coal waste

Environmental Significance		RPF / 1000	SCE Stage 5		SCE Stage 6	
			Coal Flotation Tails	Sulphide Flotation Tails	Coal Flotation Tails	Sulphide Flotation Tails
High	A	1000-10000				
	B	100-1000				
	C	10-100			Fe	Fe
Moderate		1-10	Fe<As	Pb<Fe	As	As
Low		0.1-1	Mn<Pb	Mn<As	Pb	Pb
Negligible		<0.1	Al<Cr<Zn	Cr<Zn<Al	Al<Cr<Mn<Zn	Al<Cr<Mn<Zn

4.3 Characterising Environmental Risks Associated with Sulphide-bearing Gold Wastes

Also presented as:
Opitz, Alexander; Becker, Megan; Harrison, Susan T.L.; Broadhurst, Jennifer L. (2016). Characterising Environmental Risks Associated with Sulfide-bearing Gold Wastes. In: Drebenstedt, C; Paul, M (Eds). IMWA 2016: Mining Meets Water – Conflicts and Solutions. pp 1050-1057. https://www.imwa.info/docs/imwa_2016/IMWA2016_Opitz_271.pdf

4.3.1 Introduction

The ecological impacts of pollution, including ARD, from gold mine wastes are often cumulative and their true impact may only be felt long after mining activities have ceased (McCarthy, 2011). Most commonly observed, are the immediate effects to the local flora and fauna; however, the contamination of water sources may lead to far-reaching consequences. In a study of the rivers and water sources

surrounding the Witwatersrand basin, Durand (2012) reported significant detrimental effects to local communities who use contaminated groundwater for drinking and subsistence farming. The environmental damage is not limited to animals, but may affect local soils, due to the accumulation of heavy metals and salts (Kitula, 2006). Reliable characterisation of the environmental risks associated with drainage runoff emanating from mine waste requires independent assessment of the potential to form acidity and the deportment of deleterious elements.

Evaluation of the ARD potential of waste samples can be achieved using standard ARD characterisation and prediction tools to assess the potential of waste samples to generate acidity. The independent quantification of the inherent acid-neutralising and acid-forming potentials is achieved through laboratory-scale test work, with their difference used to assess overall acidity generation (Price, 1997). Following the classification of the samples, kinetic tests can be performed on those which show acid generating potential, or for which uncertainty in the classification is observed. The kinetic tests characterise the time-dependence of the ARD generation and the composition of the resulting pollution with time (Parbhakar-Fox & Lottermoser, 2015).

While standard static characterisation tests provide a rapid assessment of the overall acid generating potential, these results are limited to the extreme chemical condition of the test methods. No information is gathered on the potential for ARD generation under microbial conditions most commonly experienced within waste deposits (Hallberg, 2010). The recent development of the biokinetic tests to account for microbial action has been demonstrated on base metal wastes (Hesketh, et al., 2010a), gold wastes (Dyantyi, et al., 2013) and coal ultrafine wastes (Opitz, et al., 2015). Furthermore, the exclusive focus on the potential for acidity generation as a proxy for ARD formation results in a lack of information regarding the deportment of deleterious elements from the waste sample during the characterisation step, particularly the environmental consequences associated with the elevated elemental concentrations within neutral drainage (Plante, et al., 2010). These samples are classified as non-acid generating and are, as per the standard screening protocols, not typically subjected to further test work (Parbhakar-Fox & Lottermoser, 2015).

Measurement of the elemental concentrations in solutions resulting from the static characterisation test may provide information regarding metal deportment under severe conditions, with the addition of sequential chemical extractions allowing for semi-quantitative information of elemental deportment under disposal conditions (Opitz, et al., 2015). The inclusion of a detailed mineralogical assessment allows for a fundamental understanding of the geochemical behaviour of waste samples within ARD characterisation tests (Becker et al., 2015). The inclusion of mineralogical analyses of waste samples in the current characterisation toolbox, either as a co-current characterisation step (Maest, et al., 2005) or a preceding characterisation step (Parbhakar-Fox, et al., 2013), was suggested previously. However, the integration of such analyses within the common ARD characterisation protocols remains limited.

The present study was undertaken to demonstrate the integrated use of test methods to analyse for the potential for acidity generation and elemental deportment for two sulphide-bearing gold wastes. In addition to experimental tests performed, analysis of sample mineralogy provided a fundamental understanding to the observed acidity generation and elemental deportment results.

4.3.2 Materials and methods

4.3.2.1 Gold waste samples

Two mine waste samples were used in the completion of this study. Sample A was sourced from a greenstone belt gold deposit. The second waste sample (B) was sourced from a historical tailings dam, generated during the processing of a Witwatersrand gold ore deposit. The compositions of the two waste samples are presented in Figure 4-20 (Opitz, et al., 2016b). Acid generating minerals consist predominately of pyrite (A:1.2 wt. %, B: 0.3 wt. %) and pyrrhotite (A: 5.8 wt. %, B: 0.1 wt. %), with small (< 0.1 wt. %) concentrations of other metal sulphides. These trace phases consist predominately of chalcopyrite, galena, and pentlandite. Acid consuming phases within the waste samples consist predominantly of fast-weathering carbonates (A: 0.9 wt. %, B: 0.01 wt. %), with intermediate-weathering

silicates such as chlorite (A:1.4 wt. %, B: 1.4 wt. %) and slow weathering Fe-oxides phases such as magnetite (A: 33.4 wt. %, B: 1.9 wt. %) also present. The majority of the waste samples, however, consist of non-reactive silicate minerals such as quartz (A:26 wt. %, B: 70.9 wt. %) and plagioclase (A: 13.5 wt. %, B: 23.9 wt. %).

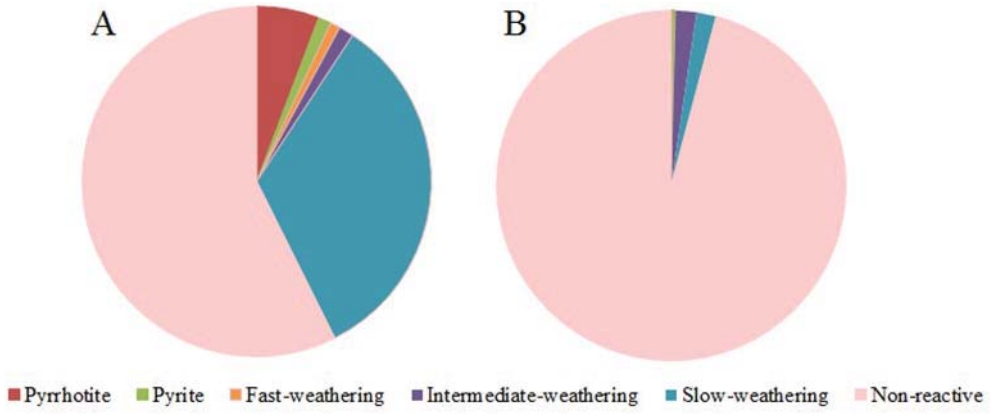

Figure 4-20 Results from the mineralogical analysis using QEMSCAN on the two gold waste samples indicating the acid-generating minerals, pyrite and pyrrhotite, and acid-consuming minerals, carbonates, chlorite and magnetite as fast-, intermediate- and slow-weathering respectively, and non-reactive mineral phases

4.3.2.2 Characterisation of the ARD potentials

The ARD potentials of the waste samples were estimated directly from sample mineralogy in accordance with the method developed by Paktunc (1999) using the difference in the theoretical acidity generated by the acid-forming minerals and consumed by the acid-neutralising phases. Standard acid base accounting tests (ABA, Lawrence and Scheske (1997)) were used to calculate the maximum potential acidity (MPA), on the basis of LECO analysis of total sulphur, and the acid neutralising capacity (ANC), determined empirically, of the waste samples. These tests were performed in conjunction with net acid generation tests (NAG, Miller et al. (1997)) in triplicate. To assess the potential for ARD generation, biokinetic tests were performed according to the method outlined by Opitz et al. (2016c) at 37°C for 90 days.

4.3.2.3 Sequential Chemical Extraction tests

Sequential chemical extraction tests were performed using a method outlined by Broadhurst et al. (2009). In this test, the waste sample is subjected to a sequential chemical leach protocol, to determine the distribution of metals to seven different fractions: water soluble, ion-exchangeable, carbonate, amorphous Fe/Mn-oxide, crystalline Fe/Mn oxide, sulphide and residual/inert.

4.3.2.4 Environmental risk assessment

The environmental risks associated with the deportment of the deleterious elements were assessed using a ranking and scoring method as outlined in Broadhurst and Petrie (2010). Here, elements are ranked and scored according to their potential environmental significance, as determined from their leachable concentration levels derived from the SCE tests, their acceptable risk concentrations as derived from water quality limits (DWAF, 1996), and their typical crustal abundance. Elements of interest were identified based on common deleterious elements within gold waste deposits (Opitz et al., 2016), with the deportment of As, Cu, Cr, Ni, Pb, and U presented. Elemental concentrations were quantified using induced coupled plasma mass spectrometry (ICP-MS) analysis using a Thermo-Fisher X-series II quadruple ICP-MS machine.

4.3.3 Results and discussion

4.3.3.1 Characterisation of the potential for acidity generation

Mineralogical Assessment

The results in Table 4-17 indicate that both samples can be classified as potentially acid generating due to the greater quantities of acid forming phases relative to the acid neutralising phases. The higher acid forming potential for Sample A as compared to that observed for Sample B, can be attributed to the greater quantity of pyrrhotite and pyrite minerals (see Figure 4-20). Similarly, the higher content of the fast-weathering minerals resulted in a greater acid-consuming potential for Sample A as compared to Sample B where the majority of the acid-consuming minerals were intermediate- and slow-weathering phases.

Table 4-17 Theoretical ARD estimates using the mineralogical composition

Sample	Acid-forming Potential [kg H_2SO_4/ton]	Acid-consuming Potential [kg H_2SO_4/ton]	ARD Estimate [kg H_2SO_4/ton]	ARD Classification
A	83.9	9.1	74.8	Potentially acid forming
B	6.7	0.3	6.4	

Static ARD characterisation tests

Significant discrepancies were observed in the quantitative acid-generating and acid-neutralising results between the mineralogical and static ARD tests (Table 4-18). The observed differences in AP and MPA calculations were due to differing sulphide values obtained from chemical and mineralogical analysis, with the LECO total sulphur method resulting in lower sulphide sulphur (A: 2.3 wt.%, B: 0.06 wt.%) than calculated from the pyrrhotite and pyrite content (A: 2.8 wt.%, B: 0.2 wt.%). On assessing different methods for determining total sulphur in geological samples, Czerewko et al. (2003) observed significant under-estimations in the total sulphur content for low-sulphur samples using LECO analysis. For the samples in this study, an under-estimation in the total sulphur content would explain the lower MPA values compared to the AP values estimated directly from sample mineralogy. Differences in calculated acid-consuming potentials may be due to the presence of intermediate- and slow-weathering minerals not being accounted for in the mineralogical estimates. Becker et al. (2015) indicated partial dissolution of these minerals phases under the relatively aggressive ANC test conditions, resulting in a higher neutralizing capacity than that predicted from quantification of the fast-weathering acid neutralizing minerals.

Although differences were observed between the estimates based on mineralogy and the static ARD test results, the overall ARD classification was unchanged for all tests for Sample A. Similarly, the NAPP results suggests a potentially acid generating classification (-20 < NAPP < 20) corresponding to that from the mineralogical estimate in the case of sample B. The elevated NAG pH value (pH 4.0 < NAG pH), however, suggested a “non-acid forming” classification for Sample B. The overall classification of the ARD potential for this sample, therefore, remained uncertain due to these discrepancies.

Table 4-18 ARD test results following static characterisation tests performed in triplicate

Sample	MPA [kg H_2SO_4/ton]	ANC [kg H_2SO_4/ton]	NAPP [kg H_2SO_4/ton]	NAG pH [kg H_2SO_4/ton]	ARD Classification
A	70.2 ± 0.7	53.2 ± 1.8	17.0 ± 1.9	2.5 ± 0.0	Potentially acid forming
B	1.9 ± 0.4	3.9 ± 0.5	-2.1 ± 0.3	6.5 ± 0.1	Uncertain

Biokinetic Tests

The pH profiles within biokinetic tests provided an indication of the relative rates of acid formation and acid consumption under the acidic, microbial conditions (Figure 4-21). The observed initial rise in solution pH for Sample A can be attributed to the dissolution of the fast-weathering carbonate minerals. The rapid decrease in solution pH thereafter was due to ferric iron precipitation and, below pH 3.5, sulphide mineral oxidation by ferric iron, as (re)generated by Fe^{2+}-oxidising micro-organisms. The biokinetic test results confirmed the potentially acid generating classification of Sample A as characterised by the static tests and mineralogical evaluation.

For Sample B, the lack of initial changes in solution pH was indicative of the lack of fast-weathering carbonate minerals within the waste sample, consistent with the mineralogical composition (Figure 4-20) and low ANC determined (Table 4-18). The subsequent absence of significant changes in solution pH with time further indicated no net acidity generation or consumption within the tests, with any acidity generated from the oxidation of the sulphide minerals neutralised by the intermediate- and slow-weathering minerals. The slight increase in solution pH was attributed to a combination of the addition of distilled water to account for the volumes lost to evaporation, and the acid consumption of the intermediate- and slow-weathering mineral phases as determined from sample mineralogy. The biokinetic test results supported a non-acid forming classification for Sample B as opposed to the potentially acid forming classification from the acid-base accounting and mineralogical estimates.

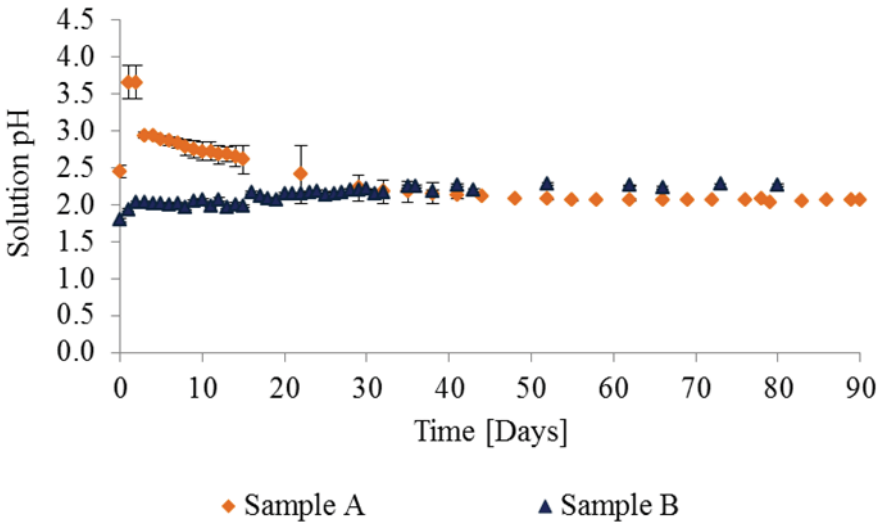

Figure 4-21 pH profiles from biokinetic tests performed at 37°C on waste samples A and B

Sequential chemical extraction (SCE) tests

Leachable element concentration levels and relative extents of mobilisation under the SCE tests conditions are presented in Table 4-19 and Figure 4-22 respectively. A comparison of results in Table 4-19 indicates that, with the exception of Cr and Ni and, to a lesser extent, leachable elemental concentrations are far higher for sample B. This is particularly so in the case of As and U. Furthermore, the relatively high mobility of elements in the leach stage 1-5 for waste sample B is indicative of the weathered nature of the sample. This is consistent with the origin of the waste, indicating natural oxidative dissolution of primary sulphide minerals such as arsenopyrite, chalcopyrite, galena, pentlandite and uraninite, and the subsequent re-precipitation of the solubilised metal ions in the form of more reactive secondary minerals and salts. These mineral forms are more readily available for dissolution at circa-neutral pH and non-oxidative acid leach conditions within the waste deposit.

Although a fairly significant percentage of the As, Pb and U in Sample A is mobilised in the first 5 leach stages, indicating some weathering, leachable concentrations remain relatively low. The majority of the Cr, Cu and Ni, furthermore, was associated with the primary sulphide phase, and only mobilised under

acidic, oxidative conditions. This was congruent with the sample mineralogy which indicated significant association of Cr, Cu and Ni with primary chromite, chalcopyrite and pentlandite minerals respectively.

Table 4-19 Leachable elemental concentrations from the SCE tests for sample A and Sample B showing concentrations available for deportment

Element	Sample A [mg/kg]				Sample B [mg/kg]			
	Stages 1-3	Stages 4-5	Stage 6	Total (Stages 1-6)	Stages 1-3	Stages 4-5	Stage 6	Total (Stages 1-6)
As	2.2	0.7	2.5	5.3	4.5	64.7	27.1	96.3
Cr	5.8	50.0	403	459	1.7	8.7	25.4	35.8
Cu	1.2	12.3	68.3	81.7	70.6	99.5	9.7	180
Ni	15.6	30.0	210	255	7.5	8.7	11.1	27.3
Pb	3.2	3.0	2.3	8.5	13.7	99.6	4.6	117
U	0.1	0.2	0.3	0.7	23.2	5.2	3.7	32.1

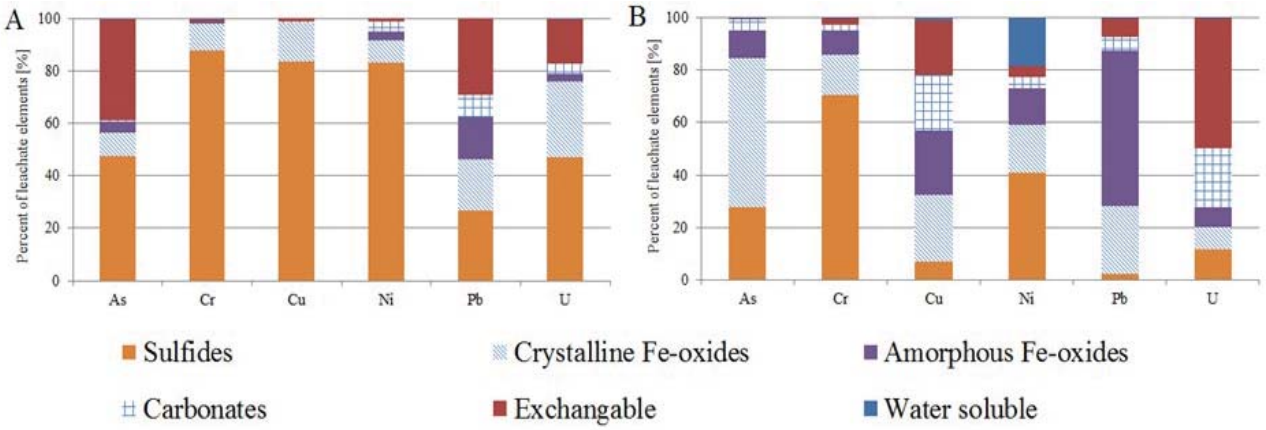

Figure 4-22 Relative extents of mobilisation of leachable elements during sequential chemical extraction (where 100% represents the total leachable concentrations over the 6 stages presented)

4.3.3.2 Environmental risk assessment

The risks associated with the elemental concentrations from the SCE tests are presented in Table 3. As a result of the relatively low concentrations of leachable elements in Sample A, particularly in readily soluble forms (SCE stages 1-5), only Ni and, to a lesser extent, Cr pose a potential risk to the environment, and then only under oxidizing acid leach conditions. As indicated above, this can probably be attributed to the dissolution of primary pentlandite (Ni) and chromite (Cr) under the relatively aggressive leach conditions consistent with stage 6 of the SCE test

The relatively high concentrations of leachable elements and weathered nature of Sample B, however, resulted in a significantly higher environmental risk profile, even under relatively mild leach conditions. In particular, a significant environmental risk was associated with the deportment of As, U and Pb across all stages. “High” risks were associated with U deportment under the stages targeting the water soluble and carbonate mineral phases (stages 1-3), and with Pb and As under the stages targeting the acid soluble Fe-oxide phases and sulphide phases resulted in significant environmental risks during the final three stages of the SCE tests.

Table 4-20 Environment risk assessment of elemental deportment measurements from SCE tests on wastes samples A and B

Environmental Significance	Risk factor	Sample A			Sample B		
		Stages 1-3	Stages 4-5	Stage 6	Stages 1-3	Stages 4-5	Stage 6
High	> 10			Ni	U	As, Pb	As
Moderate	1-10			Cr	As, Pb		
Low	1	Ni	Ni	As		U	Pb, U

4.3.4 Concluding remarks on environmental risks associated with gold wastes

The current study highlights the use of a combination of mineralogy, geochemical and chemical leach tests, together with a simple environmental risk assessment method to provide a rapid characterisation of the acid-generating potentials and trace metal deportment risks associated with sulphide-bearing wastes. The integration of the results allowed for an understanding of the minerals responsible for the acid-generating behaviour of the waste samples, and the conditions under which the elemental deportment is likely to occur. This information is key in providing guidance for more detailed risk assessment procedures, and to inform relevant risk mitigation strategies.

4.4 Conclusions: Water-Related Risk in Mine Wastes and Waste Remediation

Analysis of the ARD generation potential through a selection of approaches, including mineralogy-based calculations, acid-base accounting, the combination of NAPP and NAG analyses and batch biokinetic tests, coupled with sequential chemical extraction analysis to determine potential for metal deportment and its associated environmental risk analysis, has been applied to both coal and gold mine waste to demonstrate its potential to provide a more complete assessment of the material over a limited time span. The value of these tests has been further explored through applying them to the set of streams generated on desulphurising the fine coal waste through two-stage flotation to yield a coal concentrate, a sulphide concentrate and a final, low sulphide tailings, the latter being the bulk volume. For each of the coal and gold waste materials, two different samples were selected.

The results of the two-stage desulphurisation process performed on two ultrafine coal wastes provided insight into the overall environmental risks associated with both the feed coal waste and the “product” or final waste streams. For the Witbank coal waste, a poor separation was observed in the 2nd stage of the desulphurisation process, resulting in a 2nd Tails with a significant total sulphur content. In contrast, the separation observed during the same stage for the Waterberg ultrafine waste resulted in an appreciable decrease in total sulphur content as compared to the feed stream.

ARD static testing conducted on the process streams for the Witbank coal waste revealed that although the 2-stage desulphurisation process resulted in a decrease in total sulphur content, the 2nd Tails retained its potentially acid generating classification. This was, in part, due to the low acid neutralising component relative to the total sulphur content of this coal waste. Conversely, ARD static testing of the Waterberg samples revealed a “non-acid forming” classification for the 2nd Tails stream, indicating the overall net acid neutralising ability of this process stream. The static ARD classifications for the acid generating potential for both coal waste samples, as well as the relative abundance of the acid generating and acid consuming components, was confirmed through the use of biokinetic ARD tests.

Following the classification of the process streams for the two coal wastes, the environmental risks associated with the deportment of hazardous elements within the coal waste was explored, with particular attention paid to the “benign” 2nd Tails process stream. Through use of total sample digestion and measurement of the soluble elements within the leachate solution, Al, As, Fe and Pb were identified as elements with potential environmental risk for the Witbank sample, while Cr, Mn and Zn associated with the Waterberg ultrafine coal waste. Analysis of the leachate solutions generated from the static ARD characterisation tests identified As and Fe as the elements of particular environmental concern for

the Witbank sample under these conditions. The differences between the degree of mobility of elements, in particular Fe, suggested the presence of non-acid soluble mineral phases, such as pyrite, within the coal waste and that these contained elements of potential risk. For the results of the tests using the Waterberg sample, no environmental concern associated with the identified elements was observed, in part due to the elevated pH conditions under the NAG tests.

To aid in the understanding of the differences observed between the mobilities under ANC and NAG conditions, sequential chemical extractions were performed which partitioned the element-bearing mineral phases with respect to conditions causing their leaching. Furthermore, this approach was used to assess potential risks associated with the deportment of elemental species under conditions typical to waste disposal scenarios. It was found that there was little difference in the overall environmental risks associated with the mobility of the elements of interest between the feed and 2nd Tails process streams for the Witbank sample, suggesting incomplete separation, potentially because of incomplete liberation of the sulphidic minerals. Application of the two-stage flotation process would serve to decrease the volume of potentially hazardous material requiring disposal and would be aided by improved separations.

For the Waterberg stream, it was found that although the 2nd Tails did not possess the overall potential to form acidity, environmental risk associated with the deportment of Fe, As and to a lesser extent Pb, remained. This was in contrast with the results obtained from analysis of the leachate solutions following static ARD testing. This result was particularly illuminating given the overall “non-acid generating” classification and served to accentuate the importance of using a suite of relevant tests to ascertain the overall environmental risk.

Application of the 2-stage desulphurisation process was successful in recovering a saleable coal product and decreasing the potential for the generation of acidity for both Witbank and Waterberg ultrafine coal wastes. However, the further analysis of metals in the leachate streams and application of SCE analysis highlighted the importance of assessing metal deportment.

Similarly, a combination of mineralogy, geochemical and chemical leach tests as well as a simple environmental risk assessment were used to analyse two mineral waste samples from processing of gold-bearing minerals. These sought to enable rapid characterisation of acid generation potential and trace metal deportment risks associated with sulphide-bearing wastes. The combined use of mineralogy, static tests and biokinetic tests improved understanding of the minerals responsible for acid generation from waste samples. Combination of metal analysis in leachates and the SCE analysis highlighted conditions for elemental deportment and key metals of concern. This information is key in providing guidance for more detailed risk assessment procedures, and to inform relevant risk mitigation strategies.

The approach has demonstrated, across mining sectors, that in addition to assessing acidity, it is also important to consider the overall environmental risks, including metal deportment. This is especially important in considering the re-purposing of these waste streams. The potential environmental risks associated with the mineral waste streams necessitate careful consideration in suitable disposal of these streams. Furthermore, investigations into potential applications or re-purposing for the “benign” and “sulphide-rich” process streams need to be cognisant of the potential deportment of hazardous elements within these wastes.

CHAPTER 5: STANDARDISATION OF THE BIOKINETIC TEST

5.1 Introduction to the Standardisation of the Biokinetic Test

The additional value of application of the biokinetic test over only using the static tests for characterisation of ARD generation potential has been demonstrated in the preceding chapters. In the development of the laboratory-scale biokinetic test to date, focus was placed on providing proof of concept and interrogating the value of data from the tests in the characterising of ARD generation potential and being fit for use in modelling for prediction of ARD. Having demonstrated its value, it is now necessary to determine fully the impact of operating variables on the data set and to optimise the test to ensure its robustness, reproducibility and potential for sound interpretation.

In Chapters 5 to 8, experimental studies are presented to address the refinement of the batch biokinetic test (Chapter 5 and 6) and the development of an "open system" biokinetic test (Chapter 7 and 8). In Chapter 5, we introduce the pH-controlled and non-controlled biokinetic tests and seek to provide understanding of the effect of grind size and solids loading on the batch biokinetic study. In Chapter 6, we address the effect of inoculum properties on the duration and results of the test. In developing an "open system" biokinetic test, a "draw-and-fill" semi continuous shakeflask test is considered in Chapter 7 and a flow-through unsaturated column test in Chapter 8.

Based on these findings, it is intended to propose a rationale for selecting appropriate test conditions for the biokinetic test assay. The need for the assay conditions to take cognisance of the characteristics of the samples to be analysed is addressed.

5.2 Materials and Methods for Study on Effects of Operating Conditions on the Biokinetic Test

5.2.1 Mineral preparation

A low grade copper ore (Spence ore) was used for this study. A mass of 20 kg was received as crushed rock of approximately 5 mm in diameter. The ore was representatively split into 10 kg samples using a riffle splitter. After splitting, 10 kg was further crushed using the retch grinder (Department of Geology, University of Cape Town). The crushed ore was screened using sieve sizes 425 to 600 µm on a shaker. The remaining 10 kg was stored in a bucket and sealed to prevent oxidation.

After screening the low grade copper ore, a 600 g portion of the 425-600 µm fraction was selected. This is referred to as the head sample. This 600 g portion was representatively split into five equal fractions using a Dickie & Stockler splitter. Each 120 g fraction was milled using a rod mill for 15, 30, 45 and 60 seconds respectively. Ten rods of 260 mm x 25mm were used in a 3 ℓ coal mill at the Centre for Minerals Research laboratories (CMR, University of Cape Town). The milled fractions were then representatively split using a 10-pot rotary riffle or an 8-way Fritsch rotary sample divider or both. The particle size distribution (PSD) was determined using Malvern Mastersizer

5.2.2 Mineral and elemental analysis

The elemental composition of the low grade ore was analysed using x-ray fluorescence spectroscopy (XRF) and quantitative evaluation of minerals (QEMSCAN). Mineral groups were also analysed using QEMSCAN as well as quantitative x-ray diffraction (QXRD). In addition, QEMSCAN was used to identify the liberation and association properties of the mineral groups in the low grade copper ore. The grain size distribution of chalcopyrite and pyrite was determined.

5.2.3 The biokinetic test: the effect of varying solids loading

5.2.3.1 Non-controlled pH batch biokinetic test

The low grade copper ore was milled for 15 seconds giving a particle size distribution of D_{50} 400 µm (D_{10} of 20 µm and D_{90} of 700 µm, i.e. larger than typically used in the biokinetic test). It is noted that this represents a larger size than previously used for biokinetic tests where the mineral sample was screened as passing 150 µm. A 10-pot rotary riffle splitter and an 8-way Fritsch rotary sample divider were used to representatively split the sample into 3 g (2%w/t), 7.5 g (5%w/t) and 12 g (8%w/t) solid loading. These solid loadings were used for the biokinetic test where four flasks per solid loading were set up.

To remove inherent oxidation present in the milled samples, each solid loading mass was added into a 500 mL shake flask with 150 mL autotrophic basal salt (ABS) set to pH 2 using concentrated sulphuric acid and incubated overnight in a 30°C incubator at 150 rpm. The ABS contained 0.5 g/L of ferrous sulphate solution in order to stimulate microbial oxidation for ferric production to oxidise sulphidic components of the low grade copper ore.

After the overnight incubation period, the flask pH was corrected to pH 2 using concentrated sulphuric acid (96-98%).The flasks were then inoculated with $1*10^7$ cells/mL consisting of a mixed mesophilic culture dominated by *Acidithiobacillus ferrooxidans* and *Leptospirillum ferriphilum,* taken from the 35°C stock reactor and mixed with *Acidithiobacillus thiooxidans* dominated sulphur-oxidizing mixed culture to provide a culture with adequate sulphur and iron oxidisers. The flasks were topped up with acidified water to a total volume of 200 mL and the initial pH was set at pH 1.85 and allowed to increase without modification.

The flasks were set on an orbital shaker at 150 rpm and 37°C for a period of 90 days. During this 90 day period, the mineral sample was subjected to microbial leach conditions which enable the simulation of the biotic and acidic ARD environment. The flasks were sampled daily. Leachate was analysed for changes in pH, redox potential, total iron and ferrous iron concentrations and conductivity.

The pH measurements were made using a Metrohm 713 pH meter. The redox potential was measured using a Metrohm 704 Eh meter against a silver/ silver chloride reference electrode. Conductivity was measured using an YSI model Pro 30 (SN: 9810153AT) electrode. The electrode measures salinity, conductivity and temperature. Ferrous iron concentrations were determined colorimetrically using the 1-10 phenanthroline method using a Helios α UV-Vis spectrophotometer at 510 nm (APHA, 1998). Total iron was measured using the same method but following addition of excess hydroxylamine to the sample to promote the reduction of any Fe^{3+} ions to Fe^{2+} (APHA, 1998). Concentrations were quantified against a standard curve.

The setup of the abiotic control was similar to the non-controlled pH biokinetic test where 7.5 g (5%w/t) was used with the exception that no microbial inoculation was undertaken.

5.2.3.2 Controlled pH batch biokinetic test

The controlled pH biokinetic test allows the accelerated leaching of the minerals such that acid neutralising minerals released into solution are depleted using sulphuric acid, thereby maintaining conditions that reflect the acidic environment following onset of ARD and which support acidophilic microorganisms. The controlled pH tests were set up in the same manner to those of the non-controlled pH tests with the exception that, in the controlled pH biokinetic test, the initial pH is set at pH 1.8 and then maintained at pH 1.8 by daily titration using 0.5 M H_2SO_4. The amount of sulphuric acid added was recorded, giving the number of protons needed to maintain the sample pH at 1.8. The addition of sulphuric acid accelerates the depletion of acid consuming minerals. Under these conditions the acidophilic culture continues to leach the mineral under acid leaching conditions.

5.2.4 The biokinetic test: The effect of varying particle size

The influence of different particle sizes on the results of this test was investigated. Different batches of low grade copper ore were milled for 30, 45 and 60 seconds each, giving a particle size distribution represented by a D_{50} of 320, 210 and 110 µm respectively as determined using the Malvern analyser. The 10-pot rotary splitter and an 8-way Fritsch rotary sample divider were used to representatively split each of the milled fractions to a final solid loading of 7.5 g (5%w/t). Three replicates were set up per mill time. Due to the soft texture of the mineral, particle size was described as a function of mill time rather than as size.

The flasks were set up in the same way as the solid loading biokinetic tests (non-controlled pH biokinetic flask), the difference being a constant solid loading of 7.5 g (5%w/t) which was used for all test conditions and with varying particle size.

5.3 Results and Discussion

5.3.1 Characterisations of the feed

5.3.1.1 Bulk mineral analysis

The mineralogy of the low grade copper ore was obtained through QEMSCAN and X-ray diffraction (XRD) analysis. The most dominant acid consuming minerals present were inert quartz (41.5 wt%) followed by mica (muscovite) (24.9 wt%) and K-Feldspar (17.08 wt%). These minerals are slow weathering (Buckwalter-Davis, et al., 2015; Eary, 2006). The leading acid producing mineral was pyrite (7.62 wt%) followed by chalcopyrite (1.60 wt%). All other minerals detected by QEMSCAN and XRD were below 0.1 wt%.

5.3.1.2 Particle size distribution

The Malvern Mastersizer was used to determine the particle size distribution of the head sample (not milled) and the milled fractions. The particle size distributions are presented in Figure 5-1. The particle size distribution of the head sample showed a D_{50} of 425 µm. All other size fractions were milled from this fraction. The results showed that the 15, 30, 45 and 60 second milled fraction had a D_{50} of 400, 320, 212 and 110 µm respectively. These samples presented a D_{10} of 50, 20, 10, 5 and 4 µm for the head sample and 15, 30, 45 and 60 second milled samples respectively and D_{90} of ~500 µm for the 45 and 60 s samples and of 700 µm for the remaining samples.

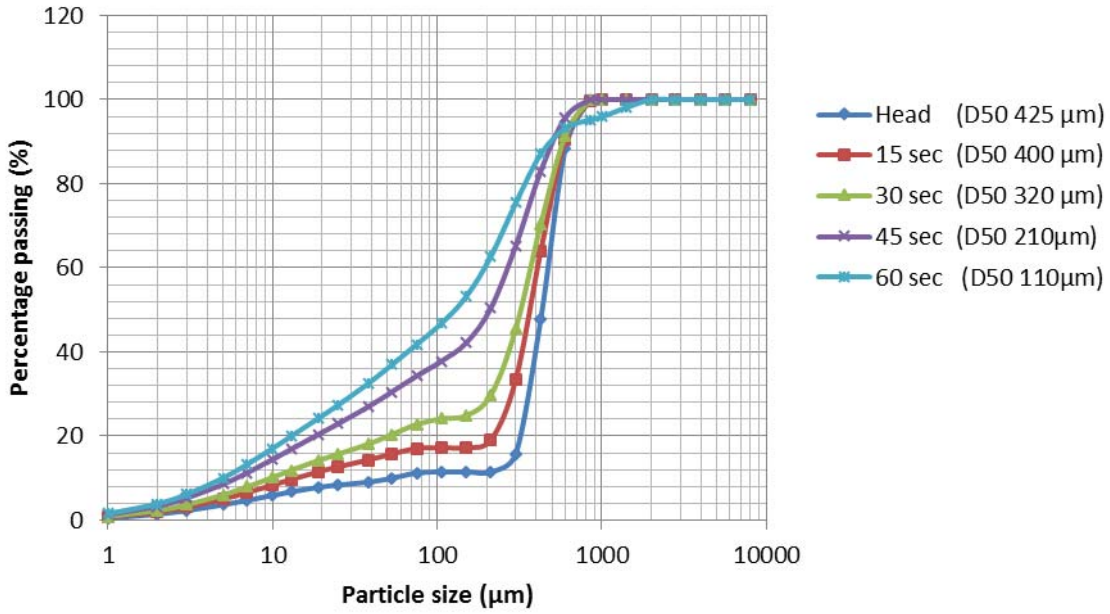

Figure 5-1 Particle size distribution of the head sample and the 15 sec milled fraction used to conduct the solid loading experiment

5.3.1.3 Grain size distribution

In addition to the particle size distribution, the distribution of the grain size, which is the size of single mineral entities, was deemed significant. A grain size distribution for the head and milled fractions of the major sulphides chalcopyrite and pyrite was analysed using QEMSCAN. This was important in understanding how the grain size in addition to the particle size influences both the generation of ARD as well as the characterisation of sulphide containing ores. The QEMSCAN grain size distribution analysis indicated that pyrite contained larger liberated grain sizes compared to chalcopyrite (Figure 5-2 and Figure 5-3). The impact of this is explored through the textural analysis in Section 5.3.1.4. The relative dimensions of particle size and grain size impact the degree of liberation, the latter being presented in the following section.

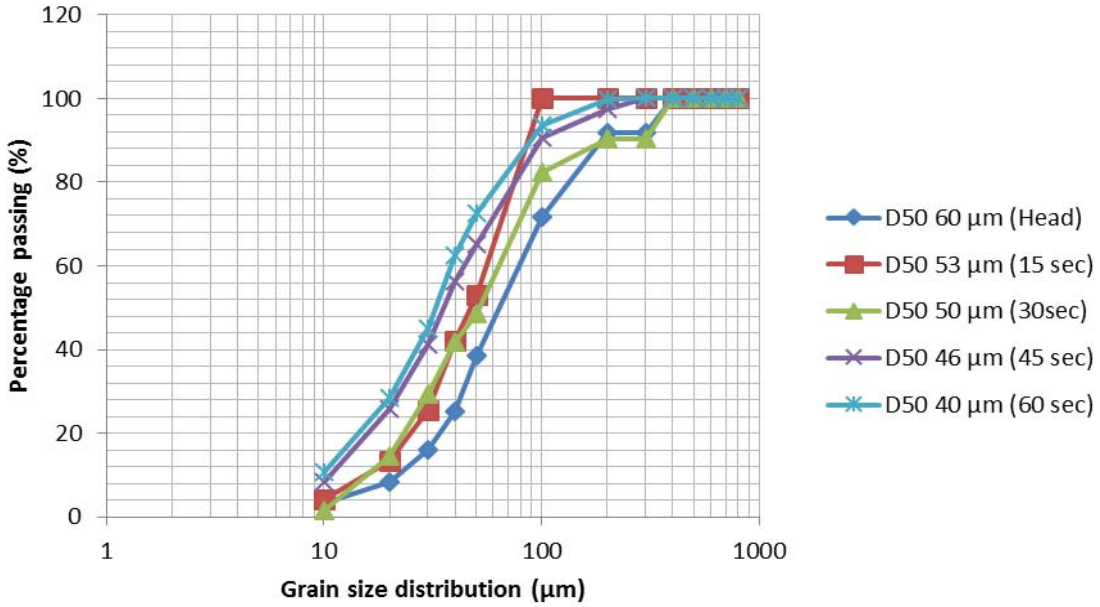

Figure 5-2 Grain size distribution of chalcopyrite in the head, 15, 30, 45 and 60 second milled samples. D_{50} values are given in the legend.

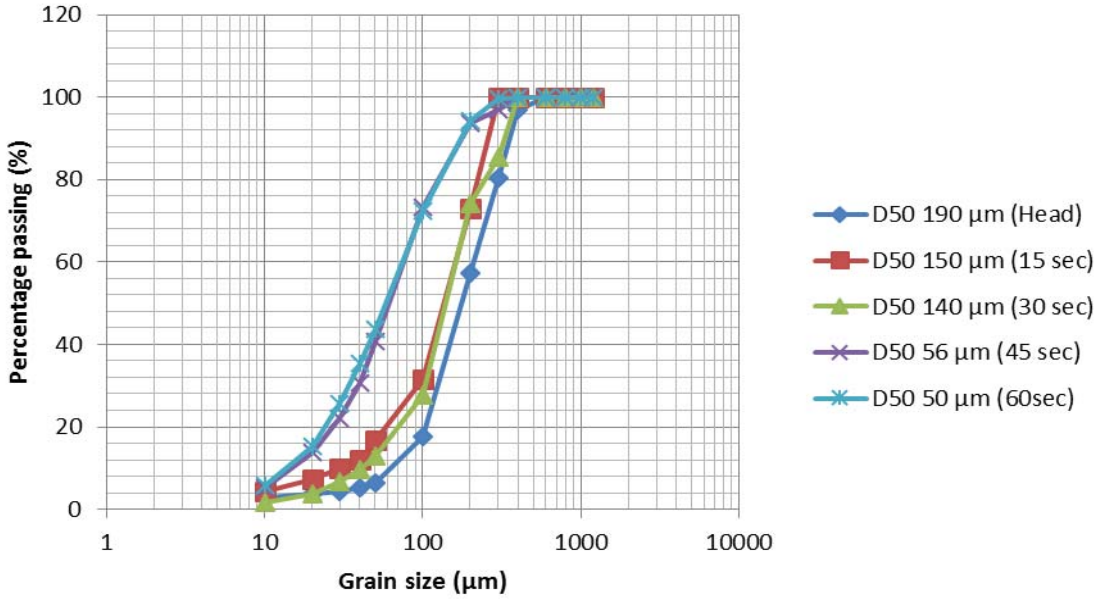

Figure 5-3 Grain size distribution of pyrite in the head, 15, 30, 45 and 60 second milled samples. D_{50} values are given in the legend.

5.3.1.4 Textural properties of the head sample

The textural properties of the ore refer to the liberation and association of the minerals within the ore, its morphology, lithology as well as the degree of weathering. Textural properties of the low grade copper ore head sample were analysed by QEMSCAN to indicate the accessibility of the minerals to leaching and reaction and thereby their potential to contribute to acid generation and acid neutralisation. These results are presented first for the ore sample and thereafter for samples milled increasingly finely for study of the effect of particle size on the UCT biokinetic test for characterisation of ARD potential.

Fully liberated pyrite was defined as mineral particle possessing more that 90% surface area as pyrite or chalcopyrite. Middlings were classified as particles containing between 30-90% pyrite or chalcopyrite as exposed surface. Locked minerals contain less than 30% pyrite or chalcopyrite as exposed surface. Liberated grains enable the oxidation of the sulphide mineral by ferric iron which is formed through microbial oxidation of ferrous iron entering solution on leaching. Association of pyrite and chalcopyrite with other minerals was defined as those having shared perimeter pixels with pyrite or chalcopyrite. The determination of the association of minerals with each other provides significant information of leachability of the mineral of interest and also indicates which lixiviant is suitable for extraction of the mineral of interest. Ghorbhani (2013) showed that the galvanic interactions involving pyrite and other sulfide minerals influenced the leachability significantly when associated with pyrite. In assessing the potential for ARD generation, the association of sulphides with gangue minerals such as silicates is important in understanding the degree to which potential acid forming reactions from sulphur containing minerals could be neutralised by acid consuming reactions from silicate containing minerals. Furthermore, the relative kinetics of these reactions are important (Dyantyi, et al., 2013; Opitz, 2013).

Figure 5-4 demonstrates the type of particles that were found in the particle map output for the feed sample studied. Figure 5-4 A shows that the presence of pyrite that was locked in by mica and quartz as well as plagioclase. Such pyrite would be available for oxidation following long term leaching or milling the sample to a fine PSD. Figure 5-4 B shows the presence of iron oxides on the surface of mineral containing other sulphides as well as pyrite and quartz. Tiny specs of pyrite are visible under the iron oxides, indicating the presence of precipitates. Figure 5-4 C shows the presence of alunite on the surface associated with quartz. Alunite is an aluminium hydroxysulphate silicate mineral that is ubiquitously found in porphyry copper deposits (Cox, et al., 2003). Alunite formation is associated with the precipitation of sulphates in the presence of iron sulphides. The presence of these minerals is an indication of natural weathering of the low grade copper ore in the environment (Bishop & Murad, 2005). A particle map analysis indicated that alunite and iron oxides were found on the surface of the particle grains largely associated with sulphide minerals, thereby indicating oxidation of the ore prior to all experiments. Figure 5-4 D shows chalcopyrite association with other sulphides and Figure 5-4 E shows the presence of liberated pyrite where pyrite is also associated with mica.

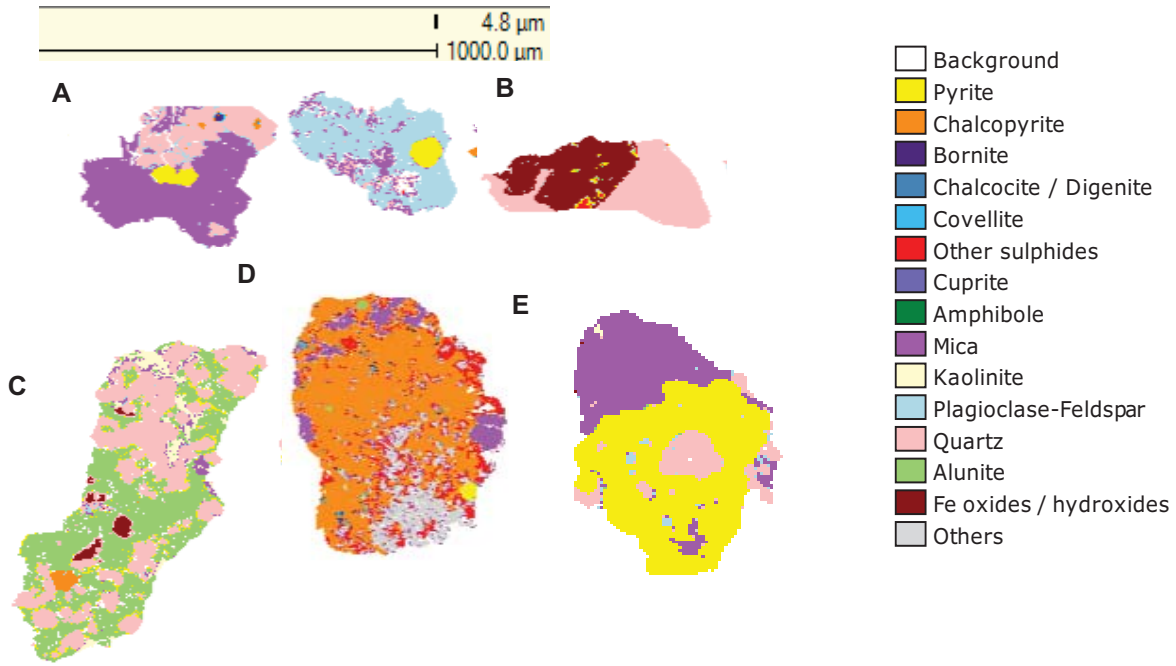

Figure 5-4 False colour QEMSCAN particle map illustrating the texture and nature of the mineral association

5.3.1.5 Textural properties of the head as a function of particle size

The formation of ARD is dependent on the surface oxidation of the sulphide-containing ore in the presence of ferric iron and acid lixiviants or the oxidation of sulphides with access to cracks and pores in the mineral along which the lixiviant can traverse. The ferric iron is regenerated from the resultant ferrous iron (slowly) by chemical oxidation or (fast) by iron- and sulphur-oxidizing microorganisms. Liberation analysis for pyrite and chalcopyrite as a function of particle size was compared against the head sample since it was expected that liberation should increase as particle size was decreased. The low grade copper ore feed was milled for 15, 30, 45 and 60 seconds, resulting in decreasing particle size. The most dominant acid producing minerals were pyrite and chalcopyrite, hence the liberation and association of these was analysed.

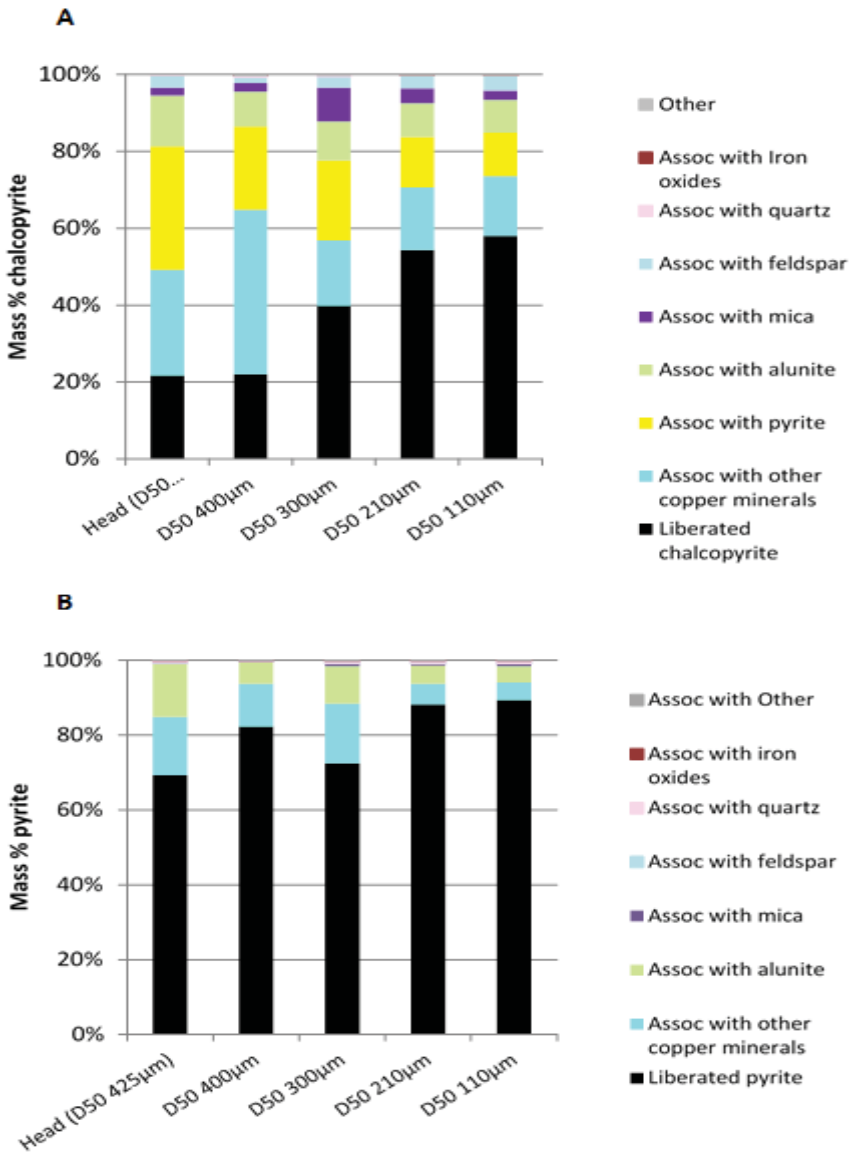

Figure 5-5 Liberation and association characterisation of chalcopyrite (A) and pyrite (B)

Most of the chalcopyrite in the head sample was locked in by other minerals, some 60% by other copper and pyrite phases. Results in Figure 5-5 A indicate that chalcopyrite liberation increased as particle size decreased (mill time increased). Chalcopyrite was also found associated with a variety of minerals ranging from other copper minerals to pyrite and acid consuming minerals such amphibole, mica and K feldspar.

An increasing trend in pyrite liberation with milling time was also noted in Figure 5-5 B, with an outlier apparent between the 15 and 30 second milled fraction. The longest milled fractions (45 and 60 sec) showed more than 85% liberation of pyrite. The pyrite was found associated with other copper minerals as well as alunite.

5.3.2 The effect of solid loading on the characterisation of sulphide containing ores using the biokinetic test

In this study, the test was conducted using a solid loading of 3 g, 7.5 g and 12 g at a fixed particle size of D_{50} 400 µm. The loading was leached by mixed mesophilic culture dominated by *Leptospirillum ferriphilum* and *Acidithiobacillus ferrooxidans* mixed in equal proportion with a culture dominated by *Acidithiobacillus thiooxidans*. Two solid loading experiments were conducted, one without daily acidification (non-controlled pH test) and one with daily acidification to hold the pH at or below pH 2.0 (controlled pH biokinetic test). The biokinetic test was operated as a closed system. Conditions used simulated the conditions leading to the formation of acid rock drainage such as the presence of acidophilic iron and sulphur oxidizing microorganisms, a moderate temperature of 37°C and an initial acidification of the environment. The test was run for a period of 90 days with periodic analysis of the leachate for pH, redox, ferrous iron concentration, ferric iron concentration and conductivity.

5.3.2.1 The leachate pH profile.

Prior to the inoculation of the non-controlled pH biokinetic test (Figure 5-6 A), the low grade ore for each respective solid loading was incubated in a flask overnight with ABS in order to allow the dissolution of metal hydroxides present on the surface of the sample which might prevent leaching. In Figure 5-6 A, presenting data for the non-controlled pH test, this phase is represented as before Day 0 (pre-inoculation stage). After the 24 h pre-inoculation stage, the pH had increased from pH 2.0 to 2.26 in the abiotic control flask (5% w/v), 2.21 in the 2% w/v flask, 2.26 in the 5% w/v flask and 2.31 in the 8% w/v flask respectively. On Day 0, the pH of each flask was corrected to pH 2 with sulphuric acid and the biotic flasks inoculated with the mixed mesophilic culture at 10^7 cells per mL. The addition of the mesophilic culture further lowered the pH to pH 1.87. In the controlled pH experiment, the flasks were prepared and inoculated in the same way on Day 0.

The presence of microorganisms in the biotic experiments enabled rapid oxidation of ferrous iron and therefore more acid was consumed than in the abiotic control in the absence of microorganisms, with a concomitant increase in pH. It was expected that an increase in solid loading would result in a proportional increase in acid consuming reactions; this is observed in the pre-inoculation stage. However, this was not observed after inoculation indicating that microbially mediated oxidation of ferrous iron occurs faster than ferric iron leaching of the mineral and therefore initial acid consumption was largely due to ferrous iron oxidation (Figure 5-6). In the abiotic control, the oxidation of ferrous iron continued at a slow rate mediated by oxygen and water. Bulk mineral analysis (Section 5.3.1.1) indicated that the sample is dominated by the minerals mica and plagioclase. These possess low acid neutralising properties and react slowly in an acidic environment; therefore, the acid neutralising ability of the mineral is not significant.

In the non-pH controlled test (Figure 5-6A), the pH increased to pH 2.1 over the first 5 days. From Days 5 to 11 a stable region can be noted where there is no decrease or increase in the leachate pH. During this period, the rate of increase in acid consuming reactions is balanced by the rate of sulphide oxidation with a concomitant release in H^+ ions. On Day 11, the pH decreased to 1.9 symbolising the point at which the solution pH is the same as the initial starting pH. A sharp decline in pH from to 1.69 is noted from Day 12 to Day 27. This represents the point at which acid producing reactions occur faster than acid consumption. The 2% w/v solid loading stabilised at pH 1.6 by Day 50 whereas the 5% w/v and 8% w/v solid loadings stabilised at a pH of 1.59 and 1.49 by the end of test. The acid production capacity of the sample increased as solid loading increased, i.e. the overall acid production outweighed the acid consumption over this period. The bulk mineralogy indicated that the dominant acid producing minerals

were chalcopyrite and pyrite respectively. These results therefore indicate that these sulphides were sufficiently reactive to induce differences in acidity within the different solid loadings.

The controlled pH biokinetic test (Figure 5-6B) mitigated formation of precipitates, should the acid consuming reaction result in a pH increase above pH 2. It also provided a favourable environment for acidophilic microorganisms to thrive. The pH profile in the non-controlled pH test (Figure 5-6 A) showed a significant consumption of acid due to microbially mediated ferrous iron oxidation which resulted in the increase of pH from pH 1.87 to 2. Hence in the controlled pH study the pH was initiated at pH 1.8 and maintained at pH 1.8 using 0.5M sulphuric acid (H_2SO_4) between Days 0 and 10. Figure 5-8 illustrates the accumulative sulphuric acid added, showing that the acid required to counter acid consuming reactions increased as solid loading increased.

In the pH controlled test, the ferric iron generated does not precipitate, but remains in solution and acts as a potent leaching agent (Figure 5-6 Leachate pH and net accumulated H^+ ions in the non-controlled pH (A) and controlled pH (B) biokinetic test, n=4 B). Here, the release of acid in the 2% w/v solid loading did not stabilise on Day 50 but continued to decline to a pH of 1.58 on Day 90 (Figure 5-6 B). It was also noted that the rate of release of acid in the 5% w/v and 8% w/v tests was similar; the pH stabilised at pH 1.5 in the 4% w/v test and pH 1.45 in the 8% w/v pH controlled test. A lower pH is observed for the 5 and 8% w/v tests than the 2% w/v test, indicating the presence of an increased proportion of reactive sulphides or liberated acid producing minerals. The release of acid producing minerals increased as solid loading increases.

In line with Figure 5-6, the balance between hydroxide ions and hydrogen ions is plotted in terms of the net accumulated hydrogen ions per experiment (Figure 5-7 A and B). The results show that the accumulated hydrogen ion concentration in the non-controlled pH tests started to increase on Day 10 (Figure 5-7A). The controlled pH test also shows the production of hydrogen ions on Day 10. This represents the point at which acid is generated at a faster rate than it is consumed.

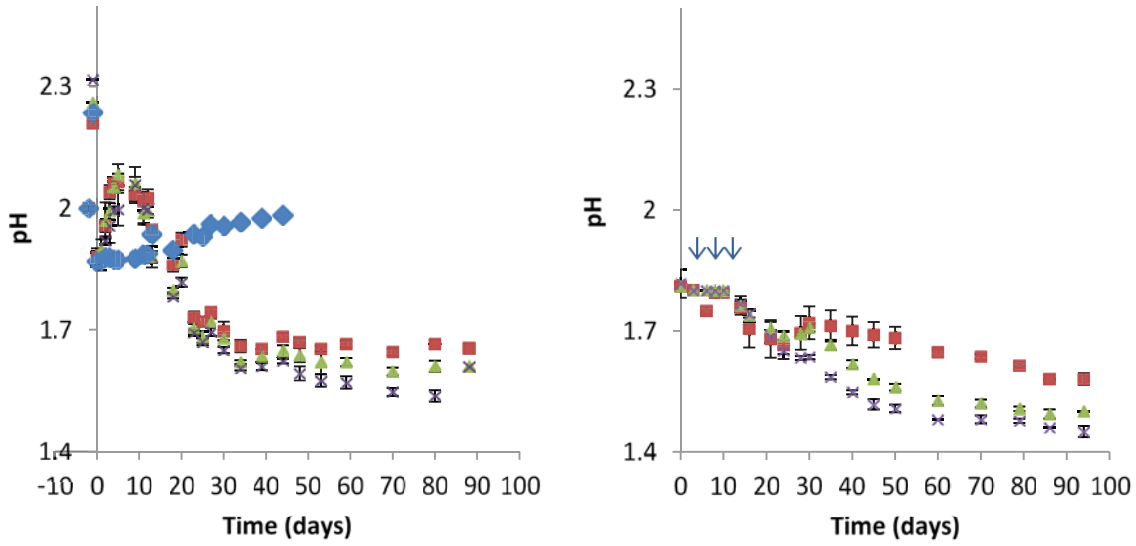

Figure 5-6 Leachate pH and net accumulated H^+ ions in the non-controlled pH (A) and controlled pH (B) biokinetic test, n=4. ■ = 2% w/v (3 g), ▲+ 5% w/v (7.5 g), X = 8% w/v (12 g), ◆ = 8% w/v (12 g) abiotic control

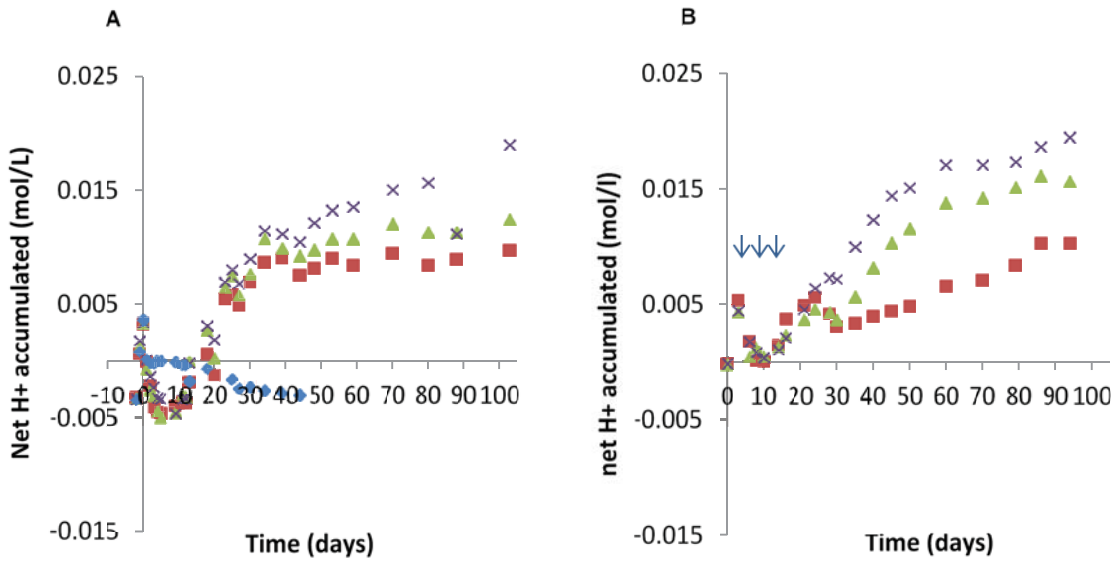

Figure 5-7 Net accumulated H^+ ions in the non-controlled pH (A) and controlled pH (B) biokinetic test, n=4. ■ = 2% w/v (3 g), ▲+ 5% w/v (7.5 g), X = 8% w/v (12 g), ◆ = 8% w/v (12 g) abiotic control

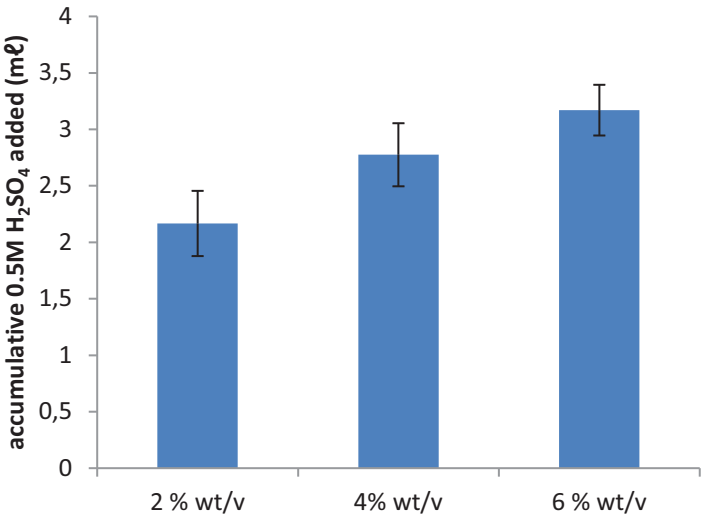

Figure 5-8 Total acid added during the controlled pH biokinetic test: 2, 5 and 8% loading

5.3.2.2 Leachate redox potential in the biokinetic test

The redox potential is an indication of the ratio of ferric to ferrous ions in solution and is described by the Nernst equation (Nemati & Webb, 1996). A high redox potential implies that the ratio of ferric iron to ferrous iron in solution is high suggesting its continual regeneration. This ratio is increased in the presence of iron oxidising microorganisms due to the oxidation of ferrous to ferric iron and is dependent on the oxygen availability (Ahmadi, 2012; Córdoba, et al., 2008; Wu, et al., 2014). In this study, an initial 500 mg/ℓ ferrous iron was present in solution and was oxidised by iron oxidisers. In both the non-controlled pH and controlled pH biotic tests, the solution redox potential increased rapidly from 430 to 700 mV (Figure 5-9 A and B). The reox of 700 mV was attained slightly sooner in the pH controlled test (1-2 days at 2% loading) than pH uncontrolled test (4 days at 2% loading), owing to conditions favouring the acidophilic iron-oxidisers. The ferric:ferrous iron ratio was, however, affected by the solids loading in each flask such that lag time for the increase in the redox potential increased with an increase in solid loading, reaching 700 mV at 4, 9 and 14 days in the uncontrolled pH experiment on exposure to 2, 5 and 8% w/v loading respectively. This is attributed to an increase in pyrite and chalcopyrite available

for leaching and therefore ferrous iron is regenerated from mineral leaching faster than the net increase in ferric iron due to microbial oxidation.

In the absence of a microbial inoculation, the redox potential increased slowly from 300 to 428 mV over a 40 day period (Figure 5-9A) indicating minimal ferrous iron oxidation over this period. After 40 days, an increase in redox potential was observed due to the inherent microbial population present on the unsterilised mineral (Bryan, 2006). In the absence of microorganisms, the oxidation of ferrous to ferric iron chemically is slow.

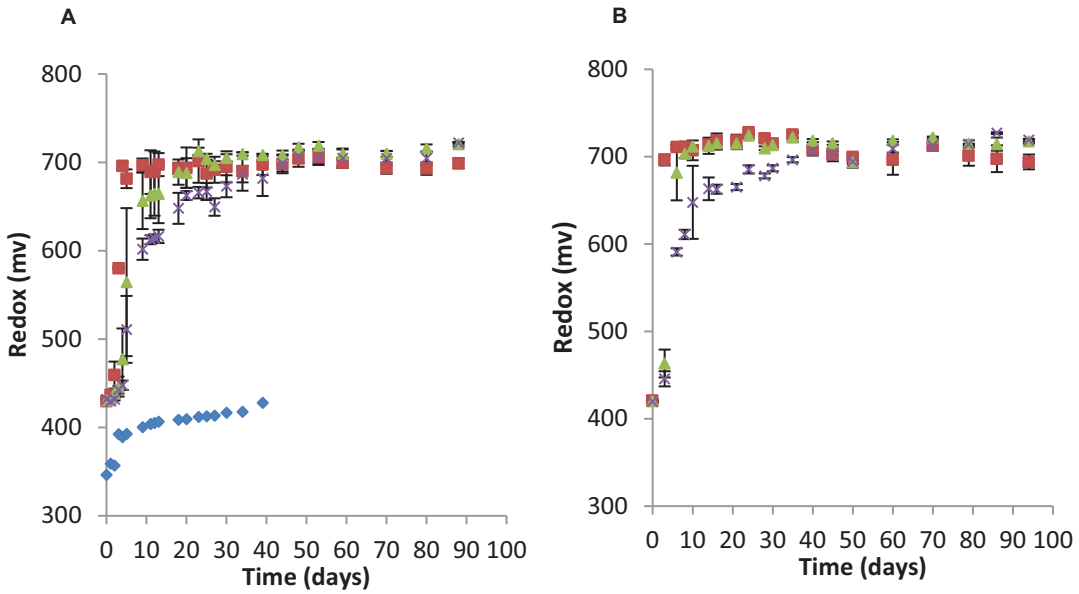

Figure 5-9 Redox potential in the non-controlled pH (A) and controlled pH biokinetic test (B) as a function of solids loading. n=4. ■ = 2% w/v (3 g), ▲+ 5% w/v (7.5 g), X = 8% w/v (12 g), ◆ = 8% w/v (12 g) abiotic control

5.3.2.3 Ferrous iron oxidation and ferric iron regeneration in the biokinetic test

In this test, an initial 500 mg/L ferrous iron was added (as ferrous sulphate) to each flask in order to accelerate the formation of ferric iron and therefore the leaching of the low grade ore, accelerating the onset of ARD generation if likely to occur and decreasing the required test time. In both the non-controlled pH and controlled pH tests (Figure 5-10 A and B), a depletion of ferrous iron was seen in each biotic solid loading case from day 0 to11 as a result of the oxidation of ferrous iron to ferric iron by iron and sulphur oxidisers. The rapid utilisation of ferrous iron in the abiotic control was not evident due to the absence of microorganisms. The abiotic control shows a fluctuation in ferrous iron present in the medium across 40 days. A similar trend of an increase in ferric iron in solution is noted in both the non-controlled pH and controlled pH biokinetic tests (Figure 5-11 A and B respectively). The ferric iron in solution increased from 58 to 1060 mg/ℓ in the non-controlled pH test and from 168 to 1061 mg/L in the controlled pH test.

In the non-controlled pH test (Figure 5-11A) the ferric iron decreases significantly from Day 11-27 across all solid loading cases. The decrease in ferric iron is due to the utilisation of ferric iron as a primary oxidizing agent as well as the formation of iron precipitates which coat refractory minerals such as chalcopyrite even at low pH, thereby limiting further oxidation or leaching of the low grade copper ore. Additionally, the normalised ferric iron data in the non-controlled pH test (Figure 5-12 A) suggests that microbially mediated leaching of the ore and therefore ferric iron regeneration became limited as solid loading increased. The liberation and association profile in Figure 5-5, demonstrates that pyrite grains

within the D_{50} 400 µm are liberated and are associated with other sulphide minerals and copper containing minerals. Pyrite has a high electrode potential and thus the association of pyrite with other sulphide minerals partially inhibits its oxidation. In this case, other sulphides are preferentially oxidised (Kwong, et al., 2003) due to the galvanic interactions mediated by differences in electrode potential within the sulphide.

The addition of 0.5 M H_2SO_4 in the controlled pH test (Figure 5-11B) resulted in the acidification of the medium, thereby creating a low pH environment. Under these conditions precipitate formation is negligible, and the effect of precipitation as observed in the non-controlled pH test is not evident. The pH was maintained below pH 1.8 under all test conditions. An increase in ferric iron leached into solution from day 0-14 is observed. Here the ferric iron stabilises to 950, 1021 and 1073 mg/L for the 2, 5 and 8% w/v respectively during the period from day 14 to day 30. The normalised ferric iron data in the controlled pH test (Figure 5-12B) shows that ferric iron regeneration became limited as solid loading increased. However, no net decrease in ferric iron was observed between days 14 to 30. The decline in ferric iron during the period from day 79 to 94 may be attributed to the formation of a passivation layer around the ore particles due to the production of reduced inorganic sulphide compounds (RISC). This would result in the preferential leaching of sulphide as an energy source by sulphur oxidising microorganism as opposed to leaching of ferrous iron by iron oxidising bacteria (Konishi, et al., 1995; Rawlings, 2005).

An increase in ferric iron was noted on day 30 to 100 in the non-controlled pH test (Figure 5-11A) when the pH was below pH 1.7. The decreased pH creates a favourable environment in which the ferric iron precipitates which coat the ore particle become soluble, allowing ferric iron regeneration through microbially mediated leaching. The ferric iron leached into solution in the 2% w/v solid loading stabilises to between 210 and 250 mg/L over day 40 to100. This can be compared to the controlled pH test (Figure 5-11 B), where ferric iron regeneration fluctuated between 817 to 849 mg/L between day 35 and 70. This indicated that proton and ferric iron mediated leaching had the greatest leaching effect on the 2% w/v solid loading. The normalised non-controlled pH ferric iron data (Figure 5-12 A) show that the rate of ferric iron regeneration in the 5 and 8% w/v was the similar. Here the ferric iron increases from 117 to 245 mg/L in the 4% w/v and from 95 to 241 mg/L in the 6% w/v solid loading respectively. The normalised ferric iron data in the controlled pH test (Figure 5-12B) shows that the amount of ferric iron in solution in the 5% w/v solid loading test fluctuated between 419 and 406 mg/ℓ while it fluctuated between 239 and 250 mg/L in the 8% w/v. A decrease in ferric iron leached into solution in the 5 and 8% w/v flasks was seen on day 103 due to the formation of RISC that coat the mineral and thus the preferential leaching of sulphides by sulphur oxidising microorganisms.

In the absence of microbial leaching in the non-controlled pH test (abiotic control 5% w/v) low levels of ferric iron are present in solution (Figure 5-11A). This suggests that ferrous iron is oxidised slowly over time.

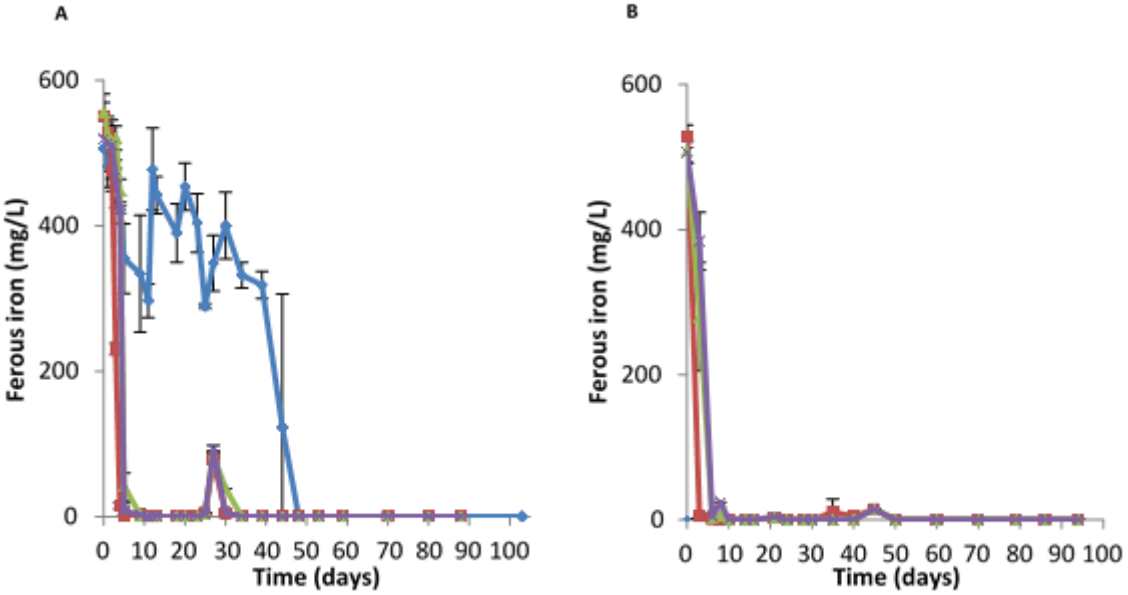

Figure 5-10 Ferrous iron in solution in the non-controlled pH (A) and controlled pH biokinetic (B) tests. ■ = 2% w/v (3 g), ▲ + 5% w/v (7.5 g), X = 8% w/v (12 g), ◆ = 8% w/v (12 g) abiotic control

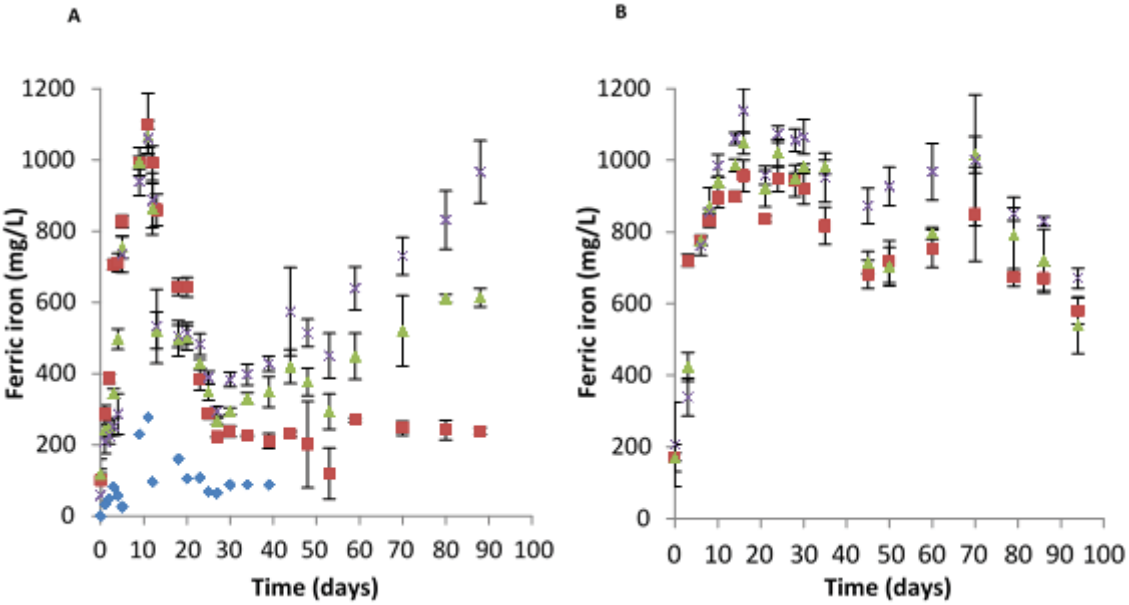

Figure 5-11 Ferric iron in solution in the non-controlled pH (A) and controlled pH biokinetic (B) tests. ■ = 2% w/v (3 g), ▲ + 5% w/v (7.5 g), X = 8% w/v (12 g), ◆ = 8% w/v (12 g) abiotic control

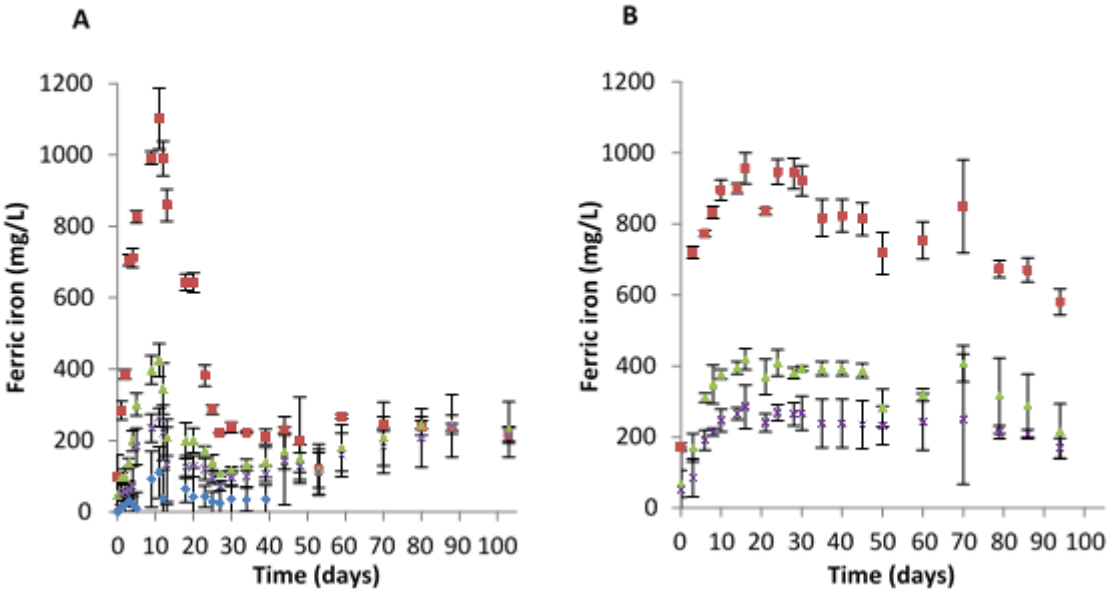

Figure 5-12 Ferric iron regeneration normalised in terms of lowest solid loading mass. ■ = 2% w/v (3 g), ▲+ 5% w/v (7.5 g), X = 8% w/v (12 g), ◆ = 8% w/v (12 g) abiotic control

5.3.2.4 The conductivity of the solution

ARD generation results in the dissolution of metals from the leaching of the sulphide ore leading to high concentrations of dissolved metals being transported into neighbouring streams and thereby perpetrating acid rock drainage pollution. Elevated sulphate concentration in water streams is often the first indicator of ARD generation. In open systems, dilution of sulphates can occur thereby making pH measurements less reliable. The conductivity of the solution can be used to measure anions and cations released into solution.

In this study the conductivity was quantified in each solid loading experiment to indicate the degree to which anions and trace metals are leached into solution. In the non-controlled pH test (Figure 5-13A) there is a steady increase of anions leached into solution. The conductivity of the leach solution for the 2, 5 and 8% w/v was measured to be 12.91, 14.42 and 15.91 mS on Day 70. These results suggest that a greater concentration of dissolved solutes was leached into solution as solid loading increases.

In the controlled pH biokinetic test (Figure 5-13B) a similar increasing trend of solution is observed. However, under pH controlled conditions the amounts of leached solids are much higher than for the non-controlled pH test. The conductivity measured in the 2, 5 and 8% w/v solid loading experiment on day 70 was 14.85, 19.84 and 21 mS respectively.

The abiotic control test (Figure 5-13A) shows a decreasing trend in the solution conductivity. Conductivity measurements are sensitive to ions released into solution and thus an increased release of sulphate from the sample would result in an increase in conductivity. However, in the abiotic control, the sample is subjected to slow oxidizing condition facilitated by oxygen and water leading to slow leaching condition and release of sulphate ions.

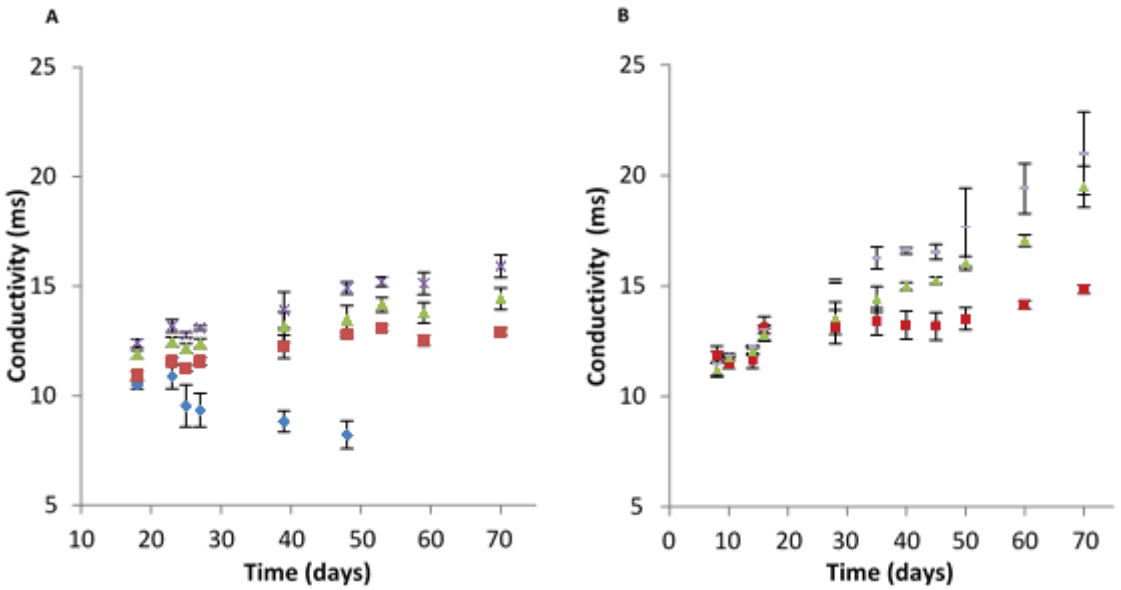

Figure 5-13 Conductivity of leachate in non-controlled pH (A) and controlled pH (B) biokinetic tests. ■ = 2% w/v (3 g), ▲+ 5% w/v (7.5 g), X = 8% w/v (12 g), ◆ = 8% w/v (12 g) abiotic control

5.3.2.5 Mineral reactivity

In order to understand the reactivity of various mineral groups and the possible leaching chemistry, the 5% w/v solid loading residue from the biokinetic experiments was analysed by XRD analysis on Day 50 and Day 90. In addition, the iron and sulphur remaining in the 5% w/v solid loading from the non-controlled pH and controlled pH experiments were analysed using atomic absorption spectroscopy (AAS) and LECO. The reactivity was determined using Table 5-1 and was calculated based on the amount of mineral that had reacted from the amount present in the original sample. It is presented in Table 5-2.

The results from the XRD analysis showed that pyrite was strongly reactive across the duration of the test in both non-controlled pH and controlled pH biokinetic tests. In the initial stages of the non-controlled pH test, from Day 0 to Day 50, chalcopyrite was unreactive. In the last stage of the test, by Day 90, chalcopyrite was reactive. A comparison against the controlled pH test shows that the maintenance of low pH enabled leaching the chalcopyrite. The only acid consuming minerals which were reactive were mica and kaolinite. These minerals are slow weathering and would contribute to acid neutralisation over a long period as a result of dissolution (Ardau, et al., 2009; Dopson, et al., 2004; Santelli, et al., 2001). Quartz was unreacted throughout the duration of the test in both non-controlled pH and controlled pH biokinetic test. Plagioclase was unreacted in the non-controlled biokinetic test as well as from Day 0 to 50 in the controlled biokinetic test; however it showed reaction by Day 90 in the controlled pH test.

Table 5-1 Mineral reactivity as calculated by XRD

Mineral reactivity	
Reacted	(>10%)
Strongly reacted	(>60%)
Formed as secondary minerals	(<10%)
Unreacted	(0-10%)

Table 5-2 The extent of minerals leaching for the biokinetic test at 5% w/v loading. Only major mineral groupings shown

	Non-controlled pH		Controlled pH	
	Day 50	**Day 90**	**Day 50**	**Day 90**
Pyrite	Strongly reacted	Strongly reacted	Strongly Reacted	Strongly reacted
Chalcopyrite	Unreacted	Reacted	Reacted	Reacted
Mica	Reacted	Reacted	Reacted	Reacted
Kaolinite	Reacted	Reacted	Reacted	Reacted
Plagioclase-Feldspar	Unreacted	Unreacted	Unreacted	Reacted
Quartz	Unreacted	Unreacted	Unreacted	Unreacted

5.3.3 The effect of particle size on the characterisation of sulphide containing ores using the biokinetic test

The formation of ARD is known to be surface reaction determined by the reactivity of sulphide particles at specific sites (Broughton & M, 1992; Lapakko, et al., 2006; Erguler & Erguler, 2015; Erguler, et al., 2014). The access of leachate to the grain surface through its liberation or the presence of cracks or pores in the mineral ore is required. Particle size distribution impacts this liberation and accessibility of mineral grains to leach solution.

In the biokinetic test, ARD formation was simulated in closed shake flasks. To investigate the effect of particle size, non-controlled pH biokinetic flask tests were conducted. Particle sizes of D_{50} 300, 210 and 110 µm at a solid loading of 5% w/v were leached by a mixed mesophilic culture dominated by *Leptospirillum ferriphilum* and *Acidithiobacillus ferrooxidans* mixed with an equal proportion of an *Acidithiobacillus thiooxidans* dominated culture. The test was run for a period of 90 days with the leachate sampled periodically; the pH, ferrous iron, ferric iron and conductivity were measured. The leachate chemistry was compared against the test conducted using the D_{50} 400 µm size fraction at a solid loading of 5% w/v, reported above.

5.3.3.1 The pH profile

In the particle size experiment, shown in grey symbols in Figure 5-14, an increase in solution pH from pH 1.8 to 1.94 was observed from day 0 to day 4, compared to an increase to pH 2.1 in the prior experiment using the D_{50} = 400 µm size fraction and described in detail above. The increase in solution pH was due to the solubilisation of acid consuming minerals present in the low grade copper ore (although these are recognised to be slow reacting minerals) as well as the oxidation of ferrous iron. On Day 6, acid began to be formed faster than it was neutralised and hence a decrease in pH is noted from Day 6 to a point between Day 30 and Day 45 in the particle size experiment (Day 35 in the D_{50} = 400 µm size fraction described above). Over this period, the pH decreased from pH 1.95 to pH 1.61, 1.58 and 1.51 for the D_{50} 300, 210 and 110 µm fractions respectively. The lower pH achieved with lower particle size suggests the availability of more liberated sulphide mineral and hence more leaching occurring

Between day 45 and 57 the pH in each particle size fraction stabilised such that the pH in the D_{50} 300, 210 and 110 µm fractions are 1.61, 1.58 and 1.55 respectively. Following a decrease in pH around Day 60, an increase in pH is observed resulting in an average pH from Day 66 to 90 in the D_{50} 300, 210 and 110 µm fractions of 1.63, 1.63 and 1.60 respectively. The presence of aluminium silicate has been shown to stabilise the pH once low levels are reached. Hence this rise in pH may be due to the release of aluminosilicates as well as other gangue minerals which were associated with the aluminosilicates (Figure 5-5) (Miller, et al., 2010). Interestingly when compared against the non-controlled pH biokinetic test conducted on the D_{50} = 400 µm fraction, the pH was in the same range. These results suggest that the reactivity of acid consuming minerals in all experiments is consistent. However the release of acid

from the oxidation of acid producing minerals increases with a decrease in particle size. Pyrite liberation (Figure 5-5) in the D_{50} 300, 210 and 110 µm fractions was 72, 88 and 89% respectively, indicating that the oxidation of sulphides is expected to increase as particle size decreases.

In the D_{50} 400 µm fraction abiotic control no acidification was observed over a period of 72 days, supporting that solubilisation of the ore was slow in the absence of acidophilic microorganisms. The biotic control test using the D_{50} 400 µm fraction shows that the presence of microorganisms leads to a faster oxidation of the ore. Direct comparison of these controls with the particle size data is not appropriate as these were conducted as different experiments with the potential for variation in inoculum, amongst others.

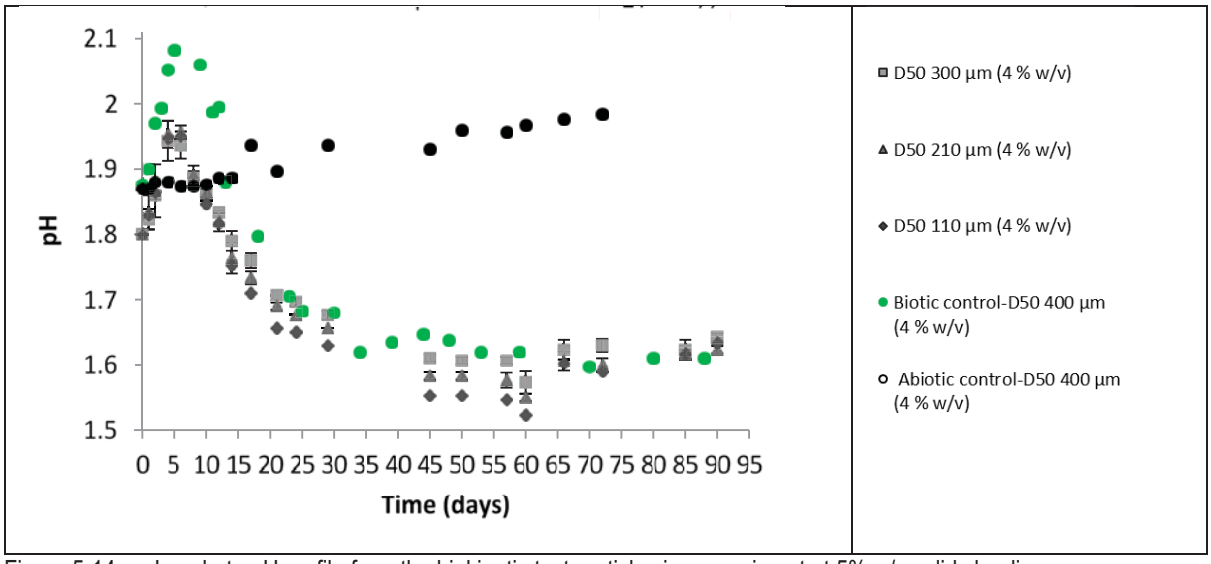

Figure 5-14 Leachate pH profile from the biokinetic test particle size experiment at 5% w/v solids loading

5.3.3.2 The redox potential

An analysis of the solution redox potential (Figure 5-15) in the D_{50} 300, 210 and 110 µm fractions showed a rapid increase in the redox potential from 424 mV to 696 mV across all particle sizes over a duration of 4 days. A high redox potential is an indication of ferric iron regeneration. The rate of ferrous iron to ferric iron conversion was higher in the D_{50} 300, 210 and 110 µm fractions than in the D_{50} 400 µm fraction used in the biotic control biokinetic test. This may result from the use of slightly different inocula since conducted as separate experiments. Alternatively, this may result from differing liberation of the mineral. The redox potential remained above 700 mV after Day 8 for the D_{50} 300, 210 and 110 µm fractions and after Day 20 for the D_{50} 400 µm fraction. The absence of microorganisms in the abiotic control resulted in low levels of the solution redox potential owing to the slow chemical oxidation of ferrous iron.

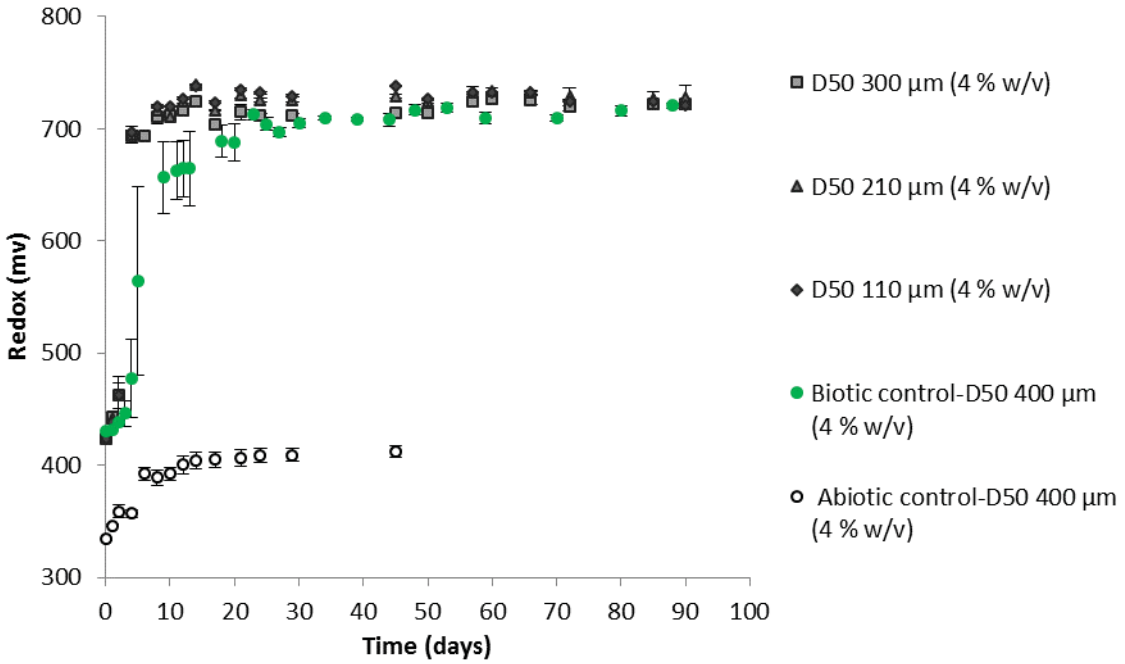

Figure 5-15 Changes in the redox potential in the solution as measured from the leachate in the biokinetic test particle size experiment at 5% w/v solids loading

5.3.3.3 Ferrous iron oxidation and ferric iron regeneration.

An initial 500 mg/L ferrous iron solution (as ferrous sulphate) was added into each flask. A decrease in ferrous iron is noted from day 0 to 4 across the D_{50} 300, 210 and 110 µm fractions. This shows that the rate of ferrous iron oxidation was the same in the presence of the D_{50} 300, 210 and 110 µm fractions; and that by day 4 all the ferrous iron had been oxidised and continued to be oxidised at the rate that it formed (Figure 5-16). This indicates that microbial activity and rate of ferrous oxidation were optimal in these size fractions. A slower rate of ferrous oxidation is noted for the D_{50} 400 µm fraction used in the biotic control biokinetic test, conducted as a separate experiment. Ferrous iron was not depleted in the abiotic control, remaining in the range 300 to 500 mg/L.

For the D_{50} 300, 210 and 110 µm fractions, a linear increasing trend in ferric iron production is observed from day 0 to day 4, where ferric iron increased from 105 mg/L to 749mg/L in the D_{50} 110 µm fraction (Figure 5-17). Between Day 4 and 8, this trend adjusts from linear to a saturation function, with the point of change depending on the particle size. Thereafter a gradually decreasing slope is noted where ferric iron increases asymptotically to a final concentration of 1309, 1464 and 1509 mg/ℓ for the D_{50} 300, 210 and 110 µm fractions respectively on day 90. An analysis of the ferric iron in solution showed that more ferric iron, and thus total iron, was present in the 110 µm fraction test in comparison with the 300 µm and 210 µm fractions, indicating increasing leaching of sulphide based on increased liberation of the sulphide mineral.

In comparison, the D_{50} 400 µm fraction biotic control biokinetic test shows an initial similar sharp increase to a maximum of 1064 mg/L ferric iron on Day 11, followed by a decrease in ferric iron to Day 27. It is hypothesised that the formation of ferric precipitates as the pH exceeds pH 1.9, and particularly pH2.0, reduces the ferric iron concentration. This high pH was not observed in the particle size study, possibly due to the presence of a more active sulphur oxidising microbial community.

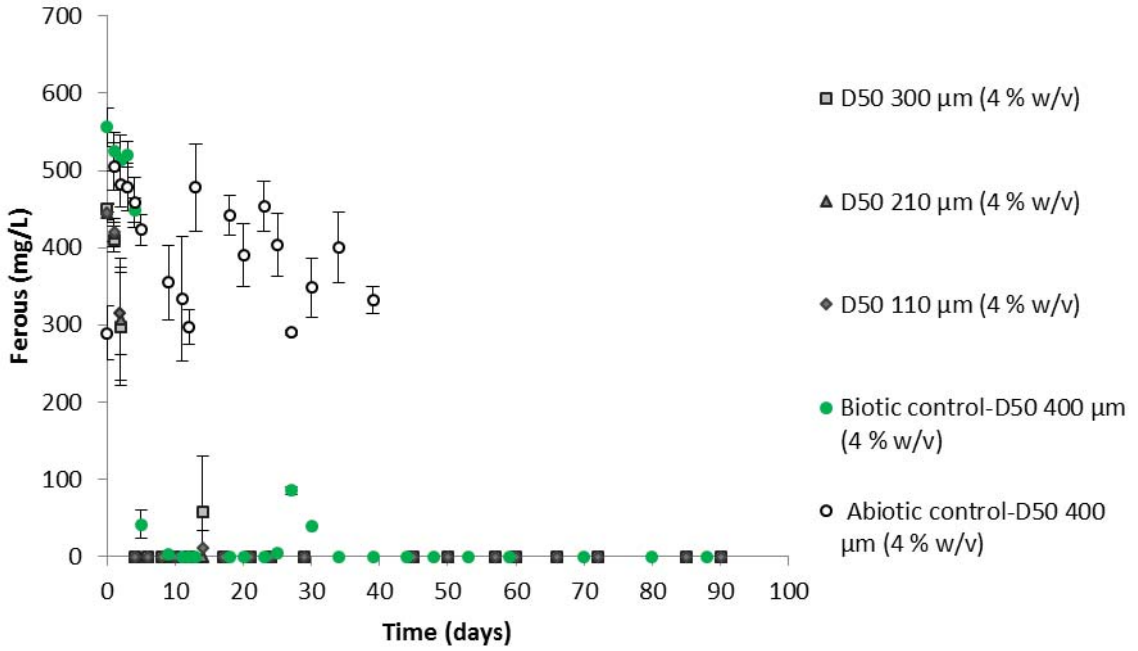

Figure 5-16 Ferrous iron concentration in the particle size experiment at 5% w/v solids loading.

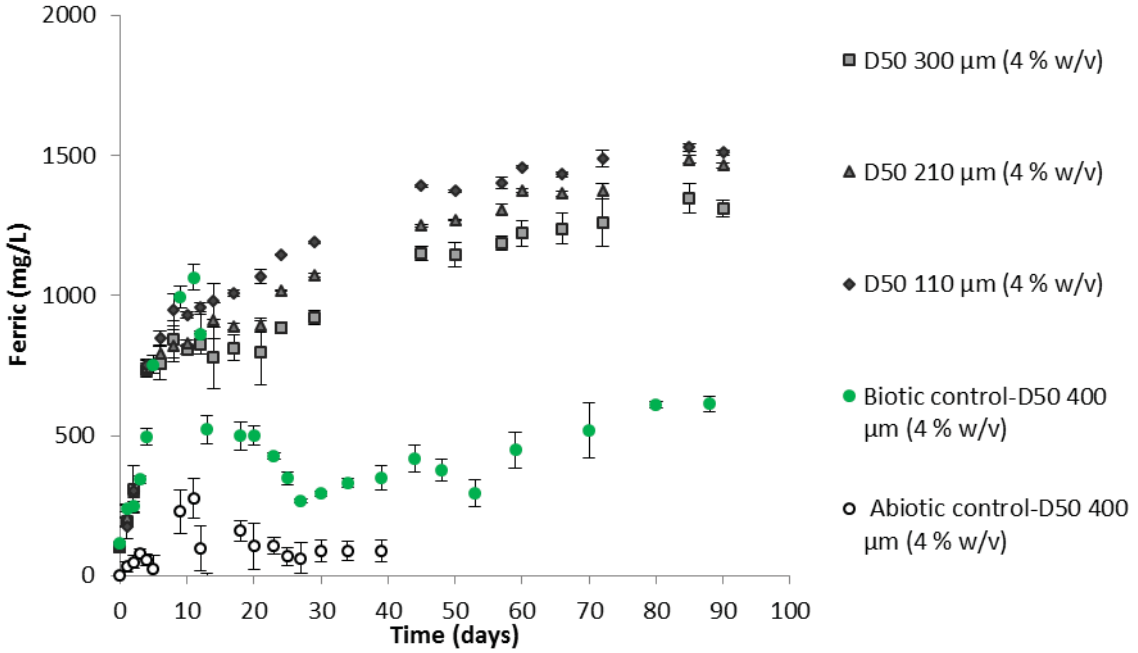

Figure 5-17 Ferric iron concentration in the particle size experiment at 5% w/v solids loading.

5.4 Concluding Comments: Operating Conditions for the CeBER-UCT Biokinetic Test

In this study, two operating variables were explored: solids loading and particle size. In considering solids loading, the sample size needs to take cognisance of sample size required for representative sampling, sample availability and impact of sample size used on the scale of test. In the CeBER-UCT biokinetic test, it is desirable to use a small scale test without limiting the potential for representative

sampling. Hence the scale selected in its development is similar to the scale of the well accepted static tests. This scale of 150 mL volume is maintained in this work, but the solids loading is varied from 3.0 through 7.5 to 12 g per test, representing 2, 5 and 8% w/v. The constraints on sample size and ascertaining representative sampling are discussed in our recent study to be presented in the Masters dissertation of Olga Guseva (expected 2020) and are not covered here. The results show that on increasing the solids loading the change in pH and ferric iron concentration is larger, allowing earlier detection of changes and increasing sensitivity. However, these changes are not equivalent when normalised, suggesting that the increased sample size results in some limitation to the reactions. Further, the increase in redox potential is delayed on use of larger sample size, resulting in the rate of ferric iron regeneration being the limiting reaction for a longer period of time over the rate of mineral leaching. It is thus proposed that the 7.5 g sample size (5% w/v) is appropriate for the biokinetic test and further reduction to 3 g (2% w/v) can be recommended, provided representative sampling is feasible (see Guseva, 2020).

While the particle size range used in this study is larger than typically used in the biokinetic test, it was appropriately applied owing to the good sulphide mineral liberation present. The study showed clearly that reduction in particle size is associated with increased liberation. Good liberation is essential to study the worst case effect with respect to ARD generation and to allow modelling of the prediction of ARD generation. In such modelling, the effect of particle size and associated liberation must be included in the model. In this study, the smallest particle size of D_{50} of 110 µm (D_{10} of 10 µm and D_{90} of 500 µm) exceeded the recommended particle size of 100% passing 150 µm for the biokinetic test but gave appropriate results. This is demonstrated by the small difference in performance with the next largest particle size. The success of this particle size is due to the 88% liberation of sulphide minerals. It is proposed that degree of liberation, while more difficult to measure, is a more appropriate indicator that particle size. In a current study in our laboratory, to be reported by Golela et al. in 2020, we are exploring the inter-relationship between particle size, grain size, degree of liberation and effectiveness of the CeBER UCT biokinetic test to build on the specifications of test conditions.

CHAPTER 6: REFINING THE INOCULUM REQUIRED FOR THE BIOKINETIC ASSAY

Also presented as:
Opitz, AKB; Harrison, STL. The effect of inoculum concentration on the biokinetic test for characterising acid rock drainage. In: Biohydrometallurgy 2016. Red Hook NY: Curran Associates Inc, Pages 412-420

6.1 Introduction to the Need for Refining the Inoculum

Characterisation of the ARD generation potential of mineral wastes centres primarily on the potential for acid generation under extreme chemical conditions (Price, 1997). The standard static acid-base accounting tests measure both the acid neutralising capacity (ANC) and the maximum potential to form acidity (MPA) based on mineral sulphide oxidation, with the difference between these values giving an estimate of the net acid producing potential (NAPP) (Lawrence & Scheske, 1997). In addition, the net acid generation (NAG) test investigates *in-situ* generation of acidity through reaction of the mineral wastes with H_2O_2. Measurement of the resulting solution pH is used an as an overall indication of ARD potential (Miller, et al., 1997). The standard tests, however, fail to account for the relative rates of acid consumption and acid generating reactions (Hesketh, et al., 2010a). These may be determined by kinetic tests, such as humidity cell tests; however, the duration of the kinetic tests is generally 6 months to multi-year tests. Furthermore, the action of Fe- and S-oxidising micro-organisms on the ARD generation rate are not accounted for in the standard chemical characterisation tests.

To address these limitations, the biokinetic test was developed (Hesketh, et al., 2010a; Broadhurst, et al., 2013). In the biokinetic test, the finely divided milled waste rock sample is prepared as a slurry, inoculated and cultured under standard bioleaching conditions. Leach rate, acidification and formation of acidity are monitored. The nature of the data collected allows data to be generated on both acid neutralisation and generation and their relative rates. Integration of the biokinetic test results with those obtained from the standard static ABA characterisation tests has been the focus of a number of studies (Hesketh, et al., 2010a; Opitz, et al., 2015) in which the value of the biokinetic tests in generation of kinetic data over a shortened time frame is demonstrated together with the confirmation of static test results. Prior to the recommendation of the biokinetic test for more widespread use, its standardisation in terms of operating conditions such as solids loading and particle size distribution, investigated by Hlongwane (2015) and presented in Chapter 5, as well as biological conditions is required. The impact of microbial inoculum and its activity are addressed in this study.

6.2 Material and Methods for Study of the Inoculum in the Biokinetic Test

6.2.1 Waste rock samples

A waste rock sample was sourced from a greenstone gold deposit at an operational gold mine, as in Section 4.3. A representatively sampled 3.5 kg sample was milled in a rod mill, with the resulting sample sieved through 150 µm sieve. Using an 8-way Fritsch rotary sample splitter, the collected milled material was statistically split into 70 g representative samples and further split for use in the biokinetic tests. Analysis of the particle size distribution of a representatively split sample indicated a D_{50} and D_{80} of approximately 25 µm and 105 µm respectively.

6.2.2 Microbial species

The inoculum used for each biokinetic test flask consisted of an equal mix of iron- and sulphur-oxidising cultures, dominated by *Leptospirillum (L.) ferriphilum* (ATC 49881) and *Acidithiobacillus (At.) caldus* (DSM 8485) species respectively. *L. ferriphilum* was grown in a 1 L batch reactor agitated at a rate of 400 rpm. The reactor was fed with solution of the following components ($g.L^{-1}$): $(NH_4)_2HPO_4$ (0.50),

$(NH_4)_2SO_4$ (1.80), $FeSO_4.7H_2O$ (5.0), K_2SO4 (1.10) and contained pyrite concentrate at a solids loading of 3% by mass. The *L. ferriphilum* strain was originally obtained from a continuous tank bioleaching mini-plant, treating a pyrite concentrate from Gamsberg, South Africa, and was maintained at a residence time of 72 h. *At. caldus* was grown in a 1L shake flask with a 700 mL working volume, agitated at 120 rpm on an orbital shaker. The culture was grown in modified 5K medium, consisting of the following ($g.L^{-1}$): $(NH_4)_2SO_4$ (2.0), K_2HPO_4 (0.5), $MgSO_4.7H_2O$ (0.5), KCl (0.1) and S (5.0) and was initially at a pH of 1.6.

6.2.3 Biokinetic tests

Biokinetic accelerated weathering tests were performed following the procedure outlined in Opitz et al. (2015). A 7.5 gram sample of the prepared waste sample was added to a total volume of 150 mL autotrophic basal salt media (Bryan et al., 2006) at pH 2.0 in each 250 mL Erlenmeyer flask. The flasks were inoculated with the mixed microbial culture to achieve the specified starting inoculum concentration (10^9 cells per ml used as standard). Biokinetic test flasks were incubated at 37°C on an orbital shaker maintained at 150 rpm for 90 days.

Initial inoculum concentrations of 10^7, 10^8, 10^9 and 10^{10} cells in 150 mL were investigated in triplicate flasks together with three, un-inoculated control flasks. To remove the initial soluble iron from the inoculum, approximately 100 mL of each of the mixed Fe-oxidising and S-oxidising were mixed and filtered through a 0.23 µm filter. After filtration, the soluble iron was removed from the filter paper through successive oxalic acid washes using excess oxalic acid. The micro-organisms retained on the filter paper were re-suspended in 10 mL ABS solution at a pH of 2.0, with microbial counts performed to quantify the total microbial concentration. Inoculation of the biokinetic flasks was achieved through addition of the appropriate volume from this solution, ensuring a total volume of 150 mL within each biokinetic flask.

6.2.4 Sampling and solution analyses

The biokinetic tests were sampled every day for the first month of the test, with sampling occurring every second day thereafter. The biokinetic flasks were analysed for pH, redox potential, ferrous and total iron concentrations and sulphate concentrations, with a 2 mL solution sample collected on each sample day. Solution pH was measured using a Metrohm 713 pH meter while the redox potential of the solutions was measured using a Metrohm 704 Eh meter against a silver / silver-chloride reference electrode. Ferrous iron concentrations were determined colorimetrically using the 1-10 phenanthroline method, with total iron concentrations determined using the same method after the addition of excess hydrolyamine. Soluble sulphate concentrations were determined turbidimetrically using the barium sulphate method.

6.2.5 Activity tests

After the biokinetic tests had been running for 40 days, activity tests were performed to gain an indication on the Fe- and S-oxidising ability of the micro-organisms present within one flask at each of the different initial inoculum concentrations. To investigate the activity of the Fe-oxidising micro-organisms, 95 mL of a 5 g/L Fe^{2+} iron solution at pH 2.0 was inoculated with 5 mL of the solution from the biokinetic test of interest. An activity test was performed on one flask from each initial inoculum concentration. To investigate the activity of the S-oxidising micro-organisms, approximately 0.25g of elemental sulphur was added to 95 mL ABS solution at pH 2.0, to which a similar 5 mL aliquot of culture from the biokinetic test was added. Activity tests were maintained at 37°C on an orbital shaker at 150 rpm for 100 hours, with regular monitoring of ferrous iron and sulphate concentrations respectively.

6.3 Results: Inoculum Concentration in the Biokinetic Test

6.3.1 Effect of changes in initial inoculum concentration under uncontrolled pH biokinetic tests

No significant effect on the starting solution pH was observed as a result of the order of magnitude differences in inoculum concentration, owing to standardisation of the initial suspending medium of the inoculum. The initial increase in pH observed across all flasks over the three days of the test was similar (Figure 6-1A), increasing from pH 2.4 following inoculation to approximately pH 5 with a concomitant decrease in redox potential to below 300 mV (Figure 6-1B), the latter assumed to result from ferric iron precipitation. For the non-inoculated flasks, a similar increase in solution pH was observed, with a higher pH value of 5.4 reached. This increase in pH was controlled by the acid neutralising capacity of the ore. Thereafter a gradual decrease in the pH of all flasks was observed to a plateau region of approximately pH 4.0 till Day 20 (except for the highest inoculum concentration). The decrease in solution pH from pH 4 to pH 2 was initiated from Day 20 for all flasks except that inoculated with 10^{10} cells in which the pH decreased from pH 4 at 12 days. The decrease in solution pH was mirrored by an increase in the redox potential due to the increased iron solubility at pH below pH 3.5 and microbial action. The rate of increase of the redox potential was similar for all inoculated flasks, increasing from 300 mV to 700 mV over a 6 to 8 day period. The redox potential of the un-inoculated flasks also increased from Day 20, albeit more gradually reaching 600 mV at Day 30 and 700 mV at Day 70. These redox potential levels in the un-inoculated controls suggested the presence and activity of inherent Fe-oxidising micro-organisms within the non-inoculated flasks, but the absence of a ferrous iron scavenger such as *L. ferriphilum* until late in the test.

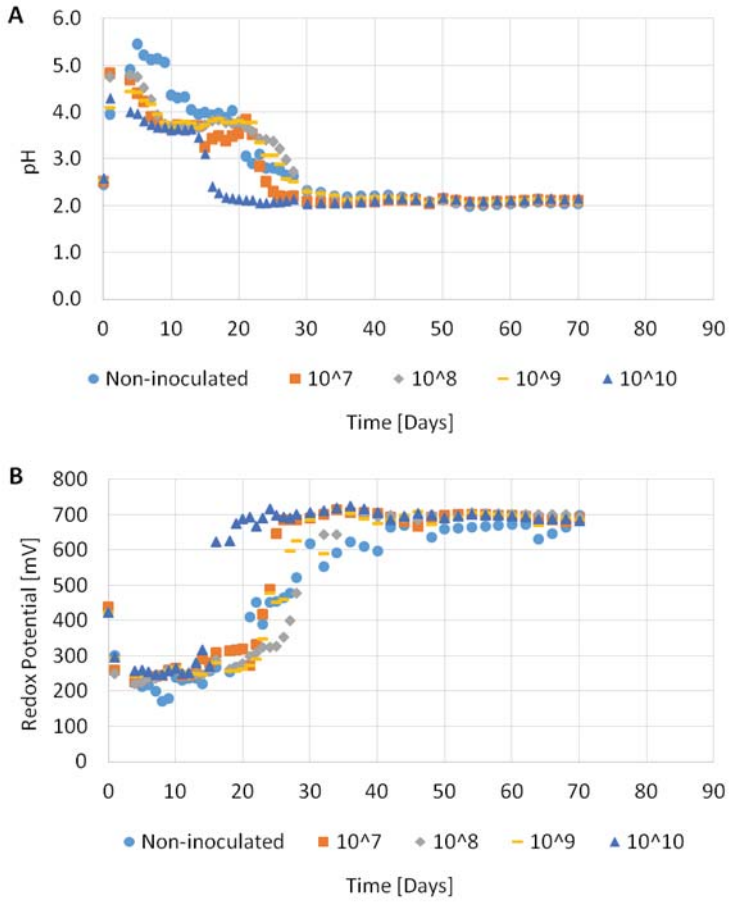

Figure 6-1 Solution pH (A) and redox potential (B) results with time for un-inoculated biokinetic tests and test with initial cell concentrations from 10^7 to 10^{10} cells in 150mL

Comparison of the ferrous iron and total iron concentrations confirmed the time period at which significant activity of the Fe-oxidising micro-organisms occurred (Figure 6-2). In all flasks an increase in ferrous iron concentration was observed over the first 10 days. In all inoculated flasks except those inoculated at 10^{10} cells, the Fe^{2+} concentration continued to increase, albeit at a slower rate, to more than 500 mg/L Fe^{2+} before the onset of microbially-mediated ferrous iron oxidation resulted in its depletion. In the flasks inoculated with 10^{10} cells, the ferrous iron concentration plateaued at 350 mg/L, presumably due to iron cycling, before decreasing from day 13 and depletion by day 16. The rapid increase in the redox potential supported the faster decrease in the ferrous iron concentration under this condition. For the other flasks, the rate of increase in ferrous iron concentration up to day 20, and the subsequent decrease in ferrous iron concentration, was similar. The increase in ferrous iron concentration was delayed in the non-inoculated flasks, increasing to 240 mg/L at day 15, i.e. approximately half that attained in the inoculated flasks due to delayed iron cycling prior to natural inoculation. Decrease of Fe^{2+} was evident from day 25 with depletion by day 30.

The difference between the inoculated and non-inoculated flasks was further highlighted by the total iron concentrations observed over the course of the experiment. The lower soluble iron concentration in the non-inoculated flasks was observed regardless of the oxidative environment due to the excess concentrations of ferric iron as compared to the ferrous iron. Interestingly, the 10^{7} and 10^{10} flasks exhibited the highest total iron concentrations, prior to decreasing concentrations.

The significant differences in the total iron concentrations observed between the inoculated and non-inoculated flasks were not observed in the sulphate concentrations between these flasks (Figure 6-3). Similar profiles were observed between the inoculated and non-inoculated flasks, with the exception of those initially inoculated with 10^{7} and 10^{10} cells, with the deviation in the sulphate concentration profiles mirroring the profiles observed in the total iron concentrations. For the flasks inoculated with these concentrations, the maximum concentrations were observed at day 40, with the decrease in the concentrations thereafter suggesting either precipitation or removal of the oxidation products due to the solution sampling. By the end of the experiment, similar sulphate concentrations were observed within the biokinetic flasks, irrespective of initial inoculation. Furthermore, an approximate constant level in the sulphate concentrations was observed from day 50.

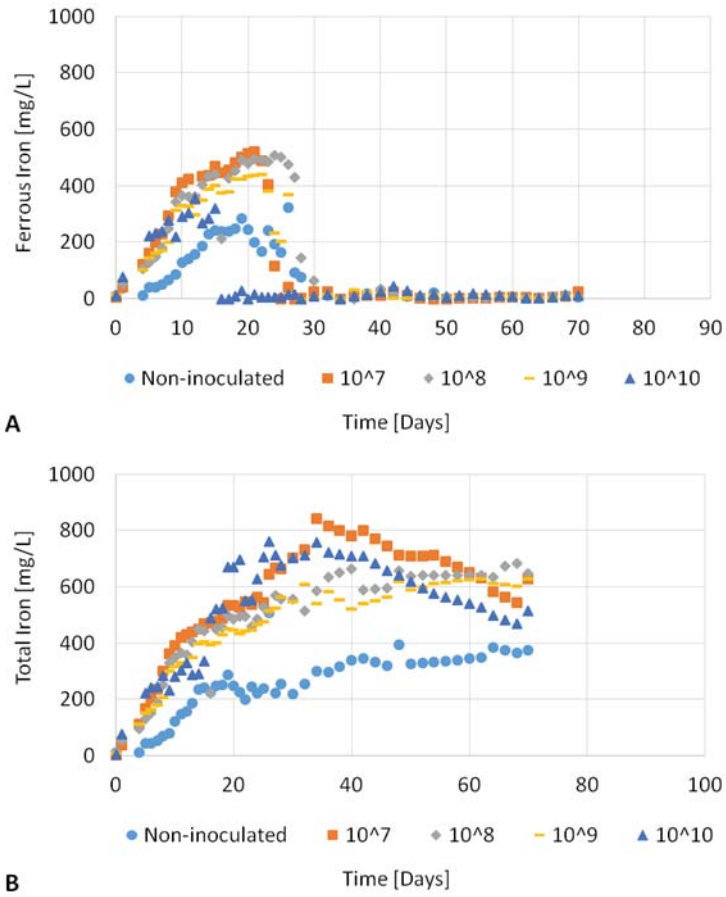

Figure 6-2 Ferrous iron (A) and total iron (B) concentrations for biokinetic tests with differing initial microbial concentrations

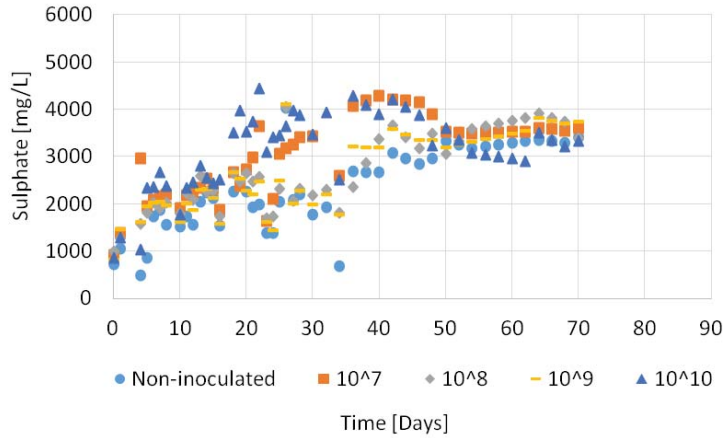

Figure 6-3 Sulphate concentration results for biokinetic tests conducted with differing initial microbial concentrations

To investigate the continued presence of the iron- and sulphur-oxidising micro-organisms within the inoculated and non-inoculated biokinetic tests, activity tests were conducted on liquid samples for one biokinetic test flask from each of the triplicates conducted at the different inoculum sizes. The data are presented in Figure 6-4. In the activity test of a healthy bioleaching culture, ferrous iron depletion is complete within 24 h. In these tests, no substantive ferrous iron oxidation was recorded in the first 24 h and depletion required 60 to 80 h. This suggested a low microbial activity. Further, the microbial activity within the un-inoculated and inoculated flasks were similar.

The microbial phase was further studied at the end of the test at 90 days. At this point, the microbial cells were collected, and DNA extracted for qPCR analysis according to Tupikina et al. (2013). The microbial copy numbers are presented in Figure 6-5 as a function of the test conditions. In these data, other bacteria" represent the difference between the copy numbers determined using the UniBact primer and *L. ferriphilum* and *At. caldus* primers, whereas "other archaea" represents the difference between the copy numbers determined using the UniArch and *A. cupricumulans* primers. These data demonstrate the low copy numbers (of the order of 10^6) relative to the inoculum concentrations. Further the dominant microbial species in these biokinetic tests are shifted substantially from the inoculum speciation.

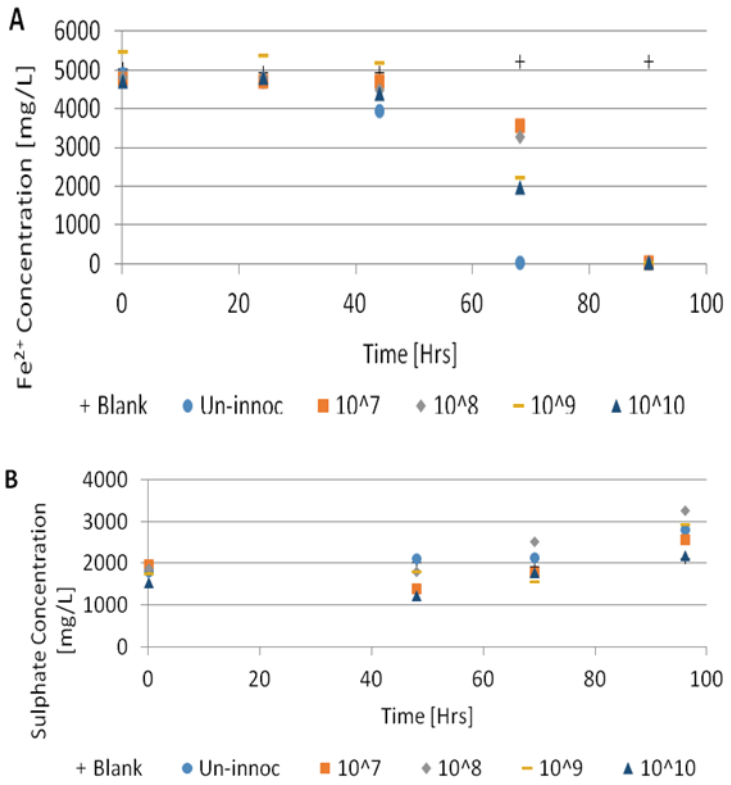

Figure 6-4 Activity test results for the un-inoculated biokinetic tests sampled at 40 h

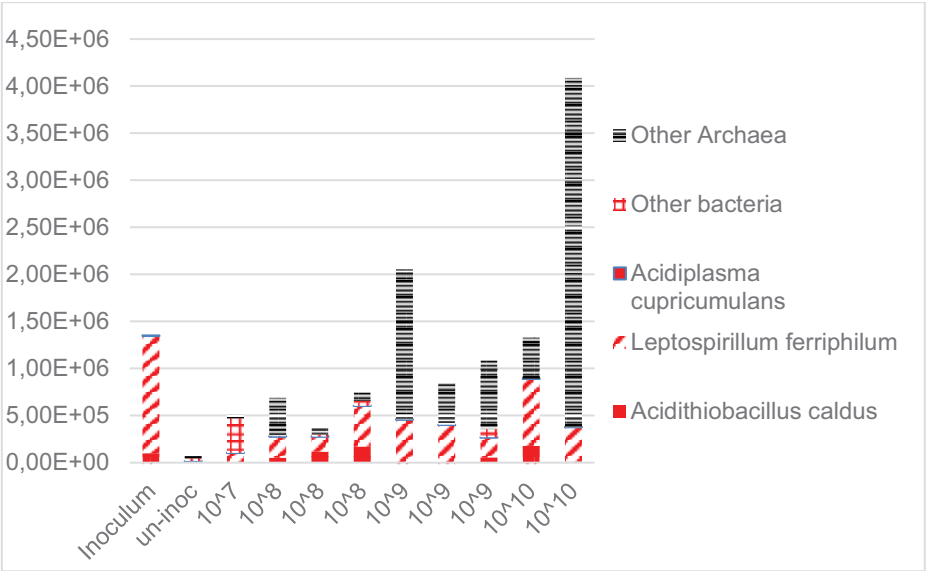

Figure 6-5 The microbial speciation determined at the end of the biokinetic tests in terms of copy number

6.3.2 Comparison of leaching under controlled and uncontrolled pH conditions in the biokinetic tests

The progression of pH controlled and uncontrolled biokinetic tests, inoculated with 10^9 cells were compared with data presented in Figure 6-6. In the pH controlled tests, the pH was corrected by titration to pH 2 at each sample point if it were found to be higher. By recording the acid addition required, the acid neutralisation capacity could be estimated. Figure 6-6A demonstrates the limited increase in pH compared to the pH elevation to approximately pH 4 for in excess of 20 days in the uncontrolled test. Figure 6-6B illustrates that maintenance of the low pH facilitated the rapid onset of ferrous iron oxidation with the establishment of a redox potential of 700 mV within 8 days compared with 30 days in the uncontrolled case. The rapid onset of ferrous iron oxidation is confirmed by data presented in Figure 6-6C while Figure 6-6D demonstrates the enhanced leaching achieved and thereby total iron in solution (>1400 mg/L in 10 days). These data confirm the value of the pH controlled biokinetic test in expediting the test.

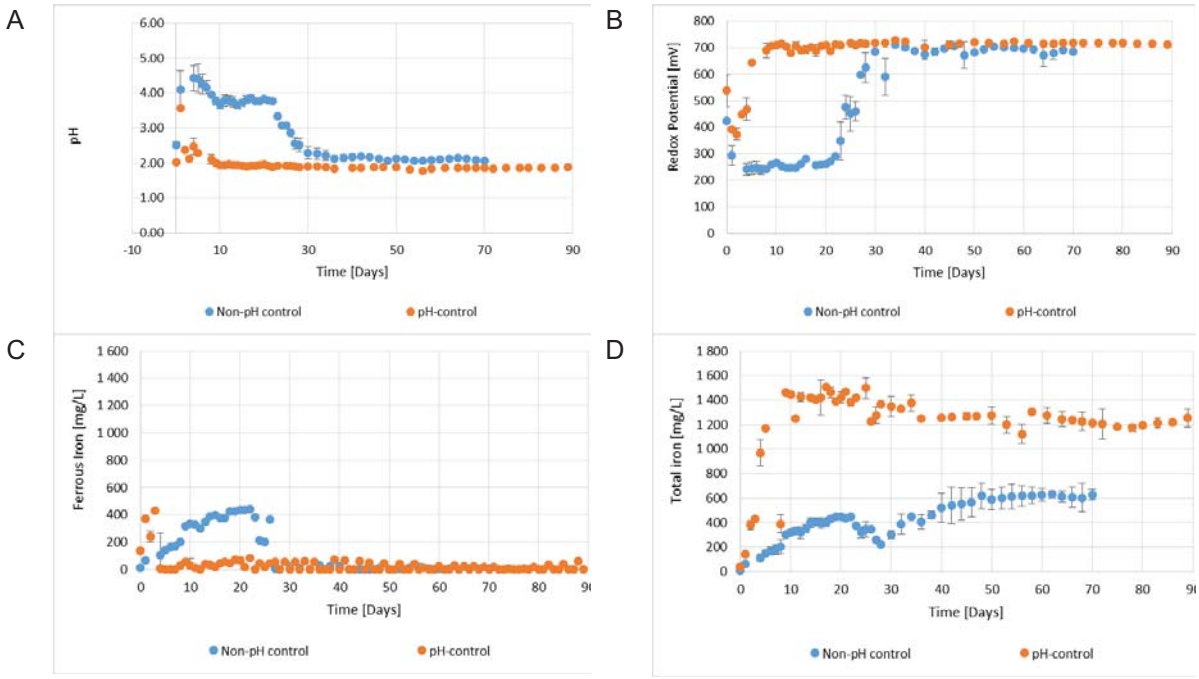

Figure 6-6 Comparison of the controlled and uncontrolled pH biokinetic tests inoculated with 10^9 cells. A: pH profile; B: redox potential profile; C: ferrous iron concentration; and D: total iron concentration, with time.

6.4 Discussion of Inoculum Concentration and pH Control of Biokinetic Test

The initial increase in solution pH observed was due to acid consumption by acid neutralising minerals present, i.e. it was controlled by the mineral ore phase and not the microbial culture. This supported the little difference in initial pH of the flasks despite differing inocula. The similar time point for the onset of decrease in pH, related to ferrous iron oxidation, in all flasks except those inoculated with 10^{10} cells suggested similar activity of the iron- and sulphur-oxidising microorganisms in these flasks. This further suggested that the initial cell concentration played no or little role in the pH profile for the flasks, with the exception of flasks inoculated with 10^{10} cells. The Fe-oxidation activity tests supported the absence of significant differences in the rate of ferrous iron oxidation regardless of initial cell concentration.

These data confirm that the active inocula had not persisted during the high pH period following acid neutralisation by the ore. In addition, the waste rock contained some pyrite and pyrrhotite which has been implicated in the formation of reactive oxygen species in the presence of fine particulates with

potential cell stress or death (Jones, et al., 2011; 2012). However, natural re-inoculation was evident and is supported by the difference in the microbial consortia in these flasks compared with the inoculum.

Through control of the pH of the biokinetic test to less than or equal to pH 2.0, significant enhancement of the progression of the test was found. This suggests that the inoculum viability is maintained and the duration of the biokinetic test can be expedited.

While the operation of uncontrolled pH biokinetic tests are critical to provide information on the acid neutralisation potential and subsequent onset of acid generation, these operating conditions may impact the effectiveness of the microbial inoculation added. This effect is dependent on the ore sample investigated and can be largely overcome by the additional operation of pH controlled biokinetic tests in which maintenance of the pH at or below pH 2 ensures conditions appropriate to the microorganisms catalysing the regeneration of the leach agents for bioleaching. Further studies will be conducted to explore this approach. In addition, the impact of the initial microbial population size and microbial composition will be investigated under conditions of pH control.

CHAPTER 7: THE SEMI-CONTINUOUS BIOKINETIC TEST FOR ARD POTENTIAL

Also presented as:
Mhlangabezi T. Golela, Alex K. B. Opitz, Mariette Smart, Seteno K. O. Ntwampe, Jennifer L. Broadhurst and Susan T.L. Harrison. 2019. The semi-continuous UCT biokinetic test provides improved characterisation of acid rock drainage potential of sulphidic waste rock by inoculated and naturally occurring microorganisms. Minerals Engineering (Under Review)

7.1 Introduction to the Semi-Continuous Biokinetic Test

Large quantities of sulphide-bearing mine waste rock and tailings undergo oxidation reactions in the presence of water and air, producing acid rock drainage (ARD). The presence of naturally occurring iron and sulphur-oxidising microorganisms in the environment facilitates the process of ARD generation through regeneration of the ferric iron and acid lixiviants responsible for the leaching of mineral sulphides to release metal ions, sulphate and acid into solution (Bryan, et al., 2006; Hallberg, 2010; Kazadi Mbamba, et al., 2012). In addition to the acidity and salinity generated, mobilisation of deleterious elements, especially heavy metals, during ARD generation adds to the potential environmental burden. An accurate, cost-effective and rapid characterisation of these waste materials prior to their disposal is required to inform their appropriate disposal strategies to minimise pollution. Furthermore, application of such characterisation approaches can assist in processing decisions being made to both maximise value recovery and minimise environmental burden potential simultaneously.

The commonly applied ARD characterisation methods used at the laboratory-scale are static chemical and kinetic tests (Smart, et al., 2002; Price, 1997; Weber, et al., 2005). The static acid-base accounting (ABA) and net acid generation (NAG) tests are used as a screening method and provide data for the potential for acid formation under chemical conditions. Following this classification, kinetic tests or humidity cell tests or both are performed on those samples which are classified as potentially acid-forming (PAF) or are inconclusive under static test conditions. Prescribed humidity cell tests provide information on the natural weathering of the wastes under humid conditions and aid in understanding the rate of ARD generation and the composition of the resulting liquor. However, the current kinetic tests used are long-term tests of six months or more, potentially requiring several years before the full ARD potential is understood. Further, these do not account for the key role played by microorganisms in the facilitation of ARD generation from mine waste.

To address the shortcomings of the conventional static tests in terms of extreme oxidising environment and kinetic ARD characterisation tests in terms of the rate of reaction, the accelerated batch biokinetic test protocol was developed as a small scale flask test, operating over 90 days under conditions of microbial activity (Hesketh, et al., 2010a). These tests are designed to allow microbially- facilitated oxidation through the addition of a microbial inoculum and a nutrient-replete medium with un-inoculated “control tests” also being carried out. Batch test conditions do not allow for the natural removal of reaction products typical of a flow-through system, thereby simulating a pond rather than historic workings or percolation through a heap or dump. Hence decoupling of the acid neutralisation and acid formation rates is required. In particular, rapid initial neutralisation due to high levels of rapidly soluble ANC in the sample may result in elevated pH conditions in the tests, which adversely affects microbial activity and leads to a delay in the acidification of the waste sample (Opitz, et al., 2016c), hence not providing good insight into its acidification potential. To address the challenges associated with waste containing an elevated neutralising content, the downward control of solution pH or the implementation of semi-continuous test conditions have been proposed (Broadhurst, et al., 2013; Hesketh, et al., 2010a; Hlongwane, 2015; Kotelo, 2013) and is presented in Chapters 5 and 6. In the pH-controlled batch

biokinetic test, the material is exposed to acidic waters continuously, allowing the depletion of rapidly dissolving ANC over a short period, where after the acidophilic microbial community can establish, facilitating acidification. Initial development of the semi-continuous draw-and-fill test has been developed to improve insight into the relative acidification and neutralisation over the batch biokinetic test protocol in ARD characterisation. This includes both intermittent removal of leachate solution containing dissolved components of ANC and inhibitory by-products seen in batch biokinetic test and subsequent introduction of low pH fresh media containing salts that mimic the acidified environment and facilitate proliferation of micro-organisms, both naturally-occurring in the samples and those used to initiate the tests. These tests are expected to allow for better understanding of the acid generating behaviour under conditions which are more representative of the flow-through conditions that occur in a waste deposit (Broadhurst, et al., 2013; Makaula, et al., 2019).

The aim of this study was to develop the semi-continuous biokinetic test to ascertain its benefit in elucidating the relative rates of acid neutralisation and generation, to determine the characterisation of ARD potential, to assess the nature and the role of the microbial consortia over a progressive leaching period performed, and the interaction of physiochemical conditions developed and microbial community and its activity under inoculated and non-inoculated, semi-continuous and batch biokinetic test conditions. Static chemical tests and mineralogical characterisation were conducted to inform and complement the biokinetic tests. A better understanding of microbial community dynamics within the biokinetic tests is expected to inform inoculation strategies for waste rock samples with differing mineralogical compositions.

7.2 Materials and Methods for Development of the Semi-Continuous Biokinetic Test

7.2.1 Sample description

Two waste rock samples were used in this study: a gold-bearing sample (GBS) sourced from a Greenstone gold deposit in Tanzania; and a low grade copper-bearing sample (CBS) sourced from Northern Chile. The mineralogical composition of the gold-bearing sample (GBS) was determined using QEMSCAN® analysis on an FEI QEMSCAN® 650F analyser and reported in Opitz et al. (2016c). The detailed mineralogy of the copper-bearing sample (CBS) was obtained directly from the mine (Opitz, 2013). Sample mineralogy is presented in Table 7-1.

Both waste rocks, GBS and CBS, were previously classified as potentially acid forming (Opitz, et al., 2016c; Opitz, 2013) using acid-base accounting (ABA) and net acid generation (NAG) (Miller, et al., 1997) conducted on material milled to 100% < 150 µm. The results are presented in Table 7-2.

Table 7-1 Mineralogical composition of the waste rock samples used in the completion of this study following QEMSCAN® analysis for the GBS (Opitz et al., 2016) and using mine data for the CBS (Opitz (2013)).

Mineral type	Mineral formula	GBS (wt. %)	CBS (wt. %)
Chalcopyrite	$CuFeS_2$	0.03	1.3
Galena	PbS	0.03	1.7
Pyrite	FeS_2	1.2	2.6
Pyrrhotite	$Fe_{(1-x)}S$	5.8	0.5
Other sulphides	ZnS, CuS, Cu_2S	0.0	0.9
Calcite	$CaCO_3$	0.9	0.0
Chlorite	$(Mg.Fe)_5Al((Si_3AlO_{10}(OH)_8$	1.4	0.5
Fe oxide/hydroxide	Fe_3O_4	33.4	16.5
Hornblende	$Ca_2(Al)_5\ Si_8O_{22}(OH)_2$	9.6	1.3
Albite	$NaAlSi_30_8$	13.6	4.8
Biotite	$K(Mg,Fe)_2Al_2Si_3O_{10}(OH)_2$	1.7	0.3
Kaolinite	$Al_2Si_2O_5(OH)_4$	0.0	4.8
Muscovite	$KAl_2(AlSi_3O_{10})(FOH)_2$	0.0	21.5
Quartz	SiO_2	26.1	42.2
Other		1.1	1.0

Table 7-2 Static results for ARD characterisation of waste rocks (Opitz et al., 2016, Opitz, 2013) indicating the potentially acid forming classification of both waste samples

Waste Sample	Sulphur Grade [%]	MPA [kg H_2SO_4/ton]	ANC [kg H_2SO_4/ton]	NAPP [kg H_2SO_4/ton]	NAG pH	ARD Classification
GBS	2.3 ± 0.0	70.2 ± 0.7	53.2 ± 1.8	17.0 ± 1.9	2.50 ± 0.0	Potentially Acid Forming
CBS	3.15 ± 0.1	96.3 ± 1.7	3.39 ± 0.2	92.9 ± 1.7	2.63 ± 0.0	Potentially Acid Forming

7.2.2 Biokinetic tests

7.2.2.1 Microorganisms used in biokinetic tests

An inoculum, made up by a 1:1 ratio of a *Leptospirillum ferriphilum* dominated culture and an *Acidithiobacillus caldus* dominated culture, both grown on pyrite, was cultured in autotrophic basal salt (ABS) medium at pH 2 (Govender, et al., 2013), supplemented with trace elements (Bryan, 2006) and 0.6% w/v pyrite. The inoculum culture was maintained in draw-and-fill mode, by withdrawing 10% (v/v) of the volume and replacing it with fresh ABS medium, on a shaking platform (120 rpm) at 37°C. Prior to inoculation, the cells were harvested by filtering 300 mL culture onto 0.22 µm cellulose filter membranes and washing with 10 mM Na-citrate buffer (pH 2) to remove soluble iron. The cells were re-suspended from the filter discs in 10 mL ABS medium at pH 2 for inoculation of the biokinetic tests. Direct microscopic cell counts of the inoculum were to calculate the inoculum volume required.

7.2.2.2 Biokinetic test procedure

Batch biokinetic tests without pH control were carried out using a refined protocol developed from those conducted by Broadhurst et al. (2013) and semi-continuous biokinetic tests modified from these. For each biokinetic test, 150 mL ABS solution at pH 2.0 was added to 7.5 g of waste rock material in a 500 mL flask. Tests were inoculated with 10^9 cells from the prepared inoculum to achieve a final microbial concentration of 6.67 x 10^6 cells/mL. Un-inoculated controls were included for each test. Flasks were incubated at 37°C and 150 rpm for the duration of the test. The biokinetic test flasks were compensated for evaporation daily by the addition of acidified water to correct for volume loss by weight,

prior to sampling. In the semi-continuous biokinetic tests, 10% total solution volume (15 mL) was removed, following a brief settling period to avoid mineral removal, and replaced with fresh ABS solution at pH 2.0. Redox potential, soluble iron and sulphate concentrations were measured in the volume removed. For the semi-continuous test, pH measurements were performed before sampling and after addition of fresh ABS medium. For the batch tests, analytical measurements were performed within flasks and a small sample volume withdrawn iron and sulphate assay. At specific time intervals, the planktonic microbial population was sampled for qPCR analysis. All tests, except microbial speciation, were conducted in triplicate, using triplicate flasks for each test condition.

7.2.2.3 Analytical methods

The pH was recorded using a 713 Metrohm pH meter while the redox potential was measured using a 703 Metrohm Eh meter and an Ag/AgCl reference electrode. The 1-10 phenanthroline method was used to measure ferrous iron (modified from Komadel and Stucki, 1988) and total iron, the latter following conversion to ferrous iron by addition of hydroxylammonium chloride. The sulphate concentration was determined using the $BaCl_2$ turbidity method (APHA, 1998).

7.2.2.4 Microbial community analysis

For the semi-continuous biokinetic tests, cells were harvested from the 15 mL withdrawal by centrifugation at 13 800 g for 10 min. Resultant cell pellets were washed twice with 10 mM Na-citrate buffer (pH 2) to remove any soluble iron and once with Tris EDTA buffer (pH 7.4) to neutralise the samples before they were stored at -20°C preceding DNA extraction. DNA was extracted and subsequently subjected to qPCR analysis using the methods detailed in Smart et al. (2017) and primers given in Tupikina et al. (2013). Results are presented as the abundance of species as a proportion of total cell numbers calculated from DNA yields. Total DNA extracted per mL test volume was calculated following the quantification of the DNA using a Nanodrop® spectrophotometer. The total DNA content of one cell was taken as 2.7 fg calculated for *L. ferriphilum* based on a genome size of 2.5 Mbp.

7.3 Results in Development of the Semi-Continuous Biokinetic Test

7.3.1 Mineralogy and ARD potential static test results for GBS and CBS

Quantification of the minerals present in each sample was used to determine the overall acid generating and acid consuming potentials based on mineral availability (Figure 7-1). The presence of a significant amount of acid-consuming mineral within the mine waste is expected to result in the progression of ARD being partially neutralised if generated simultaneously or in a batch system. The presence of a high proportion of sulphide-containing minerals would indicate rapid ARD generation. While different ratios of sulphide minerals were present in the two samples, both contained a similar total proportion of acid-generating sulphides (~ 7 wt. %). Conversely, substantial differences in the proportion of acid-consuming minerals between the GBS (36 wt. %) and CBS (16 wt. %) suggested a greater acid neutralising capacity for GBS. In addition, the difference in the neutralising behaviour of the two samples would be exacerbated by the differences in mineral reaction rates. While rapid neutralisation was expected for the GBS due to the presence of fast-reacting calcite, the dominance of the intermediate (chlorite, biotite) and slow-weathering (magnetite) acid consuming minerals in the CBS suggested acid neutralisation over an extended time frame.

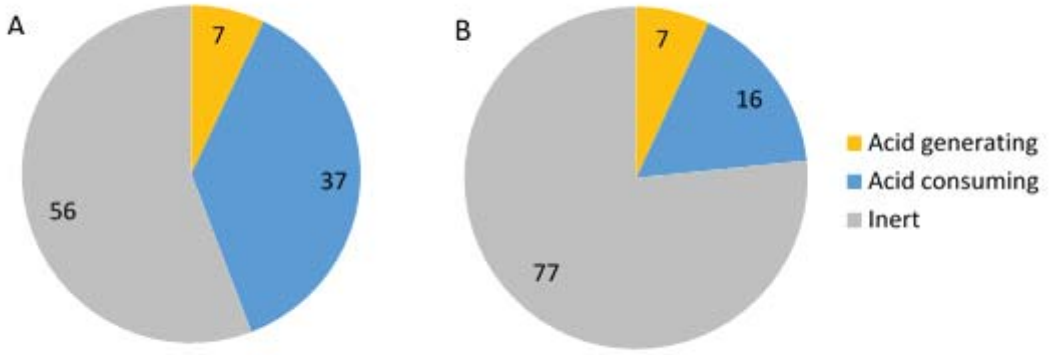

Figure 7-1 Proportion of acid generating, neutralising and inert components of gold-bearing sample(A) and copper-bearing sample (B) based on the mineralogy given in Table 7-1

7.3.2 Biokinetic tests performed on GBS

The pH in the batch biokinetic tests and semi-continuous biokinetic test of the GBS increased to pH 5.77 within the first 24 hours for both inoculated and non-inoculated tests (Figure 7-2A). In the semi-continuous biokinetic test, replacement of 10% of the test solution with fresh ABS medium at pH 2 on day 1 resulted in a reduction of the pH to 3.31. A lower increase in pH, to pH 4.63, was recorded on day two of the semi-continuous test with replacement of 10% of the solution with ABS medium resulting in pH 3.17. This behaviour of decreasing pH continued in the semi-continuous test, with pre and post medium replacement respectively reaching pH 3.38 and 2.95 on day 5, pH 2,64 and 2.54 on day 10, and pH 2.40 and 2.03 on day 15. For the non-inoculated semi-continuous test, the pH values recorded were slightly higher on days 2, 3 and 4 (5.80, 5.00 and 3.91 respectively). On day 5 the pH was very similar to that recorded for the inoculated tests, 3.42 compared to 3.38. Conversely, the pH of the inoculated batch tests continued to increase from pH 5.77 on day 1 to pH 6.7 by day 3, before decreasing between days 4 and 8 from pH 6.53 to 4.02 (Figure 7-2A). For the non-inoculated batch tests, the pH only decreased after day 6, with a decrease from 6.62 to 3.98 measured between day 6 and day 11.

The initial increase in pH observed for both semi-continuous and batch biokinetic tests was due to reaction of rapidly dissolving acid neutralising minerals such as calcite. For both batch and semi-continuous GBS tests, inoculation accelerated the generation of acidity from microbial sulphide mineral oxidation and potentially ferric iron precipitation following microbial ferrous iron oxidation. In the GBS tests, acidity generated through microbial action reacted with the acid neutralising components, moderating solution neutralisation.

The increase of the redox potential differed between the inoculated and non-inoculated tests, being more pronounced for the semi-continuous tests (Figure 7-2B). The redox potential of the inoculated semi-continuous tests increased from 360 mV on day 5 to reach a maximum redox potential of approx. 670 mV on day 8, whereas the un-inoculated test also started increasing from 360 mV after day 5, but increased gradually to 393 mV at day 11, before increasing rapidly to 660 mV on day 13. This suggested presence of an indigenous inoculum active initially with a change in microbial community effective around day 11. The batch tests showed negligible increase in redox potential till day 6, followed by a gradual increase in redox potential from 250 mV till day 14, achieving 408 and 353 mV in the inoculated and un-inoculated tests respectively. Following a plateau, redox potential increased gradually after days 26 and 30 respectively to reach a maximum redox potential of approx. 700 mV after day 36 of the tests. These data suggest that the initial inoculum added to the batch test did not tolerate the high pH period and both inoculated and uninoculated batch tests were self-seeded by indigenous microorganisms.

The increases in redox potential were mirrored by the changes in the ratio of ferrous to ferric iron with time across all tests (Figure 7-2A and B) The inoculated semi-continuous tests reached a ferrous iron concentration of 370 mg/L on day 6 relative to the 200 mg/L in the non-inoculated tests. At day 7 there was a decline in ferrous iron concentration within the inoculated tests, while the ferrous concentration in the un-inoculated test only decreased after day 12. The ferrous concentration in the batch tests displayed a much slower increase. Ferrous concentrations started increasing around day 6 for the inoculated tests, but only reached a peak in concentration (approx. 200 mg/L) on day 18. Un-inoculated tests showed a similar trend, however, the rate of ferrous generation was slower for these tests between day 6 and 12. The ferrous concentration in the inoculated batch tests decreased rapidly around day 28, whereas ferrous in the un-inoculated tests only decreased after day 32.

The differences between inoculated and non-inoculated tests may be further observed in the redox potential data and ferrous iron concentration for both tests. The oxidation of soluble ferrous iron by the iron-oxidising micro-organisms present within the inoculum resulted in a high solution potential and low ferrous iron concentration being reached over a shorter time period, following the onset of microbial activity around day 6.

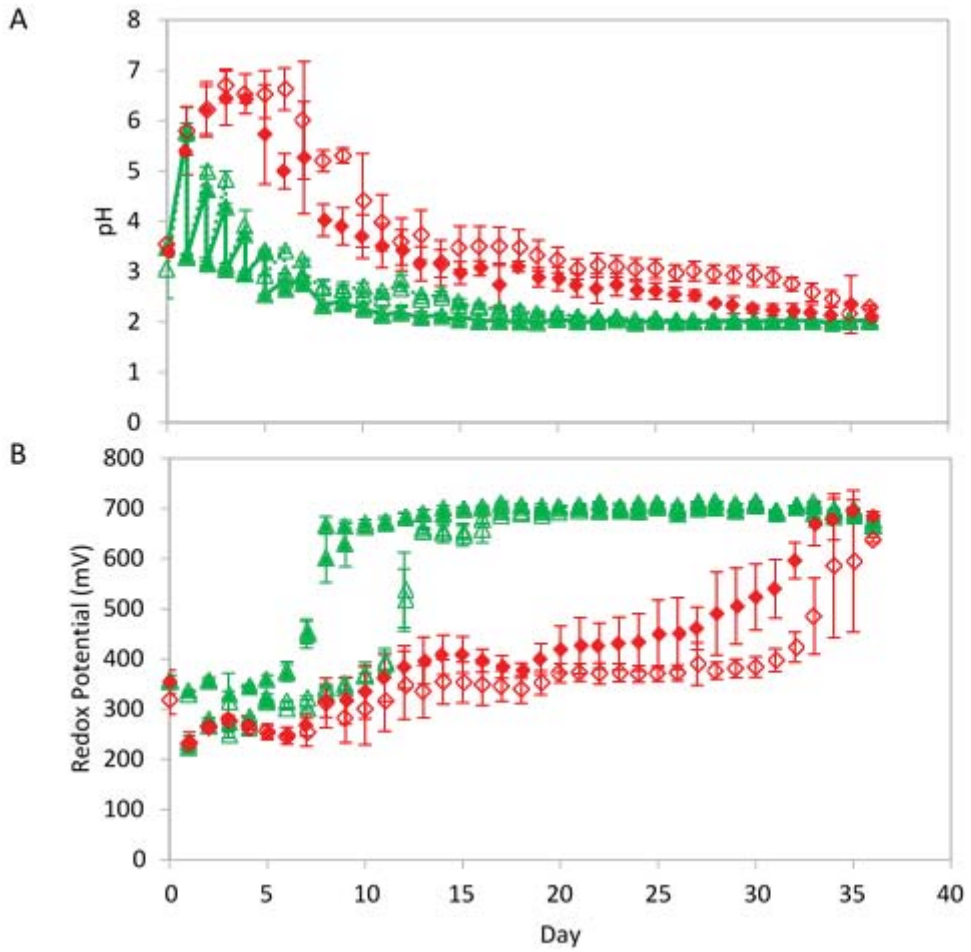

Figure 7-2 Variations in pH over time (A) for semi-continuous (▲, △) and batch biokinetic tests (◆, ◇). Two pH data points are shown for the semi-continuous tests representing the pH value before removing 10% of the supernatant and replacing it with an equal volume of ABS solution at pH 2, and the pH following addition. Lines indicate pH before removing supernatant and replacing it with ABS medium. Redox potential profile (B) with Error bars presenting standard deviation n=3 (where n represent number of flasks). The data series represent: ▲ Inoculated Semi-continuous, △ Non-inoculated Semi-continuous, ◆ Inoculated Batch, ◇ Non-inoculated Batch Biokinetic tests

For both sets of test experiments in the semi-continuous biokinetic test, a similar trend of increasing total iron concentration was observed over the initial six days, a phenomenon suggested to be indicative of chemical leaching. However, on day 12 the total iron of the inoculated samples increased to a maximum concentration of 500 mg/L. The decline in total iron observed for the semi-continuous tests was as a result of dilution created by the daily removal of 10% of the solution and replacement with fresh ABS medium. A plateau in the total iron concentration was observed for the non-inoculated tests between day 6 and 14, suggesting that the rate of removal of total iron, from the operating of the semi-continuous test, was approximately that of the rate of deportment from the waste sample.

Over the initial six days, similar sulphate concentrations were observed for the inoculated and non-inoculated semi-continuous tests (Figure 7-3C). After day 6, the sulphate concentration in the inoculated semi-continuous test increased more rapidly than that of the non-inoculated test and reached approx. 3 700 mg/L at day 13. This represents a release of some 6920 mg SO_4^{2-} per litre over this period taking into account the dilution as a result of the daily removal of 10% of the test solution, replacement with fresh ABS and the SO_4^{2-} in the ABS test medium. A similar, but more gradual, increase in sulphate concentration was observed for the non-inoculated semi-continuous test with a maximum sulphate concentration of approx. 3 100 mg/L reached after 18 days. The rapid increase in the inoculated test may be indicative of the action of sulphur oxidising organisms such as *At. caldus* included in the inoculum. Similar to the total iron concentrations, a decrease in sulphate concentrations was observed in the later stage of the semi-continuous tests, with the rate of removal and dilution of the sulphate in the test solution being higher than the rate of oxidation of the sulphide minerals. This likely suggests that for the semi-continuous tests there was a depletion of the available sulphides from the test mineral, based on an initial presence of 172.5 mg S in the 7.5 g mineral used for the test. The fluctuation thereafter may suggest dissolution of different forms of sulphur species within the mineral. The batch biokinetic tests, inoculated and un-inoculated, did not reach sulphate concentrations similar to those of the semi-continuous tests over the 30 days of the experiment.

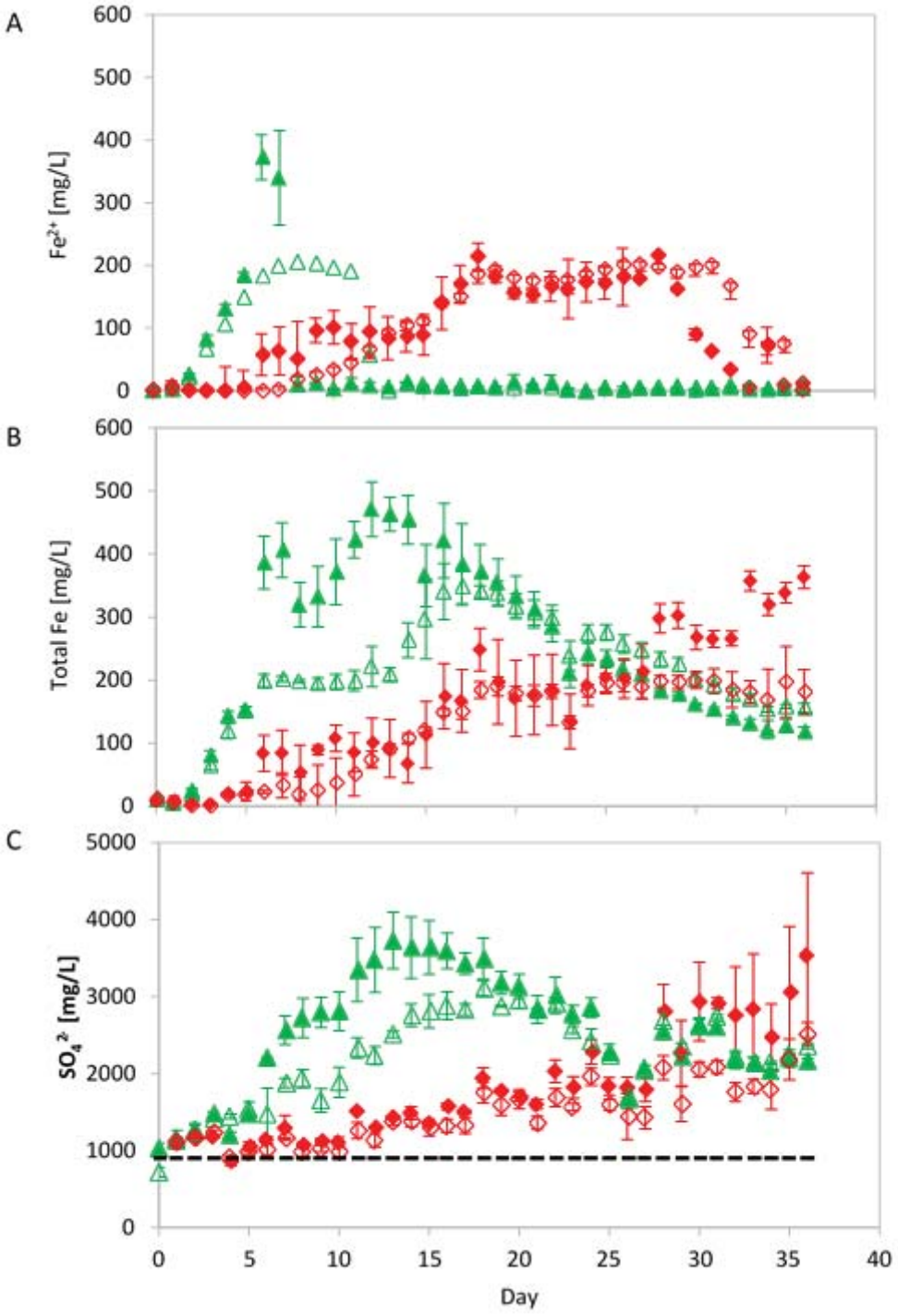

Figure 7-3 Ferrous iron (A), total iron (B) and sulphate (C) concentration profile generated from GBS as a function of time under semi-continuous (▲ △) and batch (◆ ◇) biokinetic test. The data series represent: ▲ Inoculated semi-continuous, △ Non-inoculated semi-continuous, ◆ Inoculated batch, ◇ Non-inoculated batch biokinetic tests. The dashed line (**- - -**) on graph C indicates the sulphate concentration present within the ABS medium used as test solution

Figure 7-4 shows the abundance of the microbial species in the semi-continuous biokinetic test. Sampling was performed at day 5 for both the inoculated and non-inoculated tests and again every five days following onset of increase in the redox potential within the test solution. A sample was again analysed on day 30 at the end of the test. The inoculated test was sampled at days 10 and 15 while the un-inoculated test was sampled at 20 and 25 days. For both the inoculated and non-inoculated tests,

At. caldus was the most abundant organism present at day 5. As expected, the number of *At. caldus* cells present per mL test volume was much lower in the non-inoculated tests compared to the inoculated tests owing to the lower initial cell number. The acid generated during the biooxidation of the sulphide portion of the mineral by *At. caldus* may also account for the earlier decrease in pH observed for the inoculated semi-continuous tests compared to the non-inoculated tests (Figure 7-2A). The increase in abundance of *L. ferriphilum* seen on day 10 of the inoculated test (Figure 7-4B) correlates well with the decrease in ferrous iron, substrate to the iron oxidising bacterium, observed during this time (Figure 7-3A). The generation of ferric iron together with the proton generation from the sulphide oxidation of *At. caldus*, may account for the increase in total iron observed over this period for the semi-continuous tests (Figure 7-3B).

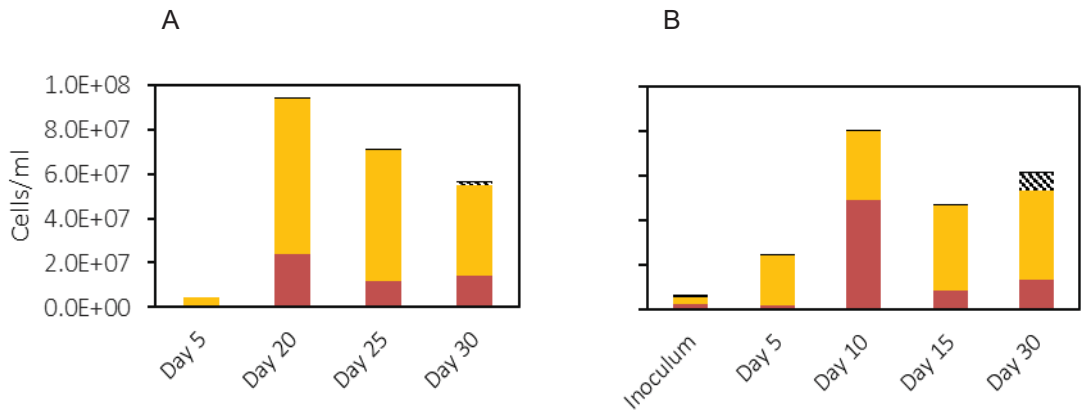

Figure 7-4 Microbial speciation determine in the non-inoculated (A) and inoculated (B) gold-bearing sample (GBS) semi-continuous biokinetic tests. Results are presented as 16S rRNA copy numbers expressed as the abundance relative to the cells/ml calculated from the DNA yields achieved

The semi-continuous biokinetic tests, with daily replacement of 10% of the solution volume with fresh ABS solution at pH 2.0, allowed for the removal of oxidation and dissolution products with time, particularly neutralisation capacity. Conversely, in the batch biokinetic test, the oxidation and dissolution products were retained in the solution, hence rapid release of acid neutralisation capacity resulted in substantial increase in solution pH, with potential to negatively affect microbial activity of the acidophilic micro-organisms. Manual control of solution pH, by the operation of a semi-continuous test, resulted in a decrease in the lag period prior to oxidative conditions within the flask experiments, with approximately half the time required to attain 700 mV as compared to the batch biokinetic flask experiments in this sample due to high ANC. This decrease in lag time was comparable to that experienced within the pH-controlled experiments reported by Opitz et al. (2016c), where the pH was adjusted daily by the drop-wise addition of H_2SO_4.

Replacement of 10% of the solution volume simulated a semi-continuous, flow-through system to better represent a typical ARD generating environment within a waste deposit. The removal of some test solution enabled the removal of oxidation and dissolution products which may limit the chemical reactions and provide a non-ideal environment for the micro-organisms within the tests, such as potentially toxic elements released from mineral dissolution and oxidation. For the tests performed on the GBS, this resulted in the dilution of acid neutralising components released from the mineral and lowered the pH conditions for the semi-continuous biokinetic tests. The removal of soluble reactant species, such as sulphides and ferrous iron, which act as substrates for the sulphur and iron oxidising microorganisms employed in these tests and of the microorganisms during the 'draw' phase may slow the rate of reaction. Where microbial growth is slower than the dilution rate of the tests, washout of the planktonic microbes may occur. This may occur under circumstances where the chemical leaching rate is slower than the rate of removal of the soluble species such as may be experienced when there is a

shift in the primary source of the iron and sulphur from easily solubilised pyrite or chalcocite components to slow-dissolving minerals.

7.3.3 Biokinetic tests performed on the copper-bearing sample (CBS)

The biokinetic tests, both semi-continuous and batch, were also conducted on a CBS containing a lower proportion of acid neutralising components, 16 wt % compared to 37 wt % for the GBS (Figure 7-1B). The pH in these tests remained close to the starting test pH conditions of 2 for the duration of the test with the highest pH, 2.5, recorded for the batch tests after 15 days (Figure 7-5A).

The redox potential in the inoculated semi-continuous test started to increase after 2 days, and the inoculated batch test after 3 days, with both tests reaching redox potential values of approx. 650 mV after 5 and 6 days respectively days (Figure 7-5B). Both the semi-continuous and batch un-inoculated tests only showed an increase in the redox potential 8 days after initiating the test and increased more gradually, over 4 days for the semi-continuous and 6 days for the batch tests, until a redox potential of approx. 650 mV were reached.

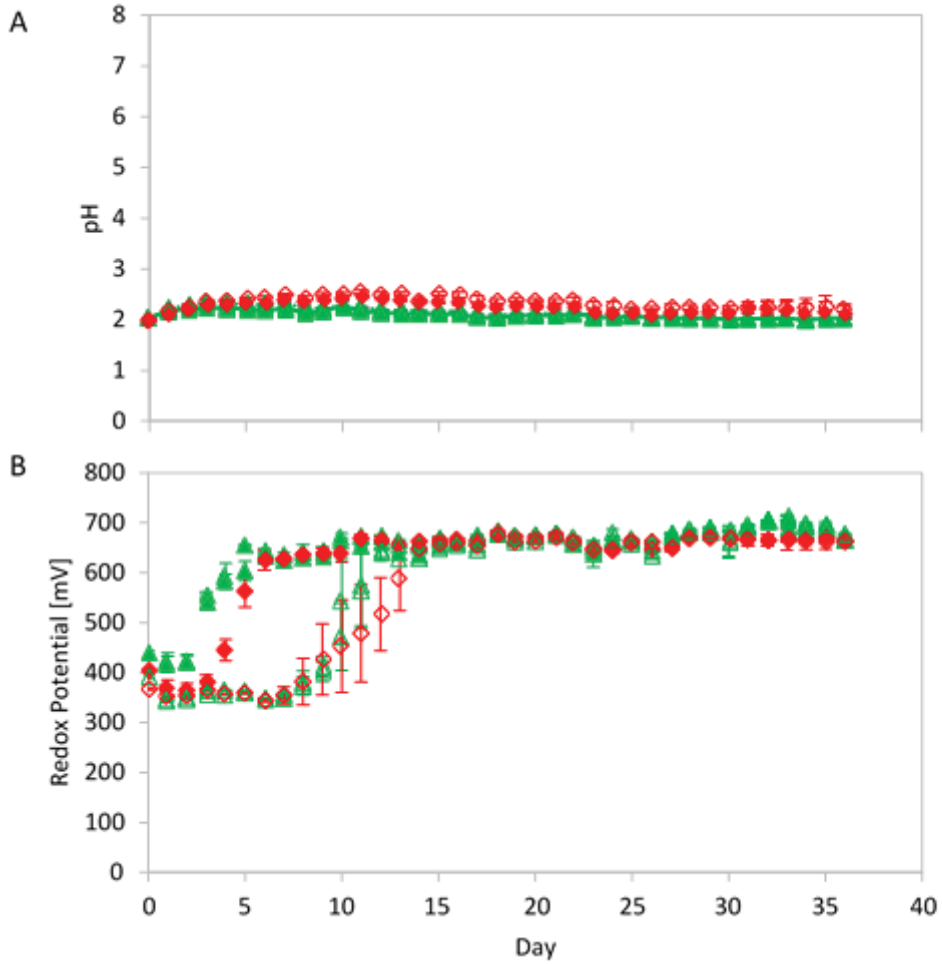

Figure 7-5 Solution pH of inoculated and non-inoculated flasks for semi-continuous (▲ △) and batch (◆ ◇) biokinetic test for copper bearing waste rock sample (CBS) as a function of time. The data series represent: ▲ Inoculated semi-continuous, △ Non-inoculated semi-continuous, ◆ Inoculated batch, ◇ Non-inoculated batch biokinetic tests

The increase in ferrous iron measured in the leachate initially was due to the mineral dissolution of the Fe-bearing minerals such as pyrite, pyrrhotite and chalcopyrite. The difference in ferrous iron concentration measured for the semi-continuous and batch tests was as a result of the dilution of the

test solution with the daily removal of 10% of the test volume and replacement with fresh ABS medium employed for the semi-continuous test (Figure 7-6A). The subsequent decrease of ferrous iron observed on day 2 for the semi-continuous and day 3 for the batch inoculated biokinetic tests respectively, is indicative of the microbial activity of iron oxidising microorganisms. The lag period of 7 days observed for the non-inoculated tests, suggested a period required for the proliferation of the natural microbial community present within the mineral sample. The total iron concentration was similar for both sets of tests for the first days of the experiments. The total iron of the semi-continuous inoculated test increased gradually until reaching a maximum concentration of 80 mg/L, while in the batch test the iron concentration fluctuated and reached a peak of 120 mg/L. This fluctuation in total iron concentration may result from both mineral leaching rates and precipitation of Fe^{3+} at pH > 2.0.

An initial increase in sulphate concentration between day 0 and 2 was observed across all tests, thereafter insignificant difference observed in the sulphate concentrations throughout the remaining duration of the tests performed on the CBS (Figure 7-6C) with the sulphate concentration oscillating around a mean of approximately 2000 mg/L. This was indicative of the formation of approx. 1100 mg-SO_4^{2-} per litre as ABS medium contains approx. 900 mg-SO_4^{2-}/L. It is recognised that the turbidity assay used to measure changes in SO_4^{2-} concentrations in this study has a large standard deviation, giving a coefficient of variance of 10-15%, hence measurement of small changes in the background of high SO_4^{2-} concentrations is difficult; however, more sensitive assays applicable to solutions containing iron are currently limited. Precipitation may further interfere with soluble SO_4^{2-} measurement.

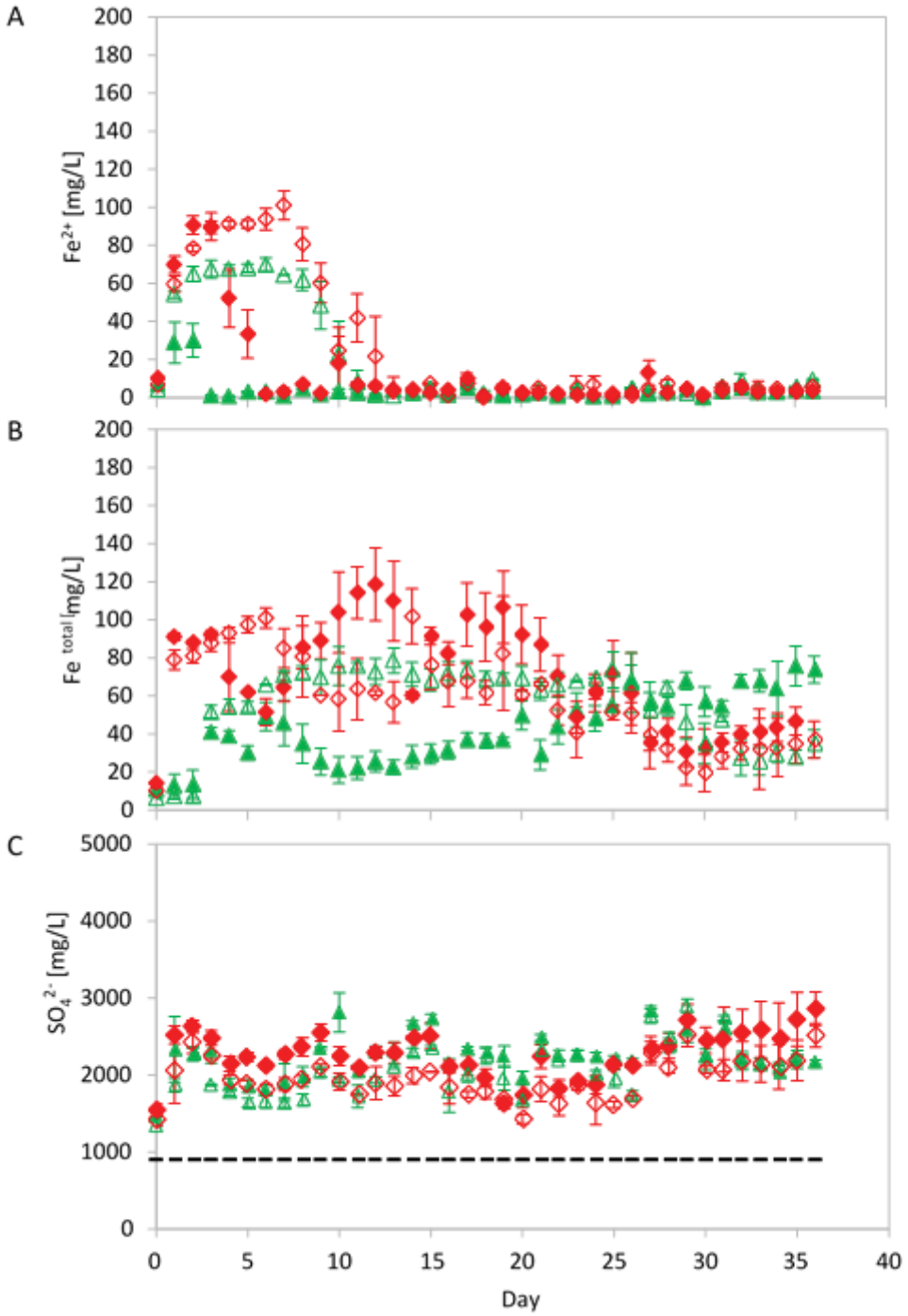

Figure 7-6 Ferrous iron (A), total iron (B) and sulphate (C) concentrations for copper bearing sample (CBS). The data series represent: ▲ Inoculated semi-continuous, △ Non-inoculated semi-continuous, ◆ Inoculated batch, ◇ Non-inoculated batch biokinetic tests. The dashed line (- - -) on graph C indicates the sulphate concentration in ABS medium used as test solution

Speciation results on the uninoculated and inoculated semi-continuous tests were performed on days 5, 15 and 30 of the tests. Results indicate the presence of significant numbers of the sulphur oxidiser *At. caldus* on day 5 of the uninoculated and inoculated tests (Figure 7-7). This may be the reason for the increase in sulphate concentration early in these tests (Figure 7-6C). For the inoculated test, the early presence of the iron oxidising species *L. ferriphilum* resulted in the decrease of the ferrous iron concentration in solution (Figure 7-6A), subsequent regeneration of ferric iron and increase in the redox potential within this test (Figure 7-5B). The delay in ferrous decrease in the uninoculated test, may be

as a result of low *L. ferriphilum* numbers as can be seen from the day 5 results and the subsequent establishment of the required cell number may have resulted in the decrease of ferrous iron observed around day 7 of the test (Figure 7-6A).

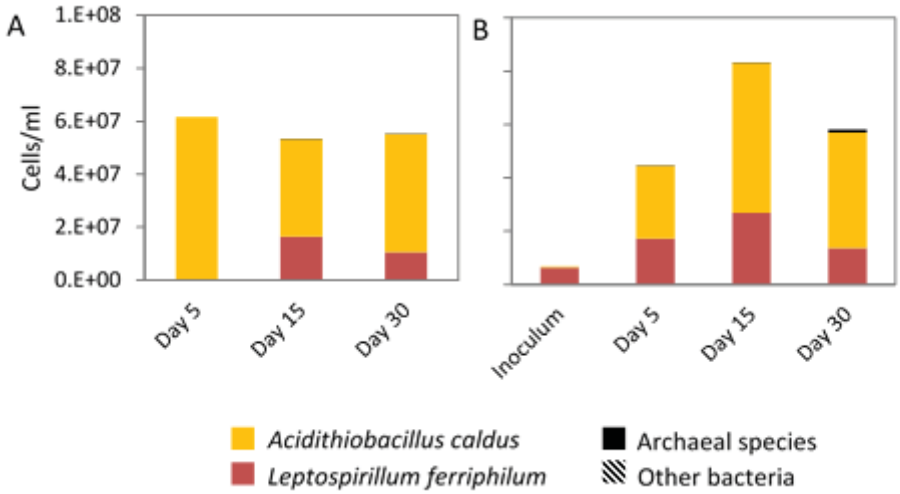

Figure 7-7 Microbial speciation determine in the non-inoculated (A) and inoculated (B) semi-continuous copper-bearing sample (CBS) biokinetic tests. Results are presented as 16S rRNA copy numbers expressed as the abundance relative to the cells/ml calculated from the DNA yields achieved

7.3.4 Comparison of the batch and semi-continuous biokinetic tests performed on high ANC GBS and low ANC CBS

The two samples, GBS and CBS, provided a comparison of the effect of neutralising capacity on the results of the biokinetic test. The greater neutralising potential, specifically the fast-weathering carbonate minerals present in the GBS, resulted in a greater initial increase in solution pH for the tests performed with no pH control. This initial dominance of the acid neutralising mineralogy on solution pH over the first 15 days was further illustrated by the lack of substantial difference between the pH profiles for the inoculated and non-inoculated tests for both samples. This is reflected by similarities in the trends observed in the redox potential and the concentrations of the sulphide oxidation products, the iron and sulphate concentrations over the same time period, suggesting that the extended period of high pH de-activated the inoculum added. In contrast, in the presence of low neutralising potential (CBS), no significant and extended high pH was observed and the inoculated tests demonstrated potential for acid generation more rapidly than the un-inoculated tests. Similarly, in the presence of high acid neutralising capacity (GBS) in the semi-continuous test, regular removal of solubilised ANC (representative of the open system expected in the mine dump environment) resulted in less extreme increase of pH and demonstrated activity of the inoculum added, providing a more representative and rapid test.

On considering the microbial communities driving acidification, the dominance of the *At. caldus* sulphur-oxidising micro-organisms relative to the *L. ferriphilum* species during the early stages of the biokinetic tests performed on both waste samples was of significance. This dominance was observed regardless of the initial increase in solution pH and optimal pH for *At. caldus* and *L. ferriphilum*, as measured through sulphur and ferrous iron oxidation rates respectively. The optimum pH of *At. caldus* for growth and sulphur oxidation is reported as pH 2.0-2.5 by Hallberg and Lindstrom (1994) and Kelly and Wood (2000) and as pH 1.5-2.0 by Plumb et al. (2008a; 2008b). The pH range in which *At. caldus* growth is supported is from pH 1.0 to 3.5 (Hallberg & Lindstrom, 1994; Kelly & Wood, 2000; Plumb, et al., 2008a); however, on increasing pH from 2.0 to 2.5-3.5, a decrease in growth of 10 fold and in sulphur oxidation rate of 5 fold is observed (Plumb, et al., 2008b). Similarly, the optimum pH for *L. ferriphilum* is reported as pH 1.4-1.8 by Coram and Rawlings (2002) and as pH 2.0 by Plumb at el. (2008a; 2008b) while growth and ferrous iron oxidation was reported between pH 1.0 and 3.5 (Plumb, et al., 2008b). Our

unpublished results show *L. ferriphilum* activity at pH 0.7. Quantification at higher pH was limited by ferric iron precipitation; however, rates lay in the range of 2-4 times lower than the maximum rate (Plumb, et al., 2008b).

The similarities in microbial community composition and dynamics between inoculated and non-inoculated tests suggests that *At. caldus* and *L. ferriphilum* are the indigenous microbial species associated with these waste rock samples responsible for catalysing ARD generation in the waste deposits. Furthermore, the differences in the time periods required for the establishment of these populations within the non-inoculated tests for the two samples, may be indicative of the effect of the elevated pH conditions on rates of growth and metabolism as a consequence of the greater neutralising capacity of GBS.

7.4 Analysis of the Development of the Semi-Continuous ARD Potential Test

This study focussed on the further development of the biokinetic test for characterisation of acid rock drainage potential through refinement of a semi-continuous biokinetic test and improved data interpretation. To conduct the study, two samples of waste rock with varying acid neutralisation capacity were used. Acid-consuming minerals (calcite, magnetite and other slow weathering minerals, including plagioclase-albite) and acid generating minerals (pyrite, pyrrhotite and chalcopyrite) were identified in the two waste rock samples studied using mineralogical techniques. The minerals present in these were leached using static ARD chemical characterisation tests, leading both samples to be classified as potentially acid-forming.

These samples were further investigated using batch and semi-continuous biokinetic tests. The composition of the waste samples directly affected the leach results obtained. In particular, high acid neutralising capacity of the wastes affected the solution pH, with consequences for the rates of both chemical and biological ARD generation. This effect was aggravated in the batch test over the semi-continuous test as the latter facilitated some washout of the neutralisation capacity solubilised in a manner more representative of the open systems encountered in natural settings. The sulphide minerals, including iron sulphides, represent the sole energy supply to the micro-organisms. The presence of easily-soluble sulphides which undergo dissolution under acidic conditions result in the development of oxidative conditions earlier through the supply of nutrients to the microbial communities.

The neutralisation of the batch biokinetic tests to pH ~ 6 in the presence of high neutralising capacity (Sample GBS) had a negative effect of the activity of the inoculum of acidophilic iron and sulphur oxidisers, especially in the batch system where solubilised acid neutralisation capacity accumulated. As a result, the progress of acidification was delayed in the batch test owing to inhibition of the planktonic inoculum added, hence the inoculated and un-inoculated batch biokinetic tests performed similarly in the presence of high neutralising capacity, as in GBS, owing to their dependence on the ore-associated indigenous microbial community. The microbial activity detected within the un-inoculated flasks of the batch biokinetic test after 6 days reflected the composition of the indigenous micro-organisms within the waste rock sample; this facilitates ARD generation in the waste deposits. Similar results were observed in the inoculated batch tests with significant ANC and high pH levels.

The use of a well-defined, mixed iron- and sulphur-oxidising inoculum provides a minimum time-frame for investigating microbial ARD generation, provided pHs approaching neutrality are not encountered. To provide a generalised test, facility must be provided for the washout of dissolved ANC over the duration of the test. The semi-continuous biokinetic test was investigated to explore this approach.

The removal and replacement of 10% (v/v) with fresh ABS solution at pH 2.0 prevented accumulation of solubilised ANC and thereby provided more realistic pH conditions. Under these conditions the relative ANC solubilisation and acid formation can be explored in the presence of the mixed-microbial inoculum, even under conditions of elevated ANC. These results demonstrated that the relative rates of acid neutralisation and acidification are not equivalent. In addition, the reduction in pH with time is less severe and more representative of natural conditions as compared to the addition of concentrated

H_2SO_4, allowing for information to be gained on the extent of initial pH increase for the waste samples. The rate of removal of lixiviates and microbial nutrients did not negatively affect the biokinetic tests performed in this study owing to the selection of a conservative residence time of 10 days. Previously, in the work of Kotelo (2013), such negative effect was observed. This highlights the importance of ensuring that the rate of replenishment of lixiviates and nutrients is equal to or exceeds the rate of their removal in the semi-continuous test. Further, the maximum specific growth rate of the microbes of interest should exceed the effective dilution rate (inverse of residence time) to prevent washout or depletion of the microbial community. The refinement of the test method with respect to the volume removed and the frequency of removal may provide a robust approach for analysis of waste samples with slower relative rates of mineral dissolution.

The approach used in this study demonstrates that knowledge of the sample mineralogy and chemistry is beneficial in the selection of the effective design of biokinetic tests for waste samples of interest, ensuring that the simplest test procedure is selected for convenience while still obtaining rigorous data on acid generation potential, as demonstrated here. It highlights the importance of use of a semi-continuous or flow through system when studying waste ore with a high ANC. Further knowledge of mineralogy informs fundamental understanding of microbially-mediated ARD generation obtained from the test conducted.

CHAPTER 8: THE FLOW-THROUGH MINI-COLUMN BIOKINETIC TEST FOR ARD POTENTIAL

Also presented as:
Makaula, DX and Harrison, STL. 2019. Establishing the flow-through biokinetic test to characterise sulfidic waste rock mineral for its potential to form ARD. Minerals Engineering. Under review.

Research Data Related to this article:
Makaula, DX and Harrison, STL. 2019. Flow through biokinetic test for ARD potential. Repository: ZivaHub | OpenDataUCT. https://doi.org/10.25375/uct.7484774

8.1 Introduction to Flow-Through Biokinetic Test

A major environmental problem facing the mineral industry and current and past mining regions harbouring sulphidic minerals is acid rock drainage (ARD), resulting from the oxidation of exposed sulphidic mineral waste rock. Oxidation of the sulphidic mineral, especially pyrite (FeS_2), in waste rock is caused by its exposure to both oxygen and water and is exacerbated by the presence of iron and sulphur oxidising microorganisms (Johnson & Hallberg, 2005; Johnson, 2003). ARD is characterised by low pH effluents with high sulphate content and may mobilise toxic metals (Akcil & Koldas, 2006; Becker, et al., 2015). The accumulation of waste material results mostly from their disposal owing to their low grade not being appropriate for economic extraction or following separation or extraction of mineral value components from ores. Such disposal has long-term implications if improperly handled (Michaud, et al., 2017). Post the disposal of sulphide-rich wastes with the potential for generating ARD, it becomes very difficult, expensive and time-consuming to control ARD-based contamination of surface and groundwater near abandoned mined areas (Erguler, et al., 2014). Thus, it is of the highest importance to characterise sulphide-bearing waste material for ARD forming potential before disposal to ensure appropriate approaches to disposal or re-purposing are used to prevent ARD being formed over the extended time frame.

A global standard practice for the characterisation of ARD generation potential, known as the “wheel approach” (Morin & Hutt, 1998), caters for laboratory, field based and whole rock geochemical assessments. The common laboratory test used as first indicator of ARD potential is the “static test” suite. These tests are fast, inexpensive and can be used easily to test multiple samples. This approach uses extreme oxidants, providing “worst case” data. It is also carried out in batch, allowing overall neutralising of acid formed based on neutralising capacity in a manner independent of their relative rates which may hide potential acid forming capacity in the long term. Through providing ‘endpoint’ data rather than a time course, no relative rates of acid consumption and production are indicated. The kinetic leach test provides an advantage when compared to static tests since this accounts for relative rates and is more representative of the actual field conditions (Bradham & Caruccio, 1991). The commonly used kinetic tests are laboratory-based column tests, humidity cells and field-based test pads (Sapsford et al., 2008). These kinetic tests, however, require long periods to generate meaningful data (several months to years), making them costly to run, often ~US$ 700-1000s (Broadhurst, et al., 2013; Parbhakar-Fox & Lottermoser, 2015) with a delay in data availability to inform disposal approaches. Furthermore, these tests do not consider the microbe-mineral interaction between the sulphide-bearing waste material and the indigenous iron- and sulphur-oxidising microorganisms.

To address these shortcomings and complement the above-mentioned tests, a batch biokinetic test was developed (Hesketh, et al., 2010a; Broadhurst, et al., 2013). The biokinetic test holds several advantages over conventional kinetic tests for measuring the ARD potential, including the delivery of meaningful data regarding the long term ARD generation potential of well liberated waste rock and its kinetics in a relatively short space of time (< 3 months) as well as being relatively inexpensive to operate

(Broadhurst, et al., 2013). Hesketh et al. (2010a) used the biokinetic test to characterise the ARD potential of de-sulphurised copper tailings. Broadhurst et al. (2013) compiled, assessed and compared the complementary nature of the biokinetic test and traditional static methods to deliver a rapid, accurate and effective characterisation of a suite of waste materials, including untreated and de-sulphurised copper tailings, copper waste rock, nickel-pyrrhotite flotation tailings, gold tailings, coal waste slurry and untreated and de-sulphurised coal discards (see Chapter 3). These studies concluded that the biokinetic test can be used to validate and improve the results obtained from simple static tests and account for microbial activity. Opitz and Harrison (2016a) studied the impact of the concentration of mixed mesophilic microbial inoculum on the duration of the biokinetic test required for characterisation of gold waste rock. Opitz et al. (2016b) collated the batch biokinetic test to the mineralogy of two gold waste rock samples. Through the integration of mineralogy, sequential chemical extraction and the biokinetic test, it was possible to detect and assess the detrimental elements leaching from the waste materials with time. While successfully augmenting the conventional test results with respect to kinetics and microbial susceptibility to leaching, the configuration of the batch biokinetic test does not represent the typical fluid contacting mechanism in the waste rock dump nor does take into account washout of neutralising capacity in an open system such as the waste rock dump where the kinetics of acid neutralisation and acid generation may differ.

Refinement of the batch biokinetic test to develop a flow-through lab-scale test is desired to remove these limitations while allowing assessment of the mineral-microbe interactions within the waste rock. Microbial activity and, in particular, the association and colonisation of the mineral surface by the microorganisms plays a key role in the generation of ARD from waste rock dumps. Several studies have targeted microbe-mineral interaction as a strategy to characterise or mitigate ARD generation. Schippers et al. (2007) analysed, geochemically and geomicrobiologically, pyrrhotite-containing tailings from a tailings storage facility (TSF) in Botswana. IMC was used to measure potential pyrrhotite oxidation rates. This facilitated estimation of the time period of ARD formation which was critical for informing safe mine closure. Sand et al. (2007) assessed ARD mitigation on several weathered rock samples over 3 years, including: 6 year old waste rock material; sorted, freshly broken, low-grade ore; and unweathered tailings material, using the detergent sodium dodecyl sulphate (SDS) as a deterrent for weathering in large lysimeters. In their study, SDS was shown to reduce microbial activity only temporarily. Makaula et al. (2017a) used a modification of the batch biokinetic test in which milled waste rock was coated onto glass beads to provide a defined reaction surface area as a precursor for a flow-through biokinetic system to demonstrate the ARD forming potential of two waste rock samples, with varying sulphide content. In this system, IMC and SEM were used to assess the metabolic activity of the mineral-associated microbial community and the degree of colonisation as a function of the available surface area; these were related to the activity in the leach solution. In the current study, the potential to develop an unsaturated, flow-through biokinetic test is explored using the same two pyrite-bearing, low grade waste rock samples, with the aim to better represent the conditions within the open system of a waste rock dump. The results obtained are compared to static tests and the shake flask-based, batch biokinetic tests using both a mineral suspension and mineral-coated beads. Furthermore, the microbe-mineral interfaces and associated microbial activity are investigated in the flow-through biokinetic system to provide improved understanding of the operating environment.

8.2 Materials and Methods for Development of the Flow-Through Biokinetic System

8.2.1 Microorganisms

The mixed mesophilic culture, containing *Leptospirillum ferriphilum*, *Acidithiobacillus caldus*, *Ferroplasma acidiphilum* and *Acidiplasma cupricumulans*, was grown on a 3% (w/v) pyrite concentrate in 0K basal salts medium made up of 3 $g.L^{-1}$ $(NH_4)SO_4$, 0.1 $g.L^{-1}$ KCl, 0.5 $g.L^{-1}$ K_2HPO_4, 0.5 $g.L^{-1}$ $MgSO_4.7H_2O$, and 0.01 $g.L^{-1}$ $Ca(NO_3)_2$ and 1 mL of 1000 × stock of trace elements (Kolmert and Johnson, 2001) in a 1 L batch stirred tank reactor at 35°C. The stock reactor was maintained by a

weekly draw and fill in which 15% (v/v) was replaced with fresh media and associated concentrate. The health of the culture was assessed through direct microscopic cell counts and redox potential. The microbial community in the reactor was maintained in the range of 1×10^9 to 4×10^9 cells mL^{-1} (Ngoma et al., 2015; Ngoma, personal communication 2018).

8.2.2 Pyrite bearing waste rock

Two pyrite bearing waste rock samples were used in this study: (A) high in sulphur (HS) and (B) low in sulphur (LS). The samples were milled and wet sieved to obtain a particle size passing 75 µm. After air drying at 37°C, the samples were split representatively. The bulk mineralogical compositions of the waste samples, acquired using QEMSCAN, are shown in Figure 8-1.

Acid generating minerals consist of predominately pyrite (LS: 13.99 wt. %, HS: 33.43 wt. %) and pyrrhotite (LS: 2.35 wt. %, HS: 3.9 wt. %). Based on the classification guidelines of acid neutralising capacity of minerals described by Dold (2010), acid consuming minerals within the waste samples consist predominantly of dissolving calcite (LS: 0.22 wt. %, HS: 0.03 wt. %), fast and intermediate weathering minerals predominantly containing garnet (LS: 2.83 wt. %, HS: 4.52 wt. %) and slow weathering minerals consisting predominantly of muscovite (LS: 14.77 wt. %, HS: 12.42 wt. %) was also present. The largest component of the waste rock consisted of inert quartz mineral (LS: 36.67 wt. %, HS: 34.76 wt. %).

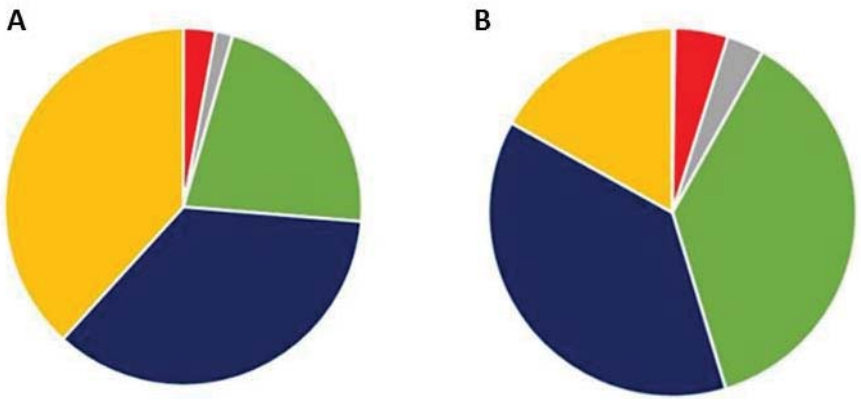

Figure 8-1 Mineralogical analysis of the two waste rock samples acquired using QEMSCAN. A (HS) and B (LS) show abundant acid forming minerals (pyrite and pyrrhotite;), rapidly dissolving mineral (calcite;), fast- (garnet;), intermediate- (Mn-Fe silicate and augite;) and slow-weathering (K-feldspar and muscovite;) acid neutralising minerals, and quartz as an inert mineral ( ).

For the mineral coated glass bead system, the milled waste rock samples were coated onto 6 mm glass beads, using Bostik glue (Africa, et al., 2013), to provide a uniform and quantifiable surface area. The coated glass beads were air-dried for a minimum of 24 hours before being sterilised by irradiation at 45 kGy dosage as described by Govender et al. (2015).

8.2.3 Static Tests

The static tests were conducted on both pyrite-bearing waste rocks using acid-base accounting (ABA) and net acid generation tests (NAG). The ABA test, conducted according to Smart et al. (2002), measures the net acid producing potential (NAPP) which represents the balance between maximum potential acidity (MPA) and the acid neutralising capacity (ANC). The NAG test was determined according to Stewart et al. (2006) and allows both acid forming and neutralising reactions to occur simultaneously. These tests were performed in triplicate.

8.2.4 Biokinetic tests

8.2.4.1 Shake flasks test

Biokinetic experiments were conducted in shake flasks containing 0K media (pH 1.6) supplemented with 0.5 g.L^{-1} Fe^{2+} as $FeSO_4.7H_2O$ and incubated at 30°C. The biotic conditions were inoculated with 10^8 cells.mL^{-1}. Two approaches were used for the flask biokinetic experiments: (1) the standard slurry test as reported by Hesketh et al. (2010a); and (2) mineral coated glass beads. For the slurry test, 7.5 g milled mineral was added to each flask containing a total working volume of 150 mL (50 g.L^{-1}). For the mineral coated beads, 100 beads of 6 mm diameter were coated with the respective mineral waste rock (~ 3.6 grams) and added to each flask with a total working volume of 100 mL (~36 g.L^{-1}). Prior to inoculation, both mineral slurry and waste rock coated beads were washed and conditioned with 0K media (pH 1.6) for 24 hours to initiate neutralising reactions. After 24 hours, the pH in the respective shake flasks was re-adjusted to pH 1.6 using concentrated H_2SO_4.

8.2.4.2 Flow-through tests

For the flow-through biokinetic test, twelve columns were operated, six of each waste rock sample. Each column was loaded with 300 waste rock mineral-coated beads of 6 mm (10.8 g milled waste rock) and operated as a continuous flow-through system. One column of each sample was conducted as an uninoculated control. Prior to inoculation, the packed columns were washed and conditioned with 0K media (pH 1.6) at a continuous flow rate of 4 mL.h^{-1} for 24 h to remove readily leachable materials and create an environment conducive for microbial attachment to the ore surface by initiating neutralising reactions in the waste rocks.

The columns were inoculated under saturation conditions (Tupikina, et al., 2014) using an upward flow of 100 mL 0K media supplemented with 10^{10} mixed mesophilic microbial cells.kg^{-1} of ore and 0.5 g.L^{-1} Fe^{2+} as $FeSO^4.7H_2O$ at a rate of 4 mL.h^{-1} in a closed circuit. The inoculum suspension was recycled for 18 h to allow microbe-mineral contacting. Thereafter, the columns were drained, and the liquid fraction collected. The effluent solution was analysed for planktonic cells remaining using total cell counts (light microscope at 1000 x magnification). A continuous downward flow of sterile fresh 0 K media (pH 1.6) supplemented with 0.5 g.L^{-1} Fe^{2+} ($FeSO_4.7H_2O$) was introduced at a rate of 4 mL.h^{-1} and the columns operated as flow-through unsaturated beds at 30°C for 30 days. Daily effluent or pregnant leach solution (PLS) samples were taken and analysed for pH, redox potential, Fe^{2+} concentration, total iron concentration and microbial cell concentration. For each waste rock, a column was sacrificed on days 1, 10, 15, 20 and 30 to assess microbial colonisation of the mineral and its activity. The control column was sacrificed on day 30.

8.2.5 Solution analysis

All pH measurements were performed using a Metrohm 704 pH metre and probe, calibrated at pH 7.0, pH 4.0 and pH 1.0 before use. Redox potential was measured relative to a silver/silver chloride (Ag/AgCl, 3 M KCl) reference, using a Metrohm 704 pH/Eh meter. The Fe^{2+} and total iron concentration in solution were measured spectrophotometrically using a modification of the phenanthroline-based colorimetric method described by Komadel and Stucki (1988).

8.2.6 SEM analysis of microbial mineral interaction

Samples of colonised mineral surface were obtained during each column sacrifice and processed according to Makaula et al. (2017b), prior to visualisation using the SEM (FEI NOVA NANOSEM 230 with a field emission gun).

8.2.7 Microbial detachment and microscopic enumeration

A modified detachment protocol, based on Chiume et al. (2012) and described by Makaula et al. (2017b), was used to recover microorganisms from HS and LS waste rock surfaces on coated beads. In the current study, the washing step was repeated 3 times to detach firmly attached microbial communities and the recovered cells were enumerated microscopically.

8.2.8 Analysis of microbial activity on the mineral

Isothermal microcalorimetry (IMC) was used to quantify metabolic activity associated with the waste rock surfaces, according to Makaula et al. (2017b). Two microbially colonised waste rock-coated beads, representative of each column sacrificed, were loaded into each empty IMC vial by sterile transfer. The maximum heat flow of each ampoule was recorded in the IMC at 30°C. Analysis was conducted on duplicate samples.

8.3 Results and Discussion of Development of the Flow-Through Biokinetic System

8.3.1 Static test results

The static test results are presented in Table 8-1 and indicate that both the LS and HS samples were acid generating. The sulphur content of the feed samples, determined by LECO analysis, were 21.04 wt% for HS and 9.97 wt% for LS, consistent with a combined pyrite and pyrrhotite content of 37.5 wt% for HS and 16.5 wt% for LS. MPA was determined from the sulphur content as 643.2 kg/H_2SO_4 for HS and 305.1 kg/H_2SO_4 for LS. The ANC values of HS and LS were 48.08 and 32.00 kg/H_2SO_4 respectively. The resultant NAPP values were 598.74 and 273.09 kg/H2SO4 for HS and LS respectively. The high sulphur content consistent with high proportionality of AF minerals in both samples, coupled with relatively low presence of AN minerals resulted in both samples being classified as potentially acid forming (PAF). The measured NAG_{pH} for HS and LS of pH 2.24 and 2.20 confirm this classification.

Table 8-1 Static ARD test results for LS and HS pyrite bearing waste rocks

Feed sample	Sulphur grade wt%	MPA kg/H_2SO_4	ANC kg/H_2SO_4	NAPP kg/H_2SO_4	NAG_{pH}	ARD classification
HS	21.04	643.2	48.08	598.74	2.24	PAF
LS	9.97	305.1	32.00	273.09	2.20	PAF

8.3.2 Performance across the biokinetic systems

The waste rock was pre-washed for 24 hours to remove acid soluble material. The pH was then adjusted to pH 1.6 prior to inoculation. Following inoculation, the pH of the un-inoculated LS control in the suspended mineral batch biokinetic test (BT) increased to pH 2.77 on day 4 (Figure 8-2A), where after it remained constant till day 13, before declining to reach pH 2.1 on day 23. The uninoculated HS reached a maximum pH of 3.48 on day 6, before it declined to pH 1.97 on day 23 (Figure 8-2A). Despite these samples being not inoculated, the decline in pH could be attributed to the action of indigenous iron- and sulphur oxidising microorganisms inherent to the waste material as this material had not been sterilised. The pH of the inoculated LS sample increased to pH 2.18 on day 4 and declined to pH 1.51 by day 12 (Figure 8-2A), where after it remained relatively constant. The pH of inoculated HS sample also reached a maximum of pH 2.2 on day 4, then declined to pH 1.51 by day 11 (Figure 8-2A). The reduced increase and subsequent decline in pH is attributed to activity of the inoculated microbial culture and the indigenous microbes facilitating the degradation of the waste rock surface.

In the batch biokinetic test using coated beads (BT-CB), the waste rock mineral coated beads were sterilised prior to the experimental run. The pH of un-inoculated LS control increased to pH 2.97 on day 17 (Figure 8-2B) and the un-inoculated HS control increased gradually to maximum pH of 3.48 on day 21 (Figure 8-2B), before decreasing slightly. The extended acid neutralisation resulted from the absence of onset of acidification owing to the absence of iron- and sulphur-oxidising microorganisms. The pH of the inoculated LS test declined from a maximum of pH 1.75 on day 3 to pH 1.45 on day 30 (Figure 8-2B) and the pH of HS test declined from pH 1.78 on day 3, to pH 1.28 on day 18 (Figure 8-2B). The column reactors packed with sterilised waste rock mineral-coated beads were, unlike the batch shake flasks, operated continuously in an open circuit with a feed containing 0.5 g.L^{-1} Fe^{2+} as $FeSO_4.7H_2O$, at

pH 1.6 (Figure 8-2C). The pH of un-inoculated column containing LS increased to pH 2.83 on day 2 due to acid neutralising capacity being solubilised, before declining to pH 1.6 by day 12 and a lowest point of pH 1.44 on day 20 (Figure 8-2C) due to the wash out of acid neutralisation by the acidified feed stream. In the HS column, the pH increased to pH 3.2 on day 2, before declining to pH 1.65 by day 12 and a minimum of pH 1.54 on day 21 (Figure 8-2C). The decline in pH could attributed to the depletion of neutralising minerals, removed by the flow-through nature of the column and its acidified feed. The pH in the inoculated LS column increased only to pH 2.27 on day 4 owing to the early onset of microbially-mediated acidification; thereafter, decreasing to pH 1.45 by day 11 and to pH 1.37 on day 20 (Figure 8-2C). In the HS column, the pH increased to pH 2.25 on day 4, before declining through pH 1.5 on day 8 and pH 1.25 on day 20 (Figure 8-2C). The pH profiles of the inoculated tests across the three biokinetic tests showed that microbial activity facilitated leaching of the sulphidic waste rock and that the rates of acidification and neutralisation were not equivalent.

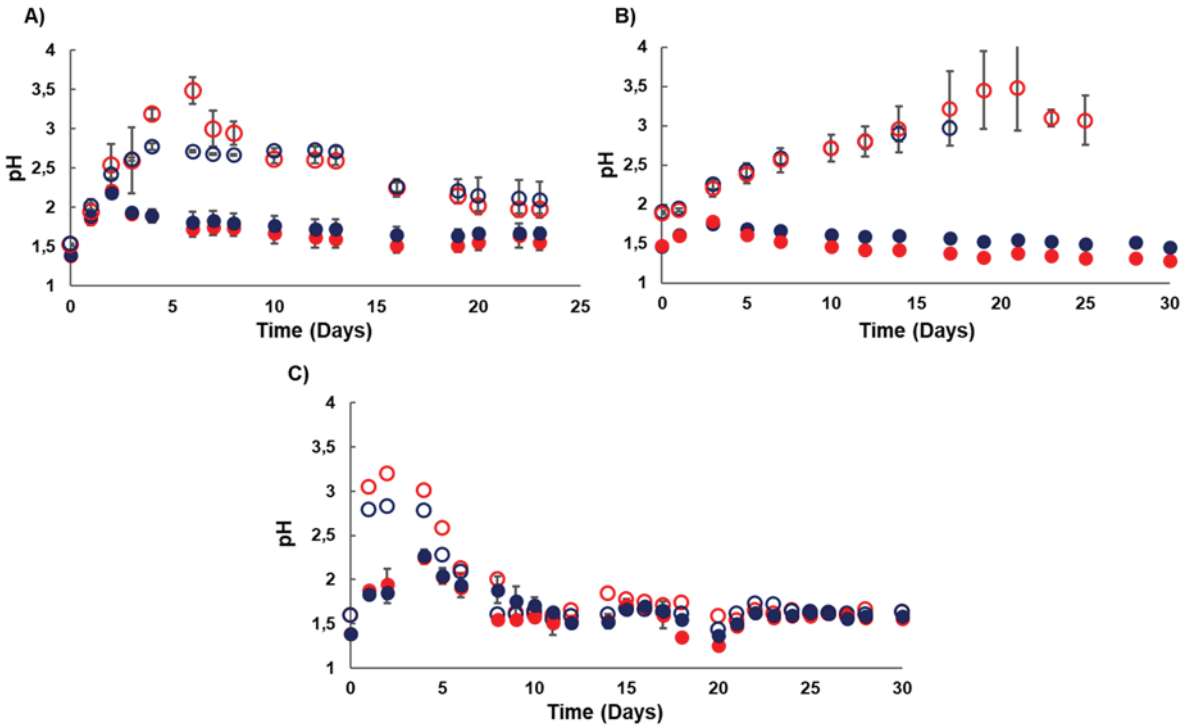

Figure 8-2 Analysis of pH across the three biokinetic test approaches, (A) batch slurry (BT), (B) batch waste rock coated glass beads (BT-CB) and (C) waste rock coated glass beads in a flow-through column (FT-CB). All experiments were conducted at 30°C.
The samples include LS un-inoculated (○), HS un-inoculated (○), LS inoculated (●) and HS inoculated (●). Error bars represent the standard deviation from the mean pH across the experimental shake flasks and columns at the same time point.

In the batch biokinetic test with un-sterilised suspended mineral (BT), the redox potential of both the un-inoculated LS and HS waste rock remained in the range ~250 mV to 300 mV until day 10. Thereafter, it increased gradually to a maximum of 666 mV and 649 mV by day 22 in the LS (Figure 8-3A) and HS tests (Figure 8-3A) respectively. The redox potential in the inoculated LS flask increased from 480 mV at the start of the run to 712 mV on day 4 and remained relatively stable thereafter (Figure 8-3A); similarly, the HS test redox potential increased from 468 mV to 696 mV in the same period and then stabilised (Figure 8-3A). In the batch test using sterilised mineral on coated beads (BTCB), the redox potential of un-inoculated LS (Figure 8-3B) and HS (Figure 8-3B) tests remained in the range 250 to 300 mV over the 17 and 25 day duration of the runs respectively. This can be attributed to the absence of viable indigenous microbial populations due to sterilisation. In the inoculated BTCB tests, the redox

potential of LS increased from 498 mV on day 1 to 683 mV on day 7 (Figure 8-3B) and that of HS from 488 mV on day 1 to 710 mV on day 10 (Figure 8-3B).

In the un-inoculated LS and HS flow-through tests using sterile mineral (FT-CB), the redox potential remained low throughout the 30 day experimental run, increasing gradually from 300 to 400 mV (Figure 8-3C). An increase in redox potential of the inoculated LS test was evident from day 10 (391 mV) up to day 21 (700 mV; Figure 8-3C), where after it remained relatively stable. The redox potential of inoculated HS test increased from 416 mV to 689 mV in the same period (Figure 8-3B). Based on solution chemistry, both waste rock minerals are demonstrated to be acid forming across all three biokinetic systems, supporting the metabolism of iron- and sulphur-oxidising microorganisms which accelerate ARD formation. In the flow-through biokinetic system, it has been shown through both solution pH and redox potential profiles that the inoculated microbial populations facilitated the degradation of the two waste rock minerals, albeit requiring longer to establish the leaching environment. Moreover, acid neutralising capacity was washed out of the columns during the early onset of acidification, negating its role in neutralisation of the acid generated from the sulphidic fraction.

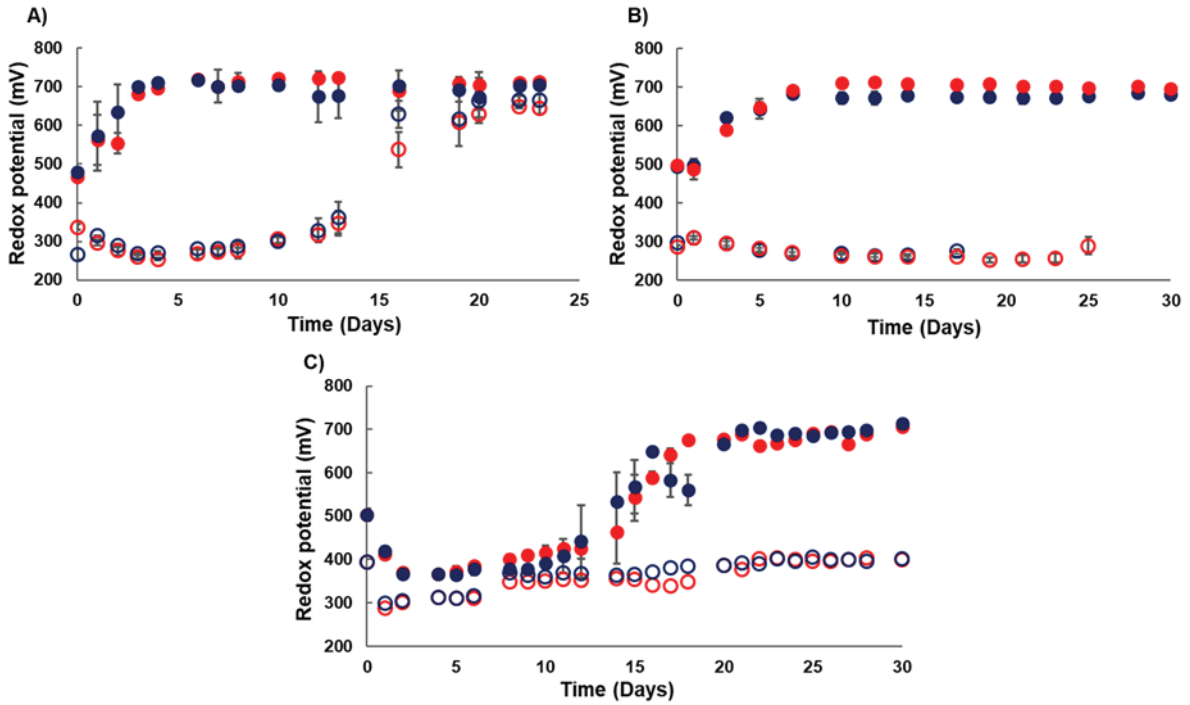

Figure 8-3 Measured redox potential across the three biokinetic test approaches, (A) batch slurry (BT), (B) batch waste rock coated glass beads (BT-CB) and (C) waste rock coated glass beads in a flow-through column (FT-CB). All experiments were conducted at 30°C.
The samples include LS un-inoculated (○), HS un-inoculated (○), LS inoculated (●) and HS inoculated (●). Error bars represent the standard deviation from the mean redox potential across the experimental shake flasks and columns at the same time point

8.3.3 SEM surface visualisation

Colonisation of the mineral surfaces from the flow-through system was analysed further by SEM. The micrographs in Figure 8-4 show leached waste rock surfaces sampled at day 10, 20 and 30. Single microbial cells (S) on the surface, colonies (C) and microbial cells embedded in EPS (E) as well as associated precipitate (P) are notable. Rod-shaped bacilli are easily distinguishable from the spirilli. Single cells are observed on the surface on both mineral samples at day 10 and day 20 (A-D) as well as at day 30 of LS (E). Colonies are visible from day 20 to day 30 on both mineral samples (C-F). On day 30, cells embedded in EPS are distinctively visible on the HS mineral surface (F). The cells attached to the mineral surface were mostly observed in, but not limited, to the regions containing surface

defects. These observations are supported by Harneit et al. (2005), Africa et al. (2010) and Ghorbani et al. (2012). Harneit et al. (2005) visualised the attachment and biofilm formation of *A. ferrooxidans* cells on pyrite coupons using atomic force microscopy (AFM) and fluorescent microscopy (FM) and revealed preferential attachment of cells to visible surface defects, attributed to improved availability of sulphide and Fe^{2+} in these areas. Africa et al. (2010) applied DAPI fluorescent staining to show that a mixed microbial culture of *A. ferrooxidans* and *L. ferriphilum* attached preferentially to the defects on pyrite and chalcopyrite surfaces of mineralogically characterised thin sections exposed to thin film flow, representative of the heap leaching environment. Similarly, Rojas-Chapana et al. (1998) proposed that nutrient concentration gradients were generated at pyrite fragmentation sites, attracting the settlement of microbes at these defect sites over others. Progressive abundance of microbial colonisation of the mineral surface was observed over the 30 day experimental run.

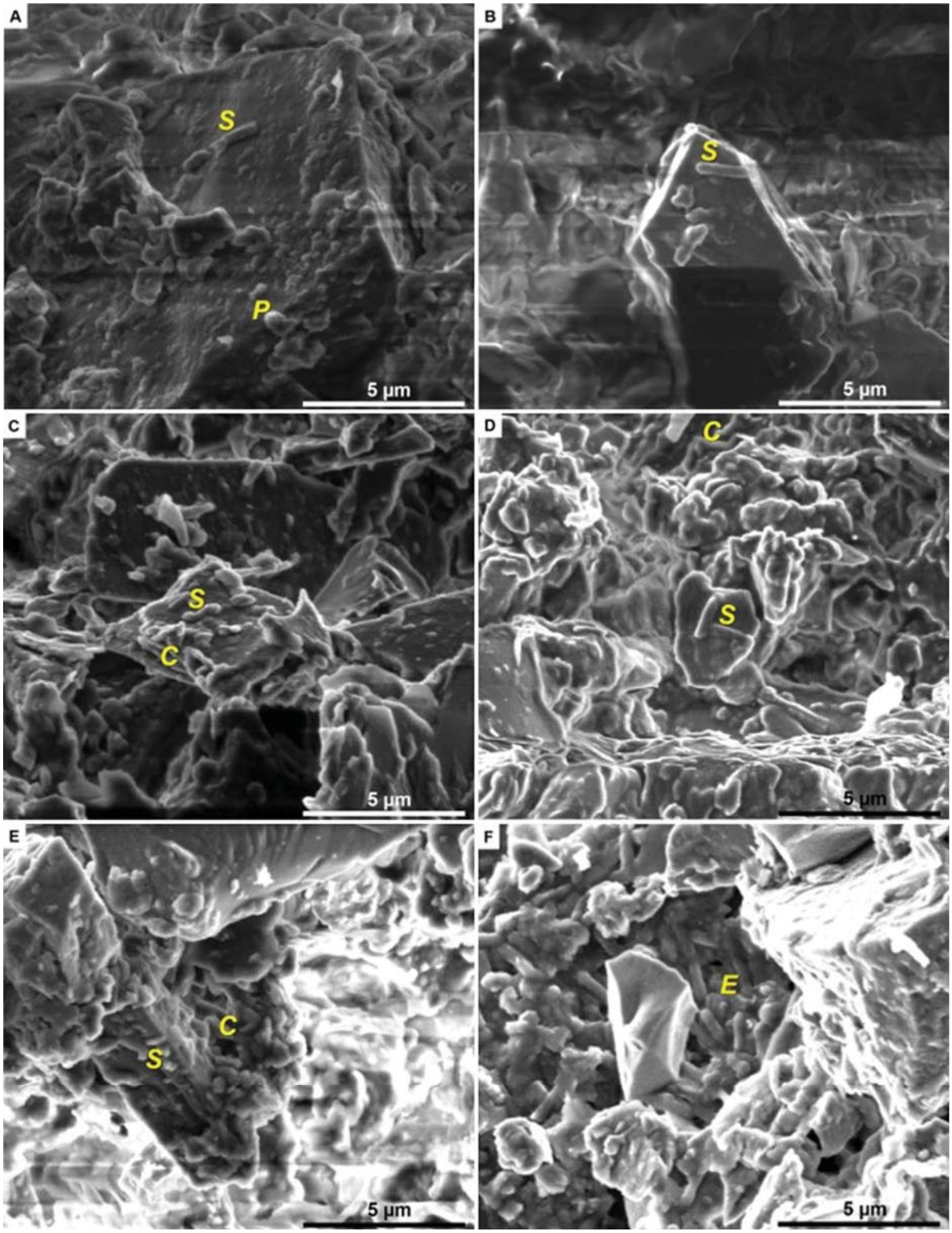

Figure 8-4 SEM images of colonised pyrite bearing waste rocks coated onto glass beads over 30 days. Microbial mineral interactions on LS surfaces are shown in micrograph A, day 10, C, day 20 and E, day 30 and interactions on HS surfaces are shown in micrograph B, day 10, D, day 20 and F, day 30. Observed surface features including single cells (S), precipitates (P), colonies (C) and EPS embedded cells (E), are labelled. A scale bar (5 µm) is shown on each image

8.3.4 Microbial coverage of waste rock surfaces

Cells were mechanically detached from the waste rock surfaces and microscopically counted. Firmly attached cell numbers, as well as the percentage microbial coverage of the mineral surface, assuming monolayer attachment, are presented in Figure 8-5.

From the initial total number of cells (3.9×10^7 cells) available for attachment in the inoculum, 4.26×10^6 and 3.71×10^6 cells respectively were firmly attached in the HS and LS columns after the 18 hour inoculation period, corresponding to 9.21×10^{10} cells.m^{-2} and 1.08×10^{11} cells.m^{-2} respectively for LS and HS systems. This equates to approximately 7% coverage for LS and 8.2% coverage for HS. At day 30, microbial populations observed on the mineral surface were 4.61×10^{11} cells.m^{-2} (34.9% coverage) on LS and 3.3×10^{11} cells.m^{-2} (35.4% coverage) on HS. A similar trend of smaller magnitude was observed by Makaula et al. (2018) on the same waste rock at a higher flow rate of 60 mL.h^{-1}, whereby cells increased from 7% LS and 8.2% HS after the inoculation phase to 17.9% and 21.6% respectively after 20 days. The observations of microbial growth on waste rock surfaces in terms of cell number was complemented by measurement of metabolic activity resulting from the oxidative processes, facilitated by the colonised cells.

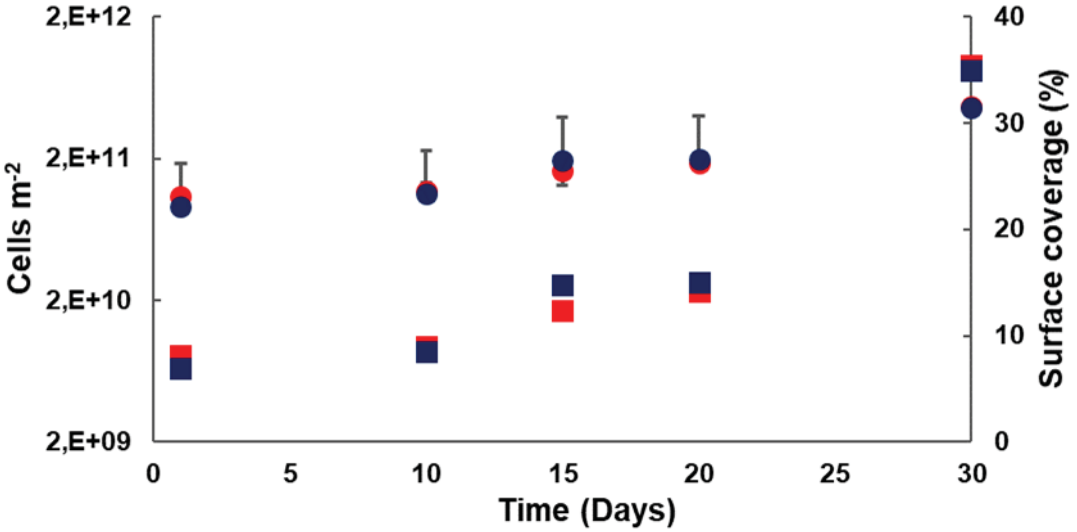

Figure 8-5 Microorganisms firmly attached to the waste rock mineral surface of LS (●) and HS (●) at each time point, as well as the calculated percentage of surface microbial coverage for LS (■) and HS (■). The degree of surface coverage was determined from the number of cells firmly attached to the surfaces. Error bars represent the standard deviation from the mean of the mineral associated and firmly attached cells across the wash repeats

8.3.5 Microbial mineral activity measurement

Microbial communities attach to solid surfaces and produce EPS for the development of a biofilm (Watnick and Kolter, 2000). Using IMC, the activity of mineral associated microbial community was quantified at different stages of the experimental run, using the maximum heat produced per unit surface (mW.m^{-2}), as shown in Figure 8-6. This activity is a combination of the heat associated with microbial Fe^{2+} oxidation as well as the ferric leaching of pyrite in the waste rock mineral. After inoculation, two beads of each waste rock sample were analysed, showing heat generation of 104 mW.m^{-2} for LS and 130 mW.m^{-2} for HS. Between the 18 hour (day 1) post inoculum measurement and day 20, the maximum heat output of both waste rock samples remained in the range 120 to 150 mW.m^{-2}. On day 30, the measured maximum heat output was 326 mW.m^{-2} for PEL-LS and 289 mW.m^{-2} for HS, indicating substantial growth and increase in metabolic activity. The microbial activity of LS and HS on day 30 was 3.1 times and 2.2-fold higher than on day 1, respectively while the attached cell numbers increased

by 5- and 3-fold respectively. A previous study conducted on these waste materials using the same microbial consortium in batch shake flasks for 15 d presented a maximum heat output of 237 $mW.m^{-2}$ for LS and 373 $mW.m^{-2}$ for HS (Makaula et al., 2017a).

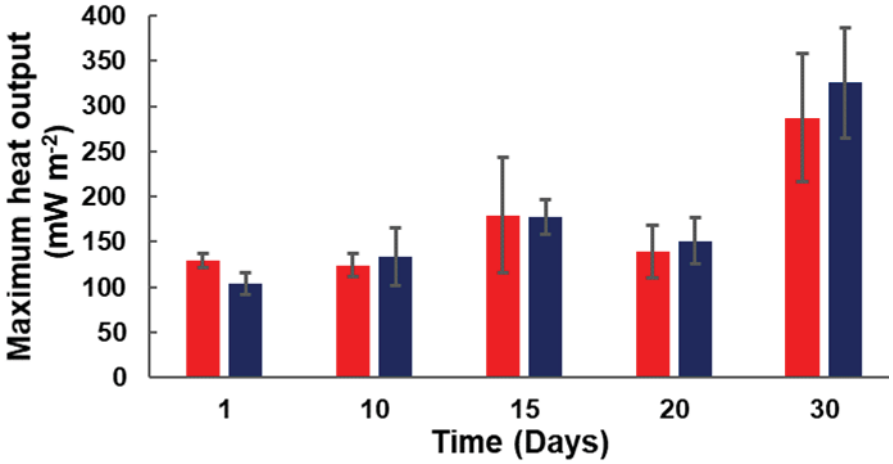

Figure 8-6 Maximum heat flow per unit surface area for HS (■) and LS (■) after day 1, 10, 15, 20 and 30 measured using the IMC. Error bars represent the standard deviation from the duplicates of each material.

8.3.6 Sulphur content of feed and leachate sample

Post the flow-through experimental run, the leached residual waste rock samples were recovered and their sulphur content analysed using LECO and compared to the feed sulphur content to determine the extent of their leach (Table 8-2). The sulphur leached from the waste rock samples after the 30 day flow-through experimental run was 0.23 g (10.2%) for the HS sample (89.8% still available) and 0.46 g (42.6%) for the LS sample (57.4% still available). A considerable amount of sulphur was still available for continued acid generation in both samples after 30 days, indicating that an extended leach time is required for complete acidification.

Table 8-2 Sulphur content of the feed samples and residual leached sample

Sample	Feed Sulphur wt%	Residual Sulphur wt%
HS sample	21.04	18.9
LS sample	9.97	5.75

8.4 Analysis of Flow-Through Biokinetic Test for ARD Potential

Mine waste is often stockpiled, post mineral extraction and processing, either as a waste material or awaiting more efficient technology or improved economic environment for further processing. This material has potential for ARD formation where sulphidic waste rock is present. To minimise environmental burden and associated socio-economic impact, it is necessary to characterise waste for potential ARD formation, before deciding on the approach to disposal or stock-piling. This enables appropriate disposal or repurposing decisions for waste materials, thereby avoiding or minimising long-term remediation requirements. All the ARD characterisation methods (static test, BT, BT-CB and FT-CB) tested in this study demonstrated that both waste rocks were potentially acid forming. The static test uses extreme oxidants to achieve ‘endpoint’ data without profiling the relative AF and AN reaction rates and does not take microbial action into consideration. In contrast, the batch biokinetic systems account for microbial action. However, due to the batch nature of the system, the acid neutralising minerals dissolved on the onset of the reaction are retained in the reaction environment, thus delaying the inception of microbial action. Furthermore, the batch test is not representative of the conditions in

the actual waste rock pile. The unsaturated, flow-through biokinetic column test offers advantage over the batch biokinetic test through contrasting the rates of acid neutralisation and acidification and showing depletion of readily acid neutralising minerals early in the experimental run. The establishment of a well colonised mineral surface was observed with the progression of the flow-through column test, with increasing microbial activity associated with increasing mineral colonisation, demonstrated by IMC, microbial cell counts and SEM respectively, within 30 days. The flow-through configuration has been shown in this study as a suitable system that is complementary to the available suite of tests to characterise the potential of acid formation in sulphide rich waste material through provision of relative kinetic data on neutralisation and acidification, their potential washout with time and the role of microbial colonisation. Further studies on waste material with lower sulphide content and over extended run periods are recommended to refine the establishment of a defined method for the flow-through test.

CHAPTER 9: CONCLUSION

Characterisation of mine waste and its potential environmental burden is critical before deciding on an appropriate disposal strategy. Increasingly, driven by the principles of industrial ecology and the desire to increasingly circularise the economy, re-purposing of this mine waste in preference to its disposal is sought. Even more importantly, prior to embarking on re-purposing applications, the environmental risk of the material must be rigorously quantified. Where sulphidic mine wastes are considered, key environmental burdens likely include generation of acid rock drainage (ARD) and deportment of metals.

In characterising mine waste in terms of ARD, the static tests of acid base accounting are most typically used. Where potential for ARD is identified, kinetic tests are used to further elucidate its potential. Static tests use extreme conditions, providing a worst case scenario of oxidation on the one hand. On the other hand, their batch nature and endpoint data do not allow the consideration of the relative rates of neutralisation and acidification. Kinetic tests which provide such data, including humidity cell tests and column tests require a time period from months to years. None of these tests account directly for the key role of microbially mediated iron and sulphur oxidation in ARD formation. These shortcomings have led to the development of the biokinetic test to provide a test able to account for microbial action, providing relative neutralisation and acidification rates and able to be carried out across multiple samples in a period of 3 months.

In this report, we explore the potential of the CeBER UCT biokinetic test, also known as the biokinetic accelerated weathering tests, by analysing data collected across a range on mine waste samples, including waste products from hardrock gold-bearing mineral beneficiation, copper-containing base metal bearing minerals, zinc-bearing minerals and waste materials from coal processing. We explore the limitations of these tests and address the impact of key operating conditions. Further we seek to refine the biokinetic test by considering pH-controlled batch tests vs non-pH controlled batch tests, semi-continuous tests and flow-through continuous tests. Further to this, we address the risk reduction of disposal of mine waste through the removal of sulphide through physical separation processing of fines. Here, we seek to explore whether a benign fraction can be produced comprising the major volume fraction for safe disposal of re-purposing. To assess this, both potential for ARD generation and metal deportment are considered.

Through analysis of static and biokinetic test data collected across a variety of mine wastes, it was demonstrated that the biokinetic test data can be used to validate static test data, resolve uncertainty in the presence of inconclusive results and provide enhanced data to inform models for ARD prediction in waste rock dumps and tailings dams. The biokinetic test provides information on the relative contribution to ARD generation expected from microbial colonisation of the mine waste. It can ascertain conditions that will either promote or mitigate against ARD generation. Further it provides relative kinetics of the acid generation and neutralisation reactions, essential to understand whether these will offset each other in a flow through system. This is achieved in a period of 3 months or less, thus providing advantage over conventional kinetic tests. Further, it is simple and inexpensive and can be applied to a significant number of samples. It represents the first rigorous method to be put forward for the characterisation of microbially-mediated ARD generation from waste rock.

Realising these advantages, it is desirable to develop a standardised protocol for the biokinetic test. In this study, we have considered the effect of specific variables such as solids loading, particle size, inoculum size and activity and pH control. Further we have studied a range of refinements to the test, including the batch test with and without pH control, the semi-continuous test and the flow-through test. These have been applied across a variety of different mine wastes. Through this, further clarity is presented on the value of the test and the set points for specific variables. However, it is recognised that the ideal test conditions are partly determined by the nature of the sample itself. While baseline

standard conditions are sought, variation is required in response to the waste mineral type. This should be recognised, with guidelines provided, to inform the tailoring of the test to the waste mineral studied.

Specific variables considered with respect to the biokinetic test include solids loading and particle size. While increasing the solids loading from 7.5 g to 12 g in a 150 mL test leads to the accentuation in pH change and iron concentration, the normalised data across sample sizes of 3, 7.5 and 12 g show that the reactions proceed best at the lower concentration. Hence, the standard sample size of 7.5 g or a smaller size of 3 g appears preferable. However, prior to confirming this, analysis of sample size required for representative sampling must be considered. This is part of an extension study currently underway and will be reported in Guseva's MSc(Eng) dissertation in 2020 and in WRC K5/2946.

The study on particle size preferred for the biokinetic test demonstrates improved data with decreasing particle size. To date a particle size of 100% passing 150 μm has been proposed. However, this depends on the degree of liberation of the sulphide minerals achieved. As near complete liberation is approached, there is limited further improvement with particle size, only a surface area effect impacting rate, not extent of reaction. This suggests that the important parameter is degree of liberation which can be estimated from the comparison of particle size and grain size. Further validation of this is underway in an extension of this study and will be reported by Golela et al. in 2020.

While pH profile of the test is a key output of the test, the profile also impacts its progression. In the presence of rapid neutralisation in a batch test, the resultant increased pH impedes the onset of microbial activity, delaying the test. The added inoculum typically does not take hold and the natural microbial activity must develop as the pH decreases with precipitation. It is proposed that for such samples the use of a dual approach on the uncontrolled batch biokinetic test and the pH controlled batch biokinetic test be used. The former allows data to be gathered on the time for onset of the acidification stage. This can be further honed by using a circum-neutral starting point. The latter allows observation of the microbially-mediated acid generation phase over the expected time period. In the analysis of a mine waste without substantive rapidly released neutralising capacity, the pH-controlled test does not add additional value.

The use of laboratory microbial communities in place of those found in natural ARD environments has been questioned. Through these studies using both performance data and metagenomic analysis of the microbial communities, it has been demonstrated that endemic communities are found on all waste rock samples. Typically, these communities include the same microbes, or microbes with the same key functions as those included in the laboratory cultures. Further, by using mixed microbial communities with both Fe- and S-oxidisers present, the cultures can shift in dominance to meet the needs of the environment. The critical variable is the activity of these communities.

In order to provide a representation of the open system typical in a mine waste disposal system, a semi-continuous system has been trialled in which a daily replacement of 10% of the sample volume is used. In this system providing a 10 day residence time, dissolved neutralising capacity is removed with time, providing a better representation of the likelihood of its availability to neutralise the acid formed. Further this prevents the artificial maintenance of high pH, allowing the microbial community activity to take hold. It is proposed that this may represent the best flask-based model of this test. It is noted that in our previous work we trialled a semi-continuous system using a 90% solution replacement which was unsuccessful owing to the washout of the microbial community. This can be selected appropriately based on knowledge of the microbial growth rate and the 10% replacement is recommended.

Taking this further, a flow-through biokinetic test has been developed in which the milled waste rock is coated onto beads allowing operation of an unsaturated packed bed representative of the waste rock dump. This again allows separation of components formed with differing reaction rates and also allows understanding of the potential for the particular mine waste to be colonised by the microbial community. The approach has been successfully demonstrated and will be further investigated to observe whether there is a minimum sulphide concentration in the mine waste at which it is relevant.

In addition to the delivery on the refined biokinetic test, we highlight in this report the necessity to consider environmental burden beyond acidification and salinisation. In particular, we consider the potential for metal deportment from mine waste. This can be assessed through determining metal concentrations following complete digestion. More meaningfully, the metal deportment to solution is considered through the sequential chemical extraction, allowing deportment to be attributed to particular environmental conditions, from aqueous, through weak acidic conditions, oxidative conditions to strong acid conditions. Similarly, deportment under ARD generating conditions can be studied. In this report we demonstrate the value of this approach, together with an environmental risk assessment, and a rigorous understanding of the ARD potential to allow the determination of disposal requirements or to assess the potential for re-purposing of the mine waste according to the tenets of industrial ecology and the circular economy.

REFERENCES

Adam, K., Kourtis, A., Gazea, B. & Kontopoulos, A., 1997. Evaluation of static tests used to predict the potential for acid drainage generation at sulfide mine sites. Transactions of the Institution of Mining and Metallurgy, Section A, Mining Industry, Volume 106, pp. A1-A8.

Africa, C., Harrison, S., Becker, M. and van Hille, R., 2010. In situ investigation and visualisation of microbial attachment and colonisation in a heap bioleach environment: the novel biofilm reactor. Minerals Engineering, 23(6), pp. 486-491.

Africa, C.J., van Hille, R.P. and Harrison, S.T.L., (2013). Attachment of A. ferrooxidans and L. ferriphilum cultured under varying conditions to pyrite, chalcopyrite, low-grade ore and quartz in a packed column reactor. Applied Microbiology and Biotechnology, 97 (3), 1317-1324

Ahmadi, A., 2012. Influence of Ferric and Ferrous Iron on Chemical and Bacterial Leaching of Copper Flotation Concentrates. International Journal of Nonferrous Metallurgy, 1(3).

Akcil A. and Koldas S. 2006. Acid mine drainage (AMD): causes, treatment and case studies. Journal of Cleaner Production 14, 1139-1145

Amaral Filho, J., 2012. Development of a framework for evaluating downstream uses of separated coal waste fractions. Technical report. Department of Chemical Engineering, University of Cape Town.

APHA, 1998. Standard methods for the examination of water and wastewaters. 20th edition. Washington, DC, USA: American Public Health Association.

Ardau, C., Blowes, D. and Ptacek, C., 2009. Comparison of laboratory testing protocols to field observations of the weathering of sulfide-bearing mine tailings. Journal of Geochemical Exploration, 100(2-3), p. 182-191.

ASTM, 2012. Standard Test Method for Laboratory Weathering of Solid Materials Using a Humidity Cell. D5744 - 12, American Society for Testing and Materials.

Becker, M., Dyantyi, N., Broadhurst, J.L., Harrison, S.T.L. and Franzidis, J.P. 2015. A mineralogical approach to evaluating laboratory scale acid rock drainage characterisation tests. Minerals Engineering, 80. 33-36.

Bergh, J.P., Falcon, R.M.S. and Falcon, L.M. 2011. Trace element concentration reduction by beneficiation of Witbank Coalfield no. 4 Seam. Fuel Processing Technology, Volume 92, Issue 4, April 2011, Pages 812-816.

Bergh, J.P., Falcon, R.M.S. and Falcon, L.M. 2013. Techno-economic impact of optimized low-grade thermal coal export production through beneficiation modelling. Journal of the Southern African Institute of Mining and Metallurgy, vol.113 n.11

Bergh, K., 2009. Trace element partitioning in the Witbank coalfield 4 seam. Johannesberg, Fossil Fuel Foundation Indaba, 11-12 March 2009, Johannesburg, South Africa (2009)

Bishop, J. and Murad, E., 2005. The visible and infrared spectral properties of jarosite and alunite. American Mineralogist, 90(7), p. 1100-1107.

Blowes, D. W., Ptacek, C. J., Jambor, J. L. & Weisener, C., 2003. The Geochemistry of Acid Mine Drainage. In: B. Sherwood-Lollar, H. D. Holland & K. K. Turekian, eds. Treatise on Geochemistry, Volume 9. s.l.:Elsevier, pp. 149-204.

Bradham, W.S. and Caruccio, F.T. 1991. A comparative study of tailings analysis using acid/base accounting, cells, columns and Soxhlets. In: 2nd International Conference of Abatement of Acidic Drainage, Montreal, vol. 1. CANMET, Ottawa, Canada, 157-173.

Broadhurst, J.L. and Petrie, J.G. 2010. Ranking and scoring potential environmental risks from solid mineral wastes. Minerals Engineering, 23, 182-191.

Broadhurst, J.L., Maluleke, W.J. and Von Blottnitz, H. 2009. Comparison and Application of Sequential Chemical Extraction Techniques for Metal Speciation in Sulphidic Copper Tailings1. 8th International Conference on Acid Rock Drainage (ICARD 2009), Skelefeå, Sweden, June, 2009

Broadhurst, J.L., Bryan, C.G., Becker, M., Franzidis, J.-P. and Harrison, S.T.L. 2013. Characterising the acid generating potential of mine wastes by means of laboratory-scale static and biokinetic tests, In: International Mine Water Association Colorado, USA, 275-280.

Broughton, L.M. and Robertson, M.A. 1992. Reliability of acid rock drainage testing. Workshop on U. S. EPA specifications for tests to predict acid generation from non-coal mining. Las Vegas, Nevada.

Bruynesteyn, A. and Hackl, R., 1984. Evaluation of acid production potential of mining waste materials: laboratory and pilot plant procedures, Faculty of Applied Science, University of British Columbia.

Bryan, C., 2006. A study of the microbiological populations of mine wastes, PhD thesis. School of Biological Sciences, University of Wales.

Bryan, C.G., Hallberg, K.B. and Johnson, D.B. 2006. Mobilisation of metals in mineral tailings at the abandoned São Domingos copper mine (Portugal) by indigenous acidophilic bacteria. Hydrometallurgy, 83, 184-194.

Buckwalter-Davis, M., Lussier-Purdy, C. and Jamieson, H., 2015. Mineralogically-Based Determinations of Neutralization and Acid Potential Using Automated Mineralogy. s.l., s.n., 1-10.

Cairncross, B., 1990. Tectono-sedimentary settings and controls of the Karoo Basin Permian coals, South Africa. International Journal of Coal Geology, 16(I), pp. 175-178

Caruccio, F., 1968. An evaluation of factors affecting acid mine drainage and ground water interactions in selected areas of Western Pennsylvania. In: Proceedings of the Second Symposium on Coal Mine Drainage Research: Bituminous Coal Research. Monroevville, PA, USA: s.n., 107-151

Chimbganda, T., Becker, M., Broadhurst, J.L., Harrison, S.T.L. and Franzidis, J.-P. 2013. Comparison of pyrrhotite rejection and passivation in two Nickel ores. Minerals Engineering, Volume 46-47, 38-44.

Chiume R., Minnaar S., Ngoma E., Bryan C. and Harrison S.T.L. 2012. Microbial colonisation in heaps for mineral bioleaching and the influence of irrigation rate. Minerals Engineering. 39, 156-164

Coastech Research Inc, 1989. Investigation of prediction techniques for acid mine drainage MEND Project 1.16.1 a, Canada Centre for Mineral and Energy Technology, Energy, Mines and Resources, Canada.

Coram, N.J. and Rawlings, D.E. 2002. Molecular relationship between two groups of the genus Leptospirillum and the finding that *Leptospirillum ferriphilum* sp. nov. dominates in South African commercial biooxidation tanks that operate at 40◦C. Applied and Environmental Microbiology, 68, 838-845.

Córdoba, E.M., Munoz, J.A., Blázquez, M.L., González, F.and Ballester, A. 2008. Leaching of chalcopyrite with ferric ion. Part IV: The role of redox potential in the presence of mesophilic and thermophilic bacteria. Hydrometallurgy, 93(3-4), p. 106-115.

Cox, D., Lindsey, D., Singer, D. and Diggles, M., 2003. Sediment-hosted copper deposits of the world: Deposit models and database: U.S. Geological Survey Open-File Report 03-107, s.l.: US Department of the Interior.

Czerewko, M., Cripps, J., Reid, J. and Duffell, C. 2003. Sulfur species in geological materials – sources and quantification. Cement and concrete composites, 25, 657-671.

Dold, B. 2010. Basic concepts in environmental geochemistry of sulfidic mine-waste management. In: Kumar, S. (Ed.), Waste Management, pp. 173-198 (http://www.intechopen.com/books/show/title/waste-management).

Dopson, M., Lövgren, L. and Boström, D. 2004. Silicate mineral dissolution in the presence of acidophilic microorganisms: Implications for heap bioleaching. Hydrometallurgy, 96(4), pp. 288-293.

Duncan, D. and Bruynesteyn, A. 1979. Determination of acid production potential of waste materials, paper A-79-29 AIME, Littleton, CO, USA: Metallurgy Society, AIME.

Durand, J. F. 2012. The impact of gold mining on the Witwatersrand on the rivers and karst system of Gauteng and North West Province, South Africa. Journal of African Earth Sciences, 68, 24-43.

Dyantyi, N., Becker, M., Broadhurst, J.L., Harrison, S.T.L. and Franzidis, J.-P. 2013. Use of Mineralogy to interpret laboratory-scale acid rock drainage (ARD) prediction tests: a gold case study. AusIMM, pp. 519-526.

Eary, L. E. and. Williamson, M.A. 2006. Simulations of the neutralizing capacity of silicate rocks in acid mine drainage environments. Montavesta, USA, ASMR 3134, pp. 564-577.

Environment Australia, 1997. Managing sulphidic mine wastes and acid drainage. Best practice environmental management in mining, Kingston, ACT 2604, Australia: Office of the Supervising Scientist, Environment Australia.

Erguler, G.K., Erguler, Z.A., Akcakoca, H. and Ucar, A., 2014. The effect of column dimensions and particle size on the results of kinetic column test used for acid mine drainage (AMD) prediction. Minerals Engineering, Volume 55, pp. 18-29.

Erguler, Z.A. and Erguler, G.K., 2015. The effect of particle size on acid mine drainage generation: Kinetic column tests. Minerals Engineering, 76, p. 154-167.

Evans, P. & Skousen, J., 1995. Effects of digestion method on neutralisation potential of overburden samples containing siderite. Gillette, Wyoming, USA, s.n., p. 696-707.

Ferguson, K. & Erickson, P., 1988. Pre-Mine Prediction of Acid Mine Drainage. In: Salomons, W. & Förstner, U., eds. Environmental Management of Solid Waste. Berlin, Heidelberg: Springer.

Florian, B. and Sand, W., 2012. Inhibition of bacterial pyrite leaching by surfactants. In: A. Mendez-Villas, ed. Microbes in applied research: Current advances and challenges. World scientific, pp. 140-146.

Galván, L., Olías, M., Cánovas, C.R., Torres, E., Ayora, C., Nieto, J.M. and Sarmiento, A.M. 2012. Refining the estimation of metal loads dissolved in acid mine drainage by continuous monitoring of specific conductivity and water level. Applied Geochemistry, 27(10), pp. 1932-1943.

Gautama, R.S. and Kusuma G.J. 2008. Evaluation of Geochemical Tests in Predicting Acid Mine Drainage Potential in Coal Surface Mine. Karlsbad, Czech Republic, International Mine Water Association.

Ghorbani, Y., Petersen, J., Harrison, S.T.L., Tupikina, O.V., Becker, M., Mainza, A.N., Franzidis, J.-P. (2012). An experimental study of the long-term bioleaching of large sphalerite ore particles in a circulating fluid fixed-bed reactor. Hydrometallurgy. 129-130, 161-171.

Ghorbani, Y., Petersen, J., Becker, M.E., Mainza, A.N. and Franzidis, J.-P. 2013. Investigation and modelling of the progression of zinc leaching from large sphalerite ore particles. Hydrometallurgy, Volume 131-132, pp. 8-23.

Govender, E., Bryan, C. G. & Harrison, S. T., 2013. Quantification of growth and colonisation of low grade sulphidic ores by acidophilic chemoautotrophs using a novel experimental system. Minerals Engineering, Volume 48, pp. 108-115.

Govender, E., Bryan, C. & Harrison, S., 2015. A novel experimental system for the study of microbial ecology and mineral leaching within a simulated agglomerate-scale heap bioleaching system. Biochemical Engineering Journal, Volume 95, p. 86-97.

Hallberg, K.B. and Lindstrom, E.B. 1994. Characterisation of *Thiobacillus caldus* sp. nov., a moderately thermophilic acidophile. Microbiology, 140, 3451-3456.

Hallberg, K.B. 2010. New perspectives in acid mine drainage microbiology. Hydrometallurgy, 104, 448-453.

Harneit, K., Göksel, A., Kock, D., Klock, J.H., Gehrke, T. and Sand, W. 2006. Adhesion to metal sulphide surfaces by cells of *Acidithiobacillus ferrooxidans, Acidithiobacillus thiooxidans* and *Leptospirillum ferrooxidans*. Hydrometallurgy. 83, 245-254.

Harrison, S.T.L., Broadhurst, J.L., van Hille, R.P., Oyekola, O.O., Bryan, C., Hesketh, A. and Opitz, A. 2010. A systematic approach to sulphidic waste rock and tailings management to minimise ARD formation. WRC K5/1831/3, Pretoria, South Africa: Water Research Commission, South Africa.

Hedin, R.S. and Erickson, P.M., 1988. Relationships between the initial geochemistry and leachate chemistry of weathering overburden samples. In: Mine Drainage and Surface Mine Reclamation. USBM Information Circular 9183. 21-28.

Hesketh, A.H., Broadhurst J.L., Bryan C.G., van Hille R.P. and Harrison S.T.L. 2010a. Biokinetic test for the characterisation of AMD generation potential of sulfide mineral wastes. Hydrometallurgy, 104(3), pp. 459-464.

Hesketh, A.H., Broadhurst, J.L. and Harrison, S.T.L. 2010b. Mitigating the generation of acid mine drainage from copper sulfide tailings impoundments in perpetuity: A case study for integrated management strategy. Minerals Engineering, Volume 23, pp. 225-229.

Hlongwane, P. 2015. Standardising the biokinetic test for characterisation of ARD potential. MSc(Eng) dissertation, Department of Chemical Engineering, University of Cape Town.

International Network for Acid Prevention, 2013. Global Acid Rock Drainage Guide. [Online] Available at: http://www.gardguide.com/index.php?title=Main_Page [Accessed 2013].

Iroala, O. 2014. Combining froth flotation with reflux classification to mitigate ARD generating potential of the Waterberg and Witbank coal ultrafines via sulfide removal (Masters thesis). University of Cape Town

Jambor, J., Dutrizac, J. and Chen, T. 2000. Contribution of specific minerals to neutralization potential in static tests. In: Proceedings 5th International Confonference on Acid Rock Drainage. Littleton, CO, USA: Society for Mining, Metallurgy, and Exploration, Inc. (SME).

Janzen, M., Nicholson, R. and Scharer, J. 2000. Pyrrhotite reaction kinetics: reaction rates for oxidation by oxygen, ferric iron, and for nonoxidative dissolution. Geochimica et Cosmochimica Acta, 64(9), pp. 1511-1522.

Jennings, S. and Dollhopf, D. 1995. Acid-base account effectiveness for determination of mine waste potential acidity. Journal of Hazardous Materials, 41(2-3), pp. 161-175.

Jiménez, A., Aroba, J., de la Torre, M., Andujar, J. and Grande, J. 2009. Model of behaviour of conductivity versus pH in acid mine drainage water, based on fuzzy logic and data mining techniques. Journal of Hydroinformatics, 11(2), pp. 147-153.

Johnson, D.B. 2003. Chemical and microbiological characteristics of mineral spoils and drainage waters at abandoned coal and metal mines. Water Air and Soil Pollution: Focus 3 47-66,

Johnson, D.B. and Hallberg, K.B. 2005. Acid mine drainage remediation options: a review. Science of the Total Environment, Volume 338, pp. 3-14.

Jones G.C., Corin K.C., van Hille R.P. and Harrison S.T.L. 2011. The generation of toxic reactive oxygen species (ROS) from mechanically activated sulphide concentrates and its effect on thermophilic bioleaching. Minerals Engineering 24 (11), 1198-1208.

Jones G.C., van Hille R.P. and Harrison S.T.L. 2012. Reactive oxygen species generated in the presence of fine pyrite particles and their implication in thermophilic minerals bioleaching. Applied Microbiology and Biotechnology 97(6), 2735-2742.

Kania, T. 1998. Laboratory methods for acid-base accounting: an update. Pennsylvania Department of Environ. Protection. Harrisburg, Pennsylvania, USA:

Kazadi Mbamba, C., Harrison, S.T.L., Franzidis, J.-P. and Broadhurst, J.L. 2012. Mitigating acid rock drainage risks while recovering low-sulphur coal from ultrafine colliery wastes using froth flotation. Minerals Engineering, Volume 29, p. 13-21.

Kelly, D.P. and Wood, A.P. 2000. Reclassification of some species of *Thiobacillus* to the newly designated genera *Acidithiobacillus* gen. nov., *Halothiobacillus* gen. nov. and *Thermithiobacillus* gen. nov. International Journal of Systematic and Evolutionary Microbiology, 50, 511-516.

Kinzler, K., Gehrke, T., Telegdi, J. and Sand, W., 2003. Bioleaching – a result of interfacial processes caused by extracellular polymeric substances (EPS). Hydrometallurgy, Volume 71, p. 83-88.

Kitula, A. 2006. The environmental and socio-economic impacts of mining on local livelihoods in Tanzania: A case study of Geita District. Journal of cleaner production, 14, 405-414.

Koehnken, L., Clarke, N., Dineen, R., Jones, W.. 2003. Present status of remediation of Mt Lyell acid drainage. In Proceedings of the Sixth International Acid Rock Drainage Conference, July 14-17 2003, Cairns, Australia. 65-70

Kolmert, A. and Johnson, D.B. 2001. Remediation of acidic waste waters using immobilised, acidophilic sulfate-reducing bacteria. Journal of Chemical Technology and Biotechnology. 76, 836-843.

Komadel, P. and Stucki, J.W. 1988. Quantitative assay of minerals for Fe^{2+} and Fe^{3+} using 1, 10-phenanthroline: III. A rapid photochemical method. Clay Minerals 36, 379-381.

Konishi, Y., Asai, S. and Yoshida, N., 1995. Growth Kinetics of *Thiobacillus thiooxidans* on the Surface of Elemental Sulfur. Applied and Environmental Microbiology, 61(10), p. 3617-3622.

Kotelo, L., 2013. Characterising the acid mine drainage potential of fine coal wastes, Masters dissertation. Department of Chemical Engineering, University of Cape Town.

Kwong, Y., Swerhone, G. and Lawrence, J., 2003. Galvanic sulphide oxidation as a metal leaching mechanism and its environmental implications. Geochemistry: Exploration, Environment, Analysis, Volume 3, pp. 337-343.

Lapakko, K., 2002. Metal mine rock and waste characterization tools: an overview. Report No. 67. International Institute for Environment and Development Mining, Minerals and Sustainable Development.

Lapakko, K. A., Engstrom, J. N. and Antonson, D. A., 2006. Effects of particle size on drainage quality from three lithologies. Poster presented at the 7th International Conference on Acid Rock Drainage (ICARD), March 26-30, 2006, St. Louis MO. R.I. Barnhisel (ed.) Published by the American Society of Mining and Reclamation (ASMR), 3134 Montavesta Road, Lexington, KY 40502. 1026-1050.

Lapakko, K. & Lawrence, R. W., 1993. Modification of the net acid production (NAP) test. In: Proceedings of the 17th Annual British Columbia Mine Reclamation Symposium: The Technical and Research Committee on Reclamation. Port Hardy, BC, Canada

Lawrence, R. W. and Scheske, M. 1997. A method to calculate the neutralization potential of mining wastes. Environmental Geology, 32, 100-106.

Lawrence, R.W. and Wang, Y., 1997. Determination of neutralisation potential in the prediction of acid rock drainage. In Proceedings of the 4th International Conference Acid Rock Drainage, Vancouver, British Columbia. 451-464.

Maest, A. S., Kuipers, J. R., Travers, C. L. and Atkins, D. A. 2005. Predicting Water Quality at Hardrock Mines. Methods and models, uncertainties and state-of-the-art. Earthworks, Washington, DC, USA

Makaula, D.X., Huddy, R.J., Fagan-Endres, M.A. and Harrison, S.T.L. 2017a Investigating the microbial metabolic activity on mineral surfaces of pyrite-rich waste rocks in an unsaturated heap-simulating column system. Solid State Phenomena. 262, 228-232.

Makaula, D.X., Huddy, R.J., Fagan-Endres, M.A. and Harrison, S.T.L. 2017b. Using isothermal microcalorimetry to measure the metabolic activity of the mineral-associated microbial community in bioleaching, Miner. Eng. 106. 33-38.

Makaula, D.X., Huddy, R.J., Fagan-Endres, M.A. and Harrison, S.T.L. 2018. Developing a flow-through biokinetic test to characterize ARD potential: investigating the microbial metabolic activity on pyrite-bearing waste rock surfaces in an unsaturated ore bed. Proceedings 11th ICARD | IMWA, Wolkersdorfer, Ch., Sartz, L., Weber, A., Burgess, J., Tremblay, G. (eds.) | MWD Conference – "Risk to Opportunity"

Makaula, D.X., Fagan-Endres, M.A. and Harrison, S.T.L. 2019. Establishing the flow-through biokinetic test to characterise sulfidic waste rock mineral for its potential to form ARD. Minerals Engineering (under review).

Malmström, M.E., Destouni, G., Banwart, S.A. and Strömberg, B.H., 2000. Resolving the Scale-Dependence of Mineral Weathering Rates. Environmental Science & Technology, 34(7), pp. 1375-1378.

McCarthy, T. 2011. The impact of acid mine drainage in South Africa. South African Journal of Science, 5/6(107), 1-7.

Michaud, M.L., Plante, B., Bussière, B., Benzaazoua, M. and Leroux. J. 2017. Development of a modified kinetic test using EDTA and citric acid for the prediction of contaminated neutral drainage. J. Geochemical Exploration, 181, 58-68

Miller, S., 2008. Development of ARD assessment for coal process wastes (ACARP project C15034). Australia: Environmental Geochemistry International Pty Ltd.

Miller, S. and Jeffery, J. 1995. Advances in the prediction of acid generating mine waste materials. In:. 2nd Australian Acid Mine Drainage Workshop. Australian Centre for Minesite Rehabilitation Research, Brisbane. 33-42.

Miller, S., Jeffrey, J. and Wong, J. 1991a. In-pit identification and management of acid forming waste rock at the Golden Cross Mine, New Zealand. In: Proc. 2nd International Conference on the Abatement of Acidic Drainage, Montreal, Sept 16-18. 137-151.

Miller, S.D., Robertson, A. and Donahue, T. 1997. Advances in Acid Drainage Prediction using the Net Acid Generation (NAG) test. 4th International Conference on Acid Rock Drainage, 1997 Vancouver, BC. 533-549.

Miller, S.D., Stewart, W.S., Rusdinar, Y., Schumann, R.E., Ciccarelli, J.M., Li, J. and Smart, R.St.C. 2010. Methods for estimation of long-term non-carbonate neutralisation of acid rock drainage. Science of the Total Environment, 408(9), pp. 2129-2135.

Mirza, A., Herrera, M. and Doyle, P. 1992. Characterization of pyrite-bearing minerals by chemical oxidation. In Emerging Process Technologies. In: S. Chandar & P. Richardson, eds. Proc. 121st SME Annual Meeting and Exhibit. Littleton, CO,USA: Soc. for Mining, Metallurgy, and Exploration, pp. 121-129.

Mitchell, P. 2000. Prediction, prevention, control and treatment of acid rock drainage. In: A. Warhurst & L. Noronha, eds. Environmental Policy in Mining: Corporate Strategy and Planning for Closure. London/New York: Lewis. 117-143.

Morin, K.A. and Hutt, N.M. 1998. Kinetic test and risk assessment for ARD. In: Proc. 5 th Annual BC Metal Leaching and ARD Workshop, Vancover, Canada.

Nemati, M. and Webb, C., 1996. Effect of ferrous iron concentration on the catalytic activity of immobilized cells of *Thiobacillus ferrooxidans*. Applied Microbiology and Biotechnology, Volume 46, pp. 250-255.

Ngoma, I.E., Ojumu, T.V. and Harrison, S.T.L. 2015. Investigating the effect of acid stress on selected mesophilic micro-organisms implicated in bioleaching. Minerals Engineering, 75, 6-13.

Nordstrom, D. K. 2011. Hydrogeochemical processes governing the origin, transport and fate of major and trace elements from mine wastes and mineralized rock to surface waters. Applied Geochemistry, 26, 1777-1791.

Opitz, A.K.B., 2013. An investigation into accelerated leaching for the purpose of AD mitigation. MSc dissertation. Department of Chemical Engineering, University of Cape Town.

Opitz, A., Broadhurst, J. L. and Harrison, S.T.L. 2015. Assessing Environmental Risks Associated with Ultrafine Coal Wastes Using Laboratory-Scale Tests. Advanced Materials Research, Volume 1130, 635-639

Opitz, A.K.B. and Harrison, S.T.L. 2016a. The effect of the inoculum concentration on the biokinetic test for characterising acid rock drainage (ARD), Biohydrometallurgy 16', MEI, Falmouth, UK,

Opitz, A.K.B., Becker, M., Harrison, S.T.L. and Broadhurst, J.L. 2016b. Characterising environmental risks associated with sulfide bearing gold wastes. Proceedings IMWA, Freiberg/Germany Drebenstedt, Carsten, Paul, Michael (eds.) | Mining Meets Water – Conflicts and Solutions

Opitz, A.K.B., Becker, M., Broadhurst, J.L., Bradshaw, D.J. and Harrison, S.T.L. 2016c The Biokinetic Test as a Geometallurgical Indicator for Acid Rock Drainage Potentials. The Third AusIMM International Geometallurgy Conference, 15-16 June 2016 Perth, Australia. AusIMM, 183-191.

O'Shay, T., Hossner, L. & Dixon, J., 1990. A modified hydrogen peroxide oxidation method for determination of potential acidity in pyritic overburden. Journal of Environmental Quality. 19, 778-782.

Paktunc, A. 1999. Mineralogical constraints on the determination of neutralization potential and prediction of acid mine drainage. Environmental Geology, 39, 103-112.

Paktunc, A., Leaver, M., Salley, J. and Wilson, J., 2001. A new standard material for acid base accounting tests. In: Securing the Future: International Conference of Mining and the Environment Skellefteå, Sweden. 644-652.

Parbhakar-Fox, A., Lottermoser, B. and Bradshaw, D. J. 2013. Cost-effective means for identifying acid rock drainage risks – Integration of the geochemistry-mineralogy-texture approach and geometallurgical techniques. The 2nd AUSIMM International Geometallurgy Conference, 2013 Brisbane, QLD.

Parbhakar-Fox, A. and Lottermoser, G.B. 2015. A critical review of acid rock drainage methods and predictions. Minerals Engineering, 82, 107-124.

Parker, G. and Robertson, A. 1999. Acid drainage. Australian Minerals & Energy Environment Foundation.

Plante, B., Benzaazoua, M. and Bussière, B. 2010. Kinetic Testing and Sorption Studies by Modified Weathering Cells to Characterize the Potential to Generate Contaminated Neutral Drainage. Mine Water and the Environment, 30, 22-37.

Plumb, J.J., Mcsweeney, N.J. and Franzmann, P.D. 2008a. Growth and activity of pure and mixed bioleaching strains on low grade chalcopyrite ore. Minerals Engineering, 21(1), 93-99.

Plumb, J.J., Muddle, R. and Franzmann, P.D. 2008b. Effect of pH on rates of iron and sulfur oxidation by bioleaching organisms. Minerals Engineering, 21(1), 76-82.

Price, W.A. 2009. Prediction manual for drainage chemistry from sulphidic geological materials (MEND report 1.20.1), British Columbia, Canada: CANMET Mining and Mineral Science Laboratories.

Price, W.A. 1997. Guidelines and Recommended Methods for the Prediction of Metal Leaching and Acid Rock Drainage at Minesites in British Columbia: Draft, Ministry of Employment and Investment. Energy and Minerals Division.

Räisänen, M., Kauppila, P. and Myöhänen, T., 2010. Suitability of static test for acid rock drainage assessment of mine waste rock. Bulletin of the Geological Society of Finland, 82, 101-111.

Rawlings, D. 2005. Characteristics and adaptability of iron- and sulfur-oxidizing microorganisms used for the recovery of metals from minerals and their concentrates. Microbial Cell Factories, 4(1), p. 13.

Rojas-Chapana, A., Bartels, C.C., Pohlmann, L. and Tributsch, H. 1998. Co-operative leaching and chemotaxis of *Thiobacilli* studied with spherical sulphur. Process Biochemistry 31, 239-248.

Sampson, M., Phillips, C. and Blake, R. 2000. Influence of the attachment of acidiphilic bacteria during the oxidation of mineral sulfides. Minerals Engineering, Volume 13, p. 373-389.

Sand, S. and Gehrke, T., 2006. Extracellular polymeric substances mediate bioleaching/ biocorrosion via interfacial processes involving iron (III) ions and acidophilic bacteria. Research in Microbiology, Volume 157, pp. 49-56.

Sand, W., Jozsa, P.-G., Kovacs, Z.-M., Sãsãran, N. and Schippers, A. 2007. Long-term evaluation of acid rock drainage mitigation measures in large lysimeters. Journal of Geochemical Exploration, 92, 205-211.

Santelli, C., Welch, S., Westrich, H. and Banfield, J., 2001. The effect of Fe-oxidizing bacteria on Fe-silicate mineral dissolution. Chemical Geology, 180(1), p. 99-115.

Sapsford, D.J., Bowell, R.J., Dey, M. and Williams, K.P. (2008). Humidity cell tests for the prediction of acid rock drainage. Minerals Engineering, 22, 25-36.

Schippers, A., Kock, D., Schwartz, M.O., Böttcher, M.E., Vogel, H. and Hagger, M. (2007). Geomicrobiological and geochemical investigation of a pyrrhotite containing mine waste tailings dam near Selebi-Phikwe in Botswana. Journal of Geochemical Exploration, 92, 151-158.

Schumann, R., Stewart, W., Miller, S., Kawashima, N., Li, J. and Smart, R. 2012. Acid-base Accounting Assessment of Mine Wastes using the Chromium Reducible Sulfur Method. Science of the Total Environment, 424(0), pp. 289-296.

Simunika, N., Broadhurst, J.L., Petersen, J., Harrison, S.T.L., and Franzidis, J.-P. 2013. Predicting the time-related generation of acid rock drainage from mine waste: a copper case study. Santiago, Chile, s.n.

Skousen, J., Renton, J., Brown, H., Evans, P., Leavitt, B., Brady, K., Cohen, L. and Ziemkiewicz, P. 1997. Neutralization potential of overburden samples containing siderite. Journal of Environmental Quality, 26, 673-681.

Smart, M., Edward, C.J., Fourie, C., Shumba, T., Iron, J. and Harrison, S.T.L. 2018. Archaeal dominated biooxidation cultures show increased resilience to operational conditions. In: Biohydrometallurgy '18, Windhoek, Namibia, 12-13 June 2018.

Smart, M., Huddy, R.J., Edward, C.J., Fourie, C., Shumba, T., Irons, J. and Harrison, S.T.L. 2017. Linking microbial community dynamics in BIOX leaching tanks to process conditions: integrating lab and commercial practice. Solid State Phenomena, 262 SSP, pp 38-42. http://dx.doi.org/10.4028/www.scientific.net/SSP.262.38

Smart, R.S.C., Skinner, B., Levay, G., Gerson, A.R., Thomas, J.E., Sobieraj, H., Schumann, R., Weisener, C.G., Weber, P.A., Miller, S.D. and Stewart, W.A. 2002. ARD Test Handbook. Project P387A Prediction and Kinetic Control of Acid Mine Drainage. Ian Wark Research Institute and Environmental Geochemistry International. www.amira.com.au/documents/downloads/P387AProtocolBooklet.pdf

Sobek, A., Schuller, W., Freeman, J. and Smith, R., 1978. Field and Laboratory Methods Applicable to Overburden and Minesoils (EPA 600/2-78-054) , Washington, DC, USA: Environmental Protection Agency.

Stewart, W.A., Miller, S.D. and Smart, R. 2006. Advances in acid rock drainage (ARD) characterisation of mine wastes. In: 7th International Conference on Acid Rock Drainage (ICARD), St. Louis, United States, pp. 2098-2119.

Tan, S. and Chan, M., 2012. Early stage adsorption behaviour of Acidithiobacillus ferrooxidans on minerals I: An experimental approach. Hydrometallurgy, Volume 119-120, p. 87-94.

Tupikina, O.V., Minnaar, S.V., Van Hille, R.P., Van Wyk, N., Rautenbach, G.F., Dew, D. and Harrison, S.T.L., 2013. Determining the effect of acid stress on the persistence and growth of thermophilic microbial species after mesophilic colonization of low-grade ore in a heap leach environment. Minerals Engineering, 53, pp.152-159.

Tupikina, O.V, Minnaar, S.H., Rautenbach, G.F., Dew, D.W. and Harrison, S.T.L. 2014. Effect of inoculum size on the rates of whole ore colonisation of mesophilic, moderate thermophilic and thermophilic acidophiles. Hydrometallurgy 149. 244-251.

US Environmental Protection Agency, 1994. Acid mine drainage prediction. EPA-530-R-94-036, Washington, DC, USA.

Valente, T. M. and Gomes, C. L., 2009. Occurrence, properties and pollution potential of environmental minerals in acid mine drainage. The Science of the total environment, 407(3), pp. 1135-1152.

Verburg, R., Bezuidenhout, N., Chatwin, T., Ferguson, K. 2009. The global acid rock drainage guide (GARD Guide). Mine Water and the Environment, 28 (4), 305-310

Wagner, N. and Tloteng, M., 2012. Distribution of selected trace metal elements in density fractionated Waterberg coals from South Africa. International Journal of Coal Geology, 94(I), pp. 225-237

Watnick, P. and Kolter, R. 2000. Biofilm, City of Microbes. Journal of Bacteriology, 182(10) 2675-2679

Weber, P., Thomas, J., Skinner, W. & Smart, R., 2004a. Improved acid neutralisation capacity assessment of iron carbonates by titration and theoretical calculation,. Applied Geochemistry, 19(5), pp. 687-694.

Weber, P.A., Thomas, J.E., Skinner, W.M. and Smart, R.S.C. 2005. A methodology to determine the acid-neutralization capacity of rock samples. The Canadian Mineralogist, 43, 1183-1192.

White III, W., Lapakko, K. & Cox, R., 1999. Static-test methods most commonly used to predict acid-mine drainage: Practical guidelines for use and interpretations. In: G. Plumlee & M. Logsdon, eds. Reviews in Economic Geology Vol. 6A,. Littleton, CO, USA: Society of Economic Geologists, pp. 325-338.

Wu, B., Wen, J.K., Chen, B.W., Yao, G.C., Wang, D.Z. 2014. Control of redox potential by oxygen limitation in selective bioleaching of chalcocite and pyrite. Rare Metals, 33(5), pp. 622-627.

Zhang, J., Ren, D., Zhu, Y., Chou, C.-L., Zeng, R. and Zheng, B. 2004. Mineral matter and potentially hazardous trace elements in coals from Qianxi fault depression area in south-western Guizhou, China. International Journal of Coal Geology, 57(I), pp. 49-61